MID-AMERICA TRANSPORTATION CENTER

Report # MATC-UNL: 004-11

Final Report
WBS: 25-1121-0005-004-11

Investigation and Development of a Test Level 6 Barrier, Phase I

Ronald K. Faller, Ph.D., P.E.
Research Professor
Midwest Roadside Safety Facility
Department of Civil Engineering
University of Nebraska-Lincoln

Jennifer Schmidt, Ph.D., P.E.
Research Assistant Professor

Joshua S. Steelman, Ph.D., P.E.
Assistant Professor

Dean Whitfield, B.S.C.E.
Graduate Research Assistant

2018

A Cooperative Research Project sponsored by
U.S. Department of Transportation- Office of the Assistant Secretary for Research and Technology

MATC

Investigation and Development of a MASH Test Level 6 Barrier

Ronald K. Faller, Ph.D., P.E. (PI)
Research Professor
Midwest Roadside Safety Facility
Department of Civil Engineering
University of Nebraska-Lincoln

Joshua S. Steelman, Ph.D, P.E. (Co-PI)
Assistant Professor
Department of Civil Engineering
University of Nebraska - Lincoln

Jennifer Schmidt, Ph.D, P.E. (Co-PI)
Research Assistant Professor
Midwest Roadside Safety Facility
Department of Civil Engineering
University of Nebraska - Lincoln

Dean Whitfield, B.S.C.E.
Graduate Research Assistant
Department of Civil Engineering
University of Nebraska - Lincoln

A Report on Research Sponsored by

Mid-America Transportation Center

University of Nebraska–Lincoln

October 2018

INVESTIGATION AND DEVELOPMENT OF A MASH TEST LEVEL 6 BARRIER, PHASE I

Submitted by

Dean L. Whitfield, B.S.C.E., E.I.
Graduate Research Assistant

Jennifer D. Schmidt, Ph.D., P.E.
Research Assistant Professor

Ronald K. Faller, Ph.D., P.E.
Research Professor and MwRSF Director

Joshua S. Steelman, Ph.D., P.E.
Assistant Professor

MIDWEST ROADSIDE SAFETY FACILITY
Nebraska Transportation Center
University of Nebraska-Lincoln
130 Whittier Research Center
2200 Vine Street
Lincoln, Nebraska 68583-0853
(402) 472-0965

Submitted to

MID-AMERICA TRANSPORTATION CENTER
2200 Vine Street
Lincoln, Nebraska 68583

MwRSF Research Report No. TRP-03-404-18

October 2018

TECHNICAL REPORT DOCUMENTATION PAGE

1. Report No. 25-1121-0005-004-11 TRP-03-404-18	2. Government Accession No.	3. Recipient's Catalog No.	
4. Title and Subtitle Investigation and Development of a Test Level 6 Barrier, Phase I		5. Report Date October 2018 6.	
7. Author(s) Dean L. Whitfield, B.S.C.E., Jennifer D. Schmidt, Ph.D., Ronald K. Faller, Ph.D., Joshua S. Steelman, Ph.D.		8. Performing Organization Report No. 25-1121-0005-004-11 TRP-03-404-18	
9. Performing Organization Name and Address Midwest Roadside Safety Facility (MwRSF) Nebraska Transportation Center University of Nebraska-Lincoln 130 Whittier Research Center 2200 Vine Street Lincoln, Nebraska 68583-0853		10. Project/Task/Work Unit No. 11. Contract © or Grant (G) No. 69A3551747107	
12. Sponsoring Organization Name and Address Mid-America Transportation Center 2200 Vine St. Lincoln, NE 68583		13. Type of Report and Period Covered Final Report: 2017 – 2018 14. Sponsoring Agency Code MATC TRB RiP No. 91994-3	
15. Supplementary Notes Conducted in cooperation with U.S. Department of Transportation, Federal Highway Administration.			
16. Abstract The objective of this research project was to develop a new, cost-effective, MASH TL-6 barrier. A literature review on prior Test Level 5 and Test Level 6 barriers was conducted, and the cost of current TL-5 and TL-6 barriers was established. Existing and modified design procedures for roadside barrier were reviewed as well as current TL-6 design forces. A preliminary TL-6 truck model was developed in LS-DYNA. The minimum barrier height to contain a tractor-tank vehicle was determined to be 62 in. for a rigid, vertical-faced barrier through LS-DYNA computer simulation. Recommendations for how to improve the tank-trailer model were presented.			
17. Document Analysis/Descriptors Highway Safety, MASH, Test Level 6, Roadside Barrier, LS-DYNA, Tractor-Tank Trailer		18. Availability Statement No restrictions. Document available from: National Technical Information Services, Springfield, Virginia 22161	
19. Security Class (this report) Unclassified	20. Security Class (this page) Unclassified	21. No. of Pages 190	22. Price

Disclaimer Statement

The contents of this report reflect the views of the authors, who are responsible for the facts and the accuracy of the information presented herein. This document is disseminated in the interest of information exchange. The report is funded, partially or entirely, by a grant from the U.S. Department of Transportation's University Transportation Centers Program. However, the U.S. Government assumes no liability for the contents or use thereof.

Acknowledgements

The authors wish to acknowledge several sources that made a contribution to this project: (1) the Mid-America Transportation Center; and (2) LBT Inc. for providing information on tank trailers.

Acknowledgement is also given to the following individuals who made a contribution to the completion of this research project.

Midwest Roadside Safety Facility

J.D. Reid, Ph.D., Professor
J.C. Holloway, M.S.C.E., E.I.T., Test Site Manager
K.A. Lechtenberg, M.S.M.E., E.I.T., Research Associate Engineer
R.W. Bielenberg, M.S.M.E., E.I.T., Research Associate Engineer
S.K. Rosenbaugh, M.S.C.E., E.I.T., Research Associate Engineer
C.S. Stolle, Ph.D., Research Assistant Professor
A.T. Russell, B.S.B.A., Shop Manager
S.M. Tighe, Laboratory Mechanic
D.S. Charroin, Laboratory Mechanic
M.A. Rasmussen, Laboratory Mechanic
E.W. Krier, Laboratory Mechanic
Undergraduate and Graduate Research Assistants

Table of Contents

List of Figures

List of Tables

Chapter 1 Introduction

1.1 Background

For run-off-road (ROR) events, roadside and median barriers, including bridge rails, have commonly been used to prevent errant motorists from striking hazardous roadside fixed objects or geometric features, which can mitigate the severity of those crashes. For some situations, it is appropriate to only utilize barrier systems that are capable of safely containing and redirecting passenger vehicles. These barrier systems typically meet the Test Level 3 (TL-3) safety performance criteria published in either the National Cooperative Highway Research Program (NCHRP) Report No. 350, *Recommended Procedures for the Safety Performance Evaluation of Highway Features* (1993) [1], or the American Association of State Highway and Transportation Officials' (AASHTO) *Manual for Assessing Safety Hardware* (MASH 2016) [2].

However, it may be necessary to use higher-performance vehicle containment barriers (i.e., TL-4 through TL-6) when the percentage of truck and other heavy vehicle traffic is high and/or the consequences of vehicle penetration beyond the longitudinal barrier is too great. Historically, TL-4 and TL-5 barriers have been implemented across the United States when truck and other heavy vehicle traffic have been considered. These TL-4 and TL-5 barrier systems have been crash tested and evaluated using single-unit trucks and tractor-van trailers, respectively, but are likely structurally inadequate and lack sufficient height to safely contain and redirect tractor-tank trailer vehicles, which often transport hazardous or flammable chemicals through heavily populated communities. When the TL-4, TL-5, and TL-6 trucks are compared, as shown in figures 1.1 and 1.2, it becomes more clear that the geometry of the tank-trailer vehicle is much different than that of the van-trailer and single unit truck vehicles. Thus, current TL-4 and TL-5 system would not be capable of safely containing and redirecting a tank-trailer vehicle.

Figure 1.1 TL-4 (20,000-lb), TL-5 (80,000-lb), and TL-6 (80,000-lb) Vehicle Sideview

Figure 1.2 TL-4 (20,000-lb), TL-5 (80,000-lb), and TL-6 (80,000-lb) Vehicle Rearview

To date, only one TL-6 vehicle containment system has been successfully tested and evaluated according to NCHRP Report No. 230 [3] using a tractor-tank trailer vehicle [4]. Designed by the Texas A&M Transportation Institute (TTI) in 1984, this combination barrier system consisted of a lower, solid reinforced-concrete parapet with an upper beam-and-post reinforced-concrete railing system, and measured 90 in. (2,286 mm) tall, as shown in figure 1.3. Unfortunately, the cost, height, and weight of this TL-6 containment barrier has prevented its widespread implementation.

Due to the TL-6 barrier's design, only a few barrier installations have been utilized in the real world thus far, leaving many situations where a TL-6 barrier is needed but is not present. These situations could include prevention and mitigation of: (1) cross median, opposing-traffic vehicle crashes involving hazardous heavy tractor tank-trailer vehicles along urban freeways and interstates and (2) tractor tank-trailer vehicle penetration or override of existing TL-4 or TL-5 barriers located on bridges, elevated road structures, or high volume roadways. These situations may create potentially catastrophic events near schools, malls, sports venues, concert arenas, military bases, international airports, critical government buildings, or other high-risk facilities.

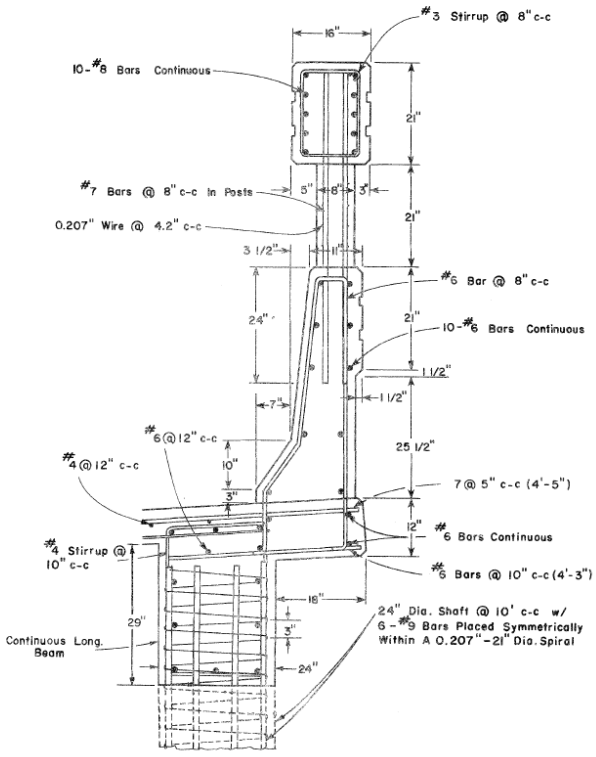

Figure 1. Cross Section of the Modified T5 Bridge Rail and Modified Bridge Deck.

5

Figure 1.3 TTI TL-6 Roman Wall [4]

In addition, state departments of transportation (DOTs) desire a TL-6 barrier option that is more economical, versatile, and easier to implement. The Virginia DOT currently uses a 90-in. (2,286-mm) tall wall design between bridge piers. This barrier is used to help prevent damage to bridge piers by errant tractor-van trailer vehicles by creating a solid wall instead of individual piers. Adding a barrier between the piers also helps to prevent an errant vehicle from snagging on the piers and coming to rest underneath the bridge. The Utah DOT is using an 84-in. (2,134-mm) tall solid concrete wall, which is installed on the roadside to shield a railroad line adjacent to a curved highway, as shown in figure 1.4.

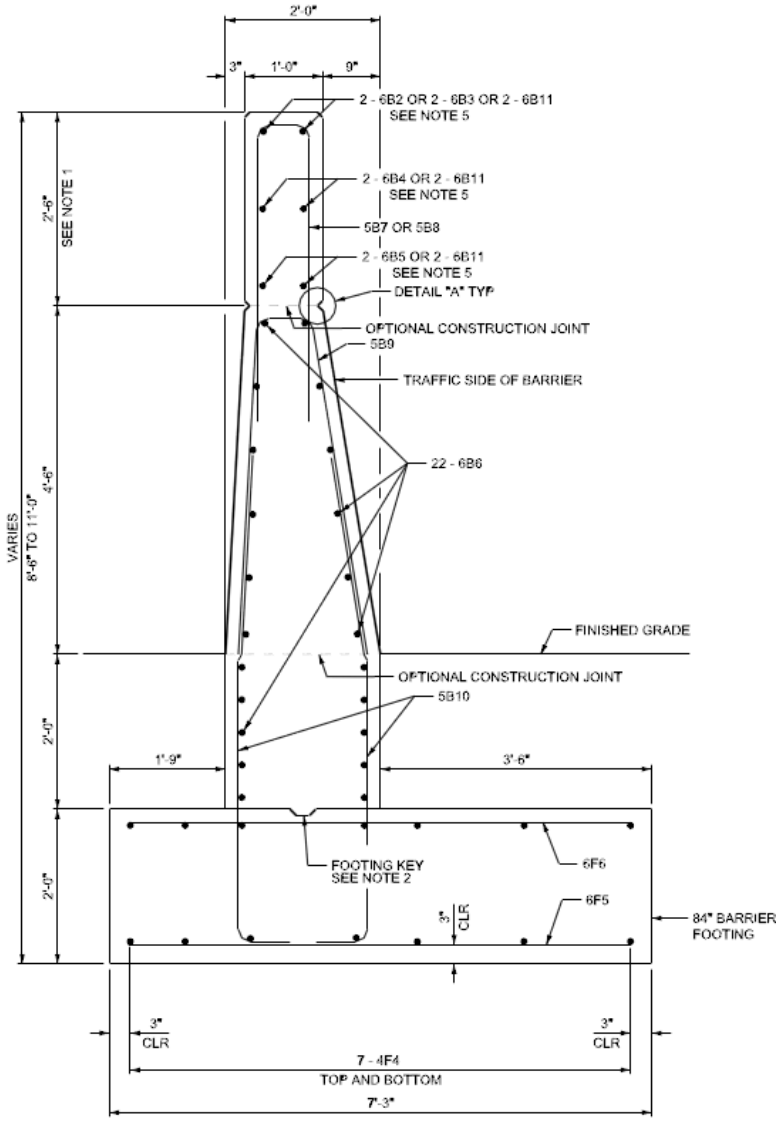

Figure 1.4 Utah TL-5 Barrier

As noted by the Federal Highway Administration (FHWA) [5], "Crashes of heavy vehicles through or over traffic barriers that result in catastrophic consequences are rare but are of extreme public concern." Heavy vehicle crashes pose a serious risk to the drivers and passengers of involved vehicles, the drivers and passengers of vehicles in the general vicinity, and to adjacent structures. Due to the likelihood of these vehicles carrying hazardous material, it is important to understand how these accidents happen, and the consequences if an accident does occur.

On May 11, 1976, a tractor-tank trailer transporting 7,509 gal (28,425 L) of anhydrous ammonia lost control and impacted the bridge rail on the ramp connecting Interstate 610 (I-610) to the Southwest Freeway (U.S. 59) in Houston, Texas [6]. This impact resulted in the tractor-tank trailer penetrating the bridge rail and leaving the ramp. As the vehicle fell, the tractor-tank trailer struck a support column of an adjacent overpass and came to rest 15 ft (4.6 m) below the bridge on the Southwest Freeway. Due to the damage from the impact with the barrier, support column, and ground, the tank was damaged, which released anhydrous ammonia. As a result of the ammonia leak, six people were killed, 78 were hospitalized, and approximately an additional 100 people were treated for other related injuries. The National Transportation Safety Board (NTSB) determined the probable cause of the accident to be the excessive speed of the tractor-tank trailer, in addition to the lateral surge caused by the liquid in the partially-loaded truck. The NTSB also stated the severity of the accident was increased due to the failure of the bridge rail to contain or redirect the vehicle.

On January 13, 2004, a tractor-tank trailer carrying 8,800 gal (33,312 L) of gasoline left the roadway in Elkridge, Maryland, and collided with the bridge rail of the ramp it was on, causing the tractor-tank trailer to roll over the top of the barrier [7]. The vehicle subsequently fell 30 ft (9.1 m) onto the roadway below at which time it exploded and caught fire. The fire from the leaked gasoline destroyed five vehicles and caused four fatalities. The NTSB listed a few factors in the probable cause of the accident, which were: (1) the failure of the driver to maintain control of his vehicle, (2) the narrow shoulder and the outdated design of the roadway, and (3) the outdated design of the guardrail to concrete parapet transition that caused the tanker to override and roll over the bridge rail.

On October 22, 2009, a 2006 Navistar International truck pulling a 1994 Mississippi Tank Company MC331 trailer hauling 9,001 gal (34,072 L) of gasoline rolled over while

traversing an at grade ramp connecting I-69 southbound to I-465 in Indianapolis, Indiana [8]. The rollover occurred when the truck driver overcorrected after drifting into the left lane from the right lane. This sudden overcorrection caused the tanker trailer to disconnect from the tractor and penetrate through a W-beam guardrail adjacent to the road. The tanker then collided with a bridge pier column of the bridge the at-grade ramp was traveling under. The collision displaced the bridge pier column and punctured the tanker trailer, releasing the petroleum gasoline, which formed a vapor cloud and ignited, causing a massive fire. The fire caused injury to the truck driver and the driver of another car, which was in the adjacent lane during the crash. Three passengers of vehicles traveling on the I-465 bridge above the accident site were also injured. The NTSB concluded that the accident was a result of the excessive speed and rapid overcorrecting of the truck driver as he drifted into the lane adjacent to him.

A TL-6 barrier utilized at these locations may mitigate some of these catastrophic events. As such, there exists a need to develop a new, cost-effective, structurally adequate, reduced-height vehicle containment system that is safe for motorists, capable of containing errant vehicle impacts with heavy tanker-truck vehicles, and prevents and/or mitigates the consequences of catastrophic crashes into high-risk facilities or highly-populated areas.

1.2 Research Objective

The objective of this research project was to develop a new, cost-effective, MASH TL-6 barrier. This barrier should be able to safely redirect vehicles ranging from 2,420-lb (1,100-kg) small passenger cars to 79,300-lb (36,000-kg) tractor-tank trailers. This barrier was initially developed as a roadside barrier but will also have median and bridge rail configurations designed. This new barrier was intended to safely and stably contain and redirect large tractor-tank trailers, while also limiting occupant risk measures in small cars and trucks. The TL-6

barrier should be aesthetically pleasing, while also being economically competitive to current TL-5 barriers.

1.3 Research Scope

The objective will be achieved through the completion of several tasks. A literature review was completed on all previous TL-6 and applicable TL-5 barrier designs. The cost of current TL-5 and TL-6 barriers was estimated. Barrier design procedures as well as TL-6 design forces were reviewed. Design criteria for the new barrier was then developed. Concepts were brainstormed, developed, and evaluated based on their ability to meet the design criteria. The minimum barrier height to contain a TL-6 tractor-tank trailer impact was evaluated using engineering analysis and computer software. Preferred concepts were designed and evaluated with finite element analysis. A summary, conclusion, and recommendations for future work were provided.

Chapter 2 Literature Review

2.1 Scope of Review

Existing barrier design and evaluation methods were reviewed. A review was then conducted on existing TL-6 crash tests. Little crash testing information exists on TL-6 barriers, thus, it was deemed necessary to broaden the scope of the literature review to also include TL-5 barriers. Barriers were investigated, and the following data was collected: height, width, amount of reinforcement in concrete barriers, vehicle properties, impact speed and angle, occupant impact velocities, occupant ridedown accelerations, and post-accident results, amongst various others.

Other geometric considerations with roadside and median barriers were reviewed, along with a review of tractor tank-trailer geometries. A study of barrier loads and loading locations was then conducted, and information was compiled.

2.2 Highway Barrier Safety Performance Criteria

Since 2009, MASH [2] has been the standard testing manual for roadside safety feature evaluation. Prior to MASH, NCHRP Report No. 230 [3] and 350 [1] provided guidance for evaluating safety hardware. MASH defines the impact conditions and evaluation criteria for each type of roadside safety hardware. For roadside parapets and barriers, MASH provides six different test levels, TL-1 through TL-6. Each test level represents different vehicle classes and impact conditions for which the barrier must safely contain and redirect errant vehicles. TL-6 barriers must be able to safely contain and redirect a 2,420-lb (1,100-kg) small car, a 5,000-lb (2,268-kg) pickup truck, and a fully-loaded 79,300-lb (36,000-kg) tractor tank-trailer. Along with specifying the weight of the test vehicle, MASH also defines the Impact Severity (IS) for each test level, which has been shown to be a good indicator of the magnitude of loading on a longitudinal barrier, as shown in Eqn 1.

$$IS = {}^{1}/_{2}\, M(V sin\theta)^2 \qquad \text{(Eqn. 1)}$$

Where:

IS = lateral component of a vehicle kinetic energy, kip-ft (kJ)
M= vehicle mass, lb (kg)
V = impact speed, ft/s (m/s)
θ = impact angle, degrees

Impact severity is dependent on the weight of the vehicle, the impact speed, and the angle of impact. A higher IS typically correlates to more force being imparted the barrier from the impacting vehicle. The full testing matrix for MASH TL-6 barriers is shown in table 2.1.

Table 2.1 MASH Test Level 6 Testing Matrix for Longitudinal Barriers

Test Level	Barrier Section	Test No.	Vehicle	Impact Speed mph (km/h)	Impact Angle deg	Acceptable IS Range kip-ft (kJ)	Evaluation Criteria[1]
6	Length-of-need	6-10	1100C	62 (100.0)	25	≥51 (69.7)	A,D,F,H,I
		6-11	2270P	62 (100.0)	25	≥106 (144)	A,D,F,H,I
		6-12	36000T	50 (80.0)	15	≥404 (548)	A,D,G

[1] Evaluation criteria explain in table 2.2.

Along with specifying the test conditions, MASH also provides safety performance evaluation criteria. Evaluation criteria for full-scale vehicle crash testing are based on three appraisal areas: (1) structural adequacy; (2) occupant risk; and (3) vehicle trajectory after collision. Criteria for structural adequacy are intended to evaluate the ability of the barrier to contain and redirect impact vehicles. In addition, controlled lateral deflection of the test article is acceptable. Occupant risk evaluates the degree of hazard to occupants in the impacting passenger vehicles. Post-impact vehicle trajectory is a measure of the potential of the vehicle to result in a secondary collision with other vehicles and/or fixed objects, thereby increasing the risk of injury to the occupants of the impacting vehicle and/or other vehicles. The evaluation criteria are shown

in table 2.2. If a test meets all the required evaluation criteria, the barrier is deemed crashworthy according to MASH.

Table 2.2 MASH Testing Evaluation Criteria

Evaluation Factors	Evaluation Criteria			
Structural Adequacy	A.	Test article should contain and redirect the vehicle or bring the vehicle to a controlled stop; the vehicle should not penetrate, underride, or override the installation although controlled lateral deflection of the test article is acceptable.		
Occupant Risk	D.	Detached elements, fragments, or other debris from the test article should not penetrate or show potential for penetrating the occupant compartment, or present undue hazard to other traffic, pedestrians, or personnel in a work zone. Deformations of, or intrusions into, the occupant compartment should not exceed limits set forth in Section 5.2.2 and Appendix E of MASH.		
	F.	The vehicle should remain upright during and after collision. The maximum roll and pitch angles are not to exceed 75 degrees.		
	G.	It is preferable, although not essential, that the vehicle remain upright during and after collision		
	H.	Occupant impact velocities (OIV) (see Appendix A, Section A5.2.2 of MASH for calculation procedure) should satisfy the following limits:		
		Occupant Impact Velocity Limits, ft/s (m/s)		
		Component	Preferred	Maximum
		Longitudinal and Lateral	30 ft/s (9.1 m/s)	40 ft/s (12.2 m/s)
		Longitudinal	10 ft/s (3.0 m/s)	16 ft/s (4.9 m/s)
	I.	The occupant ridedown acceleration (see Appendix A, Section A5.2.2 of MASH for calculation procedure) should satisfy the following limits:		
		Occupant Ridedown Acceleration (ORA) Limits (G)		
		Component	Preferred	Maximum
		Longitudinal and Lateral	15.0 G	20.49 G

2.3 Previous Crash Tests

Tables

Table 2.3 through table 2.6 contain information on two TL-6 crash tests and twelve TL-5 crash tests. Included in the tables is information relating to: barrier shape and geometry, test vehicle weights, impact conditions, and test results.

Table 2.3 Literature Review Summary for TL-6 and TL-5 Barriers

Test No.	Reference No.	Test Date	Test Agency	Barrier Description	Test Standard	Test Level
1	4	Unknown	TTI	TL-6 Roman Wall	NCHRP Report 230	6
7046-4	10	5/8/1987	TTI	TL-6 Instrumented Wall	NCHRP Report 230	6
MAN-1	11	4/16/2016	MwRSF	TL-5 Manitoba Tall Wall	MASH 2009	5
TL5CMB-2	12	7/12/2007	MwRSF	TL-5 Vertical Faced Concrete Median Barrier Incorporating Head Ejection Criteria	NCHRP Report 350	5
490025-2-1	13	8/21/2015	TTI	TL-5 TxDOT T224 Bridge Rail	MASH 2009	5
ACBR-1	14	8/28/2003	MwRSF	NDOR's TL-5 Aesthetic Open Concrete Bridge Rail	NCHRP Report 350	5
6	15	Unknown	TTI	Open Concrete Rail with mounted Steel Tube	NCHRP Report 230	5
405511-2	16	12/12/1995	TTI	TL-5 1.07-m Vertical Wall Bridge Railing	NCHRP Report 230	5
2416-1	17	9/18/1984	TTI	TL-5 Concrete Safety Shape with Top Metal	NCHRP Report 230	5
7162-1	18	8/9/1990	TTI	TL-5 Ontario Tall Wall	NCHRP Report 230	5
510605-RYU1	19	12/19/2011	TTI	TL-5 Ryerson/Pultrall GFRP-Reinforced Parapet	MASH 2009	5
401761-SBG1	20	11/16/2010	TTI	TL-5 Schöck ComBAR GFRP-Reinforced Parapet	MASH 2009	5
603911-3	21	6/17/2016	TTI	TL-5 Steel Bridge Rail for Suspension Bridges	MASH 2009	5
7046-3	10	4/7/1987	TTI	TL-5 Instrument Wall	NCHRP Report 230	5

N/A = Not Available

Table 2.4 Literature Review Summary for TL-6 and TL-5 Barriers (cont.)

Test No.	Reference No.	Barrier Height in. (mm)	Test Inertial Weight lb (kg)	Front Axle Weight lb (kg)	Tractor Tandem Axle Weight lb (kg)	Trailer Tandem Axle Weight lb (kg)
1	4	90 (2,286)	80,120 (36,342)	12,070 (5,475)	34,050 (15,445)	34,000 (15,422)
7046-4	10	90 (2,286)	79,900 (36,242)	11,840 (5,371)	33,570 (15,227)	34,490 (15,644)
MAN-1	11	49.25 (1,251)	80,076 (36,322)	9,774 (4,433)	34,066 (15,452)	36,236 (16,436)
TL5CMB -2	12	42 (1,067)	79,705 (36,154)	9,790 (4,441)	34,515 (15,656)	32,400 (14,696)
490025-2-1	13	42 (1,067)	79,760 (36,178)	10,000 (4,536)	36,460 (16,538)	33,300 (15,105)
ACBR-1	14	42 (1,067)	78,975 (35,822)	8,475 (3,844)	36,725 (16,658)	33,775 (15,320)
6	15	54 (1,372)	79,770 (36,183)	11,490 (5,212)	33,760 (15,313)	34,520 (15,658)
405511-2	16	42 (1,067)	79,366 (36,000)	11,210 (5,085)	34,249 (15,535)	33,907 (15,380)
2416-1	17	50 (1,270)	80,080 (36,324)	12,020 (5,452)	34,170 (15,499)	33,890 (15,372)
7162-1	18	41.34 (1,050)	80,000 (36,287)	11,580 (5,253)	34,360 (15,585)	34,070 (15,454)
510605-RYU1	19	41.34 (1,050)	79,650 (36,129)	9,360 (4,246)	35,060 (15,903)	35,230 (15,980)
401761-SBG1	20	41.3 (1,050)	79,220 (35,934)	9,520 (4,318)	31,980 (14,506)	37,720 (17,109)
603911-3	21	42 (1,067)	79,620 (36,115)	N/A	N/A	N/A
7046-3	10	90 (2,286)	80,080 (36,324)	11,680 (5,298)	34,140 (15,486)	34,260 (15,540)

N/A = Not Available

Table 2.5 Literature Review Summary for TL-6 and TL-5 Barriers (cont.)

Test No.	Reference No.	Impact Speed mph (km/h)	Impact Angle Deg.	Impact Severity kip-ft (kJ)	OIV Lat ft/s (m/s)	OIV Long ft/s (m/s)
1	4	51.4 (82.7)	15.0	474.0 (642.4)	8.03 (2.45)	7.20 (2.19)
7046-4	10	54.8 (88.2)	16.0	609.4 (826.2)	28.10 (8.56)	3.00 (0.91)
MAN-1	11	51.7 (83.2)	15.0	479.3 (649.8)	-16.15 (-4.92)	-2.33 (-0.71)
TL5CMB-2	12	52.8 (85.0)	15.4	523.8 (710.2)	N/A	N/A
490025-2-1	13	50.5 (81.3)	14.1	403.6 (547.1)	14.80 (4.51)	4.30 (1.31)
ACBR-1	14	49.4 (79.5)	16.3	507.5 (688.1)	18.05 (5.50)	2.99 (0.91)
6	15	49.1 (79.0)	15.0	430.6 (583.9)	18.30 (5.58)	7.60 (2.32)
405511-2	16	49.7 (80.0)	14.5	410.8 (557.0)	16.07 (4.90)	8.20 (2.50)
2416-1	17	48.4 (77.9)	14.5	393.1 (533.0)	15.49 (4.72)	6.59 (2.01)
7162-1	18	49.6 (79.8)	15.1	446.5 (605.4)	12.70 (3.87)	6.30 (1.92)
510605-RYU1	19	49.1 (79.0)	14.6	407.9 (553.0)	4.60 (1.40)	7.20 (2.19)
401761-SBG1	20	50.5 (81.3)	15.6	488.4 (662.6)	4.60 (1.40)	18.00 (5.49)
603911-3	21	49.9 (80.3)	15.1	449.8 (609.8)	12.10 (3.69)	16.70 (5.09)
7046-3	10	55.0 (88.5)	15.3	563.9 (764.5)	18.10 (5.52)	7.10 (2.16)

N/A = Not Available

Table 2.6 Literature Review Summary for TL-6 and TL-5 Barriers (cont.)

Test No.	Reference No.	ORA Lat g's	ORA Long g's	Max Dynamic Deflection in. (mm)	Permanent Set in. (mm)
1	4	11.16	1.83	4 (101.60)	0.6 (15.24)
7046-4	10	6.6	-1.1	0 (0)	0 (0)
MAN-1	11	-6.3	-4.04	2 (50.80)	0 (0.00)
TL5CMB-2	12	Unknown	Unknown	1.50 (38.10)	Unknown
490025-2-1	13	15.1	8.9	2.1 (53.34)	1.2 (30.48)
ACBR-1	14	-7.91	8.05	11.22 (284.99)	Unknown
6	15	3.3	1.2	Unknown	Unknown
405511-2	16	7.2	-2.9	0 (0)	0 (0)
2416-1	17	5.5	-2.4	10.8 (274.32)	6 (152.40)
7162-1	18	-5.1	-2	Unknown	Unknown
510605-RYU1	19	9.4	5.7	0 (0)	0 (0)
401761-SBG1	20	6.5	37.2	Unknown	Unknown
603911-3	21	8.7	10.4	2 (50.80)	0.6 (15.24)
7046-3	10	6	-2.0	0 (0)	0 (0)

N/A = Not Available

2.3.1 TL-6 Roman Wall

In 1984, TTI designed and tested the first, and only, NCHRP Report No. 230 TL-6 barrier [4]. This barrier was a modified Texas T5 reinforced concrete safety shape barrier, with a reinforced concrete post-and-beam system mounted atop, and designed and tested as a bridge rail, as shown in figure 1.3. This rail was designed using the yield line theory for reinforced concrete [9] assuming two applied loads: one 60,000-lb load applied at a height of 21 in. and a second 144,000-lb load at 84 in. above the ground surface. Knowing the approximate total load on the tandem axles of the tractor would be 34,000 lb, the researchers assumed that 10,000 lb of this load was the empty weight of the trailer, and the additional 24,000 lb was the weight of the added tank ballast. The empty 10,000 lb was expected to be transferred to the rail through the wheels at a height of 21 in., and the 24,000 lb was expected to be transferred through the tank-trailer at a height of 84 in. From past tests' accelerometer data, it was determined that the rear tandem axles of the tractor would be subjected to a lateral acceleration of approximately 6 g's. Therefore a static force of 60,000 lb (10,000 lb x 6 g's) would be applied at a height of 21 in., and 144,000 lb (24,000 lb x 6 g's) would be applied at a height of 84 in.

The modified T5 safety shape had a height of 48 in., a top width of 11 in., and a bottom width of 20½ in. The reinforcement for this section consisted of no. 6 vertical stirrups spaced at 8 in., which extended into the deck, and ten (five on the traffic side and five on the field side) no. 8 longitudinal bars which were spaced evenly throughout the section.

The upper reinforced concrete post-and-beam section totaled 42 in. in height. It consisted of 21-in. tall, 8-in. wide, and 60-in. long posts spaced at 120 in. on center i.e., 60-in. gaps between 60-in. posts. Mounted on the posts was a 21-in. tall, 16-in. wide, reinforced concrete beam. The posts contained sixteen (eight traffic side and eight field side) no. 7 vertical bars which began at the top of the reinforced concrete beam and extended down through the posts into

the safety shape. Reinforcing in the beam consisted of no. 3 vertical stirrups at 8-in. centers, and ten (five traffic side and five field side) no. 8 longitudinal bars.

The concrete barrier was mounted on a modified Texas standard 12-in. thick bridge deck. The deck cantilever extended 18 in. in length. The upper transverse bars were no. 7 bars at a 5-in. spacing, while the lower transverse bars were no. 6 bars at a 10-in. spacing. Both the upper and lower longitudinal bars were no. 6 bars spaced at 17½ in. The bridge cantilever deck was mounted on 24-in. diameter drilled shaft piers, spaced at 10-ft centers. The piers contained six no. 9 bars placed symmetrically inside a rebar spiral with 0.207 in. diameter rebar in a 21-in. diameter spiral.

The system was tested using a 1980 Kenworth tractor-trailer ballasted with water to 80,120 lb at the TTI Proving Grounds. The truck impacted the barrier at a speed of 51.4 mph and angle of 15 degrees. The point of impact was at the upstream edge of post no. 5. The truck was smoothly redirected while remaining upright throughout the whole event.

The truck sustained damage to both the right front wheel and right tandem wheels, while the cab of the truck remained intact. The tank was dented from the impact with the upper concrete beam but did not rupture. The tank sustained a small puncture from the exhaust stack, measuring ¼ in. in diameter, immediately following impact.

The barrier sustained minor cracking during impact. The bridge deck experienced minor cracking and spalling. From overhead film analysis, the upper beam had a maximum dynamic deflection of 4 in., with a permanent deflection of 0.6 in. From the mounted accelerometers and rate gyro sensors, there was a maximum roll of 17 degrees, a maximum average 0.05 sec longitudinal acceleration of -1.77 g's, and a maximum average 0.05 sec lateral acceleration of 5.54 g's.

2.3.2 TL-6 Instrumented Wall

In 1988, TTI investigated vehicle impact forces and locations on an instrumented wall [10]. A 90-in. tall reinforced concrete vertical face wall was constructed that was outfitted with accelerometers and load cells. The wall consisted of four wall segments total, each outfitted with load cells on all four corners, and one accelerometer mounted in the middle. Figure 2.1 shows one 120 x 90-in. wall segment. The wall segments were supported vertically on low friction Teflon pads to make them completely free-standing with no influence from a wall to ground connection. Vehicles ranging from small cars and pickup trucks to tractor-van and tractor-tank trailers were crashed into the barrier.

In test no. 7046-4, a 1971 Peterbilt tractor with a 1968 Fruehauf tank-trailer, weighing 79,900 lb total, impacted the wall at a speed of 54.8 mph and an angle of 16 degrees.

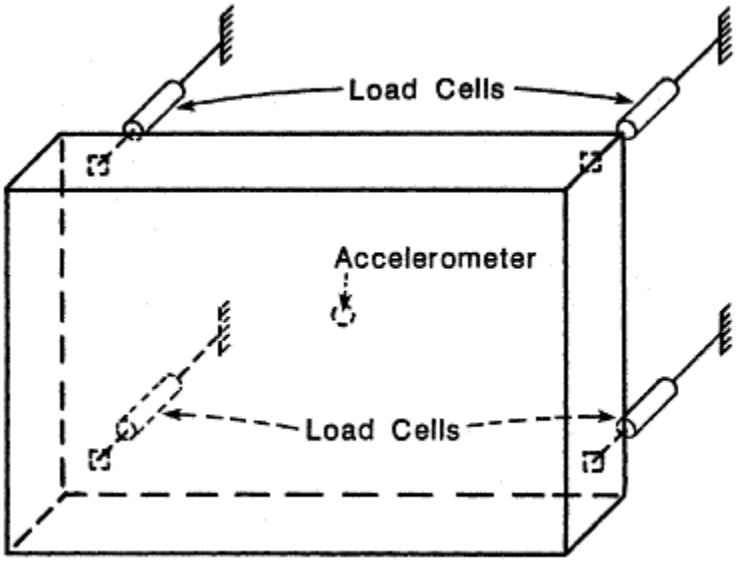

Figure 2.1 Schematic of One Instrumented Wall Segment [10]

The vehicle was equipped with triaxial accelerometers mounted over the tractor tandem axles, and biaxial accelerometers just ahead of the fuel tanker, over the trailer-tandem axles, and slightly ahead of the center of gravity of the trailer.

During the crash, data was collected from all instrumentation on the impacting vehicle, along with the load cells and accelerometer mounted to the wall. This data was then analyzed to determine the magnitude and location of the applied load. From this test it was determined that there were three main impacts in the overall crash event. Along with accelerometer and load cell data, high-speed video was also recorded.

The first impact was a 91-kip impact at a height of 36 in. From video analysis, this was determined to be the initial impact of the front of the tractor with the barrier. The second impact, from the front of the tank-trailer/tractor tandem axle, was 212-kip at a height of 40½ in. The final impact resulted in a load of 408-kip at 56 in. and was from the rear trailer tandem-axles, also known as tail slap. The graph of the loads imparted onto the instrumented wall is shown in figure 2.2.

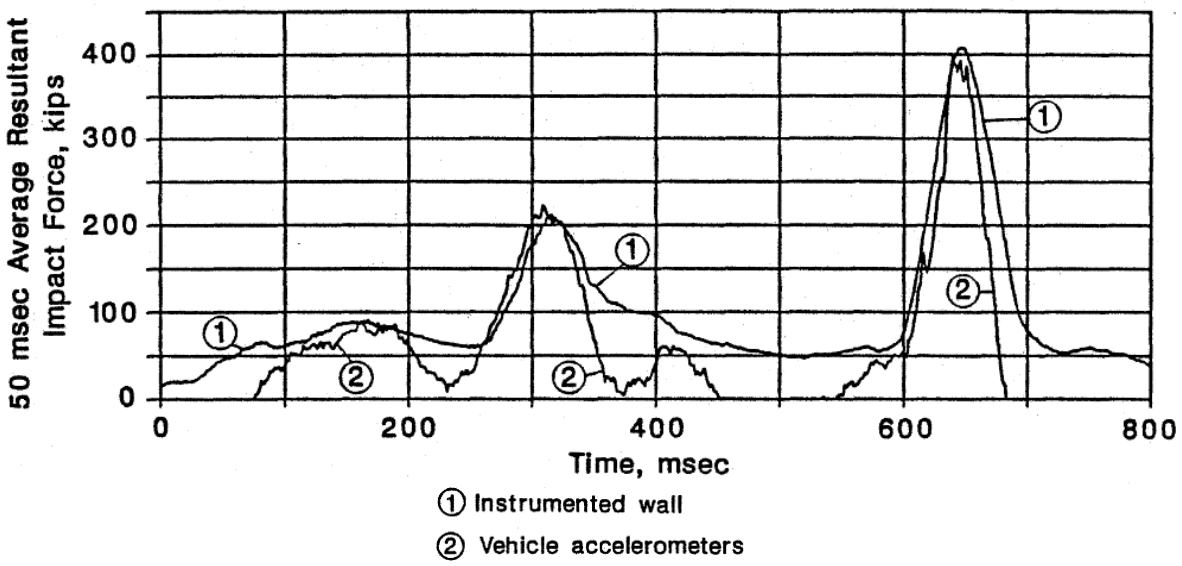

Figure 2.2 Resulting Impact Force for Tractor-Tank Trailer Instrumented Wall Impact [9]

2.3.3 TL-5 Manitoba Tall Wall

The Manitoba Tall Wall [11] was a single slope barrier designed by the Midwest Roadside Safety Facility (MwRSF) for Manitoba Infrastructure. The bridge railing configuration was 49¼ in. tall and had a 9-degree slope from the vertical traffic face, resulting in a top width of 9⅞ in. and a bottom width of 17¾ in. The rail reinforcing comprised 20M stirrups spaced at 15¾ in., with ten 15M longitudinal bars at the interior sections, as shown in figure 2.3. At the end section, the stirrup spacing was decreased to 9 in. Consequently, the interior section had a capacity of 196.48 kips, and the end section had a 196-kip capacity.

The rail was mounted on an 11-in. thick bridge deck with a 51¼-in. overhang, as shown in figure 2.4. The deck reinforcing consisted of 20M bars at 8-in. centers in the top mat, and 15M bars spaced at 15¾-in. centers in the bottom mat in the interior section. The end section deck reinforcing contained 20M bars at 4-in. centers in the top mat, and 15M bars at 8-in. centers in the bottom mat. This resulted in capacities of 27.3 kip-ft/ft and 49.5 kip-ft/ft for the interior and end sections, respectively.

The barrier was successfully tested with an 80,076-lb 2004 International 9200 Tractor and a 2001 Wabash National Trailer. The tractor tank-trailer impacted at a speed of 51.7 mph and 15.2 degrees at 1.5 ft upstream from the joint.

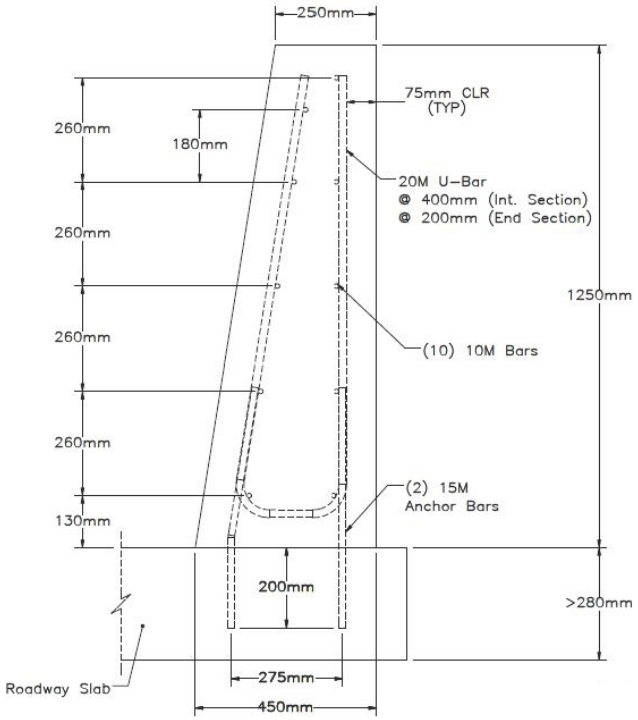

Figure 2.3 TL-5 Manitoba Tall Wall Reinforcement Layout and Dimensions [11]

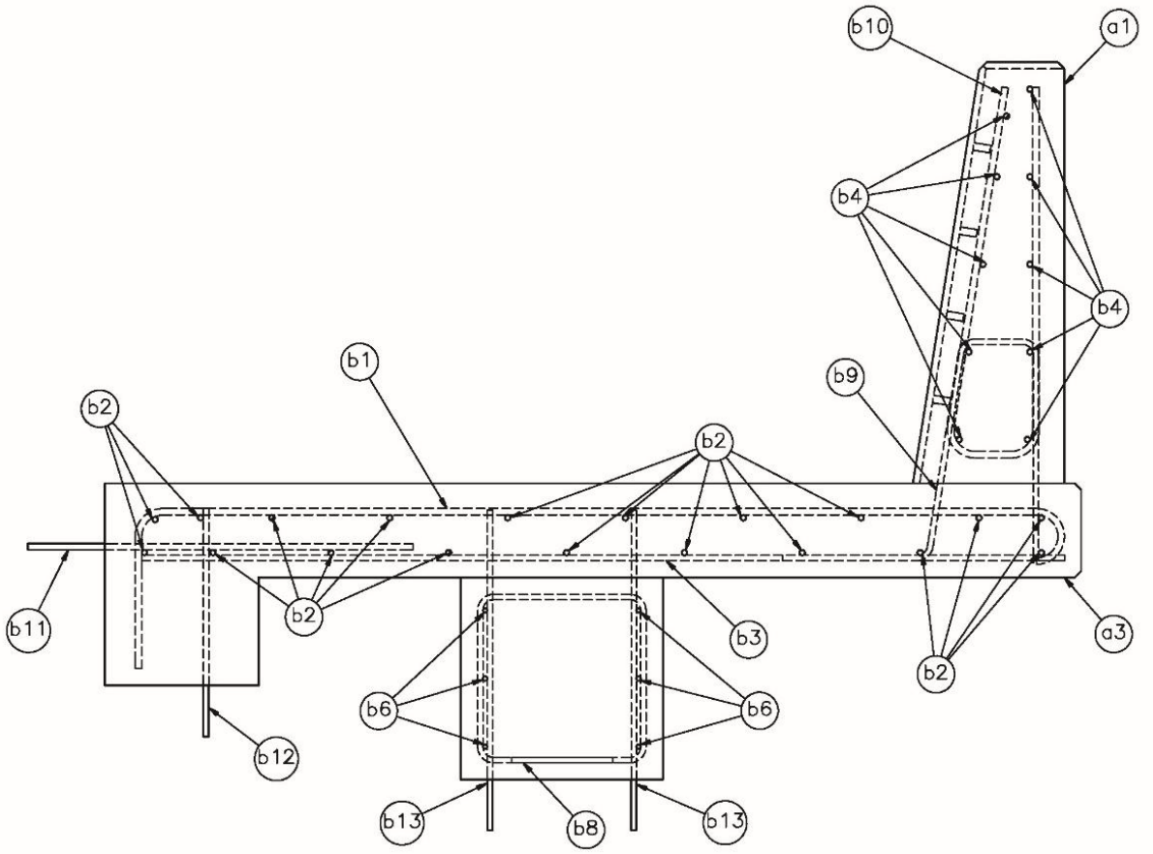

Figure 2.4 TL-5 Manitoba Tall Wall Deck Configuration [11]

2.3.4 TL-5 Vertical Faced Concrete Median Barrier Incorporating Head Ejection Criteria

In 2007, MwRSF designed a TL-5 vertical faced concrete median barrier incorporating head ejection to protect an occupant's head against head slap on the barrier [12]. The barrier was a 42-in. tall, reinforced concrete, single slope barrier, as seen in figure 2.5. The slope of the front face was 18:1 for the lower 34 in., which transitioned to a 2:5 slope for the next 2 in., and a 2:1 slope for the upper 6 in. of the barrier.

The reinforcement consisted of no. 5 stirrups spaced at 18 in. on center, which were extended into the slab below the barrier. The barrier had eleven no. 4 longitudinal bars, five on each face with one bar running along the top of the section. The section had a resistance capacity of 215.4 kips, calculated using Yield Line Analysis [9]. The barrier was successfully tested using a 1991 White GMC Conventional WG65T tractor with a 1988 Pines 48-ft Trailer weighing a combined 79,705 lb. The tractor tank-trailer impacted the barrier at 52.8 mph at an angle of 15.4 degrees and a distance of 30 ft from the upstream end of the barrier.

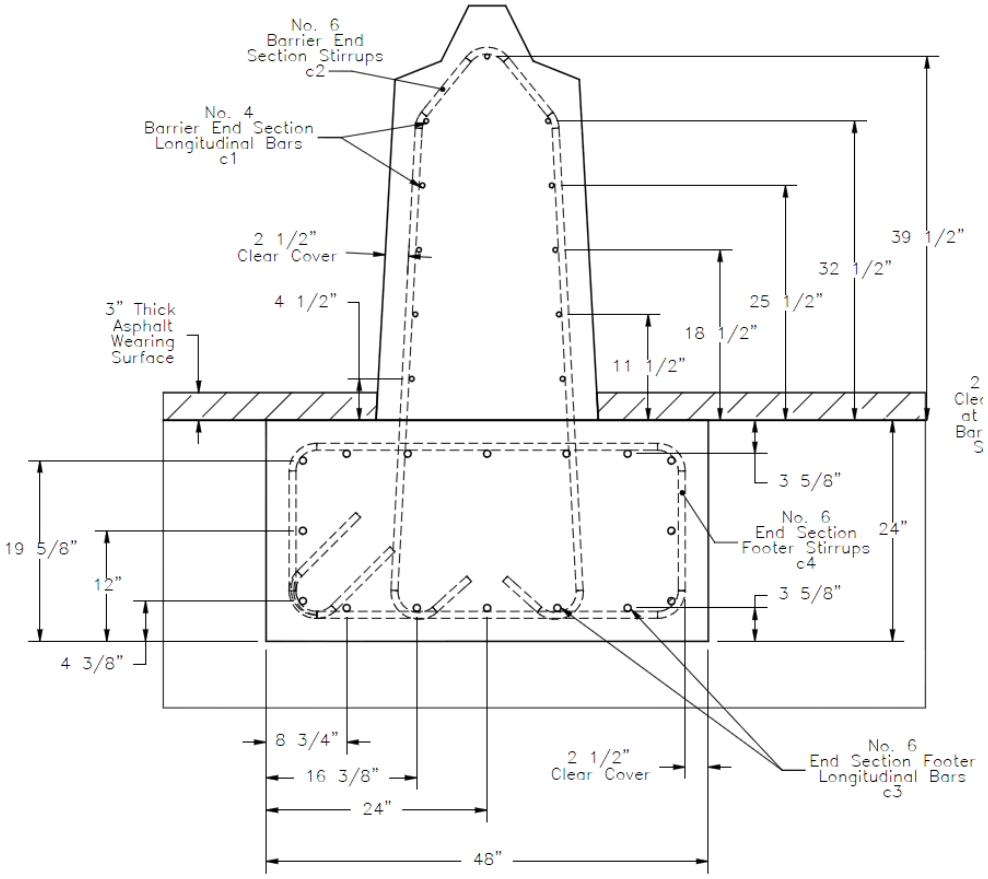

Figure 2.5 TL-5 Concrete Median Barrier with Head Ejection [12]

In addition to the barrier design, a head slap envelope was also developed during this project. Head slap is when the head of a passenger exits the vehicle, typically through the window, and makes contact with the barrier. The head slap envelope was developed by using high-speed video footage of crash tests to determine the location of the head at maximum ejection outside of an impacting vehicle's window. From this data, it was determined how far a barrier would need to be offset from the main vertical face at different heights from ground level, as shown in figure 2.6.

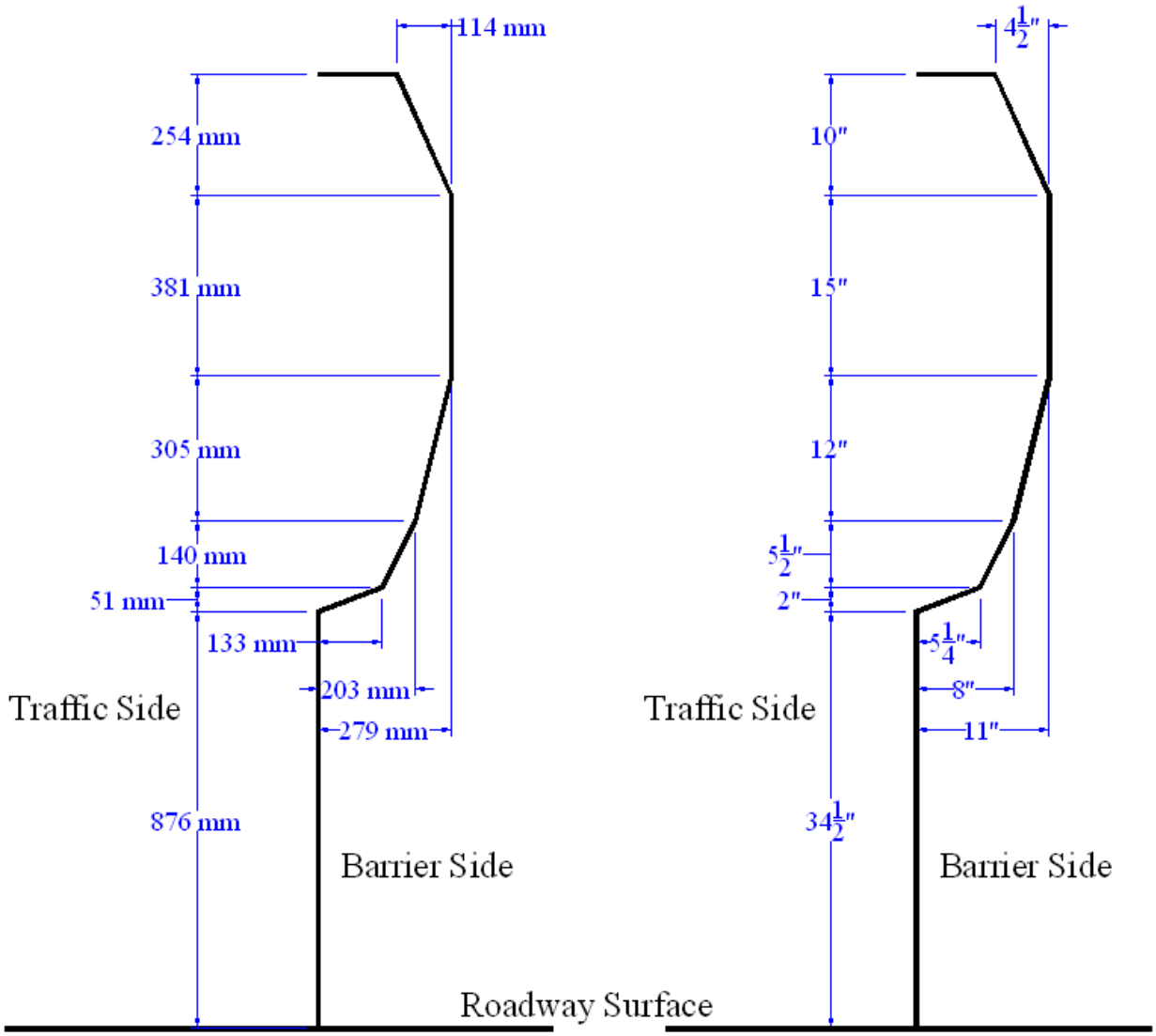

Figure 2.6 Head Ejection Envelope [12]

2.3.5 TL-5 TxDOT T224 Bridge Rail

Tested by TTI in 2015, the Texas DOT T224 Bridge Rail [13] is an Open Concrete Rail (OCR) that successfully redirected a 79,366-lb tractor-van trailer. The tractor-van trailer impacted the bridge rail at a speed of 50.5 mph, an angle of 14.1 degrees from the barrier face, and a location 2.0 feet downstream from the barrier joint.

The bridge rail consisted of a concrete curb, reinforced concrete posts, and a reinforced concrete beam mounted on top, as seen in figure 2.7. The curb was 9 in. tall by 16½ in. wide with two no. 5 bars running the length of the curb, and a U-shaped bar connecting the curb to the deck below.

The posts mounted on top of the curb were 60 in. wide, 15 in. thick, and 12 in. tall. Each post had sloping edges on both the upstream and downstream front corners, as seen in figure 2.8. This was used to prevent snagging of smaller vehicles during impacts. The posts were reinforced with six no. 5 bars in the front and two rows of five no. 5 bars (ten total) in the back face.

Mounted on top of the posts was a reinforced concrete beam measuring 21 in. tall and 16½ in. thick. The rail reinforcement consisted of no. 5 stirrup bars at 6-in. centers with ten no. 6 bars (five in each face) inside the stirrup. All bars that were in the posts extend into the rail and down into the curb.

The deck on which the barrier was mounted was 8½ in. thick with an overhang of 40 in. The deck was reinforced with no. 4 longitudinal bars spaced at 9-in. centers, no. 5 bars at 18-in. centers in the lower transverse mat, and no. 5 bars at 4½-in. centers in the upper transverse reinforcement mat.

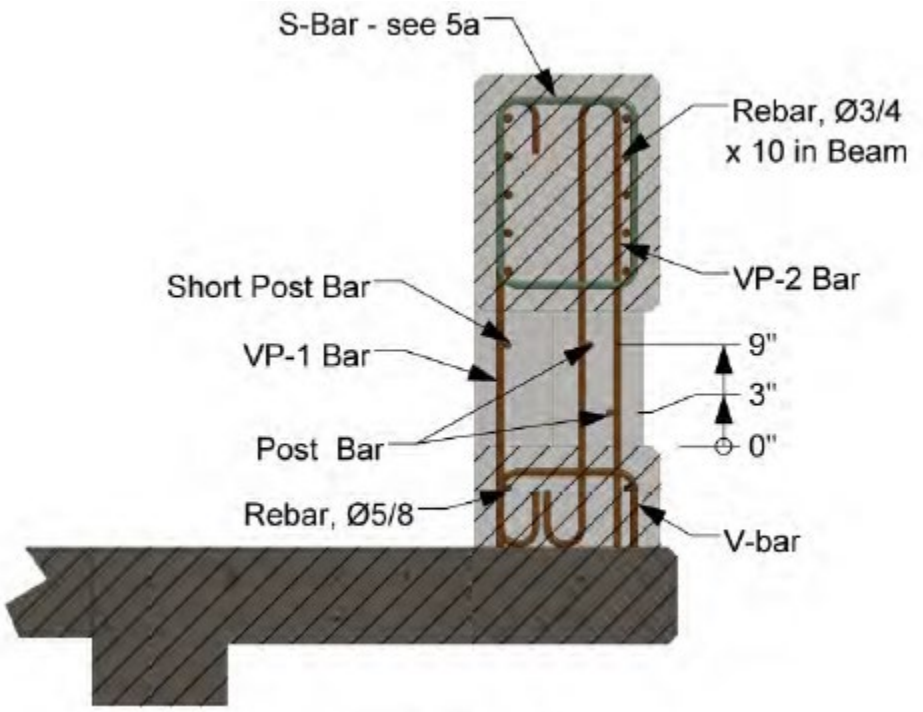

Figure 2.7 TL-5 TxDOT T224 Bridge Rail Reinforcement [13]

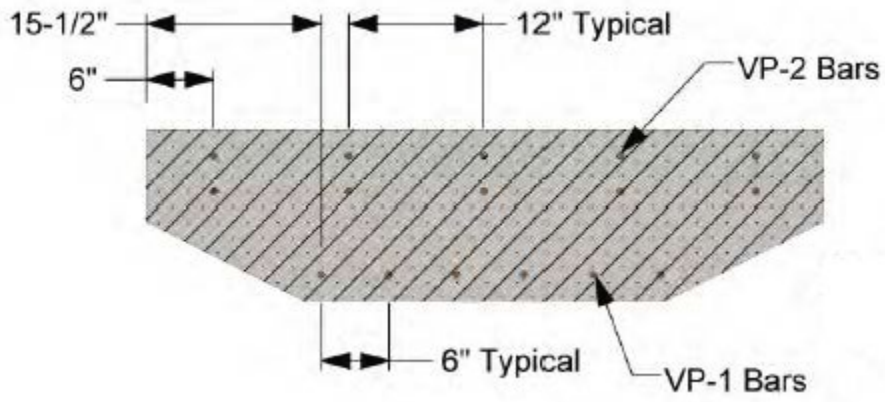

Figure 2.8 TL-5 TxDOT T224 Post Cross-Section [13]

2.3.6 NDOR's TL-5 Aesthetic Open Concrete Bridge Rail

The Nebraska Department of Roads (NDOR) TL-5 Aesthetic Open Concrete Bridge Rail [14], as seen in figure 2.9, was developed by MwRSF in 2005 and then successfully tested with a 78,975-lb tractor-van trailer. The tractor-can trailer impacted the bridge rail at 49.4 mph and 16.3

degrees. The impact location was midspan between post nos. 3 and 4. The rail was a 42-in. tall open concrete rail. The posts were 12 in. tall and 12 in. wide. Each post had three sets of two no. 4 stirrups around eight no. 6 vertical bars in the front and six no. 6 vertical bars in the back, as seen in figure 2.10. The rail was 14 in. thick and 30 in. tall. As seen in figure 2.11, the rail had slight variations in rail width for aesthetics. The rail had two no. 4 stirrups at 6-in. centers along with a U-shaped bar in the top of the rail every 12 in. The longitudinal reinforcement in the beam consisted of ten no. 6 bars, five in the traffic side and five in the field side. The rail was mounted on an 8-in. thick, 52-in. overhang bridge deck.

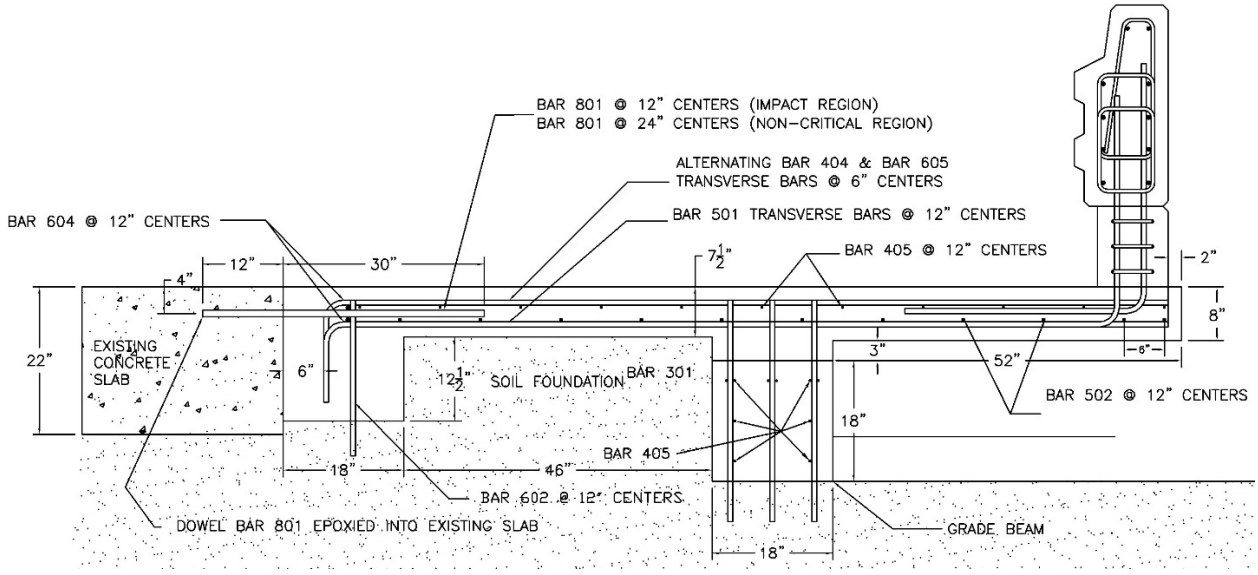

Figure 2.9 TL-5 NDOR Aesthetic OCR Test Configuration [14]

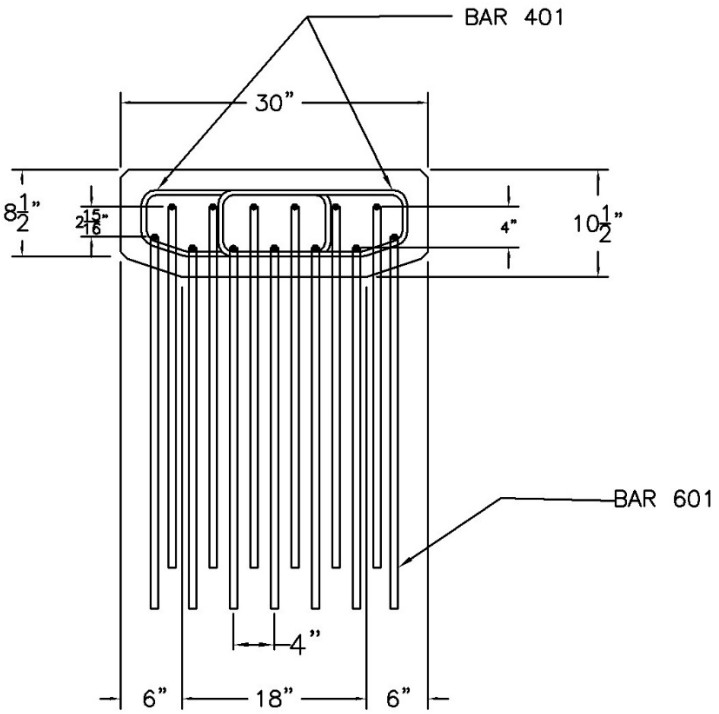

Figure 2.10 TL-5 NDOR Aesthetic OCR Post Reinforcement and Dimensions [14]

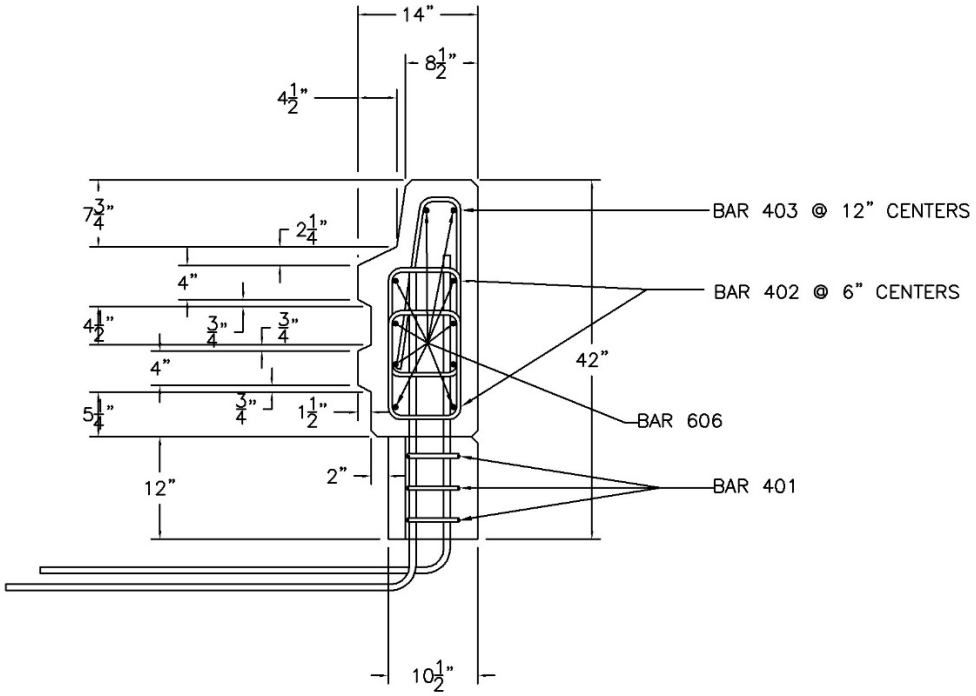

Figure 2.11 TL-5 NDOR Aesthetic OCR Reinforcement and Dimensions [14]

2.3.7 TL-5 Concrete Safety Shape with Top Metal

Developed by TTI in 1981, the TL-5 Bridge Rail to Restrain and Redirect 80,000-lb Trucks was a modified C202 open reinforced concrete post and rail system with a type C4 steel rail mounted on top [15], as shown in figure 2.12. The system was successfully tested with a 1978 Auto Car tractor-van trailer ballasted to 79,770 lb impacting the barrier at 49.1 mph, 15 degrees from the barrier face, and between post nos. 3 and 4.

The posts of the system were 13 in. high x 60 in. long x 7 in. thick. Posts were spaced at 120-in. centers, leaving gaps of 60 in. between posts. The reinforcing in the posts was thirteen vertical no. 4 bars in the traffic side and five no. 4 bars in the field side, and all bars connected down into the bridge deck and up into the concrete rail. The concrete rail was 13 in. thick x 23 in. high with ten no. 8 longitudinal bars and two 0.207-in. wire square spiral stirrups. The metal rail mounted on top was a 6-in. steel tube shaped into an 8-in. x 4⅞-in. ellipse. The steel rail was mounted to the concrete rail via two 1-in. plates at 10¼-in. centers. These posts were connected to a 1-in. plate, which was bolted to the concrete rail with four ¾-in. A325 bolts. The system was mounted on a 7.5-in. thick, 30-in. overhang bridge deck.

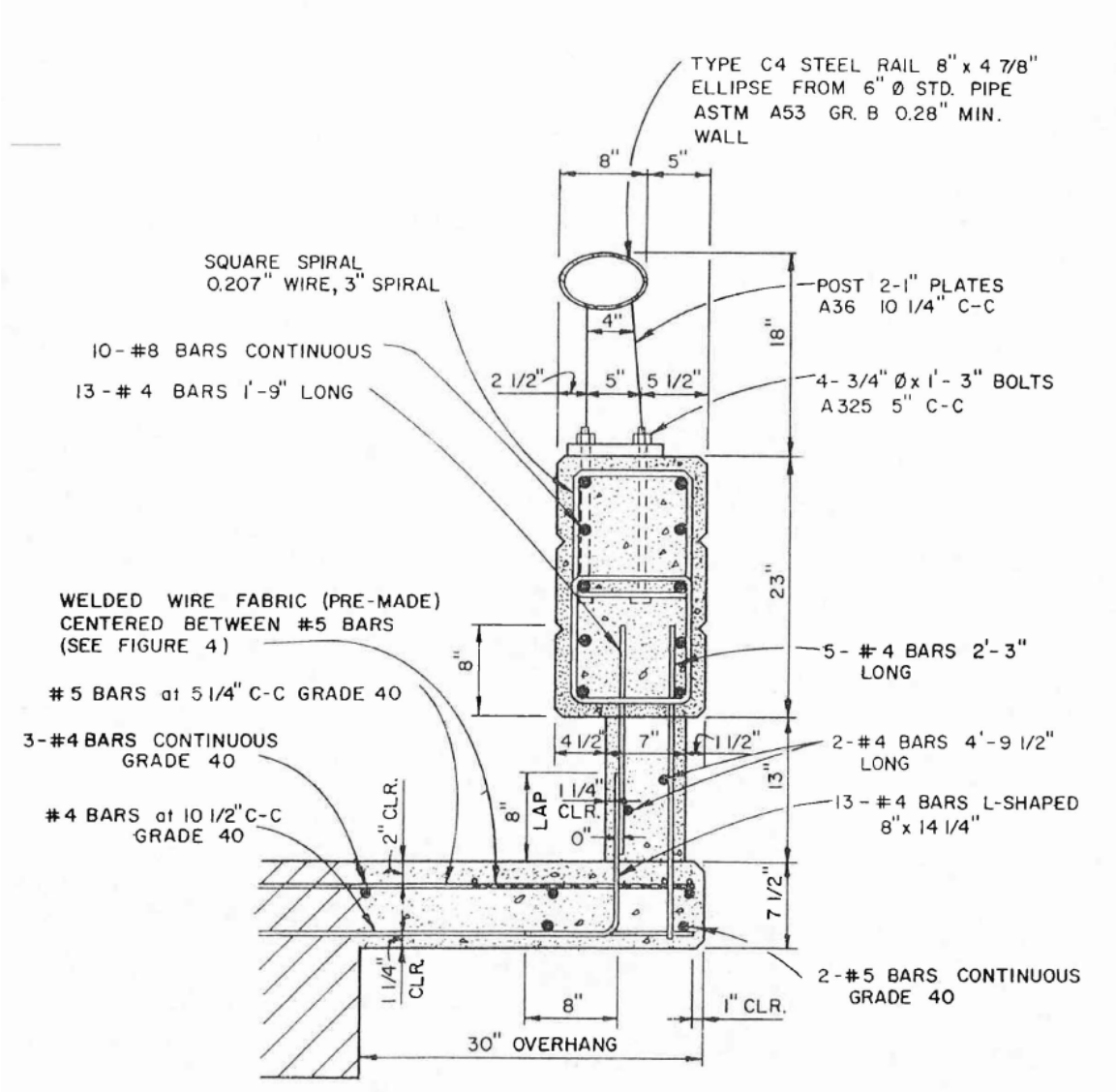

Figure 2.12 TL-5 Modified C202 with Metal Rail [15]

2.3.8 TL-5 1.07-m Vertical Wall Bridge Railing

Tested by TTI for NCHRP Report No. 350 in 1996, this vertical bridge rail safely redirected a 79,366-lb 1983 Freight Liner tractor and 1984 Great Dane van trailer [16]. The tractor-van trailer impacted the bridge rail 17.39 ft from the upstream end at a speed of 49.7 mph and angle of 14.5 degrees.

As shown in figure 2.13, this barrier was 10 in. wide for a height of 33 in. The top 8 in. section of the barrier was 12 in. wide. The reinforcement consisted of no. 5 vertical bars in both the front and back face every 12 in., with an additional no. 5 bar every 12 in. in between the other front face bars. There were ten no. 7 bars longitudinally. The rail was mounted on a 10-in. thick, 39-in. overhang bridge deck.

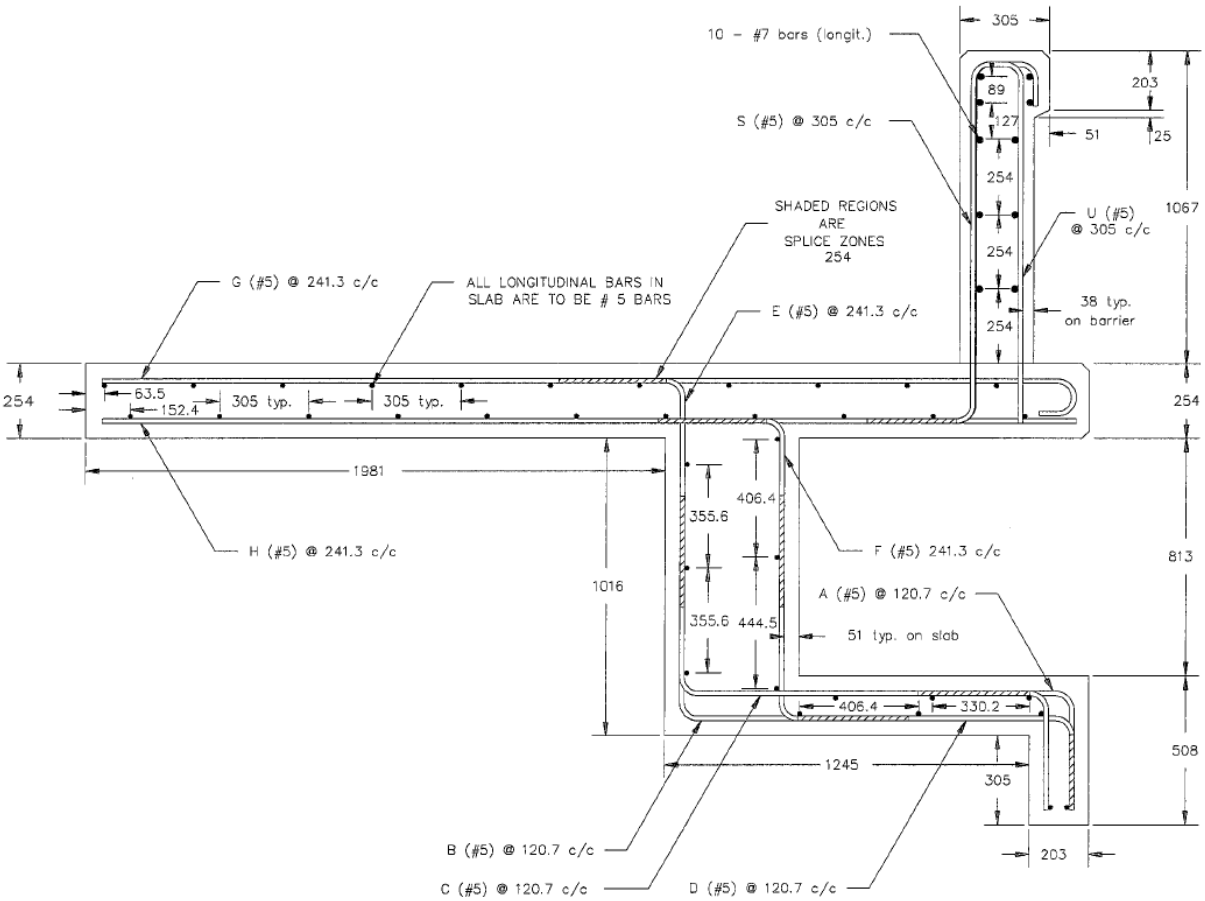

Figure 2.13 TL-5 1.07-m Vertical Wall Bridge Railing [16]

2.3.9 TL-5 Concrete Safety Shape with Top Metal Rail

In 1984, TTI investigated whether it was possible to add a metal rail onto a modified 32-in. high concrete safety shape [17]. An 18-in. tall metal rail was mounted on top of a modified Texas T5 traffic rail, as shown in figure 2.14. The modified T5 barrier was 10½ in. wide at the

top and 20 in. wide at the bottom. Reinforcement in the rail consisted of no. 5 vertical stirrups that extended down into the rail at 8-in. centers, and eight no. 6 longitudinal bars. The metal rail mounted on top was a modified Texas type C4 rail. The rail was connected to the concrete parapet via three 1-in. thick vertical steel plates. The plate groups were spaced at 8-ft 4-in. centers. Those plates were welded to the tube and to a 1-in. thick base plate, which was bolted to the safety shape with four ⅞-in. diameter ASTM-A325 bolts. The whole railing system was mounted on a 10-in. thick, 18-in. overhang bridge deck.

This system was successfully tested when a 1981 Kenworth tractor-van trailer ballasted to 80,080 lb impacted the barrier at 48.4 mph, and angle of 14.5 degrees, and at a location 26 in. downstream from post no. 5.

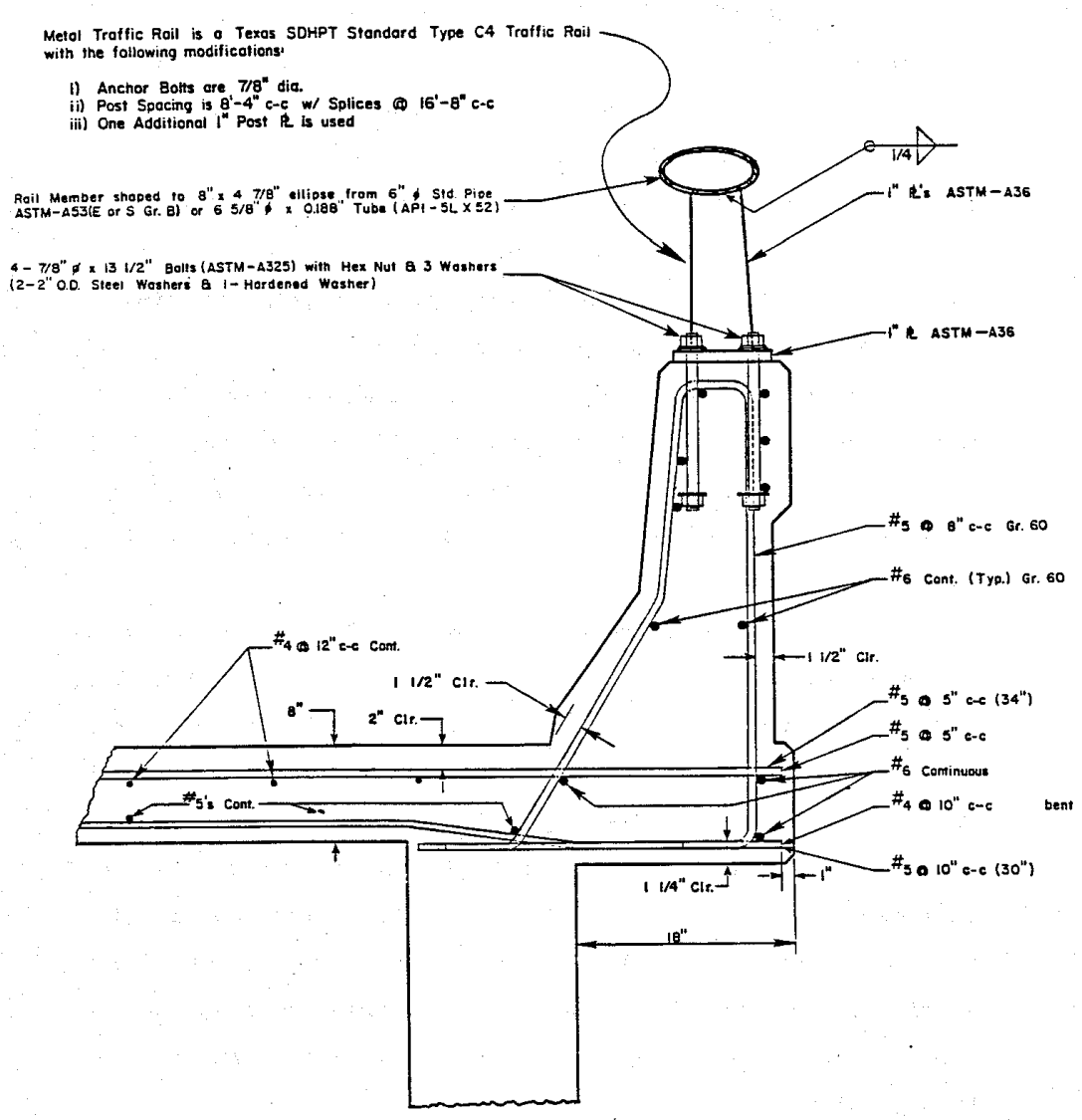

Figure 2.14 TL-5 Concrete Safety Shape with Metal Rail on Top [17]

2.3.10 TL-5 Ontario Tall Wall

Tested in 1990 by TTI, the Ontario Tall Wall [18], as shown in figure 2.15, is an unreinforced concrete median F-Shaped barrier. The safety shaped barrier was 11.4 in. wide at the top, 31.5 in. wide at the bottom, and 41.3 in. tall. The compressive strength of the concrete used in the barrier was 5,100 psi. It was successfully tested with a 1980 International Model No. F2574 tractor and 1973 Trailmobile Model A11A-1SAV trailer ballasted to 80,000 lb. The

tractor-van trailer impacted the barrier at a speed of 49.6 mph, and angle of 15.1 degrees, and a location of 87 feet from the upstream end of the system.

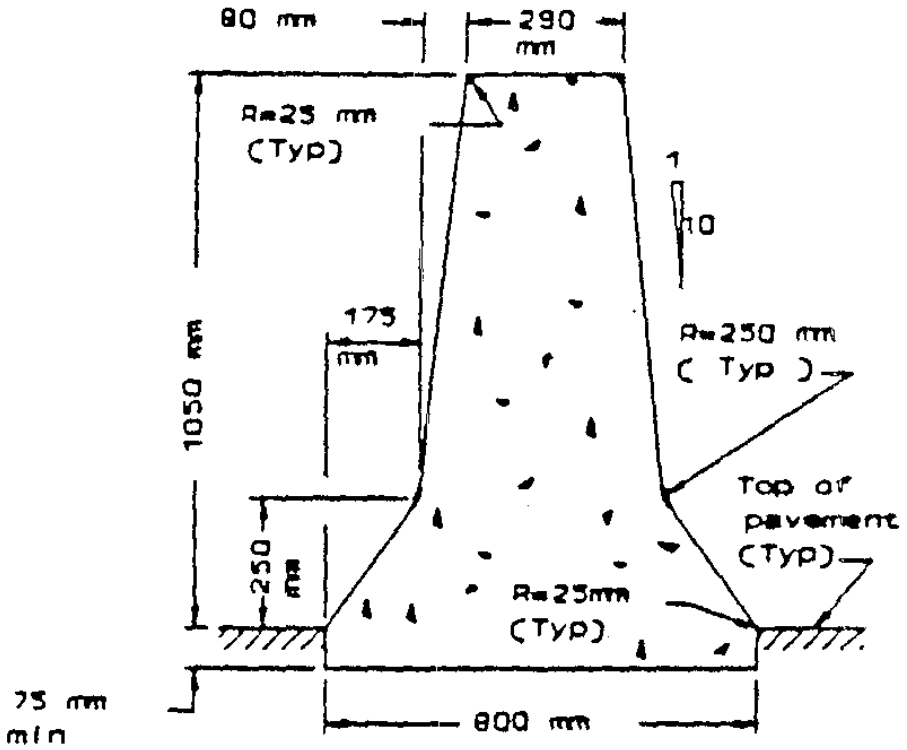

Figure 2.15 Ontario Tall Wall Dimensions [18]

2.3.11 TL-5 Ryerson/Pultrall GFRP-Reinforced Parapet

The TL-5 Ryerson/Pultrall Parapet barrier test was performed by TTI in 2012 to determine the crashworthiness of a safety shaped, glass fiber-reinforced parapet called the Ryerson/Pultrall parapet [19], as shown in figure 2.16. The Ryerson/Pultrall parapet was a single faced, safety shape parapet 8.9 in. wide at the top, 18.7 in. wide at the bottom, and 41.3 in. tall. The barrier contained one vertical 15M bar in the front face and one 12M bar in the back face spaced at 11.8-in. centers. Additionally, there was one 15M bar in the smaller bottom face, also spaced at 11.8-in. centers. All three bars extended into the deck below. Longitudinally, the

barrier contained eleven 15M bars, six in the traffic side and five in the field side. All bars, both longitudinally and vertically were V-ROD® HM glass fiber-reinforced bars. The barrier was mounted on a 14.17-in. thick, 39.37-in. bridge deck

The barrier successfully redirected a 1995 White GM TF tractor with a 1996 Great Dane 48-ft trailer, ballasted to 79,650 lb, traveling 49.1 mph, and which impacted the barrier at an angle of 14.6 degrees 36 in. downstream from the control joint.

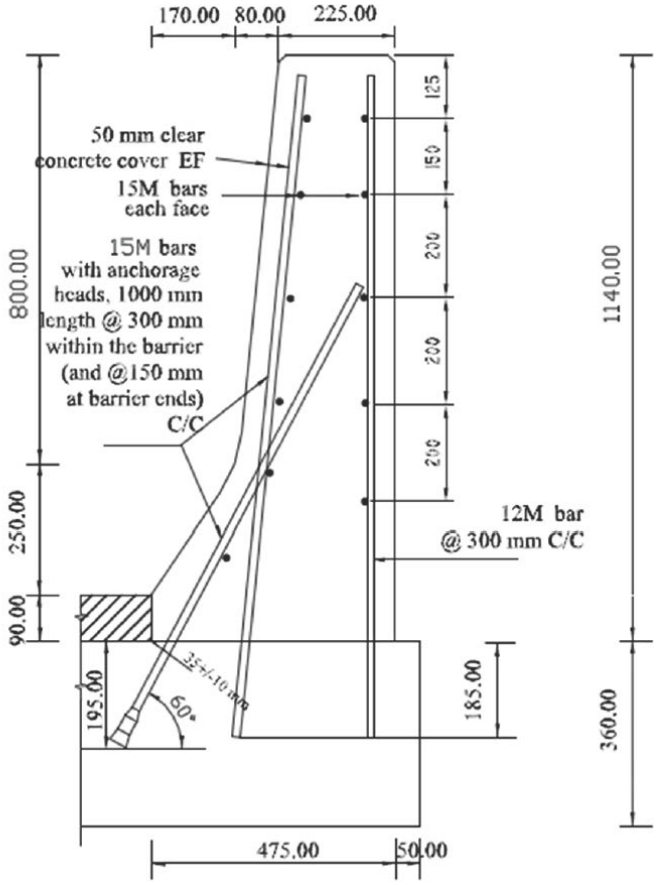

Figure 2.16 TL-5 Ryerson/Pultrall Parapet Cross Section [19]

2.3.12 TL-5 Schöck ComBAR GFRP-Reinforced Parapet

The Schöck ComBAR Parapet [20] was a safety-shaped, concrete barrier with glass fiber-reinforced polymer bars instead of the traditional Grade 60 steel rebar reinforcing. The barrier, as

shown in figure 2.17, was a single faced, safety shape barrier 8.9 in. wide at the top, 18.7 in. wide at the bottom, and 41.3 in. tall. The barrier's reinforcement was one vertical bar in both the front and back face, 0.63 in. and 0.47 in. in diameter, respectively. Additionally, there was one 0.63-in. headed bar along the lower sloped portion of the traffic face connecting the barrier and deck. All vertical bars were spaced at 11.8-in. centers and extended down into the deck. Longitudinally, there were ten 0.63-in. bars, five in the front face and five in the back face. All bars were ComBAR glass fiber-reinforced polymer. The barrier was mounted on a 14.17-in. thick, 39.37-in. overhang bridge deck.

The parapet was successfully tested with a 2000 Freightliner FL112 tractor and 1993 Strick van-trailer weighing 79,220 lb. The impact conditions for this test were a speed of 50.5 mph, an angle of 15.6 degrees, and a location 24.4 in. upstream from the control joint or 33.6 feet from the upstream end of the barrier.

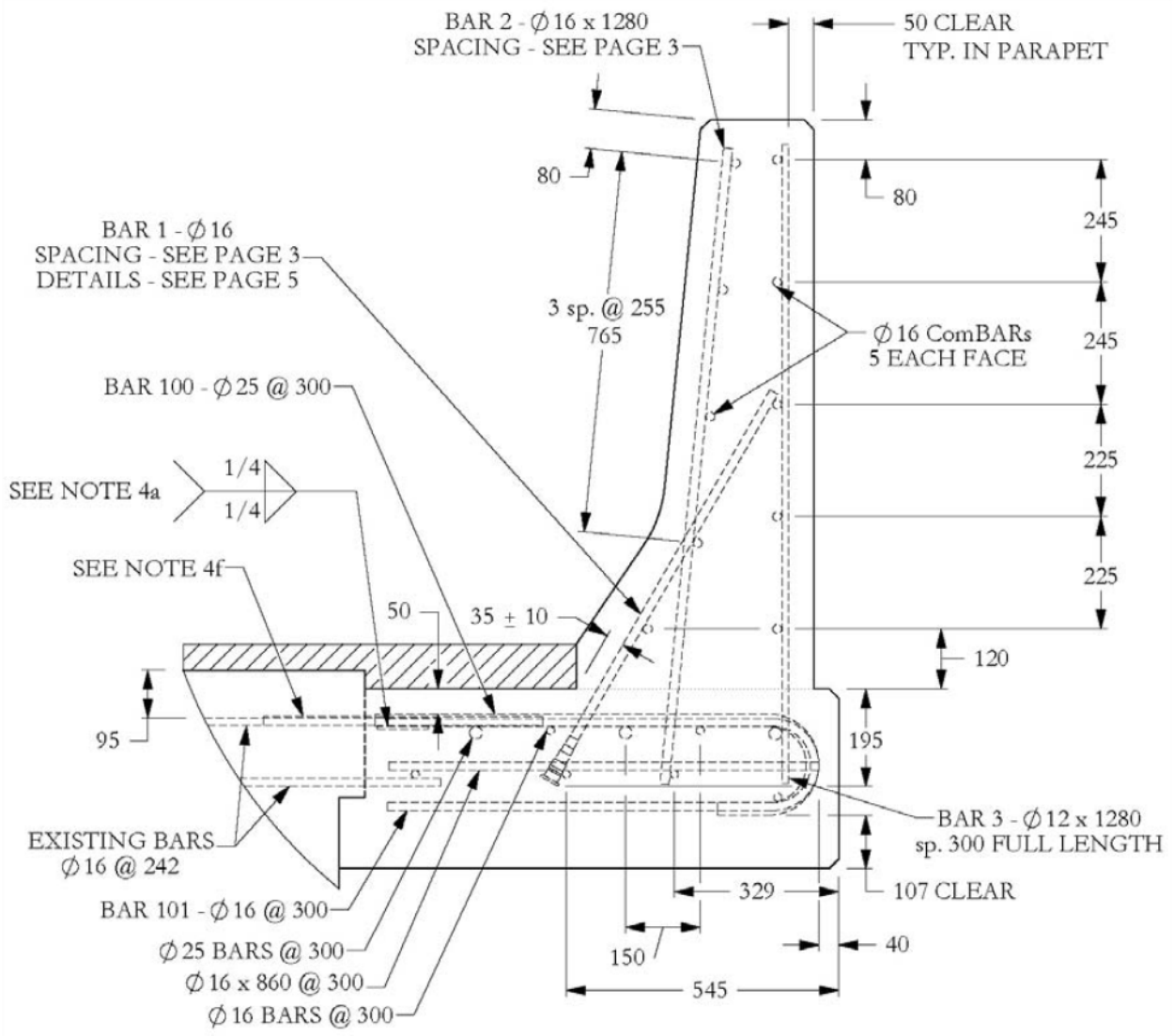

Figure 2.17 TL-5 Schöck Combar Parapet Dimensions and Reinforcement [20]

2.3.13 TL-5 Steel Bridge Rail for Suspension Bridges

Designed specifically for the Verrazano-Narrows Bridge in New York City, the TL-5 Steel Bridge Rail for Suspension Bridges [21], as shown in figure 2.18, was successfully tested using a 2006 International 8600 tractor with a 1997 Stoughton AVW 5357-S-C-AR van-trailer ballasted to 79,620 lb. The tractor-van trailer impacted the steel bridge rail at a speed of 49.9 mph, an angle of 15.1 degrees, and a location 6 in. downstream from the splice between post nos. 4 and 5.

This side-mounted steel bridge rail consisted of 3-ft 6-in. W8x28 steel beam posts at 8-ft 3-in. centers holding four hollow structural section (HSS) tube rail members. The posts were attached to the bridge deck via eight ⅞-in. bolts connecting the rail base plate to the bridge deck side mount.

The top tube was an HSS 5x3x½ mounted 40½ in. from the bridge deck surface. The two middle tubes were HSS 6x6x⅜ mounted 30 and 18 in. above the deck. The bottom element was an HSS 5x3x½ at a height of 7½ in. above the paved bridge deck. The posts were ASTM A572 Grade 50 steel, and the rails were ASTM A500 Grade B steel.

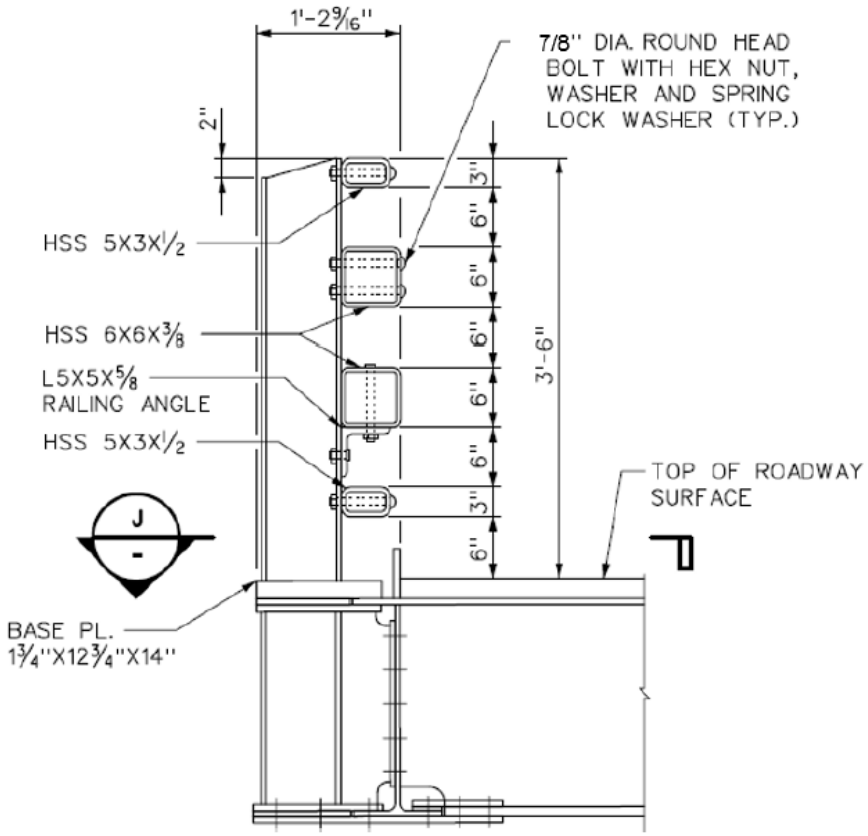

Figure 2.18 TL-5 Steel Rail for Suspension Bridges [21]

2.3.14 TL-5 Instrumented Wall

As previously described in Section 2.3.2 , TTI conducted an instrumented wall test in 1988 [9] with the intention of more accurately determining the loads imparted onto a barrier during various vehicle impacts. Test no. 7046-3 was conducted with a tractor van-trailer. The truck was ballasted to 80,080 lb and impacted the wall at 55.0 mph and 15.3 degrees. The truck sustained extensive damage during impact while the barrier sustained only cosmetic damage.

The most important elements of this test were the values received from the instrumentation on the barrier and the truck. Loads of 66 kips for the initial truck impact, 176 kips for the first tandem axle and front of the trailer, and 220 kips from the rear tandem axle and the box trailer impact were recorded from the load cells in the wall. A graph of the loads obtained from the tractor-van trailer impact into the instrument wall is shown in figure 2.19.

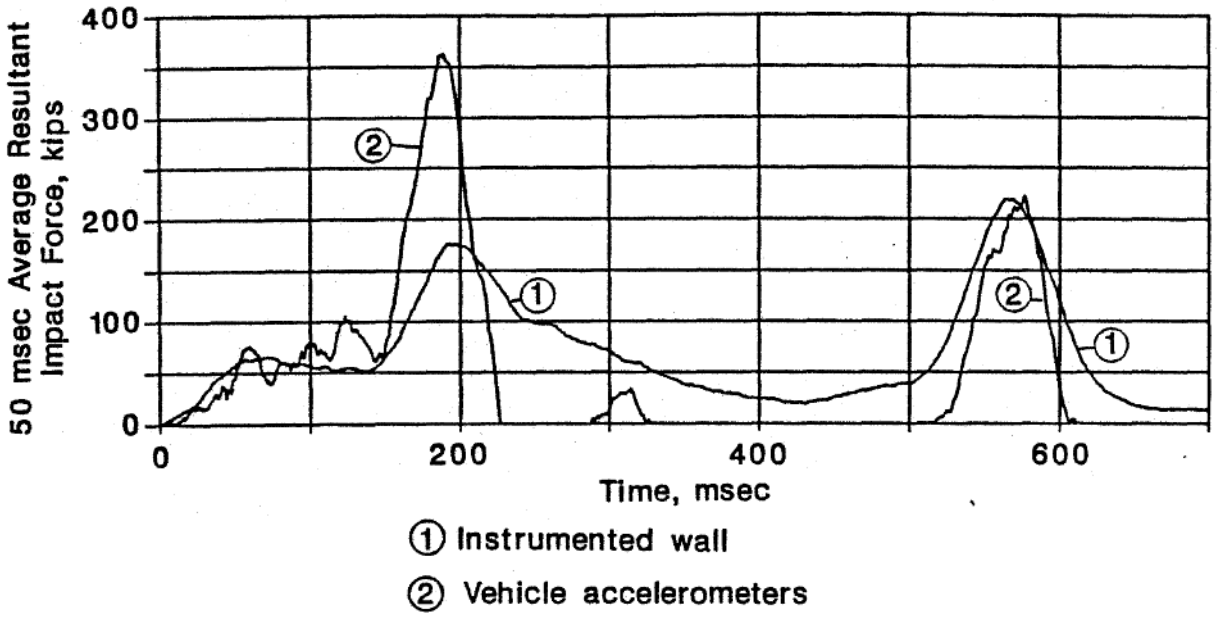

Figure 2.19 Resulting Impact Force for Tractor-Van Trailer Instrumented Wall Impact [9]

2.4 Geometric Considerations

With previous barriers that have met the TL-5 and TL-6 criteria reviewed, the next task of the literature review was to investigate different geometric parameters that contributed to the overall system design.

2.4.1 Investigation of Barrier Heights

According to *AASHTO LRFD Bridge Design Specifications* [22] Section 13.7.3.2, a 90-in. barrier is required for TL-6 applications. The commentary on this section states that the given heights for each test level have been determined through successful crash testing for NCHRP Report No. 350. This 90-in. minimum value stated by AASHTO is based on the only TL-6 barrier to be crash tested, the Roman Wal tested by TTI in 1984.

In TTI's *Analytical Evaluation of Texas Bridge Rails to Contain Buses and Trucks* [23], the researchers stated that to prevent a large tanker truck from rolling over the barrier, a minimum 57-in. high railing would be needed. This conclusion was based on calculations done with the impacting force of the truck located at the vertical center of gravity assumed to be 78 in., and the resisting force and location of the resistive force from the barrier. It is important to note that this report was published before any TL-6 full scale crash testing had occurred. Therefore, this minimum barrier height was never validated against any full scale crash testing.

2.4.2 Head Ejection Criteria

In the study/barrier design conducted by MwRSF in 2007 [12] a head ejection envelope was developed. Head slap is where the head of a passenger exits the vehicle, typically through the window, and makes contact with the barrier. This envelope was developed by using high-speed video footage of crash tests to determine the location of the head at maximum ejection outside of an impacting vehicles window. From this data, it was determined how far a barrier would need to be offset from the main vertical face at different heights from ground level. This

envelope, as shown in figure 2.6, can be used to help prevent the head of a passenger involved in a crash from contacting the barrier, also known as head slap.

2.5 Vehicle Dimensions

To better understand what happens during a tractor tank-trailer impact, it was important to understand the geometry of the vehicle. A field survey was performed to obtain measurements of tractor tank-trailer vehicles. Five tractor tanker-trailer combos and five standalone tank-trailers were measured, as shown in figure 2.20. The survey aimed to obtain the dimensions required by MASH, and additional dimensions that were believed to be pertinent to the project. A vehicle schematic with all dimensions labeled is shown in figure 2.21. The dimensions obtained in the survey are shown in Appendix A .

(a)

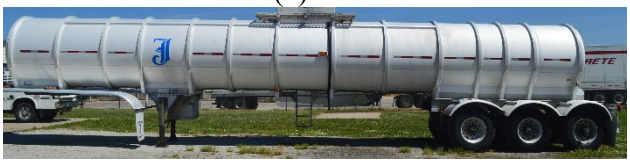

(b)

(c)

(d)

(e)

(f)

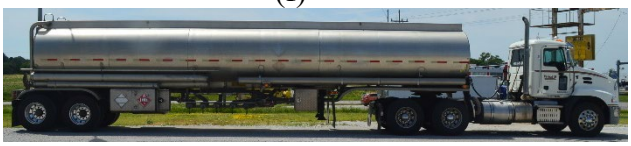

(g)

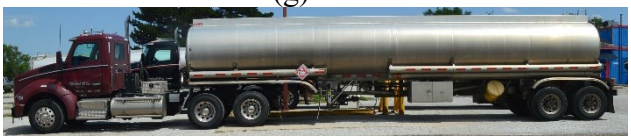

(h)

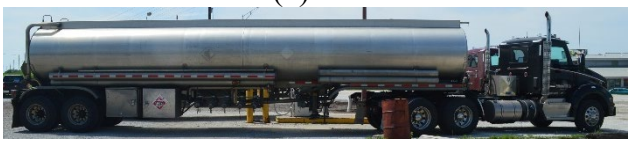

(i)

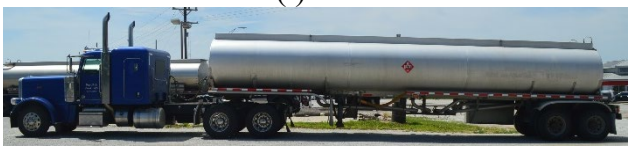

(j)

Figure 2.20 Vehicle Dimension Field Survey Vehicles, Vehicle Letter Referenced in table 2.7

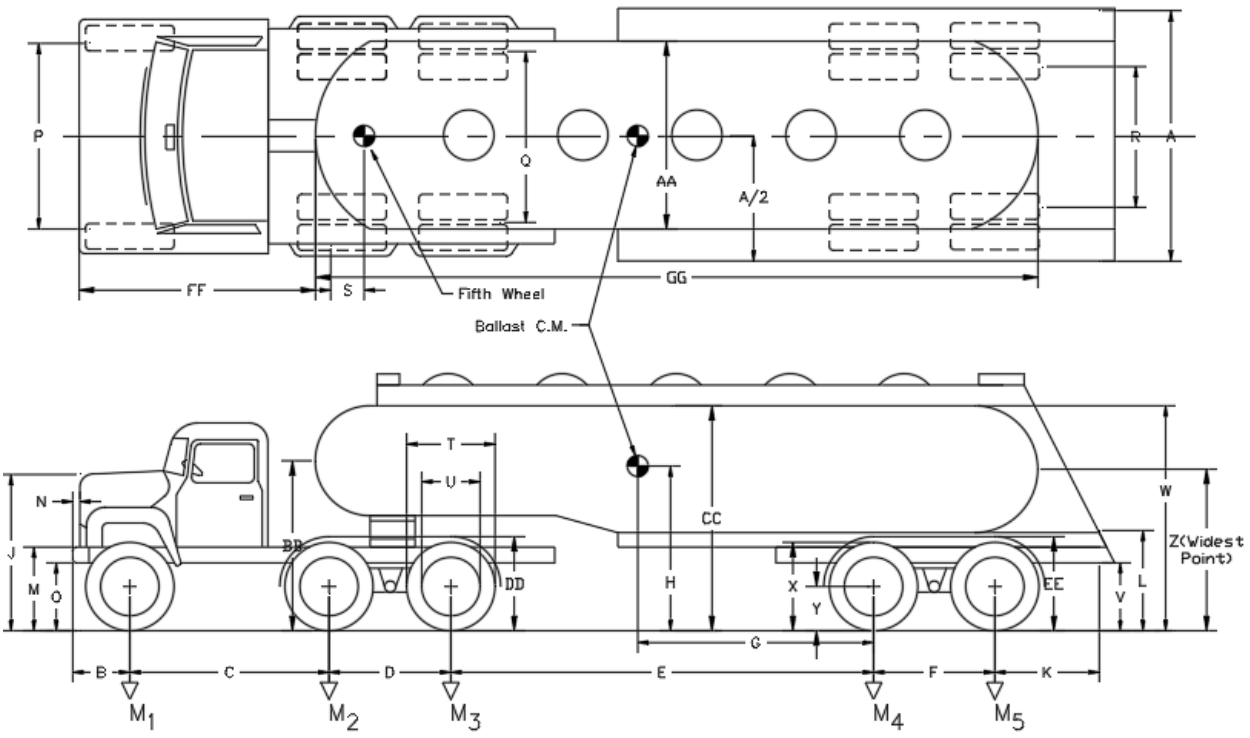

Figure 2.21 Vehicle Dimension Field Survey Schematic

Of the dimensions shown in figure 2.21, a few were seen as crucial to the project. From the dimensions measured, the heights to the widest portions of the vehicle were thought to be most important as they would contact the barrier first. Thus, the height of the wheels (X – tire height, Y – middle of rim height), the height to the widest portion of the tank (Z), the height to the bottom of the tank (L), the height to the middle of the front of the tank (BB), wheel well height (EE), top tank height (CC), and overall tank-trailer length (GG) were considered to be the most important and are summarized in table 2.7.

Table 2.7 Vehicle Dimension Field Survey Summary, Vehicle Letter Referenced in figure 2.20

Vehicle	Tractor			Trailer			Dimensions, in. (mm)							
	Year	Make	Model	Year	Make	Model	L	X	Y	Z	BB	CC	EE	GG
a	Unknown	Kenworth	W900	2016	Walker	N/A	54	38.5	19.5	86	94	120	44	500
							1371.6	977.9	495.3	2184.4	2387.6	3048	1117.6	12700
b	N/A	N/A	N/A	Unknown	Polar	N/A	52	41	20.5	86	90 1/2	120	47 1/2	563
							1320.8	1041.4	520.7	2184.4	2298.7	3048	1206.5	14300.2
c	N/A	N/A	N/A	1971	Butler	N/A	48	40	19	84	87	119	51	467
							1219.2	1016	482.6	2133.6	2209.8	3022.6	1295.4	11861.8
d	Unknown	Mack	CXU16	1998	Walker	N/A	50	39	19.5	84	89	120	48	500
							1270	990.6	495.3	2133.6	2260.6	3048	1219.2	12700
e	N/A	N/A	N/A	1971	Butler	N/A	46	30	19.5	81	88	118	46	464
							1168.4	762	495.3	2057.4	2235.2	2997.2	1168.4	11785.6
f	N/A	N/A	N/A	1969	Butler	N/A	45	39	19	81	81	118	45	440
							1143	990.6	482.6	2057.4	2057.4	2997.2	1143	11176
g	2014	Mack	Pinnacle	1989	Fruehauf	TAG-F2-ESF-9200	55	41	20.5	87	92	118	49	488
							1397	1041.4	520.7	2222.5	2336.8	2997.2	1244.6	12395.2
h	2017	Kenworth	T880	Unknown	LBT	Unknown	55	40	20	86	89.5	117	51	488
							1397	1016	508	2184.4	2273.3	2971.8	1295.4	12395.2
i	2017	Kenworth	T880	1995	LBT	TAG-F2-ESF-9200	55	41	21	88	91	119	52	489
							1397	1041.4	533.4	2235.2	2311.4	3022.6	1320.8	12420.6
j	Unknown	Peterbilt	Unknown	1994	LBT	TAG-F2-ESF-9500	53	40	20	86	93	117	50	486
							1346.2	1016	508	2184.4	2362.2	2971.8	1270	12344.4

N/A = Not Applicable (Tank-Trailer had no tractor)
Trailer model was not able to be determined
Unknown = Information was not available

2.6 Applied Forces and Locations

Due to the lack of TL-6 crash data, the location and magnitude of the loads applied to the barrier from the impacting tractor tank-trailer is not well defined. Two crash tests and two design specifications have provided TL-6 load magnitude and height. A summary of the pertinent loads and application points for the TL- 6 truck is shown in table 2.8.

Table 2.8 TL-6 Loads and Application Heights

Source		TL-6 Barrier Test No. 2911-1	TTI Instrumented Wall 1988	AASHTO 1989 Guide Specifications for Bridge Railings	AASHTO 2012 LRFD Bridge Design Specifications
Reference		[4]	[10]	[24]	[22]
Year		1984	1988	1989	2012
Test Level		TL-6	TL-6	PL-4t	TL-6
Type		Test	Test	Design Guide	Design Guide
Tractor Front	**Transverse Load (kips)**	-	91	200	-
	Longitudinal Load (kips)	-	-	60	-
	Vertical Load (kips)	-	-	18	-
	Height (in.)	-	36	19 thru (23 to 33)	-
Tractor Tandem	**Transverse Load (kips)**	160*	212	200	-
	Longitudinal Load (kips)	-	-	50	-
	Vertical Load (kips)	-	-	18	-
	Height (in.)	-	40.5	51	-
Trailer Tandem	**Transverse Load (kips)**	-	408	200	175
	Longitudinal Load (kips)	-	-	50	58
	Vertical Load (kips)	-	-	18	80
	Height (in.)	-	56	74 min - 84 max	56

- = Undefined or not present in given source
* = Estimated from accelerometers, see Section 2.6.3

2.6.1 Design Specifications

The AASHTO 1989 *Guide Specifications for Bridge Rails* [24] provides the most comprehensive loading matrix. The 1989 Guide Specifications PL-4T loading matrix specifies a 200-kip lateral load at a height from 19 in. to an upper range of 23 to 33 in. for the impact of the tractor. Along with the tractor load, a load is specified for the front of the trailer/tractor tandem axle of 200 kips at 51 in. above ground level. Lastly, a 200-kip load for the rear tandem axle of the tank trailer is to be applied between 74 and 84 in. According to the *Guide Specifications*.

The 2012 *AASHTO LRFD Bridge Design Specifications* [22] provides much detail on loads and locations. In Section A13.2-1, a transverse load of 175-kips applied at the top of the barrier is specified. According to the same section, the minimum height for a TL-6 barrier is 90 in. Therefore, the 2012 *AASHTO LRFD Bridge Design Specifications* recommends a load of 175 kips at 90 in. from the ground's surface.

2.6.2 TTI Instrumented Wall

As previously discussed in Section 2.3.2 , test no. 7046-4 of the 1988 TTI Instrumented Wall involved a 1971 Peterbilt tractor with a 1968 Fruehauf tank-trailer weighing 79,900 lb impacting an instrumented wall at 54.8 mph and an angle of 16 degrees. The maximum load recorded by the wall load cells was 408 kips at a height of 56 in., as shown in figure 2.22, which corresponds to the time when the rear trailer tandem axles impacted the wall.

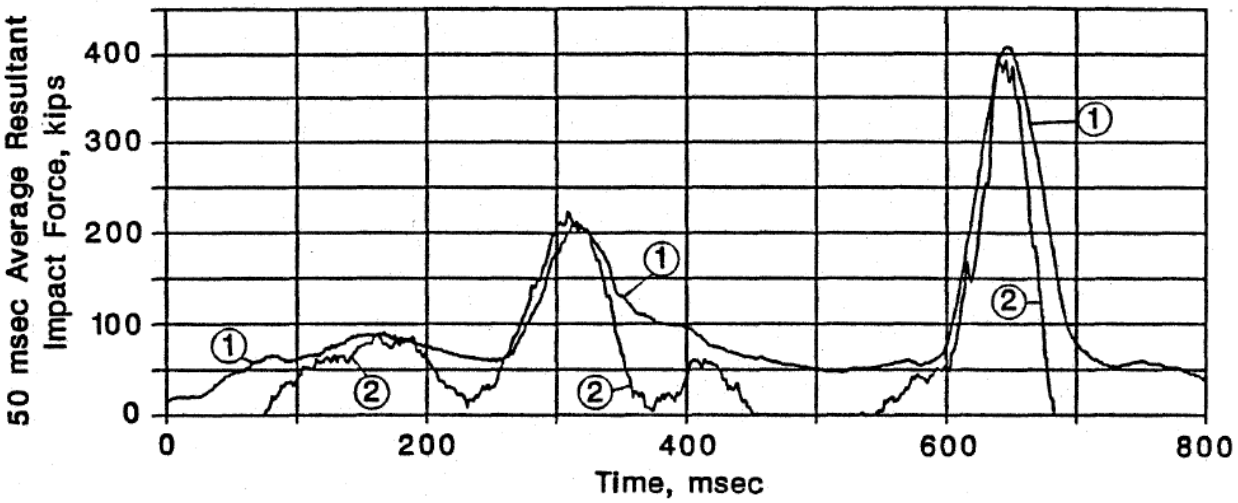

Figure 2.22 TL-6 TTI Instrumented Wall Force vs. Time

2.6.3 TL-6 Barrier Test

As discussed in Section 2.3.1 , in 1984, TTI designed the only crash-test-proven TL-6 barrier [4]. This barrier was tested with a 1980 Kenworth tractor tank-trailer ballasted with water to 80,120 lb. The vehicle was equipped with one rate gyro and one triaxial accelerometer mounted above the tractor tandem wheels. The lateral and longitudinal accelerations from that test were averaged over a rolling 50-msec time period and combined with the vehicle yaw to estimate the force vs. time graph. The averaged data was transformed into orthogonal components with orientations normal and tangent to that of the barrier system using Eqn. 2 & 3:

$$A_N = A_x * sin(\theta) + A_y * cos(\theta) \quad \text{(Eqn. 2)}$$

$$A_T = A_x * cos(\theta) - A_y * sin(\theta) \quad \text{(Eqn. 3)}$$

Where:

A_N = acceleration normal to the barrier
A_T = acceleration tangential to the barrier
A_x = vehicle's local acceleration in the longitudinal direction
A_y = vehicle's local acceleration in the lateral direction

The acceleration was then multiplied by the mass of the vehicle at the location of the accelerometer, i.e., the mass of the tractor and trailer above the tractor tandem wheels.

Using this procedure, the force vs. time graph was calculated, as shown in figure 2.23. A maximum 160-kip force was estimated. In table 2.8, this force was recorded as a tractor tandem force because the acceleration data was obtained at the tractor tandem axle and the weight on the tractor tandem was used in the force calculations. Accelerometers were not located above the other axles, so those forces could not be estimated.

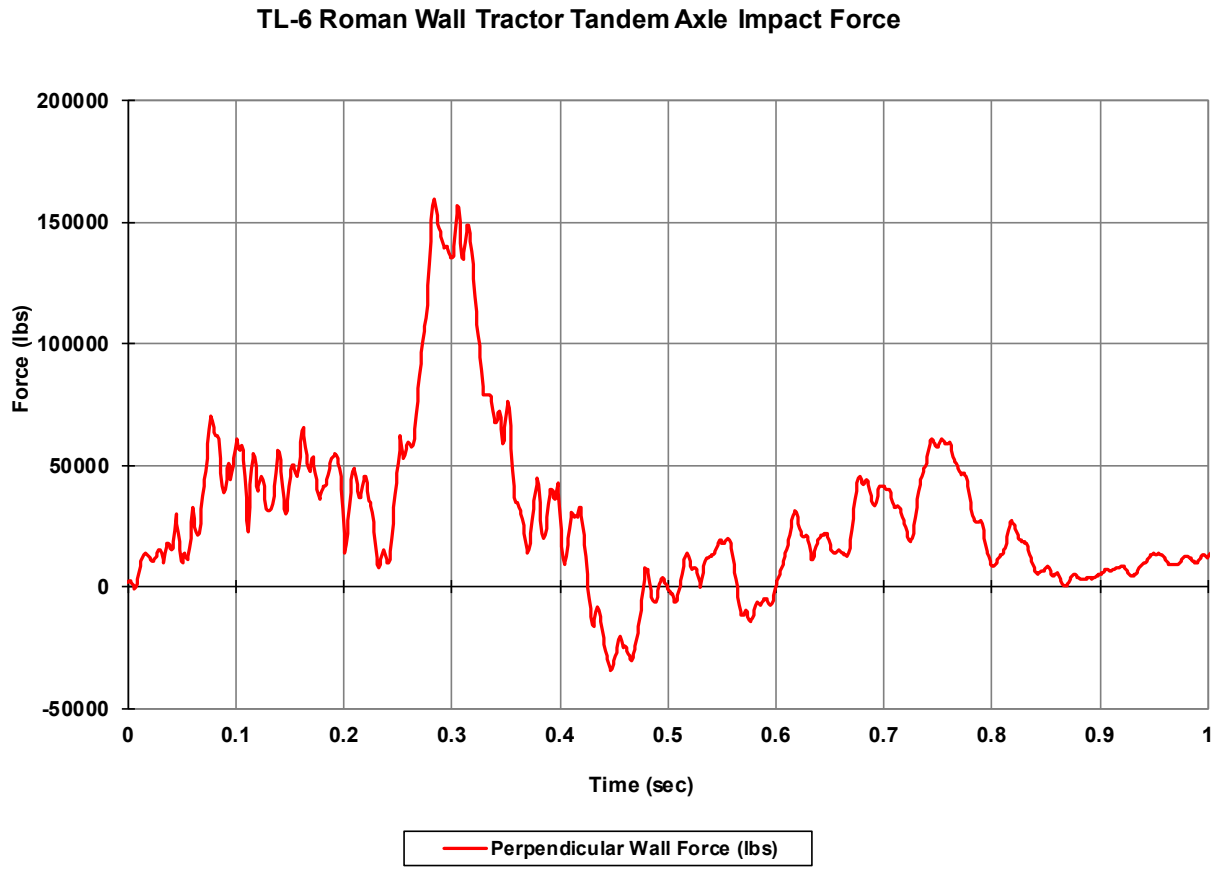

Figure 2.23 TL-6 Roman Wall Tractor Tandem Axle Impact Force vs. Time

2.7 Yield Line Analysis

Developed by TTI in 1984 [23], Yield Line Analysis is a technique for determining the resistive capacity of reinforced concrete parapets and rails. Yield Line Analysis uses the balance of external work onto the system and internal energy absorbed to estimate an overall system

capacity. A schematic of yield line cracks and applied loads [23] is shown in figure 2.24 for a solid interior wall section.

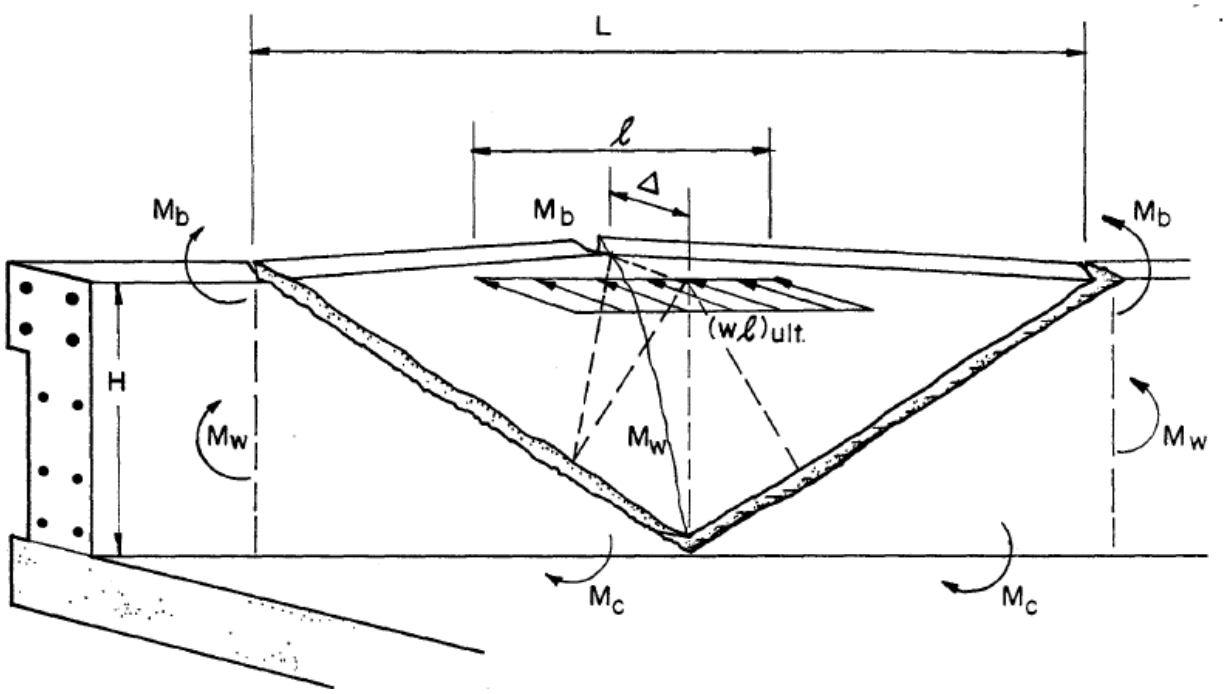

Figure 2.24 Yield Line Schematic [23]

The external work on the system is the impacting force from the vehicle over a certain length on the rail and the corresponding deflection. The internal energy absorbed by the system is a sum of the products of moment capacities of various rail elements and the amount of rotation during an impact event.

2.7.1 External Work

External work (EW) is defined as the total load on any given segment, multiplied by the deflection at the centroid of the load of that segment. A segment of the wall is defined as the section from maximum deflection (Δ) to the nearest point of no deflection, or where the yield line crack is located at the top of the rail. The length of this segment along the barrier line is defined as $^{L}/_{2}$, with the total length of involvement *L* because there is one segment on each side

of the point of maximum deflection in an interior section of the rail. An overhead illustration of these deflections and lengths are shown in figure 2.25 below.

l = Length of loading
L = Length of rail involvement
w = Distributed load magnitude
Δ = Maximum deflection of rail
Δ' = Deflection at midspan of loaded portion of rail segment

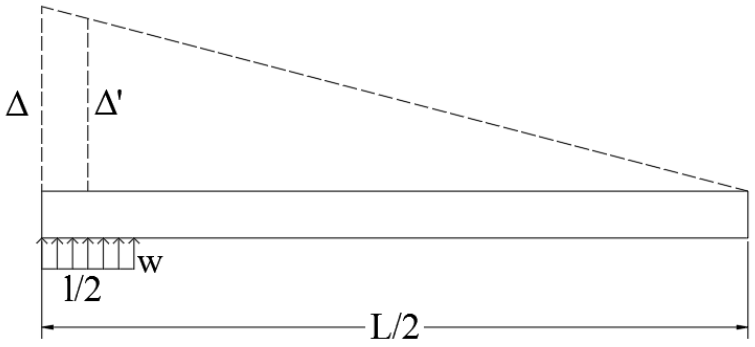

Figure 2.25 External Work on Segment

With a segment defined, the applied load on that segment can be calculated. The load will be centered where maximum deflection occurs, with an applied load on one segment equal to $W = w\left(l/2\right)$, where w is the distributed load and l is the total length of loading. The centroid of the loading will be at a distance of $L' = L/2 - l/4$ from the point of no deflection. Using similar triangles, the deflection at the centroid of loading, Δ', can be determined. The centroid deflection is $\Delta_c = \frac{\Delta(L/2 - l/4)}{L/2}$. Multiplying the total load on the segment by the deflection at the centroid of the segment and by two segments returns Eqn. 4. The external work equation can be further simplified to Eqn. 5.

$$EW = 2 * W * \Delta_c = 2(w)\left(l/2\right)(\Delta)\left(\frac{L/2 - l/4}{L/2}\right) \quad \text{(Eqn. 4)}$$

$$EW = (w)(l)(\Delta)\left(\frac{L - l/2}{L}\right) \quad \text{(Eqn. 5)}$$

2.7.2 Internal Energy Absorbed

The internal energy (IE) absorbed by the system is defined as the moment capacity of a given element multiplied by the displacement of that segment. In the case of a moment, the corresponding displacement will be a rotation. An overhead schematic of the applicable moments, lengths, and displacements is shown in figure 2.26. M_b can be defined as the moment capacity of a beam element. A beam element is any element that has different dimensions or material properties than the main wall, and is mounted above the main wall. M_w can be defined as the moment capacity of the main wall portion. This capacity should be calculated using the full height of the main wall.

M_b = Moment capacity of a beam element
M_w = Moment capacity of the main wall
θ1, θ2 = Angle of rotation of rail
L = Length of rail involvement
Δ = Maximum deflection of rail

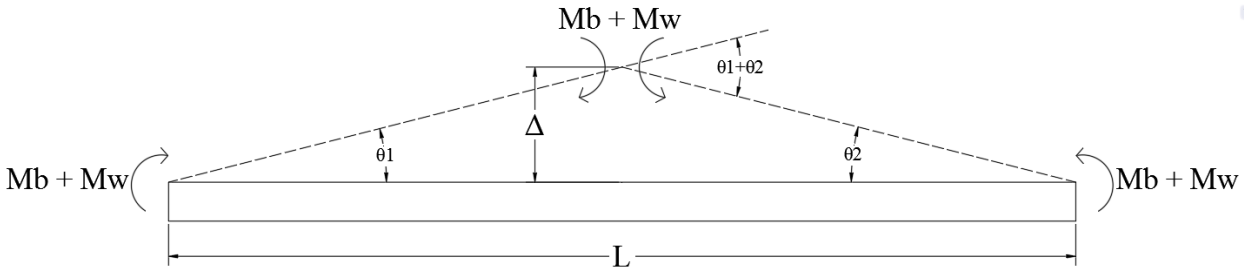

Figure 2.26 Internal Energy Absorbed by System (1)

The rotations θ_1 and θ_2 can be simplified using the small angle theorem. For a small deflection Δ relative to the overall length L, $\theta_1 = \theta_2 = tan\left(\frac{\Delta}{L/2}\right) = \left(\frac{\Delta}{L/2}\right) = \frac{2\Delta}{L}$. Combining the resistive moments with their respective rotational displacement yields the following internal work equation, as shown in Eqn. 6 through 9.

$$IE_1 = M_b\theta_1 + M_w\theta_1 + M_b\theta_2 + M_w\theta_2 + M_b(\theta_1 + \theta_2) + M_w(\theta_1 + \theta_2) \quad \text{(Eqn. 6)}$$

$$= 2M_b(\theta_1 + \theta_2) + 2M_w(\theta_1 + \theta_2) \quad \text{(Eqn. 7)}$$

$$= 2M_b\left(\frac{4\Delta}{L}\right) + 2M_w\left(\frac{4\Delta}{L}\right) \quad \text{(Eqn. 8)}$$

$$IE_1 = \frac{8M_b\Delta}{L} + \frac{8M_w\Delta}{L} \quad \text{(Eqn. 9)}$$

With the resistive moments about the vertical axis calculated, the resistive moments and rotational deflections about the horizontal longitudinal axis can be determined. An illustration of those moments is shown in figure 2.27 below.

M_c = Cantilever moment capacity of the main wall
Δ = Maximum deflection of the rail
H = Height of the rail
θ = Angle of rotation of rail

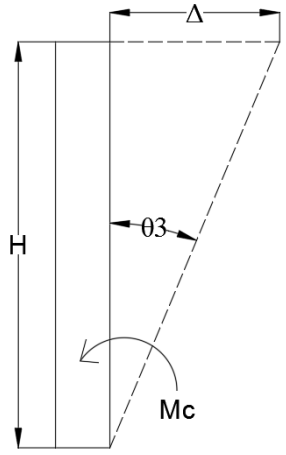

Figure 2.27 Internal Energy Absorbed by System (2)

The rotation θ_3 can be simplified like previous rotations to be $\theta_3 = \frac{\Delta}{H}$, where Δ is again the maximum horizontal displacement and H is the height of the rail. Taking the product of the rotational displacement and the resistive moment gives the internal energy equation Eqn. 10. The rotation, θ, can then be substituted in Eqn. 10 to produce Eqn. 11:

$$IE_2 = M_c L \theta_3 \quad \text{(Eqn. 10)}$$

$$IE_2 = M_c L \frac{\Delta}{H} \quad \text{(Eqn. 11)}$$

Depending on the geometry of the wall, the weakest section is typically at the base of the wall, but in some scenarios, a different section of the wall may be used. M_c has a unit of moment per unit length and is multiplied by the length of involvement L. The overall internal energy is found by Eqn. 12 and then expanded to Eqn. 13:

$$IE = IE_1 + IE_2 \quad \text{(Eqn. 12)}$$

$$IE = \frac{8M_b\Delta}{L} + \frac{8M_w\Delta}{L} + \frac{M_c L\Delta}{H} \quad \text{(Eqn. 13)}$$

2.7.3 Equation Derivation

Since Yield Line Analysis is a work-energy balance, the external energy applied to the system is equal to the internal energy absorbed by the system, as shown in Eqn. 14, which can be rearranged to produce Eqn. 15.

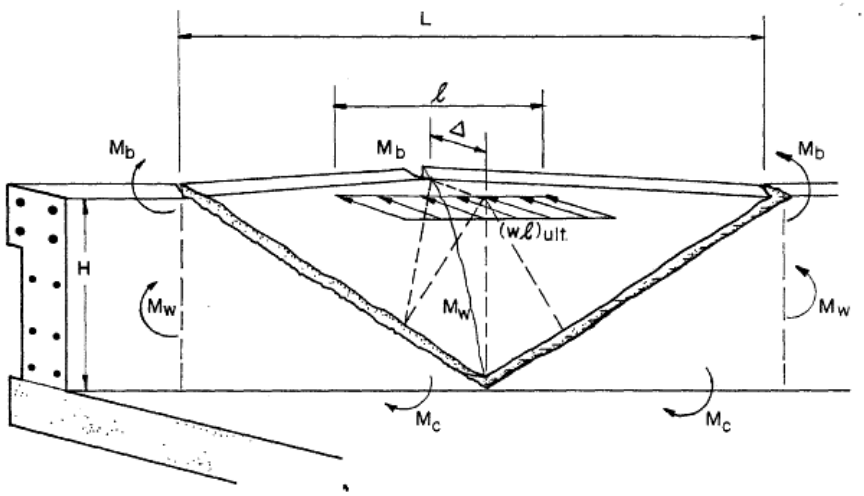

Figure 2.28 Yield Line Failure Diagram [9]

$$wl\Delta\left(\frac{L-{}^{l}/_{2}}{L}\right)=\frac{8M_b\Delta}{L}+\frac{8M_w\Delta}{L}+\frac{M_cL\Delta}{H} \quad \text{(Eqn. 14)}$$

$$wl=\frac{\left(\frac{8M_b}{L}\right)+\left(\frac{8M_w}{L}\right)+\left(\frac{M_cL}{H}\right)}{\left(\frac{L-{}^{l}/_{2}}{L}\right)} \quad \text{(Eqn. 15)}$$

The moment capacities of the beam (M_b), wall (M_w), and cantilever (M_c) can be determined through basic reinforced concrete design equations. The length over which the load is distributed (l) is given in the *AASHTO LRFD Bridge Design Specification* Chapter 13 [22], and load application height (H) is to be assumed by the designer based on the design problem. The length of involvement (L) is unknown. To determine L, take the derivative of wl can be found with respect to L, i.e., $\frac{d(wl)}{dL}$, and set equal to 0, as shown in Eqn. 16. Eqn. 16 can then be simplified in Eqn. 17 through 20.

$$\frac{d(wl)}{dL}=\frac{-8M_b}{\left(L-{}^{l}/_{2}\right)^2}+\frac{-8M_w}{\left(L-{}^{l}/_{2}\right)^2}+\frac{2LM_cH\left(L-{}^{l}/_{2}-HM_cL^2\right)}{H^2\left(L-{}^{l}/_{2}\right)^2}=0 \quad \text{(Eqn. 16)}$$

$$\frac{d(wl)}{dL} = -8M_b - 8M_w + \frac{2LM_c(L-{}^{l}/_{2})}{H} - \frac{M_cL^2}{H} = 0 \quad \text{(Eqn. 17)}$$

$$8M_b + 8M_w = \frac{2LM_c{}^{l}/_{2}}{H} + \frac{M_cL^2}{H} \quad \text{(Eqn. 18)}$$

$$L^2 - 2L\,{}^{l}/_{2} = \frac{8M_bH}{M_c} + \frac{8M_wH}{M_c} \quad \text{(Eqn. 19)}$$

$$L^2 - 2L\,{}^{l}/_{2} - \frac{8H(M_b+M_w)}{M_c} = 0 \quad \text{(Eqn. 20)}$$

The equation is a quadratic equation that can be solved to determine L. The quadratic equation is shown and solved in Eqn. 21 through 23.

$$L = \frac{-2({}^{l}/_{2}) \pm \sqrt{\left(-2\frac{l}{2}\right)^2 - 4(1)\left(\frac{-8H(M_b+M_w)}{M_c}\right)}}{2} \quad \text{(Eqn. 21)}$$

$$L = \frac{l \pm \sqrt{l^2 + \frac{32H(M_b+M_w)}{M_c}}}{2} \quad \text{(Eqn. 22)}$$

$$L = \frac{l}{2} \pm \sqrt{\left(\frac{l}{2}\right)^2 + \frac{8H(M_b+M_w)}{M_c}} \quad \text{(Eqn. 23)}$$

Chapter 3 Existing Tl-6 Barrier Analysis

The TTI TL-6 Roman Wall [4] was analyzed to determine an overall resistive impact capacity. Due to the multiple components of the Roman Wall (i.e., a lower parapet, posts, and an upper rail), no existing capacity estimation method could easily combine all of the components to determine an overall resistive capacity. Thus, multiple different methods were used to estimate the static capacity. It should be noted that none of these methods take into account the dynamic behavior of the material or the dynamic nature of a vehicle impacting the barrier. The true dynamic capacity of the barrier is expected to be greater than the estimated static capacity of the barrier. However, it was difficult to estimate the dynamic capacity due to many unknowns. Thus, the static capacity was estimated. All detailed calculations for the capacity of the Roman Wall are shown in Appendix B .

3.1 Yield Line Analysis

The Yield Line Analysis (YLA) method was performed using the assumption that if the barrier were to experience excessive cracking, the barrier would reach ultimate capacity at one of three cross-sections shown in figure 3.1: (1) the rail post to lower parapet connection, (2) the slope break point of the lower parapet, or (3) the lower parapet to foundation connection. These three sections were chosen because they represented discontinuities in the barrier geometry, which are also critical sections that could fracture.

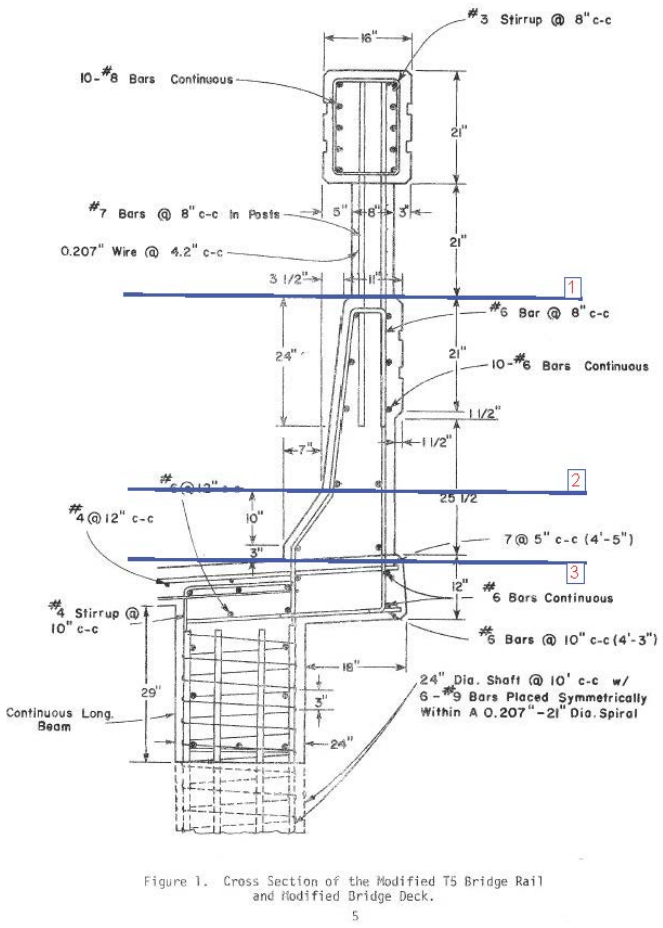

Figure 1. Cross Section of the Modified T5 Bridge Rail and Modified Bridge Deck.

5

Figure 3.1 Yield Line Analysis Three Ultimate Capacity Sections Diagram

3.1.1 Ultimate Capacity Section 1

This ultimate capacity section assumed that the barrier would reach maximum capacity at the connection between the posts and the lower parapet. It was also assumed that the lower parapet was completely rigid. The open rail Yield Line Analysis was used to calculate the capacity for this failure mode. The equation used for this method was:

$$wl\left(\frac{L-l/2}{L}\right)=\frac{8M_b}{L}+\frac{M_c(L-G)}{H} \quad \text{(Eqn. 24)}$$

Where:

w = applied load (kip/ft)
l = length of applied load (ft)
L = length over which failure occurs (ft), calculated by:

$$L=\frac{l}{2}+\sqrt{\left(\frac{l}{2}\right)^2+\frac{8HM_b}{M_c}-\frac{Gl}{2}} \quad \text{(Eqn. 25)}$$

Where:

M_b = beam moment capacity (kip-ft)
M_c = cantilever wall moment capacity (kip-ft)
G = hap between posts (inside to inside) (ft)
H = loaded height of the railing (ft)

The beam moment capacity of this railing was calculated as the moment capacity of the 21-in. tall reinforced concrete rail about the vertical axis. Thus M_b was calculated to be 202.1 kip-ft. The cantilever wall moment capacity was calculated over a 1-ft length of the post. A-2 in. cover was used from the concrete face to the edge of the vertical bars. An area of 0.84 in^2/ft for the front and back reinforcing was used in the calculation. A cantilever wall capacity of 19.33 $\frac{kip-ft}{ft}$ was calculated for M_c. A loading height of 42 in., or 3.5 ft, was chosen, i.e., loaded at the top of railing. A gap of 5 ft and a length of applied loading of 8 ft was used per *AASHTO LRFD Bridge Design Specifications* [22]. *L* was calculated to be 20.99 ft and *wl* was found to be 204.26 kip when loaded at the top of the railing.

3.1.2 Ultimate Capacity Section 2

This ultimate capacity method was assumed to happen at the location where the slope of the lower parapet changes (i.e., a height of 13 in. above the bottom of the barrier). To calculate the capacity of this ultimate capacity section it was assumed that the lower parapet portion would contribute a cantilever moment capacity (M_c) about the longitudinal barrier axis, and a wall

moment capacity (M_w) about the vertical axis over 1 ft of barrier length. The rail of the upper reinforced concrete railing was assumed to contribute only a beam moment capacity (M_b). The posts did not contribute to the capacity due to the Yield Line Analysis method used in these calculations only considering continuous barrier elements. The Yield Line method that considers discontinuous elements (posts) is a separate method that will be utilized in later calculations.

The cantilever moment capacity over a 1-ft length of the lower reinforced concrete parapet was calculated to be $M_c = 30.59 \frac{kip-ft}{ft}$. The wall moment capacity about the vertical axis of the lower parapet was calculated to be $M_w = 82.66$ kip-ft. It was assumed that the average width of the barrier was 12.75 in. The beam moment capacity of the upper reinforced concrete rail was calculated to be $M_b = 202.1$ kip-ft. As in the previous ultimate capacity section; l was 8 ft per *AASHTO LRFD Bridge Design Specifications* [22], and H was 77 in. To calculate L and wl, Eqn. 23 and Eqn. 15 were used respectively. L was calculated to be 26.23 ft, and w was calculated to be 250.1 kips. Thus, the barrier had a total capacity of 250.1 kips when loaded at the top of the upper concrete railing.

3.1.3 Ultimate Capacity Section 3

The third ultimate capacity section was at the base of the lower concrete parapet at the location of the barrier to foundation connection. This calculation was completed similarly to ultimate capacity section 2. The wall moment capacity M_w was calculated using the summation of two wall capacities. The first (upper) section, shown in figure 3.2, had a width of 12.75 in. and a height of 35 in., and was the same section as the parapet section from failure section 2. The second (lower) section, as shown in figure 3.2, had a width of 17.5 in. and a height of 13 in. The upper and lower sections were calculated to have moment capacities of 82.99 kip-ft and 32.02

kip-ft, respectively. The two wall moment capacities were added together to get a total wall moment capacity of M_w = 115.01 kip-ft.

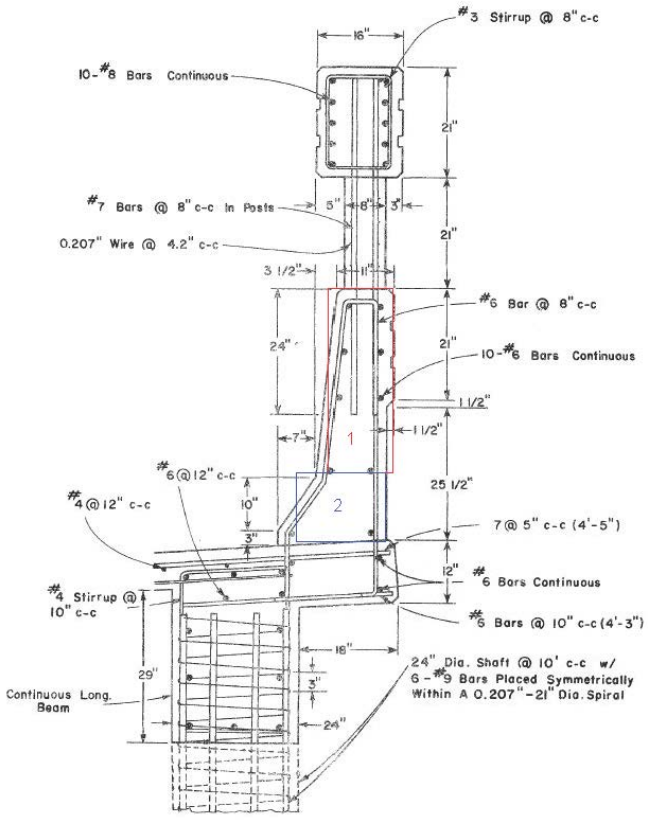

Figure 3.2 Ultimate Capacity Section 3 Mw Sections

The cantilever moment capacity was calculated using the horizontal cross section at the base of the reinforced concrete parapet. This cross section had a width of 12 in. (the cantilever moment capacity is done over a 1 ft length of barrier) and a thickness of 21.5 in. This cross section was reinforced with 0.66 $in.^2$ steel reinforcing per foot on both sides of the section, which resulted in a moment capacity of $M_c = 56.58 \frac{k-ft}{ft}$.

The beam moment capacity was calculated the same way as ultimate capacity sections 1 and 2, and was M_b = 202.1 k-ft. The posts were assumed to provide no structural capacity to this ultimate capacity section for the same reason as in failure section 2. Per *AASHTO LRFD Bridge Design Specifications* [22], l was 8 ft. For this ultimate capacity method, a loading height of 7.5 ft (90 in.) was used, which is equal to the total height of the barrier. To calculate L and wl, Eqn. 23 and Eqn. 15 were used, respectively. L was calculated to be 22.77 ft, and wl was calculated as 343.82 kips. Thus, this ultimate capacity section had a capacity of 343.82 kips when loaded at the top of the upper rail.

In summary the capacity of the 3 sections were calculated to be 204.3 kips, 250.1 kips, and 343.8 kips for the ultimate capacities sections 1, 2 and 3, respectively. The weakest cross section was ultimate capacity section 1, or the connection between the lower parapet and the reinforced concrete posts.

3.2 Sum of Moments

The sum of moments capacity was calculated by determining summing the moments of the wall and the reinforced open concrete rail, utilizing their respective capacities and heights. This method was created to be a simple, easy way to calculate the capacity of a rail that contained two distinct parts. In Section 3.1 , the contribution of the upper open concrete rail was not calculated using Yield Line Analysis for Open Concrete Rails, instead, it was simply considered to be a beam element in the Yield Line Analysis calculations for Reinforced Concrete Parapets. By calculating the capacity of the lower parapet and upper open rail separately and using statics to determine an overall moment capacity, the contribution of the upper rail was thought to be more realistic. The capacity of the reinforced concrete rail was previously determined in Section 3.1.1 to be 204.26 kips.

The ultimate capacity of the lower parapet was calculated using Yield Line Analysis of the concrete parapet [23], as previously discussed in Section 2.7 . The wall moment (M_w) and the cantilever moment capacity (M_c) were previously calculated in Section 3.1.3 to be M_w=115.01 kip-ft and M_c=56.58 kip-ft/ft, respectively. The overall wall capacity was calculated using M_c, M_w, and a loading length of 8 ft to be 367.84 kips via Eqn. 23 and Eqn. 15.

When the geometry of the overall barrier was considered, it was assumed that the parapet would resist a load at its tallest point (48 in.) and the reinforced open concrete rail would also resist load at its tallest point (90 in.). Summing the moments created by each load and its distance from the bottom of the overall rail returns Eqn. 26:

$$\sum M_{bottom} = (204.26k * 90in.) + (367.84k * 48in.) = 36039.72\ k - in. \quad \text{(Eqn. 26)}$$

The overall capacity can be estimated with an assumed load application height. For an assumed load height of 90 in. (top of barrier), the resistive capacity will be 400.44 kips. If a lower load height of 56 in., the location of maximum load according to the TTI Instrumented Wall Test [10], is assumed, the resistive capacity increases to 643.57 kips.

3.3 Combination Method

The combination method was developed by TTI [23]. The combination method utilizes the capacities and heights of individual barrier elements (rail, posts, and parapet) and calculates one overall resistive capacity (R), and the effective height (H), as shown in Eqn. 27 and 28 respectively:

$$R = P_p + P'_R + P'_w \quad \text{(Eqn. 27)}$$

$$H = \frac{P_p h_R + P'_R h_R + P'_w h_w}{R} \quad \text{(Eqn. 28)}$$

Where:

P_p = ultimate capacity of the posts (kip)

P_R' = ultimate capacity of the rail over the total span (kip)
P_w = ultimate capacity of the parapet of the total span (kip)
P_w' = reduced capacity of parapet due to post load being resisted by the parapet $= \frac{P_w h_w - P_p h_R}{h_w}$ (kip)
h_w =lower parapet height (ft)
h_r = upper rail total height (ft)

A schematic representation of the different heights and capacities is shown in figure 3.3.

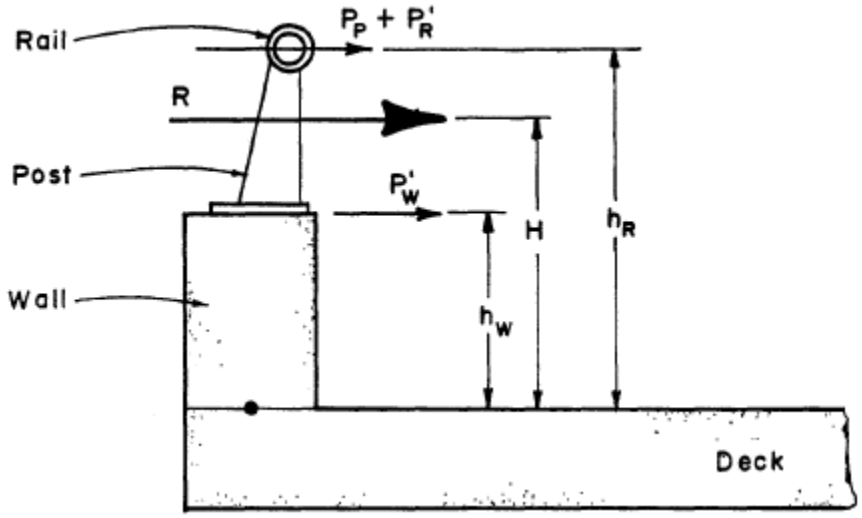

Figure 3.3 Combination Method Heights and Capacities Schematic

3.3.1 Standard Combination

The standard combination method, created by TTI [23] and discussed in Section 3.3 , utilized basic moment capacity calculations of all parts of the system as individuals and did not consider the strength of one part affecting the capacity of connected parts. For this method it was assumed that the ultimate capacity of the rail would be determined over a certain number of spans. The ultimate capacity was defined as the time at which a plastic hinge would form in the rail. This would result in any posts located between the hinges in the rail to also experience plastic hinging. This number of spans was varied from 1 to 8. As the upper rail deformed, the posts would also deform. Once the posts deformed significantly and reached their maximum

moment capacity it was assumed that the posts would be considered failed. Once a post was considered to be failed it would not contribute to the capacity of the rail to which they were attached. The rail was considered fixed at the two ends without any additional loads or bracing in the span from the attached posts. This assumption was made due to the continuity of the rail; even at the point of hinging in the rail it is still connected to the rest of the rail and would act more like a fixed connection than pinned.

The ultimate capacity of a single post was determined based on the lesser of either the ultimate moment capacity about the longitudinal axis or the ultimate shear capacity, with a load applied at the top of the rail. The ultimate moment capacity of a single post about the longitudinal axis was calculated to be 96.67 k-ft. If the load is assumed to be applied at the top of the rail, the moment arm that would result in the largest moment in the post would be the height of the rail (42 in.), which would result in a maximum load of $\frac{96.67\ k-ft}{(3.5\ ft)} = 27.63\ kips$. The ultimate shear capacity of the post was calculated using:

$$\phi V_n = \phi(V_c + V_s) \quad \text{(Eqn.29)}$$

Where:

V_c = shear capacity of the concrete (kip)
V_s = shear capacity of the steel stirrups (kip)

The posts contained no stirrup reinforcing, thus the post shear capacity equation can be simplified to:

$$\phi V_n = \phi(2\lambda\sqrt{f_c'}\, b_w d) \quad \text{(Eqn. 30)}$$

$$\phi V_n = 0.75 * 2 * 1 * \sqrt{3600} * 60 * 8 = 43.2\ kips \quad \text{(Eqn. 31)}$$

The ultimate capacity of a single post is 27.63 kips.

The ultimate capacity of the reinforced concrete rail, not including the posts, was determined based on the length (number of spans) being considered. The maximum allowable moment capacity for the rail was determined to be 202.1 k-ft. From this capacity, the load that would need to be applied to generate this moment inside the beam could be calculated for each different failure length considered. The load was assumed to be distributed over 8 ft. The ultimate capacity of the rail can be seen as P_r in table 3.1.

The ultimate capacity of the lower concrete parapet was calculated previously in Section 3.2 to be 367.84 kips. The reduced parapet capacity was calculated in accordance with Eqn. 28.

Due to the load being an 8-ft distributed load, and one span being 5 ft in length, the capacity of the rail for a length of one span is simply the capacity of the rail over one span plus the capacity of the parapet, because no posts are contained within the span. This capacity and height are calculated as:

$$(R = wl) = \frac{12M_{max}}{l} + 367.84k = \frac{12*202.1\ k-ft}{5\ ft} + 367.84k = 852.58\ kips \quad \text{(Eqn. 32)}$$

$$H = \frac{485.04*90+367.84*48}{852.88} = 71.89\ in. \quad \text{(Eqn. 33)}$$

The capacity for all spans is shown in table 3.1.

Table 3.1 Standard Combination Capacities and Heights

Spans	P_p (kips)	P_r (kips)	P_w' (kips)	R (kips)	H (in.)
1	N/A	485.04	367.84	852.88	71.89
2	27.63	119.05	316.03	462.76	61.32
3	55.26	66.95	264.23	386.44	61.28
4	82.89	47.02	212.42	342.33	63.94
5	110.52	36.32	160.62	307.46	68.06
6	138.15	29.61	108.81	276.56	73.48
7	165.78	25.01	57.00	247.79	80.34
8	193.41	21.64	5.20	220.25	89.01

3.3.2 RISA Combination

The RISA combination method was created to attempt to incorporate the load that would be imparted on the upper rail from a post, even if the post was at plastic moment. The standard combination method calculated the capacity of the rail over a certain length and assumed it to be simply supported with no intermediate supports or reactions. It was thought that this was not an accurate representation of how the upper open concrete rail would perform and that if the posts reached plastic moment or ultimate capacity, they would still provide some resistance and bracing to the rail mounted atop. The RISA combination method utilized the same equations as the standard combination method, with a change to how the ultimate capacity of the rail is calculated. RISA 2D [25] was used to draw the rail from two to six spans, and a 27.63-kip load was placed in a direction opposite of the 8-ft distributed load at every post within the span that was assumed to have reached ultimate capacity. The applied 8-ft distributed load was then increased until the maximum moment in the beam was approximately equal to the maximum allowable moment of the rail, 202.1 k-ft. The RISA models for two through six spans are shown in figure 3.4.

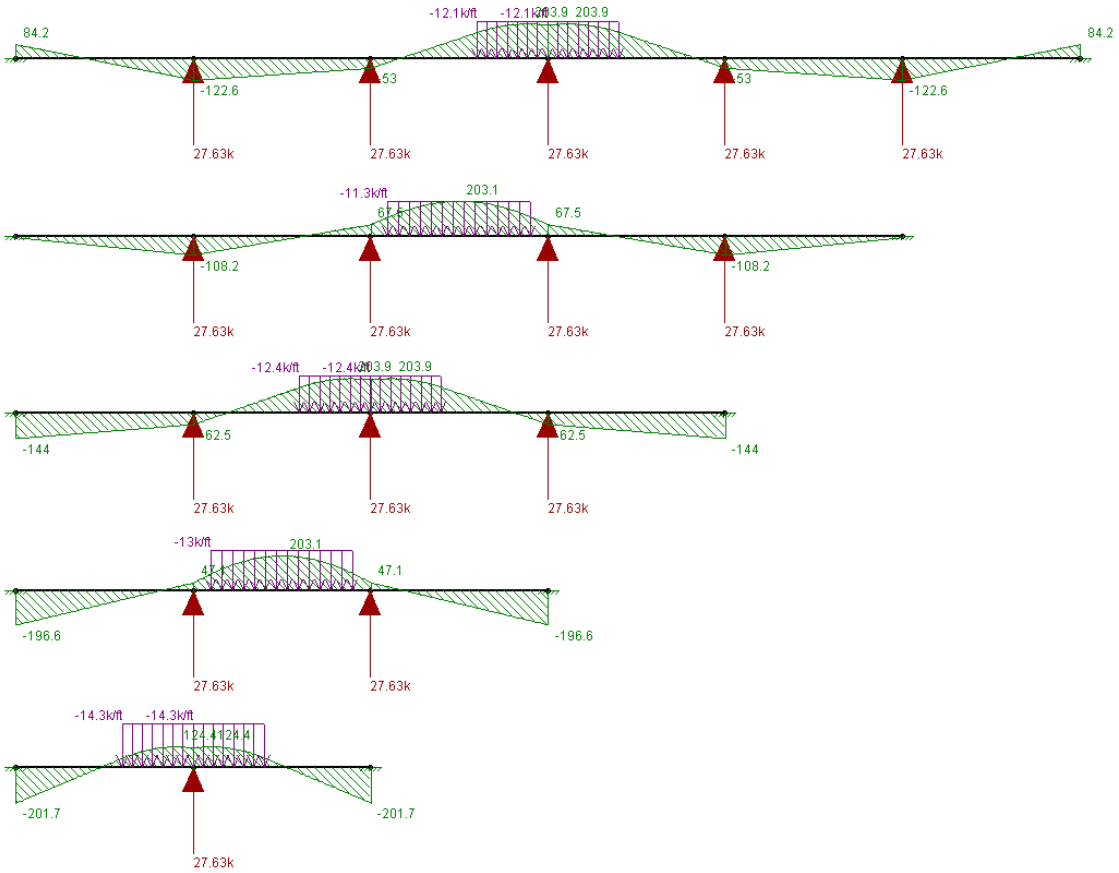

Figure 3.4 RISA Combination Method Model

The applied load for each number of spans was then used as the ultimate capacity of the rail in the combination calculation. The post capacity and parapet capacity were 27.63 kips and 367.84 kips, respectively, which were the same as the standard method. The single span capacity was the same as calculated in Section 3.3.1 . The capacities and height for all spans are shown in table 3.2. Overall, the capacity increased when the contribution of the posts which were assumed to be at ultimate capacity was incorporated in the RISA combination method, with the one exception being the two-span failure.

Table 3.2 RISA Combination Capacities and Heights

Spans	P_p (kips)	P_r (kips)	P_w' (kips)	R (kips)	H (in.)
1	N/A	485.04	367.84	852.88	71.89
2	27.63	114.40	316.03	458.06	61.02
3	55.26	104.00	264.23	423.49	63.79
4	82.89	99.20	212.42	394.51	67.38
5	110.52	90.40	160.62	361.54	71.34
6	138.15	96.80	108.80	343.76	76.71

3.3.3 Inelastic-Rail Method

The Inelastic-Rail Method was created as another way to more accurately estimate the capacity and contribution of the upper open concrete rail. It was thought that utilizing the post-and-beam railings method, as presented in *AASHTO LRFD Bridge Design Specifications* [22], for an inelastic approach to the reinforced concrete post and rail system, and conventional Yield Line Analysis [9] for the lower concrete parapet would result in the most accurate capacities for the two main components of this barrier. The combination method equations shown in Eqn. 27 and Eqn. 28 would then be used to obtain one overall capacity from the contribution of the two main barrier components (the lower parapet and upper open concrete rail).

The post-and-beam method calculated one capacity for the reinforced open concrete post and beam railing system based on the number of railing spans being considered.

For an even number of spans:

$$R = \frac{16M_p + (N-1)(N+1)P_pL}{2NL - L_t} \quad \text{(Eqn. 34)}$$

For an odd number of spans:

$$R = \frac{16M_p + N^2 P_p L}{2NL - L_t} \quad \text{(Eqn. 35)}$$

Where:

L = post spacing of a single span (ft)
L_t = transverse length of distributed vehicle impact load (ft)
M_p = inelastic, yield line resistance of all rails contributing to plastic hinge (kip-ft)
P_p = horizontal force capacity of a single post (kip)
R = total ultimate resistance of the railing (kips)

The transverse length of distributed vehicle impact was specified to be 8 ft by *AASHTO LRFD Bridge Design Specifications* [22]. The resistance of all the rails contributing to the plastic hinge (M_p) was previously calculated in Section 3.1.1 as M_b, and was equal to 202.1 k-ft. The horizontal capacity of a single post (P_p) was also calculated in Section 3.3.1 to be 27.63 kips. The total ultimate resistance of the railing for one to six spans is shown in table 3.3.

Table 3.3 Post-and-Beam Inelastic Capacity

Spans	R (kips)
1	1685.88
2	315.517
3	203.498
4	170.125
5	159.223
6	157.827

With the rail capacity calculated, an overall capacity can be established using the combination method previously presented. The Inelastic-Rail Method capacities are shown in table 3.4.

P_w' = reduced capacity of parapet due to post load being resisted by the parapet
R_{tot} = overall resistive capacity from combination method, Section 3.3
H = effective height from combination method, Section 3.3

Table 3.4 Inelastic-Rail Method Capacities and Heights

Spans	R (kips)	P_w' (kips)	R_{tot} (kip)	H (in.)
1	1685.88	367.84	2053.72	82.48
2	315.52	316.03	631.55	68.98
3	203.50	264.23	467.73	66.27
4	170.12	212.42	382.55	66.68
5	159.22	160.62	319.84	68.91
6	157.83	108.81	266.64	72.86

3.4 Incremental Analysis Method

The incremental analysis method is a technique that utilizes the reserve capacity of a member even after the plastic moment has been reached at one point in the section. This method loads an element, in this scenario the upper reinforced concrete rail, until the maximum moment in the element is reached. Although the maximum moment is reached in the element, it still has some reserve capacity, thus the element can continue to take load until a collapse mechanism is formed. For this method, an incremental analysis was performed on the reinforced concrete post and beam section of the TL-6 Roman Wall. A model of the rail was created in FTOOL [26] consisting of ten spans, pinned at the end with springs at each post location.

To determine the spring constant, the maximum load over the maximum deflection needed to be determined. It was assumed that if the railing system were to be loaded at the top of the railing that two forces would develop in the center of the rail, a horizontal shear force and a moment about the longitudinal axis. A schematic of the assumed loading is shown in figure 3.5.

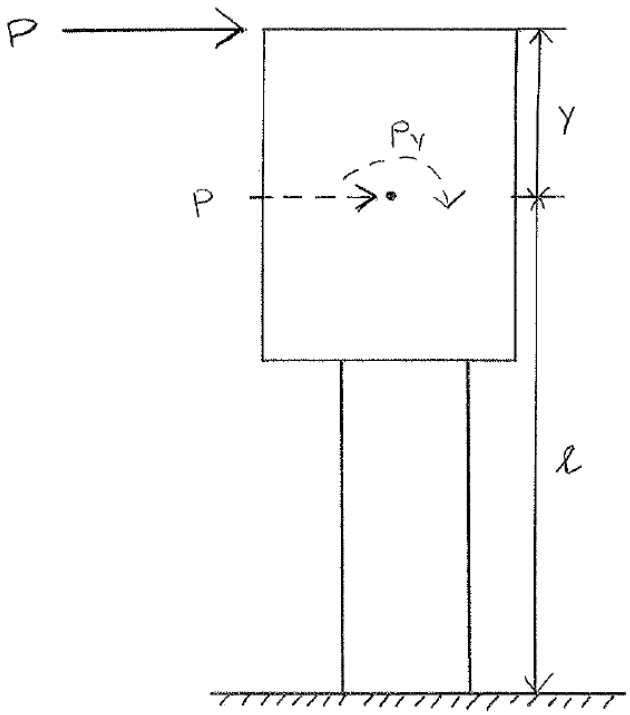

Figure 3.5 Assumed Post Loading Schematic

The maximum deflection of a point load at the end of a cantilever, in this case caused by the horizontal shear load, is known to be $\frac{Pl^3}{3EI}$. The deflection created by the moment was calculated using virtual work to be $\frac{Pyl^2}{2EI}$. The total maximum deflection is the sum of the two, and the stiffness of the railing (assumed to be the spring constant used in FTOOL) is the load over deflection.

$$\Delta_{max} = \frac{Pl^3}{3EI} + \frac{Pyl^2}{2EI} \quad \text{(Eqn. 36)}$$

$$\frac{P}{\Delta_{max}} = \frac{3EI}{l^3} + \frac{2EI}{yl^2} \quad \text{(Eqn. 37)}$$

Where:
P = post load (kips)
l = height to middle of rail (in.)
E = modulus of elasticity of concrete (kip/in.^{2})

I = cracked moment of inertia of post (in.^{4})
y = distance from top of rail to middle of rail (in.)

The moment of inertia was calculated using the cracked section to be I_{cr} = 591.33 in^4 for a single post. The modulus of elasticity was $E_c = 33(w^{1.5})\sqrt{f_c'} = 33(145^{1.5})\sqrt{3600} = 3{,}457{,}141\ psi$. Thus the stiffness of the springs is 7728.72 kip/ft. The detailed calculations can be found in Appendix B.4 .

The moment of inertia of the beam which represented the rail was 7.37555*10^3 in.^{4} and the area was 336 in.^{2}. The initial FTOOL model is shown in figure 3.6.

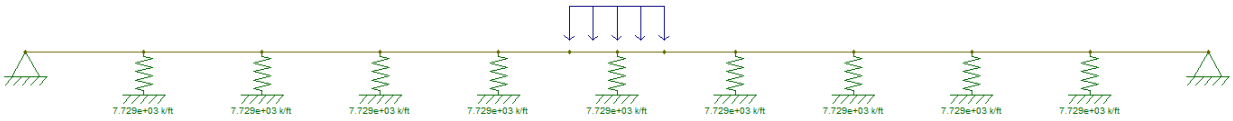

Figure 3.6 Initial FTOOL Model

With the initial model set up the incremental analysis could begin. It was assumed that either one of two things could update the model, either maximum moment in the rail being reached or a post failing. To determine which would happen first, the magnitude of the distributed load was increased until a moment of 202.1 k-ft was seen in the beam or a load of 27.63 kips was seen in a spring.

The first loading phase resulted in the middle three posts failing (reaching 27.63 kips) at an applied load of 8.67 k/ft over the middle 8 ft. The middle three posts failed before the maximum rail moment was seen. The failed posts were then removed and a point load of 27.63 kips was placed at that location. The load was then increased again (loading phase 2) until one of the two failure modes was present. The next failure mode to be present was the formation of the

beam's maximum moment in two locations, 1.2 ft to either side of the middle post, at an applied load of 11.75 k/ft. The model that created the two hinges is shown in figure 3.7. The moment diagram after loading phase 2 is shown in figure 3.8.

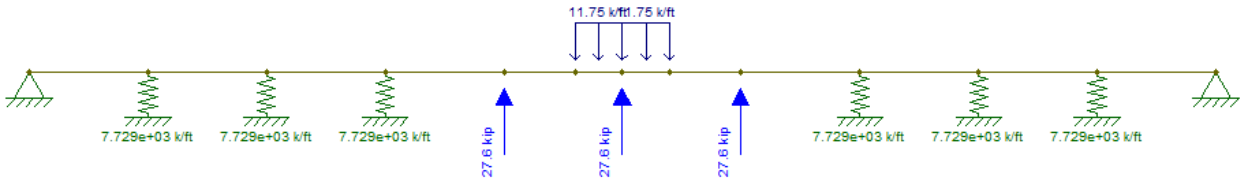

Figure 3.7 Incremental Analysis Loading Phase 2

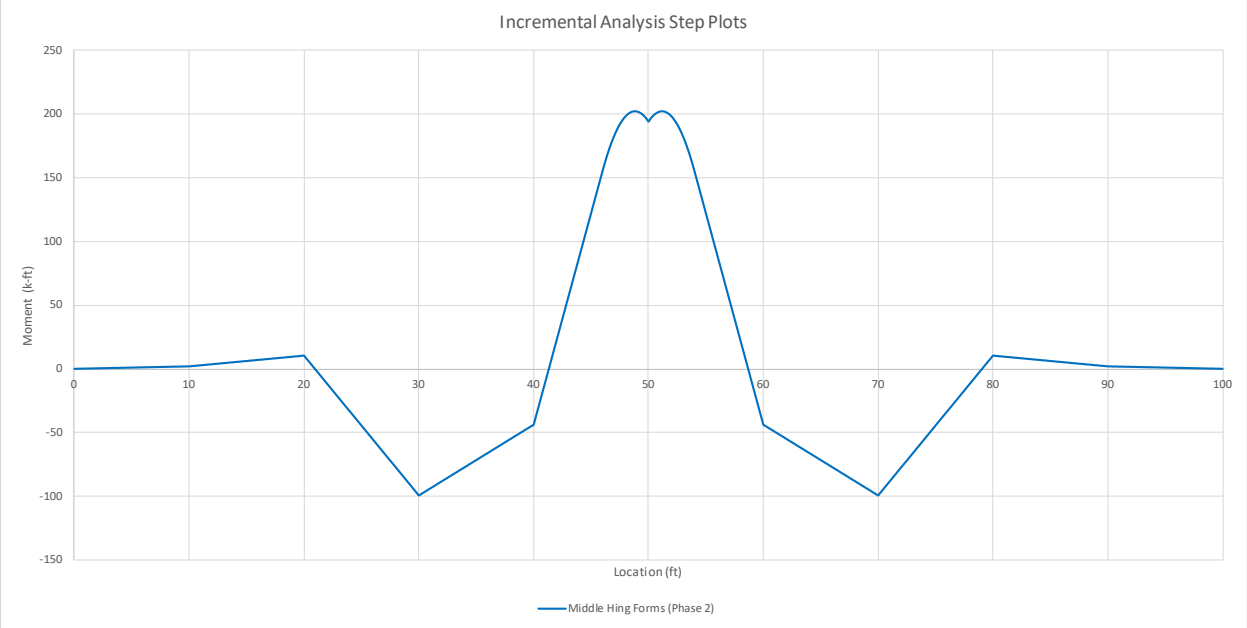

Figure 3.8 Moment Diagram after Loading Phase 2

After loading phase 2 there were three failed posts and two plastic hinges in the beam. The reserve capacity of the beam was calculated by taking the maximum moment that could be supported at a given point along the beam (202.1 k-ft), and subtracting out the moment created by loading phase 2. The model was changed to reflect the failures and loading could then be reapplied to the beam. The model for loading phase 3 is shown in figure 3.3.

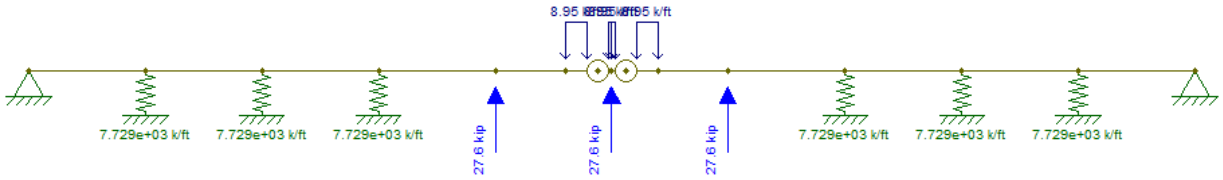

Figure 3.9 Incremental Analysis Loading Phase 3

With the changes made to the model, a load of 8.95 k/ft was applied to the beam before the reserve moment capacity of the beam was seen at any location along the beam. The reserve moment capacity was reached at two locations, 30 ft to either side of the middle post. With the addition of two more hinges formed in the beam section, a collapse mechanism was formed, and the ultimate capacity of the rail was met. A plot of the moment created by loading phase 2, loading phase 3, and the total moment is shown in figure 3.10.

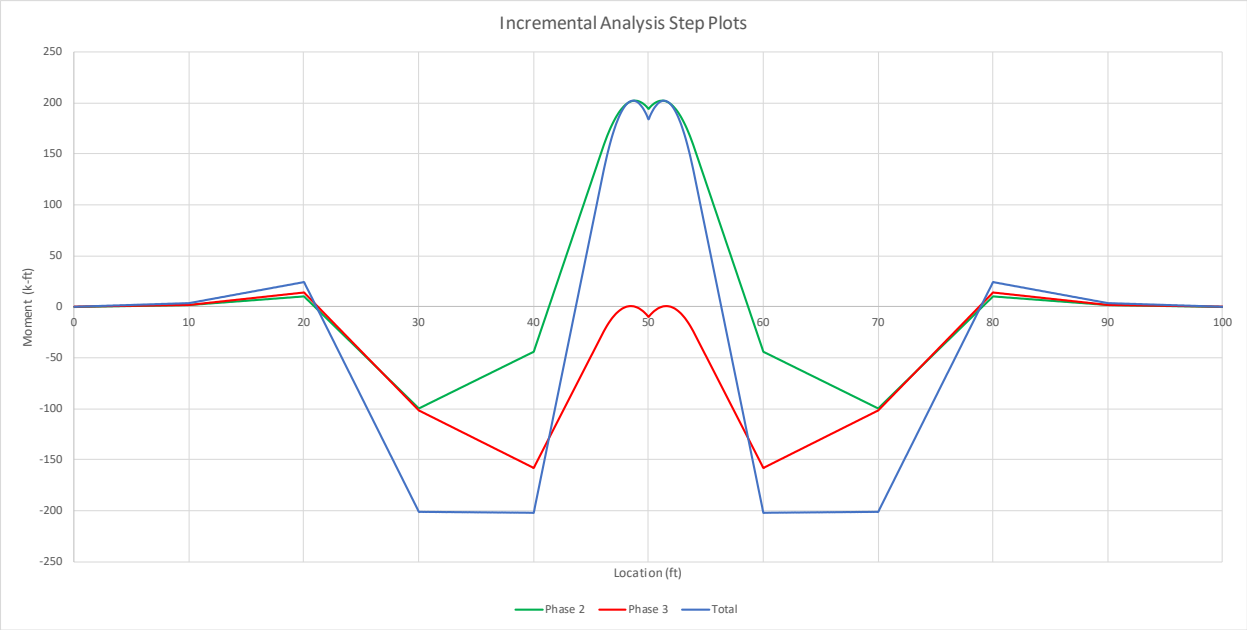

Figure 3.10 Moment Diagram after Loading Phase 3

With a collapse mechanism formed, the overall applied load that the reinforced concrete post and beam system can take is $w = 11.75\frac{k}{ft} + 8.95\frac{k}{ft} = 20.7\frac{k}{ft}$.

To get an overall capacity for the system the combination method was used. With the two final plastic hinges in the beam forming 30 ft to either side of the middle, it was assumed that the length of failure of the lower parapet would be the same as the length of failure of the post and rail system, 60 ft. Utilizing Yield Line Analysis as previously described, and new value of L=60 ft, a parapet capacity of 925.75 k was determined. The rail capacity was determined to be $wl = 20.7\frac{k}{ft} * 8ft = 165.6\ kips$. Using the combination method, the overall capacity can be calculated as follows:

$$P_w' = \frac{P_w h_w - P_p h_r}{h_w} = \frac{(925.75*48)-(5*27.63*48)}{48} = 666.72k \quad \text{(Eqn. 38)}$$

$$R = 666.72\ k + 165.6\ k = 832.32\ k \quad \text{(Eqn. 39)}$$

$$H = \frac{(666.72*48)+(165.6*90)}{832.32} = 56.36\ in. \quad \text{(Eqn. 40)}$$

Using an Incremental Analysis along with the combination method, a capacity of 832.32 kips at a height of 56.36 in. was determined.

3.5 Discussion

Nine methods were utilized to analyze and estimate the capacity of the existing TL-6 Roman Wall. A comparison of the capacity based on the different methods is shown in table 3.5. Each method calculated the capacity at a different height. The capacity was then normalized to a height of 56 in. to help more accurately compare the different method's capacities. The Yield Line Ultimate Capacity Section 1 provided the lowest capacity. The Incremental Analysis method provided the highest capacity. For this discussion it was assumed that the system had a

capacity over a length of six spans for the standard combination, RISA combination, and inelastic-rail methods. A length of six spans was determined from the high speed video of the full scale crash test where it appeared that the barrier deflection occurred over approximately six spans.

Table 3.5 Existing TL-6 Barrier Capacity Summary

Method	Capacity (kips)	Load Height (in.)	Normalized Capacity (kips)
YL Ultimate Capacity 1	204.3	90	328.3
YL Ultimate Capacity 2	250.0	90	401.8
YL Ultimate Capacity 3	343.8	90	552.5
Sum of Moments	400.4	90	643.5
Sum of Moments	643.6	56	643.6
Standard Combination	276.6	73.5	363.0
RISA Combination	343.8	76.7	470.9
Inelastic-Rail	266.6	72.9	347.1
Incremental Analysis	832.3	56.4	838.2

The Yield Line Analysis (YLA) calculations provided a simple calculation of the capacity of the barrier, but lacked the ability to fully consider how the multiple components in the system interacted with one another. The YLA calculations ignored the capacity of the posts and how the fully loaded posts may contribute to the capacity of the parapet, rail, and the posts to either side. Thus, the capacity calculated using YLA were a good estimate but should not be considered the most accurate due to the lack of involvement from the posts.

The Sum of Moments method utilized the same individual component capacities that the YLA method uses, but an overall capacity was calculated based on static equilibrium. This method has many of the same drawbacks and benefits of the YLA method. While the sum of moments method was simple, it ignored the contribution from the posts once they reached their ultimate capacity.

The standard combination method considered the capacity of the system changes with deformation occurring over various span lengths. The drawback to the combination method was that the rail capacity decreased significantly as the number of spans being considered increased. This decrease was due to the assumption that the posts carry no load after reaching ultimate load.

In reality, the posts could transfer some resistance to the rail after ultimate if complete fracture does not occur, thus increasing that rail's overall capacity. This method also required an assumption to be made about over how many spans the system would fail.

The RISA combination method changed the standard combination method assumptions with how the capacity of the rail was calculated. The addition of the post loads resisting the impact load increased the capacity of the open concrete rail as the number of spans being considered increased. This method was believed to be more realistic, as during a real crash event even when the posts reach maximum loading, they would still provide resistance to the rail deformation unless complete fracture occurred.

The inelastic-rail method calculated the capacity of the upper rail based on the Post-and-Beam *AASHTO LRFD Bridge Design Specifications* [22]. This method increases the capacity of the rail when compared to the standard combination, but less than the RISA method. The advantage to this method was that the calculations were relatively simple and it did not require any additional analysis software.

The incremental analysis method was similar to the RISA method, but did not consider multiple different numbers of spans. A capacity was calculated where plastic hinges would form. It was believed that this method more accurately captured the true behavior of the upper rail. By considering the reserve capacity of the rail after the first plastic hinge formed, but before a collapse mechanism was formed, the rail capacity was much larger than the capacity based on the maximum moment capacity of the posts and rails.

In summary, several methods were evaluated. It cannot be determined which method is the most accurate. It is the researchers' opinion that the static capacity of the barrier is between 350-400 kips with a 56-in. load height. Thus, the targeted capacity for the new barrier would be

in the same range. However, none of the methods presented accounted for the dynamic behavior of the barrier under a full scale crash test.

Chapter 4 Design Criteria

Several design criteria were established to help guide the design of a new TL-6 barrier. These design criteria were separated into three categories: (1) required criteria, which were criteria that must be met by the design and testing of the new barrier; (2) preferred criteria, which were criteria that were desired, but if they could not be accommodated, would not affect the crashworthiness of the new barrier; and (3) optional criteria, which were criteria that would be implemented if feasible and not cost prohibitive.

4.1 Required Criteria

The new barrier must be able to pass all MASH TL-6 evaluation criteria, which includes MASH test designation nos. 6-10, 6-11, and 6-12 and all safety performance criteria associated with each test. This bridge rail was initially be designed for a roadside configuration as opposed to a median configuration. The barrier shall have interior and exterior sections designed so that all points along the barrier meet the capacity requirements. The design will also include an adequate foundation design.

Using information gathered in the literature review and from the analysis of the existing TL-6 Roman Wall barrier, two different design loads were determined. The first static design load was 350 kips for a rigid barrier, and the second was 300 kips for a semi-rigid or deformable barrier. In estimating the capacity of the Roman Wall to be between 350 and 500 kips, and knowing that the damage to the barrier was minimal, the researchers selected the lower of the estimated Roman Wall capacity to be the new barrier largest capacity. The semi rigid or deformable load was lowered by 50 kips, as this was the estimated load that could be absorbed by the deformation of the barrier. These design loads were to be applied as static loads knowing that the actual dynamic load was around 400 kips for a 90-in. tall rigid wall [10]. As mentioned in Chapter **Error! Reference source not found.**, there will not necessarily be a definitive design

procedure to use for the barrier. Thus, these were only targeted values to use in initial design. The semi-rigid and deformable barriers were designed with a lower, load due to their ability to deform and absorb a portion of the impact energy. However, these design loads were only initial targets and may need to be adjusted throughout the design process.

The largest dynamic load typically comes from the rear tandem impact with rigid walls [10]. Due to the geometry of the tractor tank-trailer vehicle at the rear tandem axle, the load was to be split between two locations, the first being the center of the rear tandem wheels approximately 21 in. from the bottom of the barrier and the second being the lower of 85 in. (middle of the tank-trailer) or the top height of the barrier, as shown in figure 4.1. The magnitude of the two loads was derived from the empty weight of the trailer at the rear tandems being approximately 12,000 lb and the loaded weight being 34,000 lb. With about one-third of the loaded weight being from the tractor itself, it was assumed that about one-third of the design static load would transfer through the middle of the rear tandem wheels, or a height of 21 in. above the bottom of the barrier. The additional two-thirds of the loaded weight on the rear tandem axles is from the addition of the ballast. Thus, this load was assumed to be transferred to the barrier through the lesser of either the middle of the tank (85 in.), which would likely contact the barrier first, or the top height of the barrier, as the tank would lean heavily on the top of lower-height barriers.

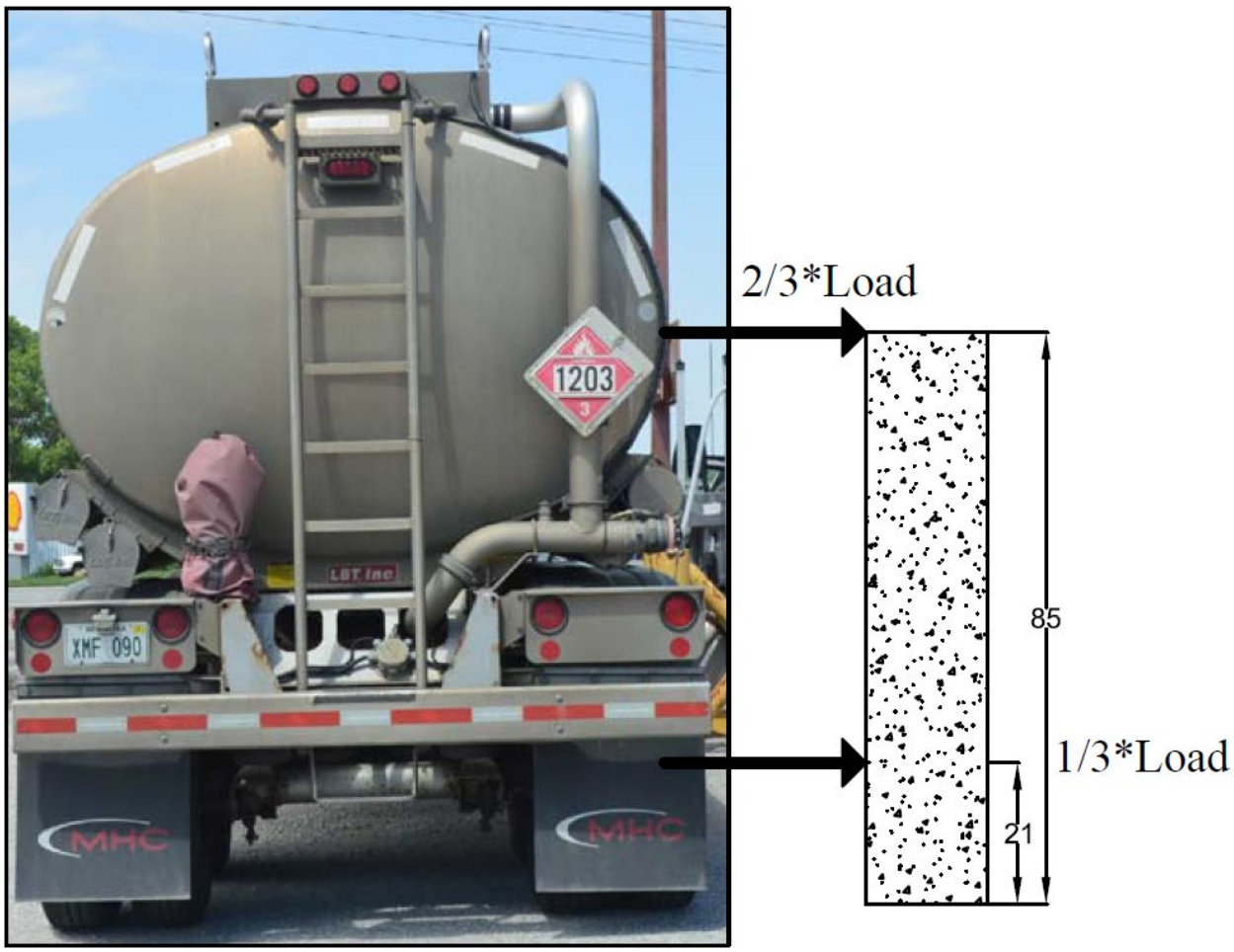

Figure 4.1 Loading Height Schematic

The criteria for geometry is based on vehicle geometry and anticipated roadside constraints. The roadside configuration of the barrier must not have a base footprint width greater than 24 in. and a future median design base footprint width must not exceed 36 in. to be similar to existing barriers. The barrier height will be minimized as much as possible and should not exceed 90 in. Based on the initial literature review and investigation, a barrier height as low as 56 in. has been suggested previously. However, the minimum barrier height will be further explored throughout the project.

The cost of the barrier must be competitive with that of current TL-5 barriers from a benefit-cost perspective. That is to say if the cost of the designed barrier is more than current TL-

5 barriers, some major benefit must be present in the TL-6 barrier over the TL-5 barrier. Some of the costs that will be considered are material, formwork, and labor. It should be noted that this criteria is somewhat subjective, as material cost can vary widely across the United States. Additionally, since TL-6 barriers are used scarcely, it is hard to quantify the benefit. The cost of current TL-5 barriers was estimated to be $140/ft, and the cost of the TL-6 barrier in current dollars was estimated to be $295/ft. These costs include only the material and construction of the barrier itself, this does not include any material or construction costs for the foundation. The new TL-6 barrier should have a cost that is less than the previous TL-6 barrier and should be competitive with current TL-5 barriers.

The barrier must be able to withstand a secondary impact of any level after a TL-3 impact, at the same location as the initialTL-3 impact. Thus, no permanent damage that would affect the performance of the barrier under the subsequent impact of any TL-3 though TL-6 impact is acceptable after a TL-3 impact.

4.2 Preferred Design Criteria

Preferred design criteria are criteria that will be considered when designing the barrier but are not required to be met by the design or in the results of the full scale crash test. It is preferred that the barrier be able to withstand a secondary impact at the same location after a TL-5 impact. In addition, the trailer should not rupture during or after the crash event due to contact with any part of the barrier. The tank-trailer in MASH test designation no. 6-12 should remain upright and not rollover during or after impact to prevent spillage of the contained liquid throughout the crash event. It is also preferred to have a width less than 15 in. based on a state DOT request.

After a roadside configuration is fully designed, both a median and bridge rail configuration will be considered in future phases. Thus, it is preferred that the design of the

roadside configuration be easily adaptable to median and bridge rail configurations. The geometry of the barrier should take into consideration the sightline criteria of state DOTs. The ability for water to drain off of the traffic side of the barrier is also preferred. Aesthetics and long term durability are also preferred based on the state survey responses.

4.3 Optional Design Criteria

The only optional design criteria is to incorporate the previously-developed head ejection envelope, as shown in figure 2.6, into the cross-sectional geometry of the barrier to protect against head slap. Head slap is where the head of a passenger exits the vehicle, typically through the window, and makes contact with the barrier. Incorporating this envelope into the front face geometry of the barrier could help to reduce the occurrence and severity of head slap if a passenger's head exited the vehicle during the crash event.

4.4 Pooled Fund State Survey

To help establish the design criteria, a survey of the Midwest Pooled Fund States was conducted in order to determine which criteria were most important to the agencies that would be using this barrier. A series of questions, presented below, were asked of the states in order to determine whether a design criteria should be categorized as required, preferred, or optional. The survey questions and responses are presented below:

1) What is your level of need for a Test Level 6 barrier?

    1 – Very High

    0 – High

    1 – Moderate

    4 – Low

    5 – None

2) Would you be likely to use a new TL-6 barrier if the system per foot cost was any of the options noted below? This cost includes material and installation for the barrier, it does not include the foundation. For reference a 49 in. single-slope TL-5 barrier has a cost of approximately $140/ft. The number of states responding to each item is shown below.

Price Range	Yes	Maybe	No
$100 - $150	5	2	1
$150 - $200	4	3	1
$200 - $250	3	2	3
$250 - $300	2	2	4
$300 - $350	0	3	5
$350 +	0	3	5

3) The current height of the existing TTI TL-6 barrier is 90 in. We believe that this height can be considerably lower. Would you be likely to use a new TL-6 barrier if the height was any of the options noted below? The number of states responding to each item is shown below.

Height Range	Yes	Maybe	No
42 - 49 in.	4	0	4
50 - 59 in.	4	2	3
60 - 69 in.	2	3	3
70 - 79 in.	1	5	2
80 - 89 in.	1	3	4
90 + in.	0	3	5

4) This barrier will be designed to sustain no damage at Test Level 3. If the TL-6 barrier was subjected to a TL-5 impact (80,000-lb tractor-van trailer at 50 mph and 15 deg) and needed repair afterward, would this be acceptable?

0 – Yes, if significantly damaged

3 – Yes, if moderately damaged

5 – Yes, if only minor damage

1 – Possibly

1 – No

5) This barrier will be designed to sustain no damage at Test Level 3. If the TL-6 barrier was subjected to a TL-6 impact (80,000-lb tractor-tank trailer at 50 mph and 15 deg) and needed repair afterward, would this be acceptable?

1 – Yes, if significantly damaged

6 – Yes, if moderately damaged

3 – Yes, if only minor damage

0 – Possibly

0 – No

6) How important is meeting sightline criteria in a TL-6 barrier?

2 – Very

4 – Somewhat

2 – Not at all

7) This barrier will be initially designed for use in one specific area of the road, either median, roadside, or as a bridge rail. Please rank the following configurations from 1 to 3, with 1 being the most desired. The number of states responding to each item is shown below.

Configuration	Rank 1	Rank 2	Rank 3	Average Rank
Roadside	4	2	2	1.75
Median	1	4	3	2.25
Bridge Rail	4	2	2	1.75

8) Rank the following design parameters based on importance from 1 to 6, with 1 being the most important. It should be noted that parameters starting with "Other –" are responses created by the responding state. The number of states responding to each item is shown below.

Parameter	Rank 1 (Most Important)	Rank 2	Rank 3	Rank 4	Rank 5	Rank 6 (Least Important)	Average
Low Cost	1	3	1	1	1	1	3.125
Low Barrier Height	2	0	0	4	2	0	3.5
Barrier Configuration	1	2	4	1	0	0	2.625
Maintaining Sightline Criteria	2	0	0	1	3	2	4.125
Low Maintenance Requirement	4	2	1	0	0	1	2.125
No damage to bridge deck at design impact	1	0	0	0	0	0	-
Other - TL-6 Compliance	1	0	0	0	0	0	-
Other - Do not build where SD is a problem	1	0	0	0	0	0	-
Other - ZOI Barrier Use	0	0	1	0	0	0	-

9) Are the following materials acceptable for use in the TL-6 barrier? The number of states responding to each item is shown below.

Material	Yes	Possible	No
Reinforced Concrete	8	0	0
Structural Steel	5	3	0
Elastomer/Rubber	1	6	1

10) Please rank the following concepts from 1 to 3 with 1 being the most preferred. The number of states responding to each item is shown below.

Reinforced concrete wall (could be single slope)	Reinforced concrete wall with steel post and rail (could be single slope)	Energy absorbing (Similar to a RESTORE Barrier)
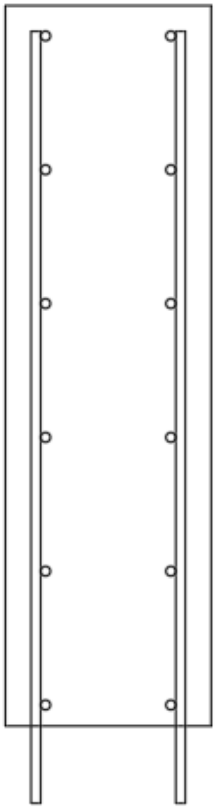	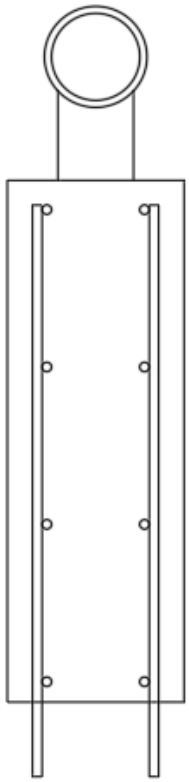	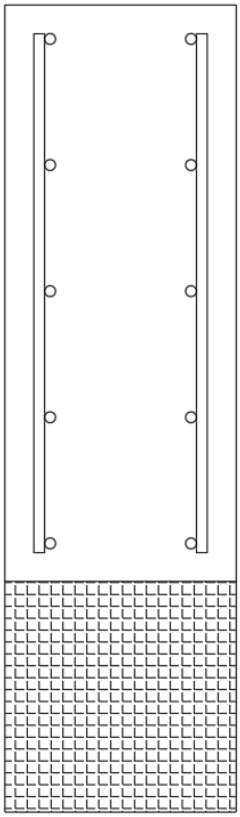

Concept	Rank 1	Rank 2	Rank 3
Reinforced Concrete Wall	3	2	1
Combination Rail	2	3	1
Energy Absorbing	0	0	6

11) Are there any additional considerations that should be incorporated into a new TL-6 barrier design?

A) We have one location where a TL-6 barrier has been considered. Due to the low use of a TL-6 barrier, it has been considered a lower priority than more highly used lower test level barrier systems.

B) Under TL-6 design impacts, bridge deck damage is not acceptable.

C) I would only use this barrier in areas where I could get the required horizontal sight distance. I would also not want a barrier that subjects small cars to head slap. I would not want to kill/injure more small car drivers to protect against the very small chance that a tanker trailer would hit the obstruction.

D) This test could be used to help provide design guidance for stability (foundation design) and durability of barrier walls. Since this is the largest test level vehicle, we would recommend capturing how forces are translated to the foundation and verifying minimum expansion joint spacing to keep the barrier from failing/overturning/sliding.

E) Using a strong structural design as well as detailing techniques (such as corner chamfers) could help establish some design guidance so that these barriers can survive higher force impacts with minimal or no damage.

F) If we used this barrier, it would most likely be as a better ZOI barrier. Collecting the ZOI values for the tank "lean" over the barrier would be most helpful. Additionally, the barrier height should be 54" or taller to meet ZOI needs.

G) A minimal/no deflection barrier is desired. Ideally, with no more than a 15" overall thickness. In order for us to effectively use as a ZOI barrier in retrofit conditions, limited space is available. A wider footing could be used if necessary, but ideally, the extra width of the footing should be on the impact side of the barrier (since the bridge pier would limit the orientation of the footing.

H) With these larger barriers it would be nice if you could plow snow next to these without damaging the barrier(occasional bump) and have the ability to at least throw some snow through safe non-snagging type openings in the barrier.

I) We currently have only a small handful of locations that use TL-5 barrier. I think it would be even more rare for us to install TL-6 barriers. My guess is if we found a location that needed TL-6 barrier, it would be a reactionary move and cost of the barrier would be less important.

J) Aesthetic considerations. This will be a highly visible roadside feature and should be made to be relatively attractive.

K) Long-term durability would be essential. Elastomer/rubber would only be acceptable if it had a 30 year design life.

Chapter 5 Barrier Concepts

Barrier concepts were brainstormed and evaluated to determine their overall feasibility. Concepts were divided into three general categories: (1) "rigid" concepts that should have minimal deflection, (2) "semi rigid" concepts that contain a rigid component and a deformable component, which may deflect under impact, and (3) "deformable" concepts that contain energy-absorbing parts or are designed to deflect during impact. Rigid concepts were designed for a total static load of 350 kips, and the semi-rigid and deformable concepts were designed for a total static load of 300 kips, as previously discussed in Section 4.1 . For all concepts, pros and cons were developed and used to determine the overall feasibility. The pros, cons, and feasibility are presented for each concept in the following sections. A few examples of each feasible concept are presented, and calculations for each presented example can be found in Appendix C . It should be noted that the examples presented in this section are preliminary concepts that have calculated capacities designed to meet the required loading. Although the concepts have the required capacity, they are not guaranteed to work as intended and meet all required MASH criteria.

All barrier concepts would have a foundation designed, which is not shown in this chapter for simplicity. In addition, the connection between the barrier and the foundation is shown in the following sections for illustrative purposes only and has not been designed.

5.1 Rigid Concepts

Rigid concepts were designed to have negligible deflections, and they would experience high loads due to higher accelerations. As previously discussed, rigid concepts were subjected to a total load of 350 kips. The total load was split into two individual loads, two-thirds of the load (233 kips) through the tank at the top of the barrier up to 85 in., and one-third of the load (117 kips) through the rear tandem axle at 21 in.

5.1.1 Solid Wall (Concept 1)

The Solid Wall concept is a simple reinforced concrete wall, as shown in figure 5.1. This barrier concept was designed using Yield Line Analysis [9] with a total load of 350 kips. The total 350-kip load was split into two loads, 117 kips at a height of 21 in. above the roadway surface, and 223 kips at the top of the barrier. Yield Line Analysis was only developed for a single load, rather than two separate loads. Thus, using the two separate loads, one equivalent total load was applied at the top of the barrier, determined using static equilibrium. It should be noted that the traffic face of the barrier could be designed as either single slope or vertical front face. To determine the feasibility of this concept, the pros and cons were determined.

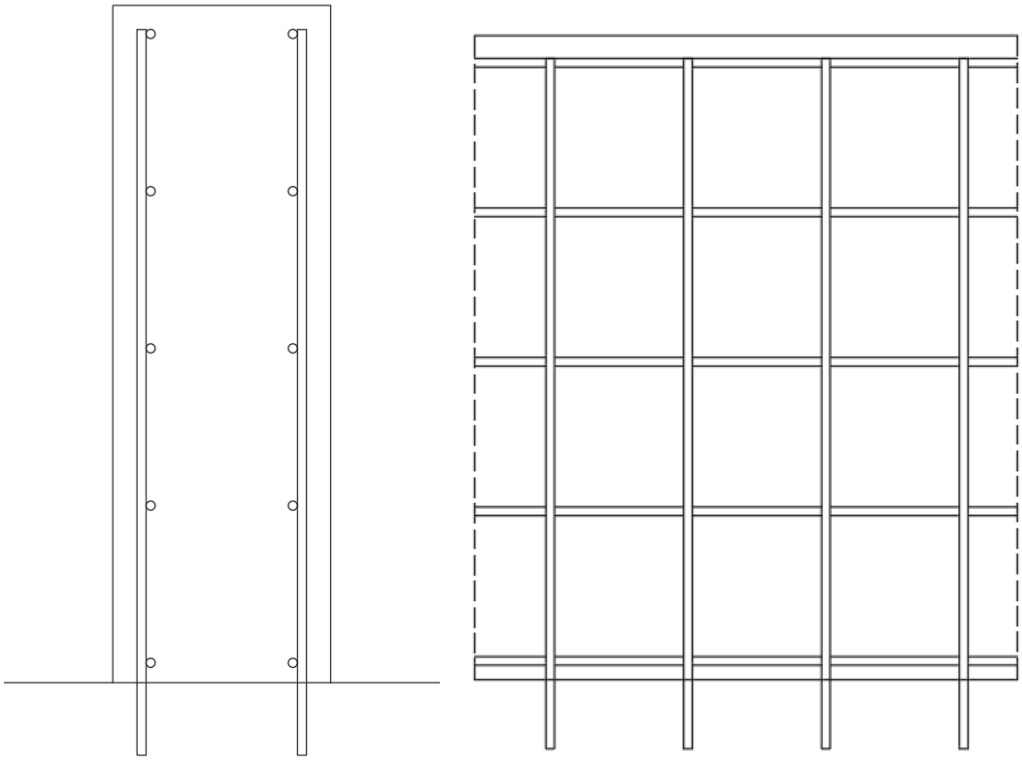

(a) Cross-Section (b) Elevation

Figure 5.1 Concept 1 – Solid Wall

The pros of the Solid Wall concept include:

- Obtaining the desired capacity within the barrier height and width constraints should be easily attainable
- Interior and exterior sections could be designed to meet loading requirements
- Conventional reinforced concrete barrier construction methods could be used
- Likely low construction cost
- Likely low potential for the trailer to snag/puncture on any element of the barrier
- Damage at lower test level impacts (TL-3, TL-4, and TL-5) would be minimal since this barrier is similar to existing barriers

The cons of the Solid Wall concept include:

- Accelerations in MASH test designation no. 6-10 could approach maximum thresholds presented in MASH [2] as the traffic face of the barrier becomes more vertical
- A fully rigid wall leads to the highest impact forces possible for the given impact
- As the height of the barrier increases, the width must also increase to maintain the required capacity. The height of the barrier may increase to a point where the width of the barrier exceeds the maximum allowable width specified in the design criteria, in order maintain vehicle stability
- As this concept height increases the sightline is reduced

From the pros and cons determined for the Solid Wall concept, it was determined to have a high likelihood of meeting the design criteria. Two examples of preliminary concept designs for Concept 1 are shown in figure 5.2.

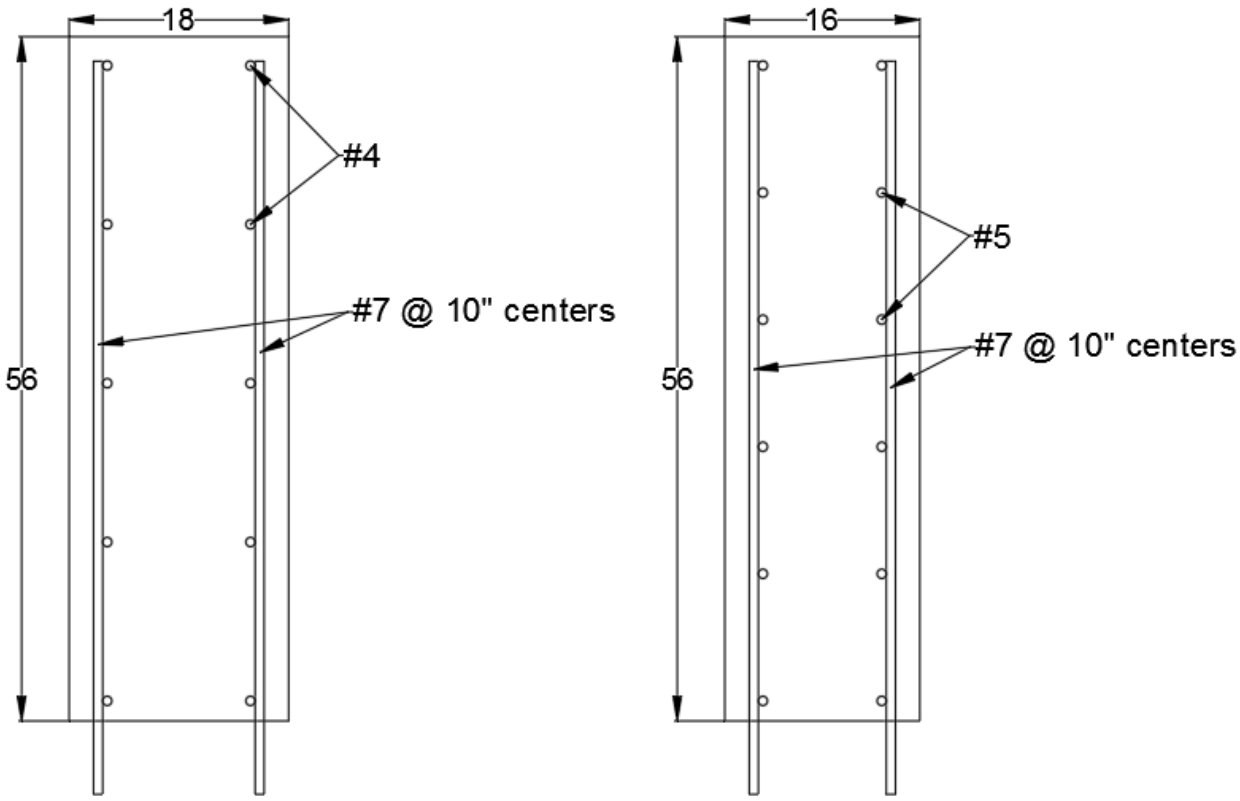

Figure 5.2 Concept 1 – Solid Wall Examples

5.1.2 Rigid Wall and Rigid Rail (Concept 2)

The Rigid Wall and Rail concept, as shown in figure 5.3, has two main elements, a rigid lower reinforced concrete wall and an upper steel rail. The lower reinforced concrete rail was designed using Yield Line Analysis [9] for loads of 117 kips at a height of 21 in., and 233 kips at the top of the barrier due to the load transferring through the railing posts. Using static equilibrium, the two loads were combined into one load applied at the top of the concrete parapet. The rail was designed to ensure that it remained as rigid as possible throughout impact. To do this it was assumed that the rail would remain elastic, thus the yield moment capacity of the rail must exceed the maximum moment created by the tractor-van trailer impact. In addition to the rails remaining elastic, the posts were also assumed to remain elastic. It was assumed the

rail would distribute the load to the two posts on either adjacent side of the distributed rail loading. Thus, four posts in total must have a yield moment and shear capacity greater than that which is generated by the tractor-van trailer impact. The same assumption was made for the base plate. These assumptions ensure that neither the base plate, post, nor rail will reach yielding during the impact event.

The lower parapet shown in figure 5.3 is in the vertical configurations. The barrier could have either a vertical or single slope traffic side face.

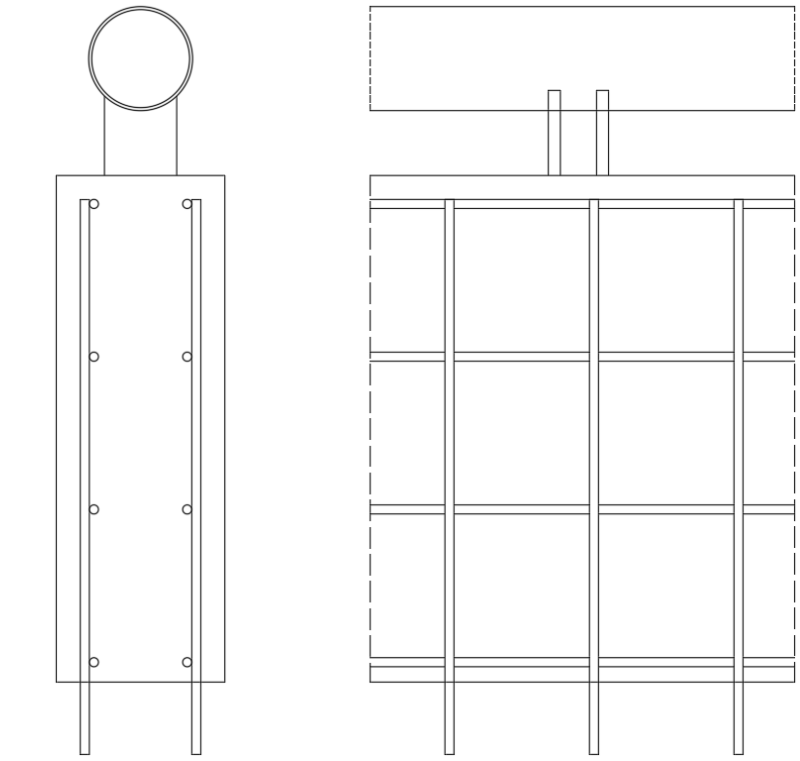

(a) Cross-Section (b) Elevation

Figure 5.3 Concept 2 – Rigid Wall and Rigid Rail

The pros of the Rigid Wall and Rigid Rail concept include:

- Obtaining the desired capacity within the barrier height and width constraints should be easily attainable

- Interior and exterior sections could be designed to meet loading requirements
- Conventional reinforced concrete barrier construction methods and steel rail manufacturing should make construction moderately easy
- Likely low to medium construction cost
- Damage at lower test levels (TL-3 and TL-4) will likely be minimal
- The ability for passengers to see through the barrier (sightlines) and snow to be pushed through/over the barrier are likely adequate at lower parapet heights

The cons of the Rigid Wall and Rail concept include:

- Accelerations in MASH test designation no. 5-10 could approach maximum thresholds presented in MASH [2] as the traffic face of the barrier becomes more vertical
- Potential for trailer to snag/puncture on steel rail components
- Potential damage of the steel rail system at TL-5

From the pros and cons for the Rigid Wall and Rail system, it was determined to have a high likelihood of meeting the design criteria. One example of a system that was designed to meet the capacity requirements is shown in figure 5.4.

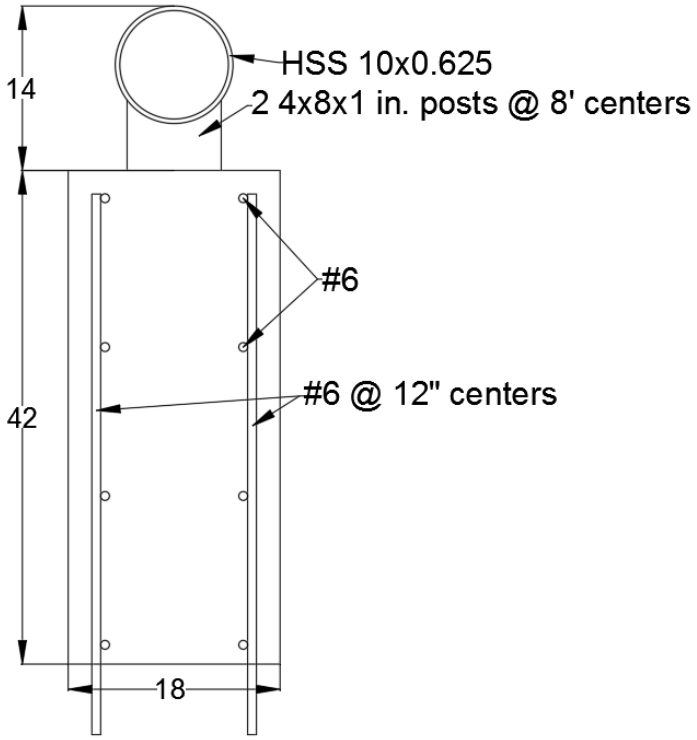

Figure 5.4 Concept 2 – Rigid Wall and Rigid Rail Example

5.2 Semi-Rigid Concepts

The semi-rigid concept category contained barrier concepts that involved a rigid lower reinforced concrete parapet with a deformable railing attached to the top of the parapet. The concepts were designed so that the majority of the impact load would be resisted by the lower parapet, and the upper rail would absorb some kinetic energy through deformation and transfer the load from the tank down into the lower parapet. The upper rail was necessary to stabilize the tank-trailer and prevent rollover. It was assumed that the lower parapet would experience negligible deflection, and the upper rail would displace and deform.

5.2.1 Rigid Wall with Deformable Rail (Concept 3)

The Rigid Wall with Deformable Rail concept, as shown in figure 5.5, was designed with two elements, a rigid lower reinforced concrete wall and a deformable upper steel rail. The upper rail could have various shapes, as shown in figure 5.5. The lower reinforced concrete wall was designed using Yield Line Analysis [9] with one 100-kip load located at 21 in. above the barrier base, and another 200-kip load located at the top of the barrier from the transfer of load in the steel rail through the posts. For this concept it was initially assumed that all the load on the upper rail would transfer down into the wall, even with the deformation of the posts and rails.

The upper deformable rail was designed in accordance with the Post-and-Beam method in Section A13.3.2 [22] for a load of 200 kips at the top of the rail. A capacity of 200 kips was targeted over four or more spans in the Post-and-Beam calculation. This was to ensure that the rail would have enough length to significantly deform, which in turn would deform the posts within the deformed rail section and absorb some of the impact energy. This four-span target was an initial assumption and could be modified at any time.

The lower wall is shown to have a vertical traffic face in figure 5.5, but could be designed with a single slope or other traffic face geometry.

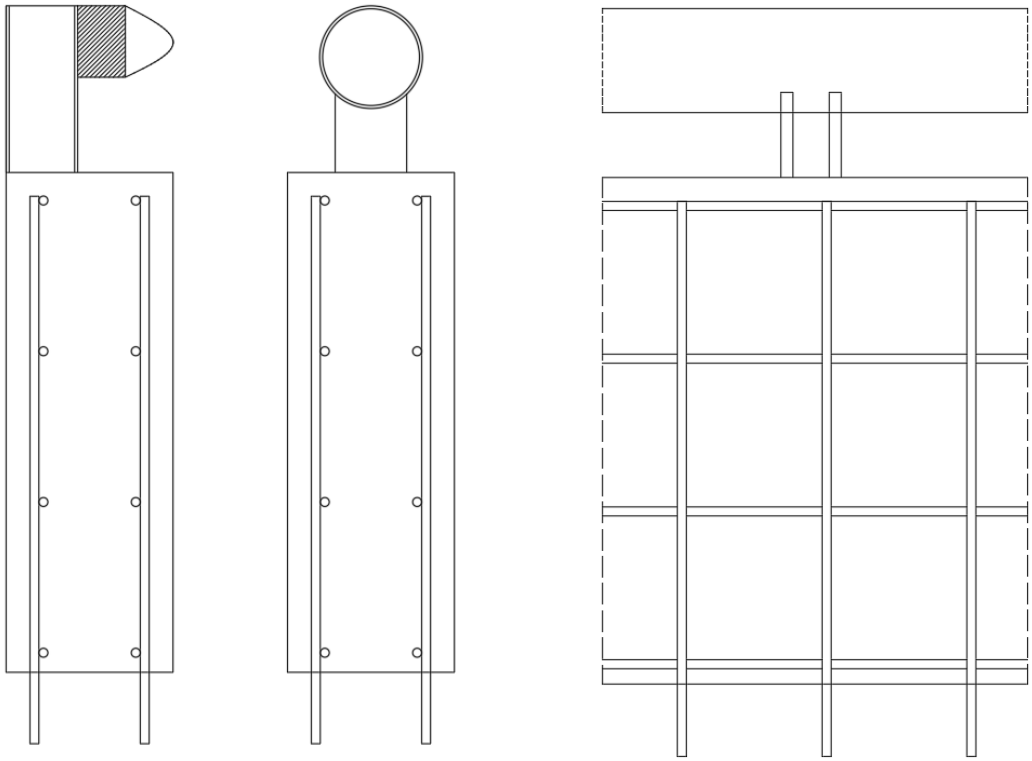

(a) Cross-Section (b) Elevation

Figure 5.5 Concept 3 – Rigid Wall and Deformable Rail

The pros of the Rigid Wall and Deformable Rail system include:

- The semi rigid design likely means lower overall impact forces
- Obtaining the desired capacity within the barrier height and width constraints should be easily attainable
- Interior and exterior sections could be designed to meet loading requirements
- The top rail can be designed specifically to prevent tank-trailer roll
- Conventional reinforced concrete barrier construction methods and steel rail manufacturing should make construction moderately easy
- Likely low to medium construction cost
- The ability for passengers to see through the barrier (sightlines) and snow to be pushed through/over the barrier are likely adequate at lower parapet heights
- Damage at lower test levels (TL-3) will likely be minimal

The cons of the Rigid Wall and Deformable Rail system include:

- Accelerations in the small car and pickup test could reach maximum thresholds presented in MASH [2] as the traffic face of the barrier becomes more vertical
- Potential for trailer to snag/puncture on steel rail components

- Potential damage of the steel rail system at TL-4 and TL-5

From the pros and cons for the Rigid Wall and Deformable Rail concept, it was determined to have a high likelihood of meeting the design criteria. One example of a system that was designed to meet the loading requirements is shown in figure 5.6.

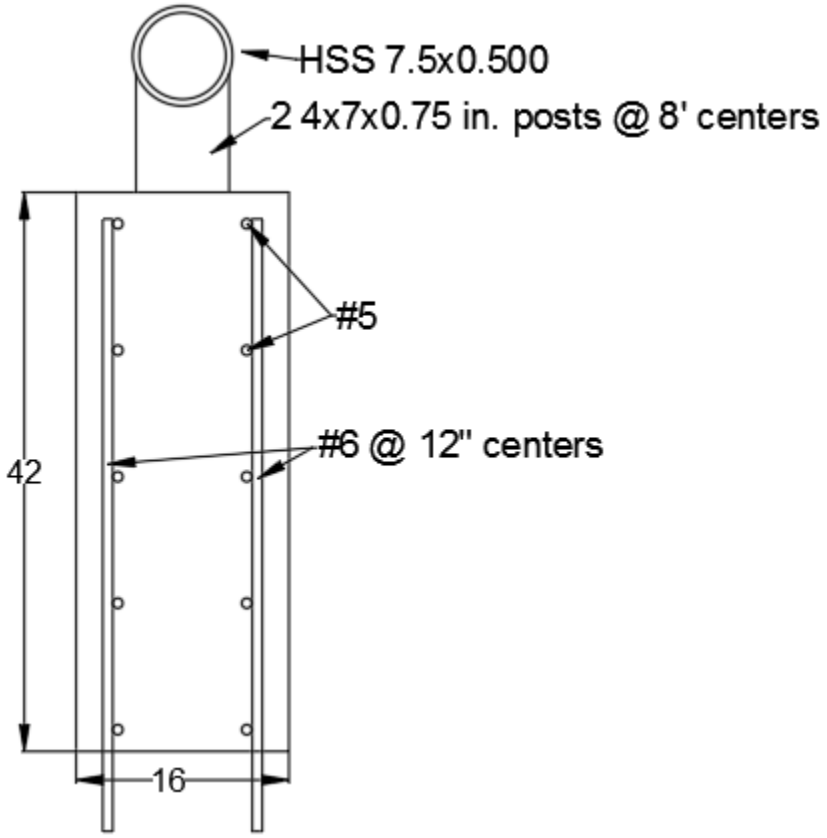

Figure 5.6 Concept 3 – Rigid Wall and Deformable Rail Example

5.2.2 Rigid Wall with Absorbing Rail (Concept 4)

The Rigid Wall with Absorbing Rail family of concepts, as shown in figures 5.7 through 5.11, consist of a lower reinforced concrete wall with an elastomer post rail system mounted atop. The lower concrete wall was designed using Yield Line Analysis [9] with one 100-kip load at 21

in. above the barrier base and another 200-kip load at the top of the barrier from the transfer of load through the railing posts.

The energy absorbing railing system was designed so that the posts do not reach yielding. This allows all the load to be transferred from the rail down through the posts and into the elastomer blocks. The elastomer blocks were designed to absorb one-seventh of the overall impacting energy. This energy level was selected to match the assumed design decrease in load from 350 kips for the rigid system to 300 kips for the semi rigid system, which was a decrease of one-seventh. The total impact energy was determined by looking at the speed and angle at which the rear tandem axle of the trailer impacted the barrier in a previous crash test, which was when the max load occurred [10]. It was determined that the rear tandem axle, which had a weight of approximately 34,000 lb, impacted the barrier at a speed of 15 mph and an angle of 90 degrees. This speed and weight corresponds to a total kinetic energy of 273 k-ft, thus the targeted energy absorption was 468 k-in.

The first concept for the upper rail was a steel rail mounted atop the elastomer posts, as shown in figure 5.7. The steel rail consisted of a steel tube connected to the elastomer posts via steel posts. The rail was designed similarly to Concept 3 and was allowed to experience yielding. Allowing the rail to yield ensures that there is significant deflection in the rail which will be transferred through the posts (which must remain elastic) and in turn displace that elastomer pads, where the impacting energy can be dissipated. As with previous concepts, the lower concrete wall could be designed with a vertical or single slope front face.

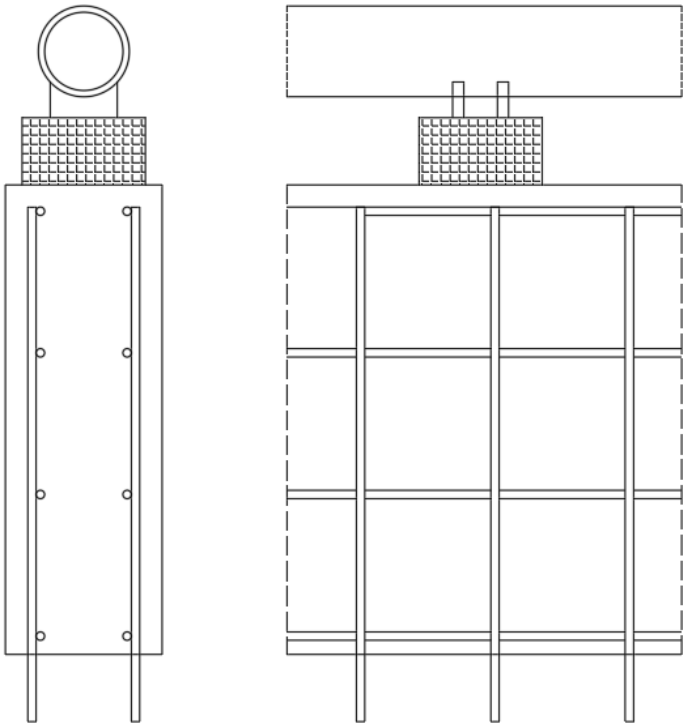

(a) Cross-Section (b) Elevation

Figure 5.7 Concept 3 – Rigid Wall and Absorbing Steel Rail

The pros of the Rigid Wall and Absorbing Steel Rail system include:

- The semi rigid design likely means lower overall impact forces
- Obtaining the desired capacity within the barrier height and width constraints should be easily attainable
- Interior and exterior sections could be designed to meet loading requirements
- Top rail can be designed specifically to prevent tank-trailer roll
- The ability for passengers to see through the barrier (sightlines) and snow to be pushed through/over the barrier are likely adequate at lower parapet heights

The cons of the Rigid Wall and Absorbing Steel Rail system shown in figure 5.7 include:

- Accelerations in the small car and pickup test could reach maximum thresholds presented in MASH [2] as the traffic face of the barrier becomes more vertical
- Potential for trailer to snag/puncture on steel rail components
- Potential damage of the steel rail system at TL-5
- Higher construction cost due to the expensive elastomer posts
- Attachment between steel, elastomer, and concrete components may be difficult and costly

From the pros and cons for the Rigid Wall and Absorbing Steel Rail system, it was determined to have a moderate likelihood of meeting the design criteria. One example of a system that was designed to meet the required loading conditions is shown in figure 5.8.

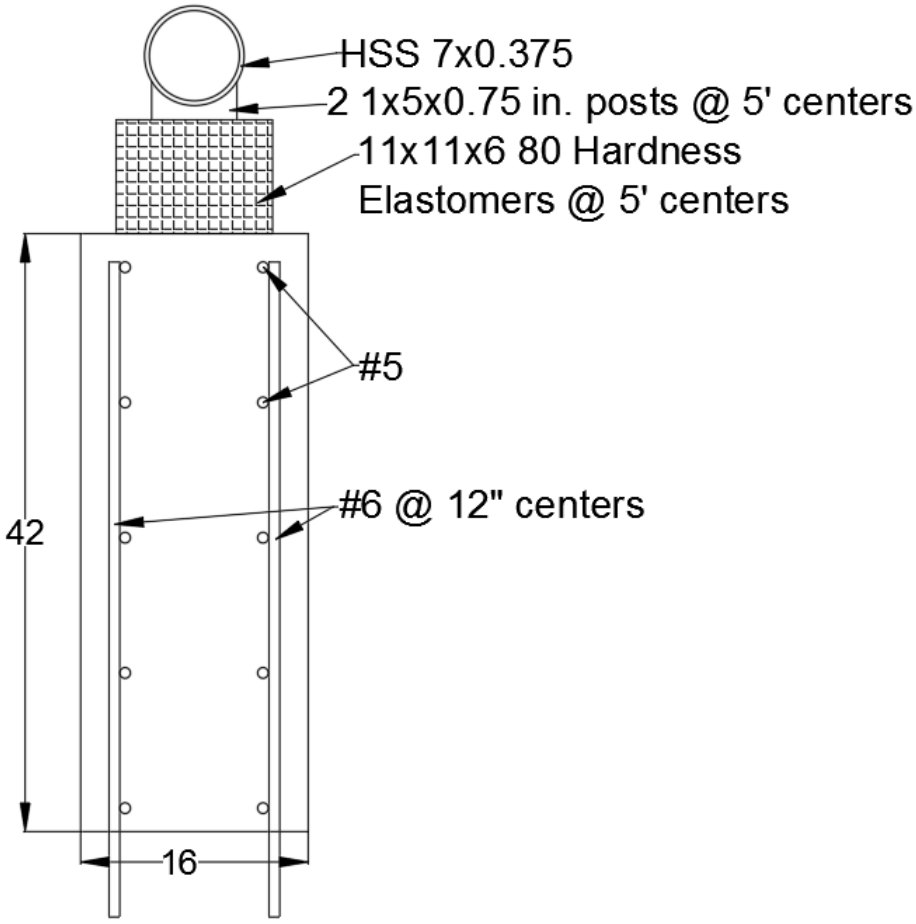

Figure 5.8 Concept 3 – Rigid Wall and Absorbing Steel Rail Example

The second configuration for the Rigid Wall and Absorbing Rail concept involves the use of a reinforced concrete beam/rail mounted atop the elastomer posts. For this concept the reinforced concrete beam was designed to have the same moment capacity as the steel rail from the previous configuration. A schematic of the Rigid Wall and Absorbing Concrete Rail is shown in figure 5.9.

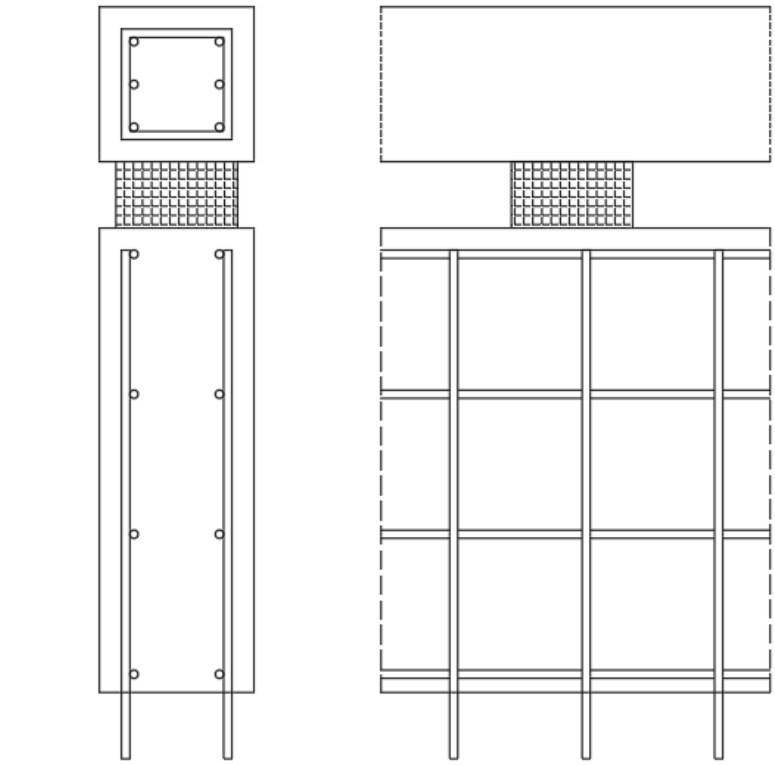

(a) Cross-Section (b) Elevation

Figure 5.9 Concept 3 – Rigid Wall and Absorbing Concrete Rail

The pros of the Rigid Wall and Absorbing Concrete Rail system include:

- The semi rigid design likely means lower overall impact forces
- Obtaining the desired capacity within the barrier height and width constraints should be easily attainable
- Interior and exterior sections could be designed to meet the loading requirements
- The top rail can be designed specifically to prevent tank-trailer roll
- The ability for passengers to see through the barrier (sightlines) and snow to be pushed through/over the barrier are likely adequate at lower parapet heights
- The opportunity for the trailer to snag/puncture on an element of the barrier is small
- Damage at TL-5 would likely be minimal

The cons of the Rigid Wall and Absorbing Concrete Rail system include:

- Accelerations in the small car and pickup test could reach maximum thresholds presented in MASH [2] as the traffic face of the barrier becomes more vertical
- High construction cost due to the elastomer posts and the difficult in-field connection between all of the components
- Attachment between the elastomer and concrete components may be difficult

From the pros and cons for the Rigid Wall and Absorbing Concrete Rail system, it was determined to have a moderate feasibility to meet the design criteria. One example of a system that was designed to meet the loading requirements is shown in figure 5.10.

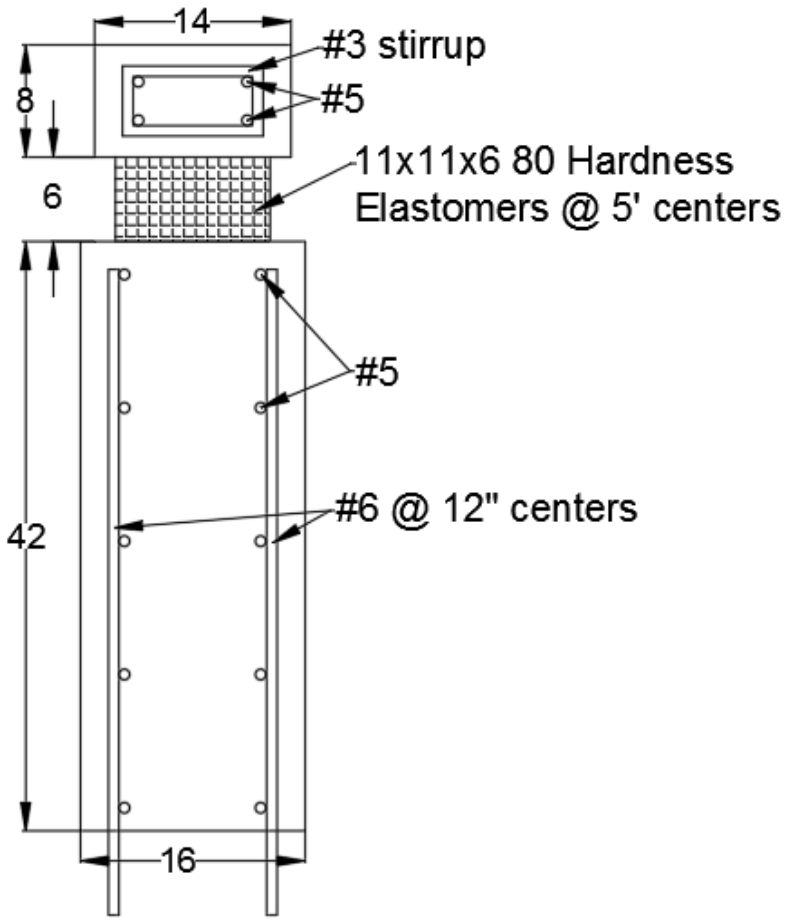

Figure 5.10 Concept 3 – Rigid Wall and Absorbing Concrete Rail Example

The last absorbing rail system concept was the Rigid Wall and Tall Elastomer Post Absorbing Rail system, as shown in figure 5.11. This system consisted of a tall elastomer post with a steel tube mounted on the side. This system was envisioned to perform similarly to the steel rail system, shown in figure 5.7, where the rail would be loaded, deform, and in turn deform the posts. Initial design and brainstorming suggested that the posts would need to be a minimum

of 14 in. tall. From the calculations presented for the loading of the elastomer posts in 0 of Appendix C , the maximum load on a single post would be greater than 20 kips. When considering the height and width/thickness (initially assumed to be around 6 in.) of the post, it was determined that using a post this tall and narrow was not feasible. Without significantly increasing the post dimensions, there was concern that the post may not be strong enough to support the weight of the rail, let alone withstand the force and deformation of an impact. This concept would also likely cost much more than the Rigid Wall and Absorbing Steel Rail system, without providing significantly more benefits. For these reasons, the Rigid Wall and Tall Elastomer Post Absorbing Rail system was deemed not feasible and was not investigated further.

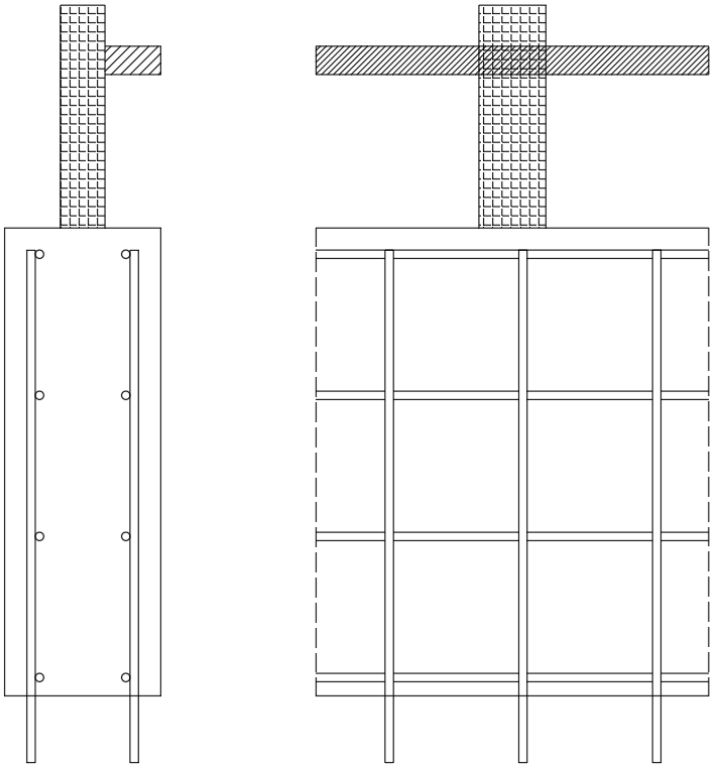

(a) Cross-Section (b) Elevation

Figure 5.11 Concept 4 – Rigid Wall and Tall Elastomer Post Absorbing Rail System

5.3 Deformable Concepts

The deformable concepts category contained barrier concepts that would experience significant displacements and deformations under TL-6 impact conditions. The deformable concepts were designed to absorb much of the impacting energy through deflection while safely containing and redirecting the vehicle.

5.3.1 Steel Rail (Concept 5)

The Steel Rail concept, as shown in figure 5.12, consisted of three horizontal steel rails connected by vertical steel posts. This concept was designed with two loads, the first being 100 kips at a height of 21 in. above the barrier base, and the second being 200 kips at the top of the barrier if the top height was less than 85 in., or at 85 in. if the top height was 85 in. or greater. The barrier was designed using the Post and Beam method in Section A13.3.2 [22]. It was targeted to have four or more posts reach ultimate load and deform. This number of posts reaching ultimate loading would ensure that the rail would behave more as a deformable system, rather than a more rigid system if only one or two posts reached ultimate load. The system would be anchored to the road surface via base plates and anchor rods.

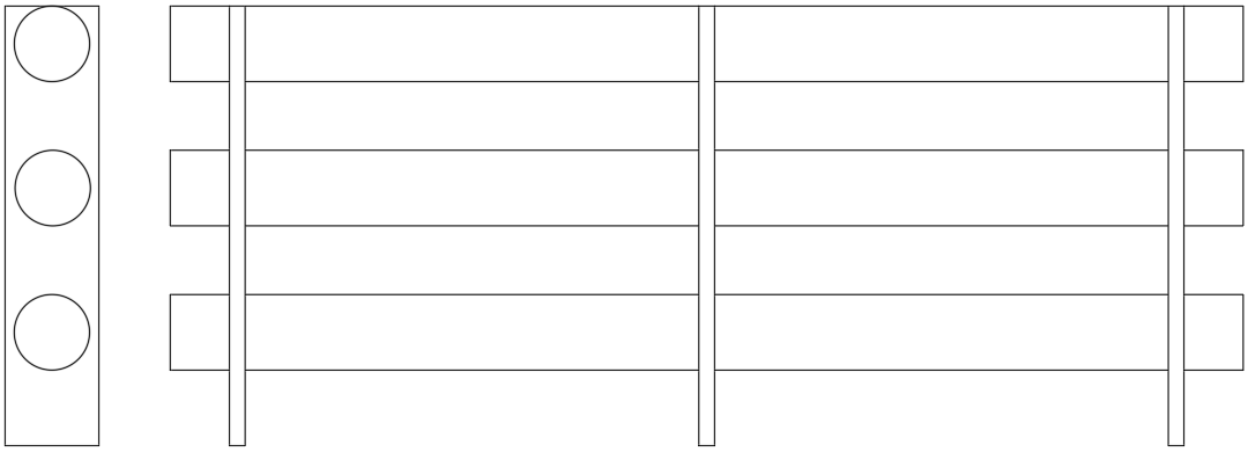

Figure 5.12 Concept 5 – Steel Rail

The pros of the Steel Rail system include:

- The deformable nature of this system will result in low impact forces, which will likely result in lower acceleration for the small car and pickup
- Obtaining the desired capacity within the barrier height and width constraints should be possible
- Interior and exterior sections could be designed to meet loading requirements
- Sightline criteria can likely be achieved

The cons of the Steel Rail system include:

- Potential for the trailer of the TL-6 vehicle to snag/puncture on a component of the barrier
- Potential for the small car and pickup to underride the lower rail or extend in between rails and snag on a post
- Damage will occur at all test levels, especially TL-4 through TL-6
- High construction and repair costs

From the pros and cons for the Steel Rail system, it was determined to have a moderate feasibility to meet the design criteria. One example of a system that was designed to meet the loading requirements is shown in figure 5.13.

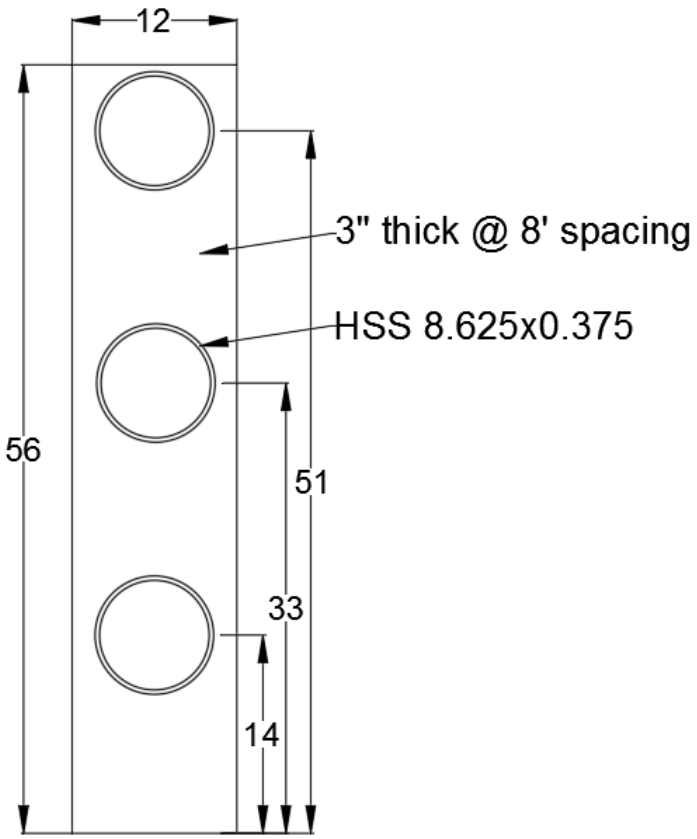

Figure 5.13 Concept 5 – Steel Rail Example

5.3.2 Crushable Wall (Concept 6)

The Crushable Wall concept, as shown in figure 5.14, had two main components: the first was an outer wall capable of transferring the impact load to the second component, the inner, crushable, energy absorbing material. This inner material could be foam, aluminum honeycomb, or another material that is able to crush and absorb the energy from impact. This material would likely be very expensive, especially in the quantity that would be needed for a significant length of barrier. Many of the brainstormed energy absorbing materials would require more maintenance than the conventional reinforced concrete and structural steel typically used in roadside barriers. Depending on the energy absorbing material, there is potential for damage at lower test levels if the material is deformable at lower loads.

For a roadside application, the traffic-side wall would be allowed to displace while the field-side wall would have to be connected to the road surface via anchor rods. In the configuration shown in figure 5.14, a median use would not be possible due to one wall having to be anchored and one being free to move.

Due to the very high cost, difficult construction and maintenance, and likely damage at all test levels, this concept was deemed not feasible to meet the design criteria and was not pursued further.

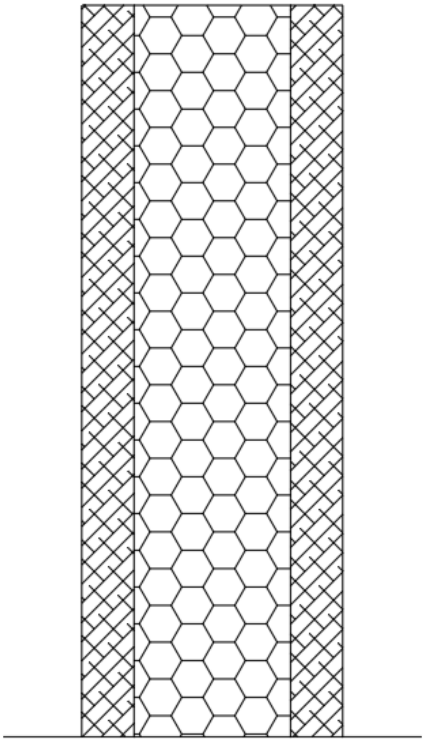

Figure 5.14 Concept 6 – Crushable Wall

5.3.3 Deformable Wall (Concept 7)

The Deformable Wall concept, as shown in figure 5.16, contained an upper reinforced concrete beam mounted to elastomer posts that were attached to the road surface, and was

inspired by the RESTORE Barrier shown in figure 5.15 [27]. When a large vehicle impacted the barrier, the whole system would displace and rotate, absorbing that energy of the impact and redirecting the vehicle. This concept was subjected to two loads: (1) 100 kips at 21 in. above the ground surface, and (2) 200 kips at the top of the barrier for barrier heights less than 85 in. or at 85 in. for barrier heights greater than or equal to 85 in. This barrier would be anchored to the roadway via anchor rods attached to the elastomer posts.

Figure 5.15 RESTORE Barrier [27]

The pros of the Deformable Wall concept include:

- Due to the deformable nature of this concept the impact forces and accelerations would be lower than that of a rigid system
- Obtaining the desired capacity within the barrier height and width constraints should be possible

- Interior and exterior sections could be designed to meet loading requirements
- The ability for the whole system to displace and rotate will help allow the trailer to roll, but prevent the trailer of the TL-6 vehicle from rolling completely over the barrier if the barrier height is sufficient
- Minimal damage at TL-3, TL-4, and possibly TL-5
- Minimal risk of tank-trailer to snag/rupture on elements of the barrier

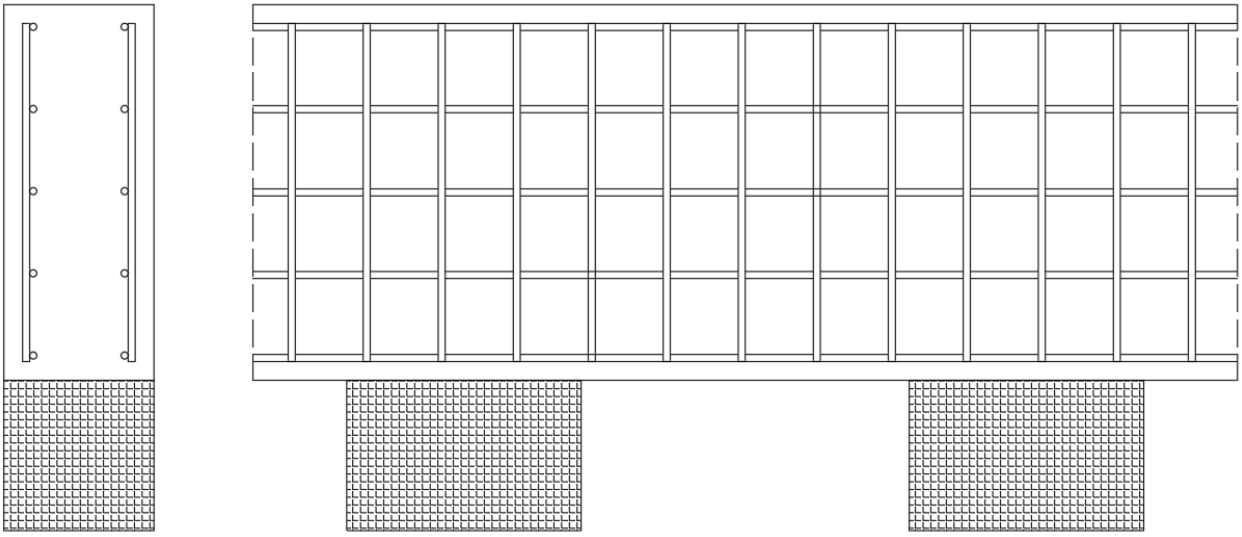

Figure 5.16 Concept 7 – Deformable Wall

The cons of the Deformable Wall concept include:

- Likely very high construction cost due to the use of elastomer and the difficulty of placing the reinforced concrete wall on top of the posts
- Sightline worsens as the height of the barrier increases
- Attachment of elastomer/rubber material to concrete could pose a challenge if simple anchor roads are not strong enough or the concrete pullout of the anchor rods in the wall is not strong enough
- The mass of the reinforced concrete section could negatively affect the energy absorbing characteristics, as the posts would have to resist not only the weight of the truck but also the weight of the barrier itself
- The potential exists for the small car and pickup to underride the reinforced concrete wall and snag on a post
- The whole system may need an alternate support system if the elastomer posts are not strong enough to support the reinforced concrete beam mounted atop; this could look like the metal feet in the RESTORE Barrier [27]

From the pros and cons for the Deformable Wall system, it was determined to have a moderate feasibility to meet the design criteria. An example of a system for Concept 7 that was designed to meet the required loading is shown in figure 5.17.

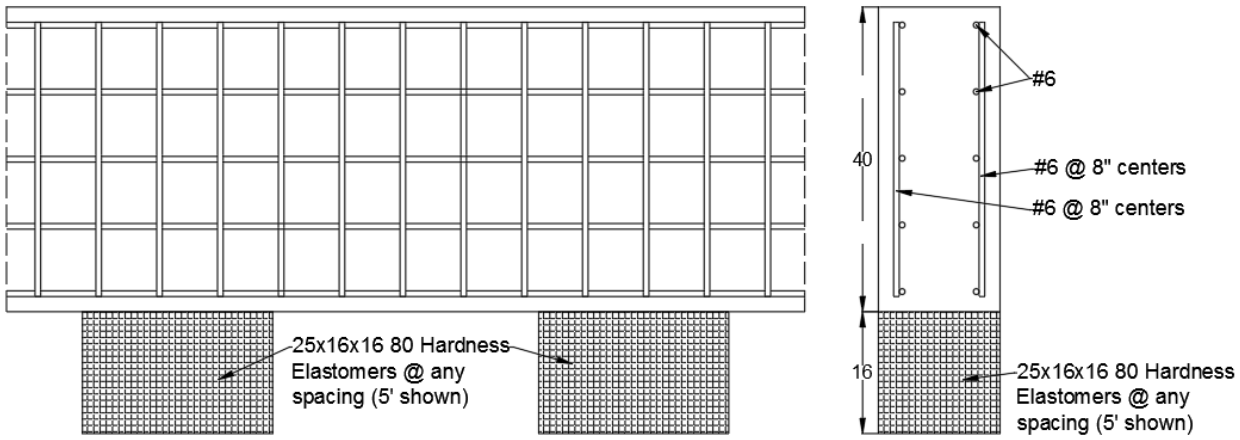

Figure 5.17 Concept 7 – Deformable Wall Example

5.4 Preferred Concept

With all concepts brainstormed, initial designs created, and pros and cons established, the preferred concepts for this project were established. Concepts 1, 2, and 3 were determined to have the highest feasibility of working and meeting the design criteria. These concepts were chosen for their simple design, easy construction, and likely ability to meet the required and many of the preferred design criteria. For parts of this project concept 1 will be used in simulation with a full scale TL-6 tractor-tank trailer vehicle. For that portion concept 3 will be used, as this was thought to be the most promising concept of the 3 preferred concepts.

Chapter 6 Minimum Barrier Height Analysis

In order to optimize the design of a new TL-6 barrier, a minimum barrier height needed to be established. The minimum barrier height was considered to be the height needed to contain and prevent rollover of a tank-trailer vehicle. In order to determine this height, a TL-6 vehicle model was created, and simulations were conducted with the vehicle model impacting rigid barriers of various heights.

6.1 Vehicle Model

A tractor-tank trailer vehicle model was created in LS-DYNA [28], as shown in figure 6.1. This tractor-tank trailer truck model was created by modifying an existing TL-5 tractor-van trailer truck model, as shown in figure 6.2, originally developed by a research team at Battelle, Oak Ridge National Laboratory and the University of Tennessee at Knoxville [29-31] and modified by Chuck Plaxico of Roadsafe, LLC and John Reid of MwRSF. The van body on the TL-5 vehicle was removed, leaving the original tractor and the rear tandem axle.

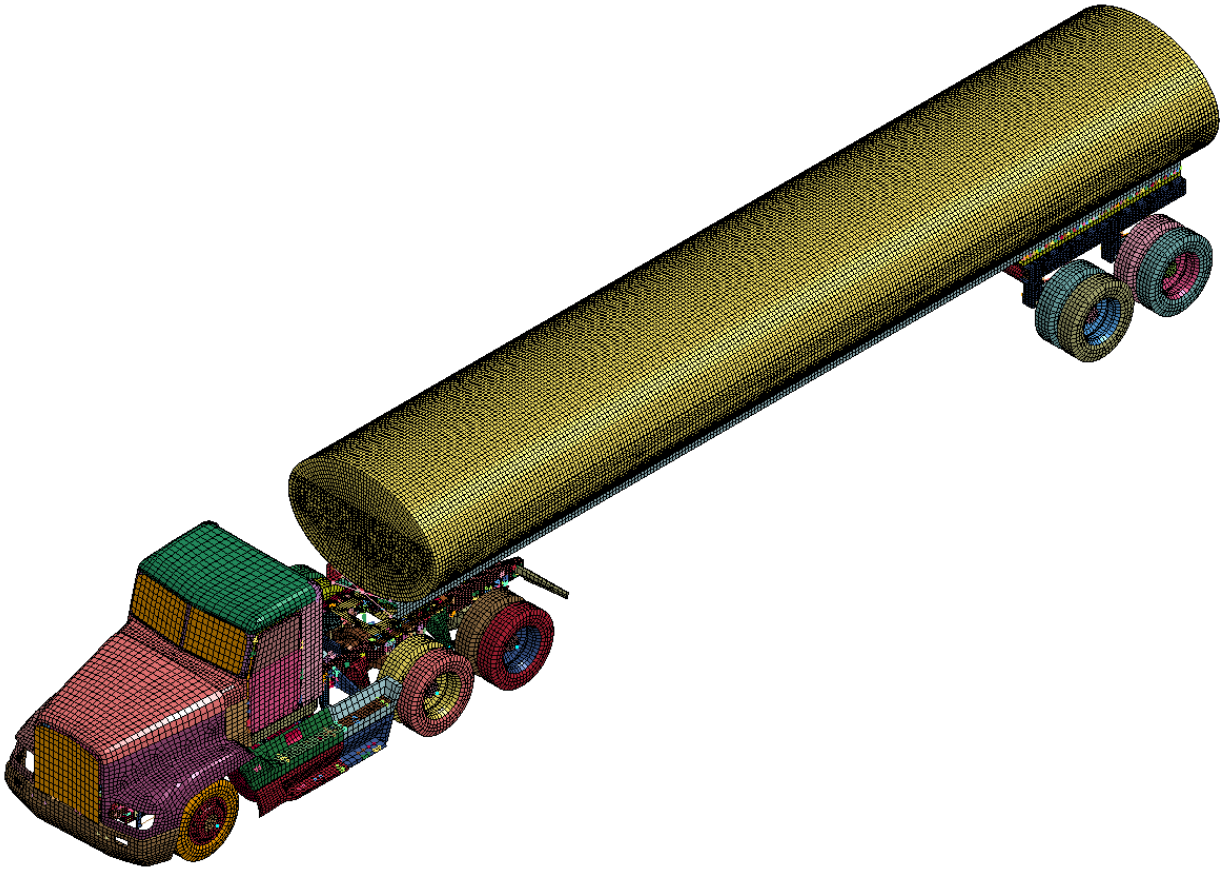

Figure 6.1 TL-6 Truck Model

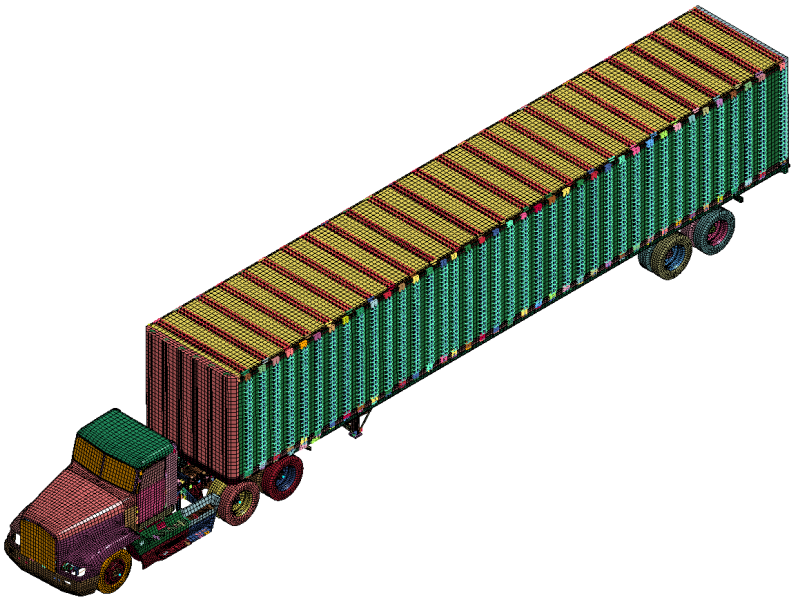

Figure 6.2 TL-5 Truck Model

The TL-6 truck geometry was determined based on the measurements taken during the vehicle dimension survey, outlined in Section 2.5 . The tank was an elliptical cylinder 92 in. wide, 63 in. tall, and 488 in. long. The tank shells were ¼ in. thick. The tank was attached to two C-channel rails with 4-in. wide flanges and an 8-in. tall web, ½ in. thick. Two 4-in. x 4-in. square tube spacer rails were also between the C-channels and the rear tandem axle to align the tank at the correct height. Spanning between the two C-channels at the front of the tank was a fifth-wheel plate which was used to attach the tank to the fifth wheel attachment used in the previous TL-5 model. The parts of the trailer were connected with *CONSTRAINED_NODAL_RIGID_BODIES (CNRBs).

The ballast for the model was solid elements with a pure Lagrangian element formulation (ELFORM=1) with the properties of water. This element formulation was relatively simple when compared to other material element formulations that can be used to model fluid. The material properties assigned to the ballast were those of water at room temperature (72°F), i.e., a density of 1.0 E-6 kg/mm^3, Poisson's Ratio of 0.2, and bulk modulus of 2.15. The empty vehicle weight was 25,050 lb, and 54,793 lb of water ballast was added, resulting in a total weight of 79,843 lb. Details on the parts used in the trailer of the TL-6 truck model are shown in figure 6.3 and table 6.1. The TL-6 vehicle model was prescribed a velocity of 50 mph.

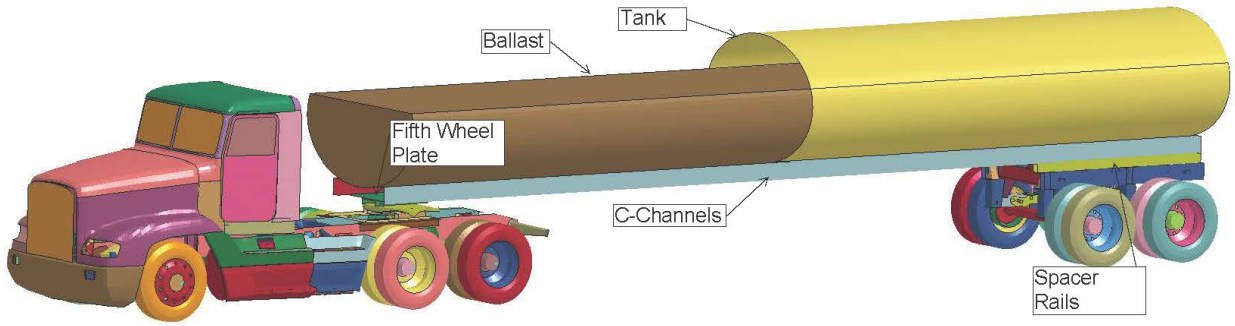

Figure 6.3 TL-6 Truck Parts (Some Parts Hidden for Clarity)

Table 6.1 Tl-6 Trailer Model Parts

Part Name	Element Type	Element Formulation	Material Type	Material Formulation
Tank	Shell	Fully Integrated (16)	5454-H32 Aluminum	Piecewise, Linear Plasticity
C-Channels	Shell	Fully Integrated (16)	T304 Stainless Steel	Piecewise, Linear Plasticity
Spacer Rails	Shell	Fully Integrated (16)	T304 Stainless Steel	Piecewise, Linear Plasticity
Fifth-Wheel Plate	Shell	Fully Integrated (16)	T304 Stainless Steel	Piecewise, Linear Plasticity
Ballast	Solid	Constant Stress (1)	Water	Elastic

6.2 Simulation Validation

To validate the TL-6 vehicle model, a simulation of the Instrumented Wall Test [10] was created, as shown in figure 6.4, and the results were compared. Sixteen rigid walls, created using *RIGIDWALL_PLANAR_FINITE, were used to simulate the 16 load cells that were placed behind four wall sections in the full scale crash test, which were 120 in. by 90 in. tall. Each simulated wall was 60 in. long and 45 in. tall. The truck model impacted the barrier model at 15 degrees and 54.8 mph (88.19 km/h) at a point approximately 90 in. from the upstream edge, which is similar to the impact conditions in the full scale crash test. Sequential photographs of the simulation are shown in figure 6.5.

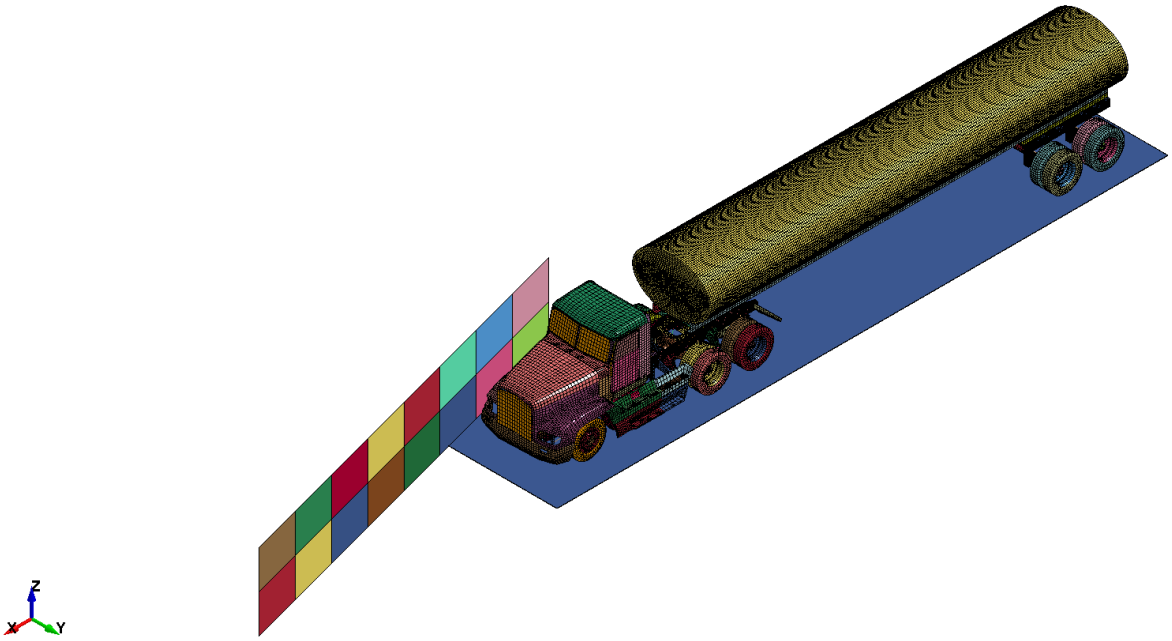

Figure 6.4 Instrumented Wall Simulation

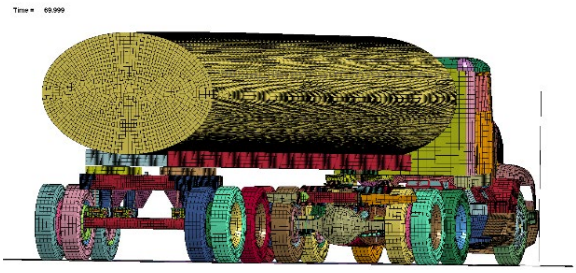

t = 0 msec

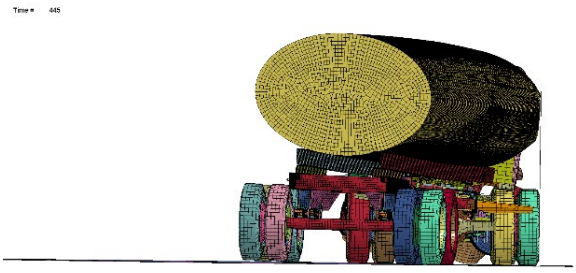

t = 375 msec

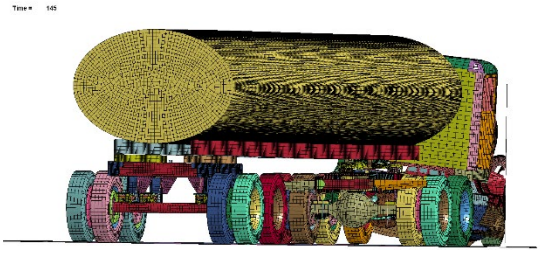

t = 75 msec

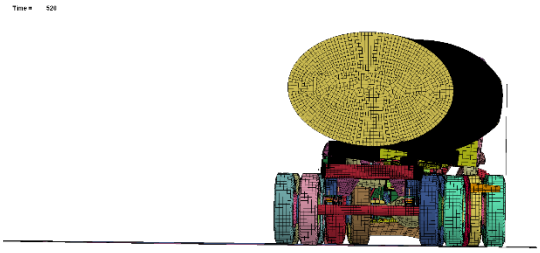

t = 450 msec

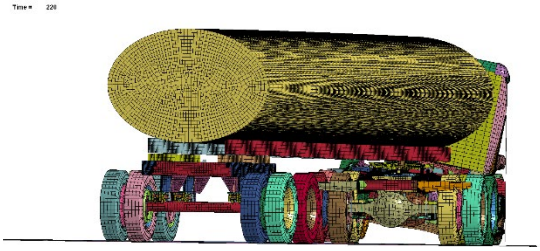

t = 150 msec

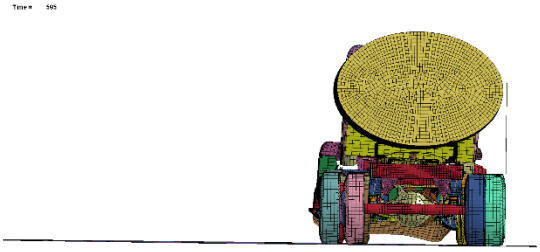

t = 525 msec

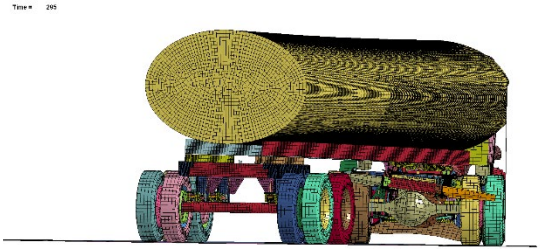

t = 225 msec

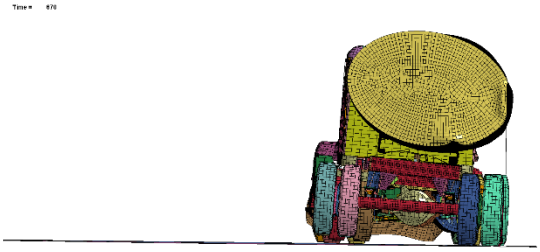

t = 600 msec

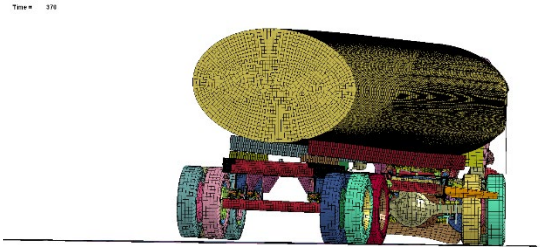

t = 300 msec

Figure 6.5 Instrumented Wall Validation Simulation Sequentials

Angular displacements were recorded in the full-scale crash test at the center of gravity of the tractor. From the simulation, the x, y, and z rotational velocities of the tractor were exported and the Euler roll, pitch, and yaw could be calculated. The angular displacements were compared between the simulation and full scale crash test, as shown in figure 6.7. A schematic of the angular displacements is shown in figure 6.6. The pitch for both the simulation and the full scale crash test were minimal. The yaw from both the simulation and test followed the same trend, with the simulation having higher magnitudes after approximately 175 msec. Finally, the roll was very similar for the first 275 ms, but then diverged afterward. The initial roll being similar between the simulation and the test was a good indication that the beginning of the simulation, or the tractor impact into the barrier, was representative of the full scale crash test. However, the tank impact was less accurate.

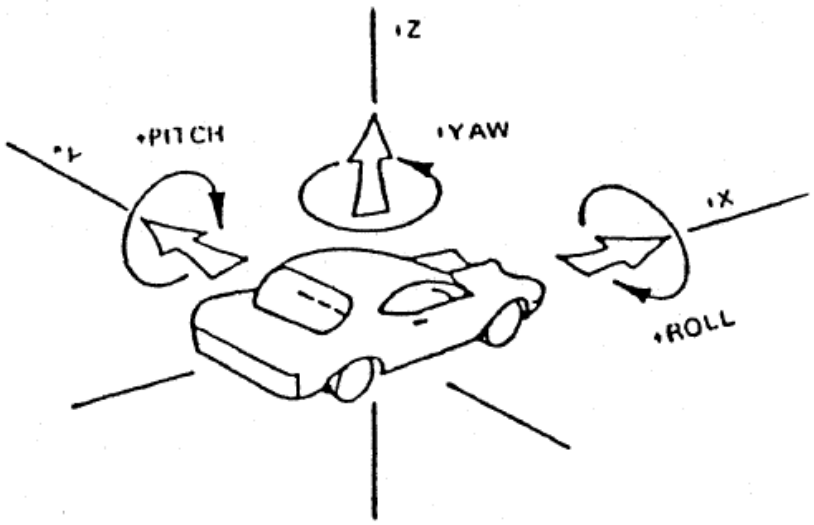

Figure 6.6 Angular Displacement Schematic

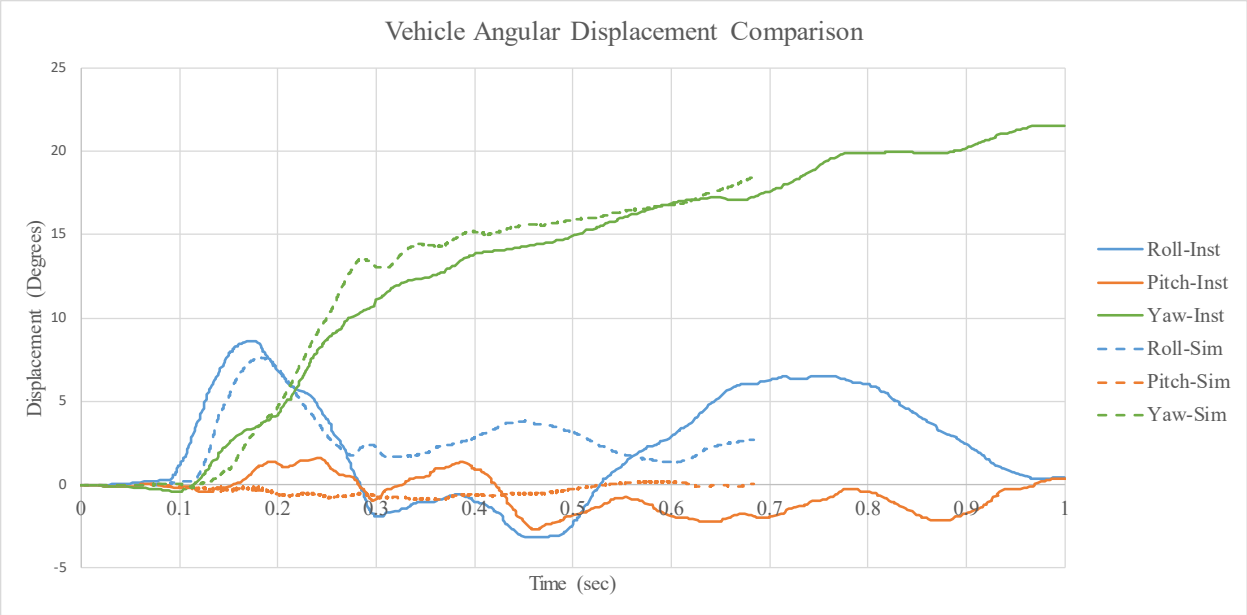

Figure 6.7 Vehicle Angular Displacement Comparison

The accelerations at the tractor model accelerometer were compared to the accelerometer data from the crash test, which was also located at the tractor c.g. A comparison of the lateral and longitudinal accelerations are shown in figures 6.8 and 6.9, respectively.

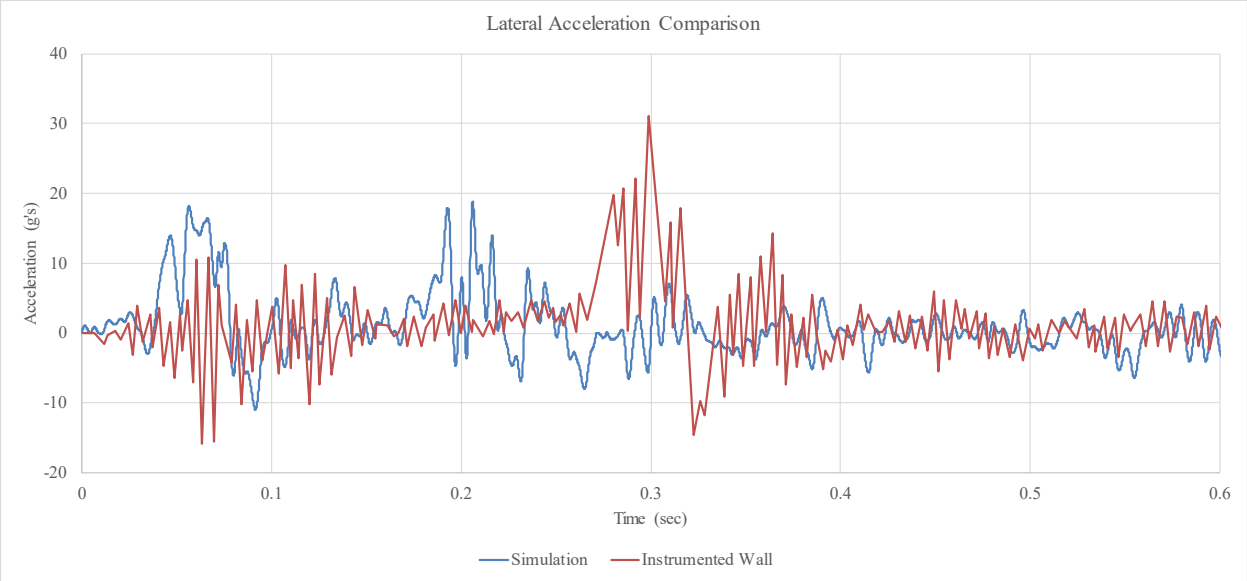

Figure 6.8 Lateral Acceleration Comparison

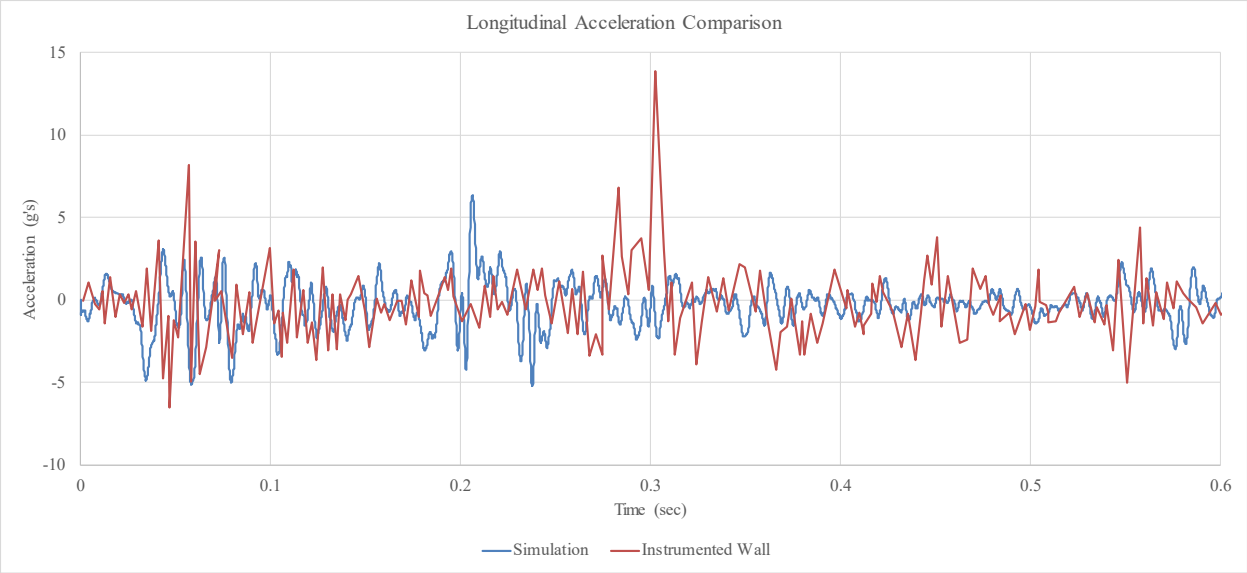

Figure 6.9 Longitudinal Acceleration Comparison

From the lateral acceleration comparison, the initial impact of the tractor (the first set of peaks) was larger in the simulation than the Instrumented Wall test, but not significantly. The second peak, which occurred about 100 msec sooner in the simulation than the full scale test and was a result of the front of the tank impacting the barrier, was larger in the full scale test than the simulation. The largest 50 msec average in the Instrumented Wall test was reported as 12.3 g as compared to 8.7 g in the simulation. Overall, the general trend of the two tests was similar, but the magnitude and timing was shifted.

The longitudinal acceleration shows similar trends to that of the lateral acceleration. Increased accelerations during the tractor and front trailer impact occurred in the full scale test versus the simulation. The largest 50 msec average in the full scale test was 2.1 g versus 1.0 g in the simulation data. Again, the general trend was similar, with the full scale test having higher values throughout.

The forces exerted on the simulated barrier were extracted from the rigidwalls. A 50-msec rolling average was applied, as shown in figure 6.10, to match the filtering performed on

the Instrument Wall test data. The forces from all of the walls were then added together, resulting in a total load. The loads from the simulation and the Instrumented Wall test are shown in figure 6.11. When comparing the forces, three distinct peaks can be seen: the front of the tractor, the front of the trailer and tractor tandem axle, and the rear tandem axle tail slap. The time at which these impacts occurred were shifted. However, the time between peaks appears very similar between the Instrumented Wall test and the simulation results.

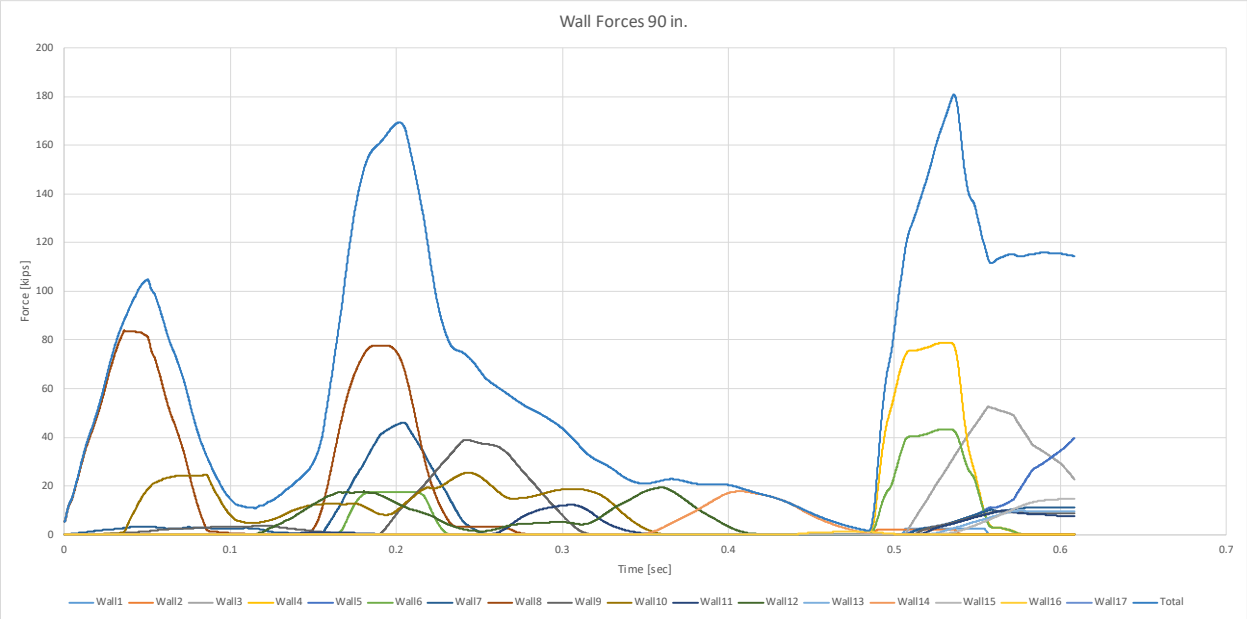

Figure 6.10 90-in. Model Wall Forces

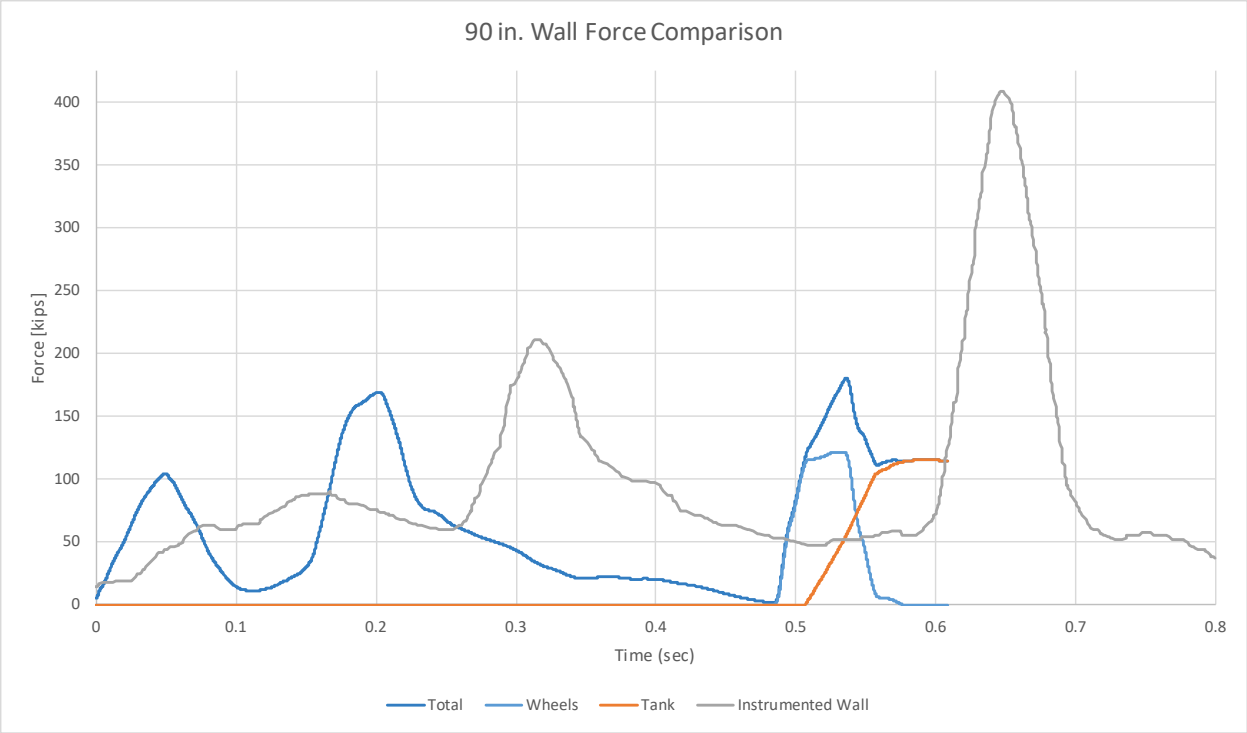

Figure 6.11 Wall Force Comparison

The most important aspect was the magnitude of the load being imparted onto the barrier. To determine the total force, all sixteen walls were summed together. The first peak load in the Instrumented Wall test was 91 kips as compared to 104 kips in the simulation. The second peak loads were 212 kips and 169 kips for the Instrumented Wall and simulation, respectively. Lastly, the largest expected load, the rear tandem, exerted 408 kips in the Instrumented Wall test and 181 kips in the simulation. This load was much lower than expected from the rear tandem. The rear tandem load was separated, that from the tires of the rear tandem axle and that from the tank. Due to the height of the walls, the bottom walls were summed to get the axle load and the upper walls were summed to get the tank load. The tank and the rear tandem axles exerted a very similar peak load. The tank load was expected to be twice that of the axle load based on previous assumptions. Thus, there were some concerns that the simulation was not accurately representing barrier forces.

When analyzing the wheel and tank loads in figure 6.11, the wheels impact the wall first, followed by the tank. Thus, their peak forces did not align. This shift was thought to be one of the main reasons that the total load was much smaller than the actual load. To determine if this had an effect, a new barrier model was created with the top walls moved 4.21 in. (160.9 mm) toward the traffic side of the barrier, which was the lateral distance from the outside of the rear-tandem tires to the outer-most point on the tank, as shown in figure 6.12. This change allowed both the tank and the rear tandem axle to impact the barrier at the same time, as shown in figure 6.13, as opposed to the rear tandem impacting before the tank impact as it rolled toward the barrier.

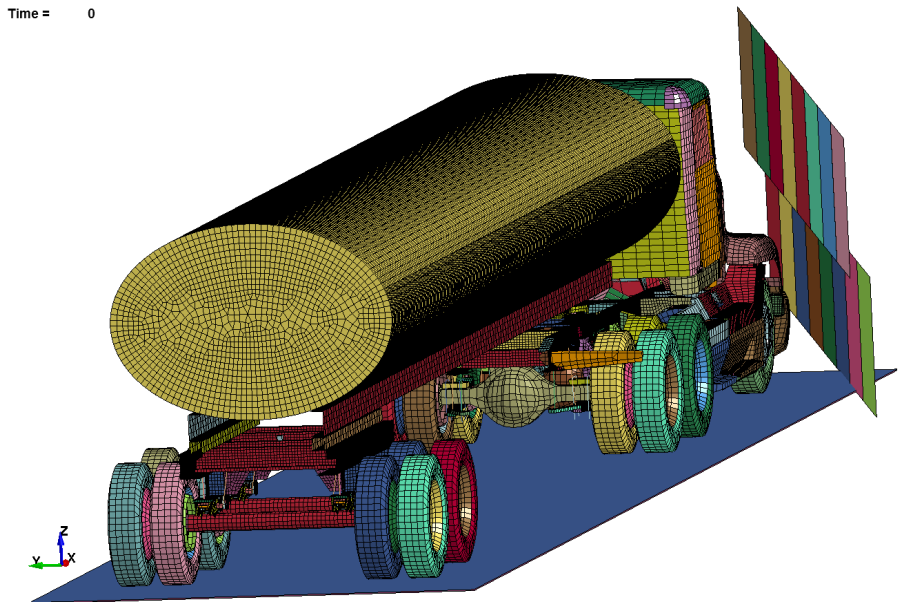

Figure 6.12 Modified 90-in. Wall Simulation

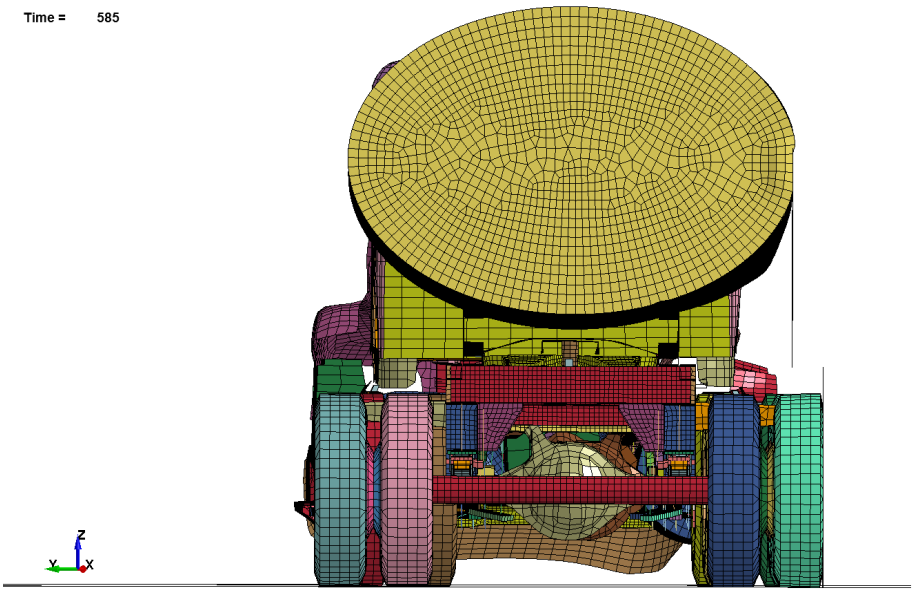

Figure 6.13 Modified 90-in. Wall Simulation Impact

Moving the barrier toward the traffic side allowed the maximum impact force from the rear tandem tires and the tank to occur at the same time, resulting in a much higher load than in the previous simulation. The load in all rigidwalls is shown in figure 6.14. There were three different impacts, with each subsequent impact increasing in magnitude. The first impact was 108 kips, the second was 173 kips, and the final impact was 243 kips.

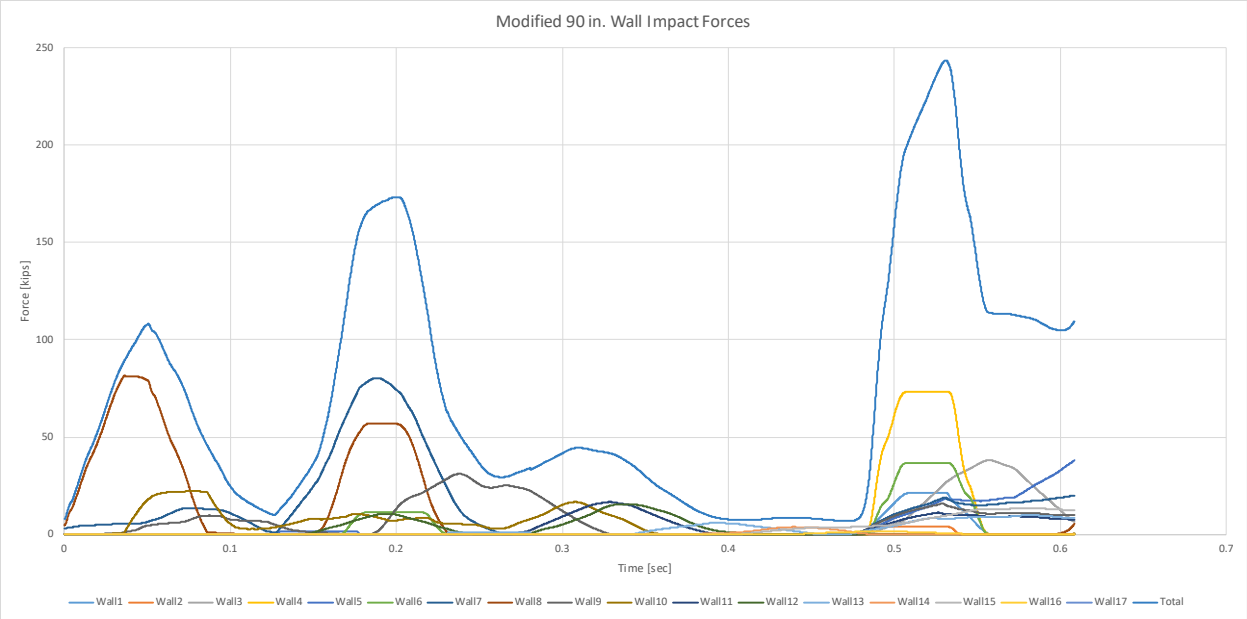

Figure 6.14 Modified 90-in. Wall Impact Forces

A comparison of the original, modified, and Instrumented Wall loads is shown in figure 6.15. The wheel and tank loads for the original and modified simulations were very similar in magnitude. In the original simulation, the wheels impacted first and approximately 50 ms later, the tank rolled toward the barrier before it impacted, thus the two components never exerted their maximum load at the same time. In the modified system, while the loads are approximately the same magnitude, they occurred closer in time; thus, the sum of the two loads was much greater.

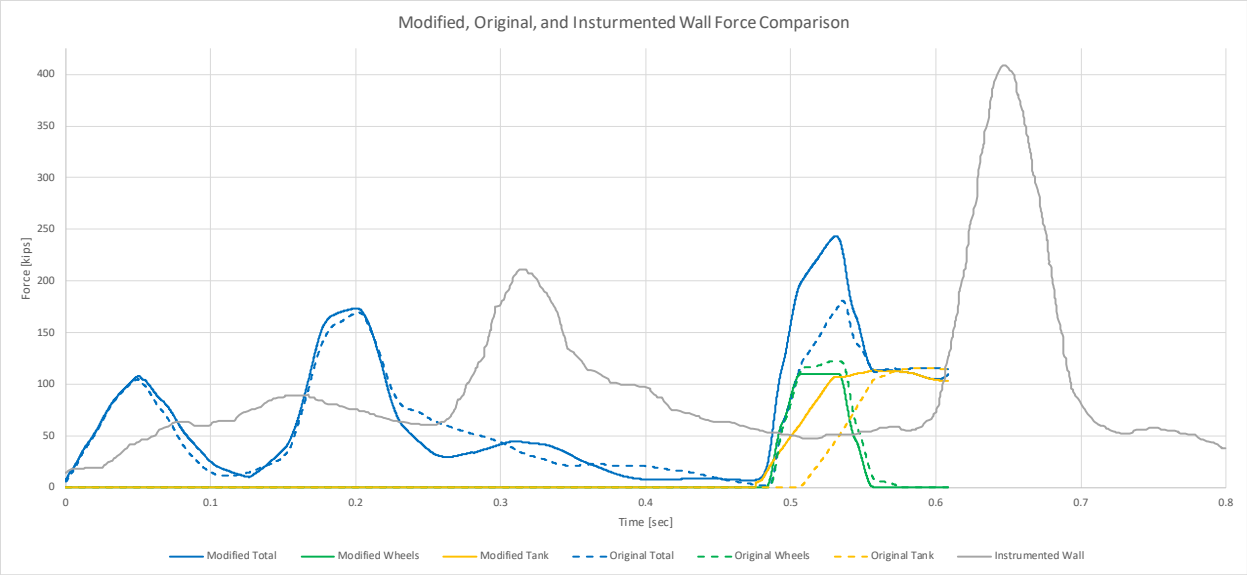

Figure 6.15 Modified, Original, and Instrumented Wall Force Comparison

While the modified simulation did not directly portray the barrier configuration used in the Instrumented Wall test, the impact force was closer in magnitude to that which occurred in the Instrumented Wall test. It was determined that the new TL-6 truck model was not representative of the impact from the Instrumented Wall test. However, the geometry of the new truck model was different than the 1971 tractor and 1968 trailer from the Instrumented Wall test, as the truck model was based on much newer tractor-trailers. Since no recent TL-6 crash tests exist, it may not be possible to fully validate a new truck model with old tests with outdated test vehicle. Thus, the new TL-6 truck model was continued to be used for the remainder of the study. However, the barrier forces and results were used cautiously considering the limitations of the model.

6.3 Lower Barrier Height Simulations

The original Instrumented Wall validation simulation, although not fully validated as forces were underpredicted, was used to further study the minimum barrier height for a TL-6 vehicle. The model layout is shown in figure 6.16. The length of the sixteen rigidwalls were kept

consistent, but the height was lowered based on the overall barrier height that was being simulated. The heights of each rigidwall were made to be one-half of the overall barrier height that was being simulated. Two additional rigidwalls, one longitudinal wall at the end of the system, and one 18-in. wide wall on the top face of barrier were added to the sixteen original rigidwalls. These two additional rigidwalls were added to more accurately represent the length of a real installation and to allow the tank to lean on top of the barrier during a full scale crash test. This configuration was selected so that the applied force magnitude and location could be analyzed separately for different wall locations.

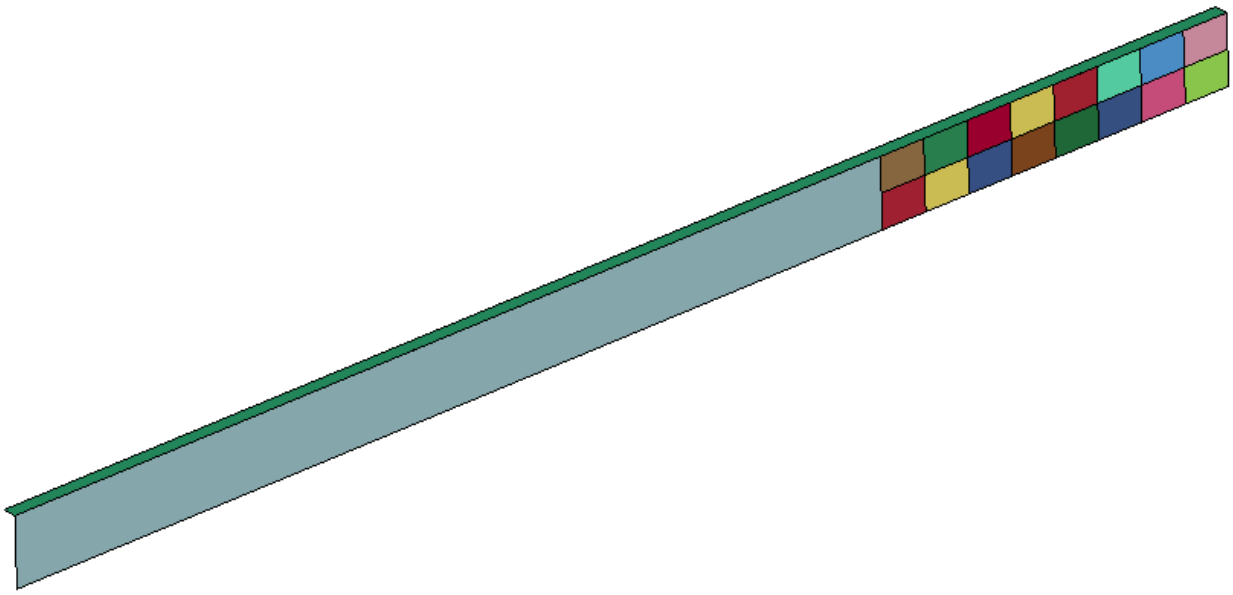

Figure 6.16 Barrier Height Study Example Barrier

In total, 17 simulations were run at the following heights: 50, 55, 60 through 70, 75, 80, 85, and 90 in. The vehicle impacted the barrier at 50 mph and an angle of 15 degrees to simulate a MASH test designation no. 6-12 test. The impact point was the same as in the simulation validation, approximately 90 in. downstream from the upstream barrier edge. Sequential photographs of four different barrier heights, 50, 62, 70, and 90 in., are shown in figures 6.17

through 6.20, respectively, as exemplar results of short, moderate, and tall barriers. These barrier heights of 50, 62, 70, and 90 in. were used throughout this chapter to illustrate general trends for each parameter as the barrier height changed.

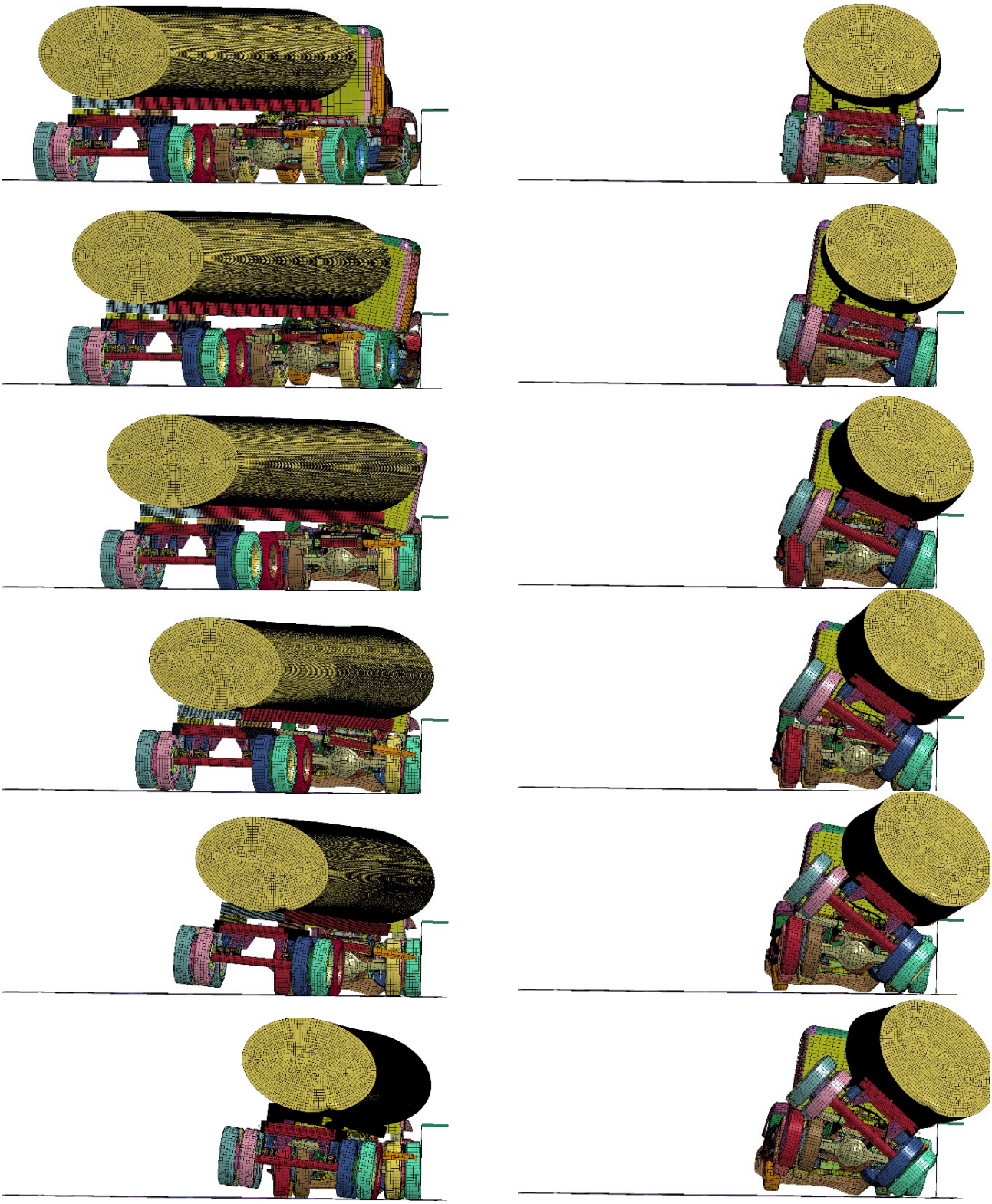

Figure 6.17 50-in. Barrier Sequentials (every 100 ms)

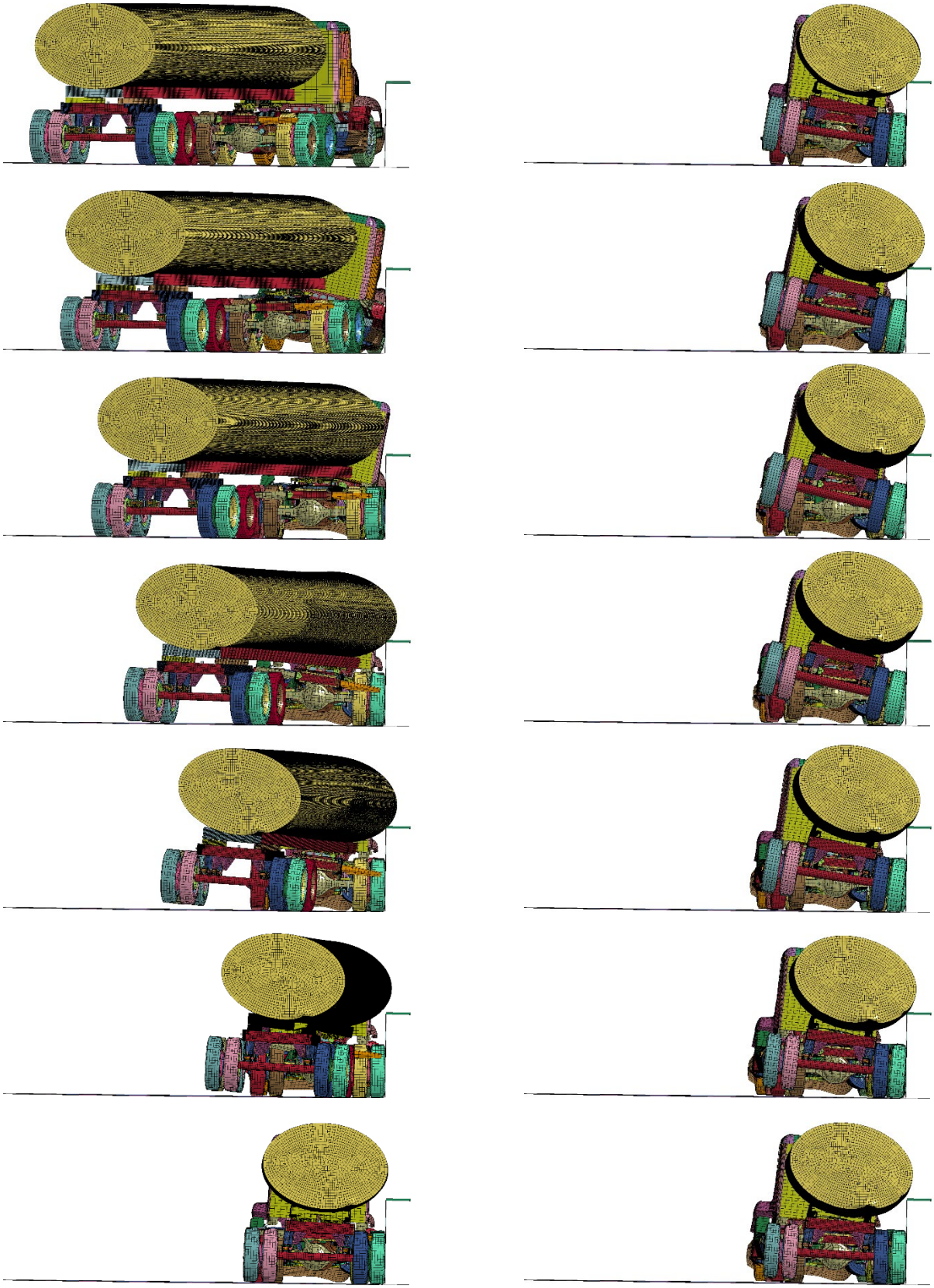

Figure 6.18 62-in. Barrier Sequentials (every 100 ms)

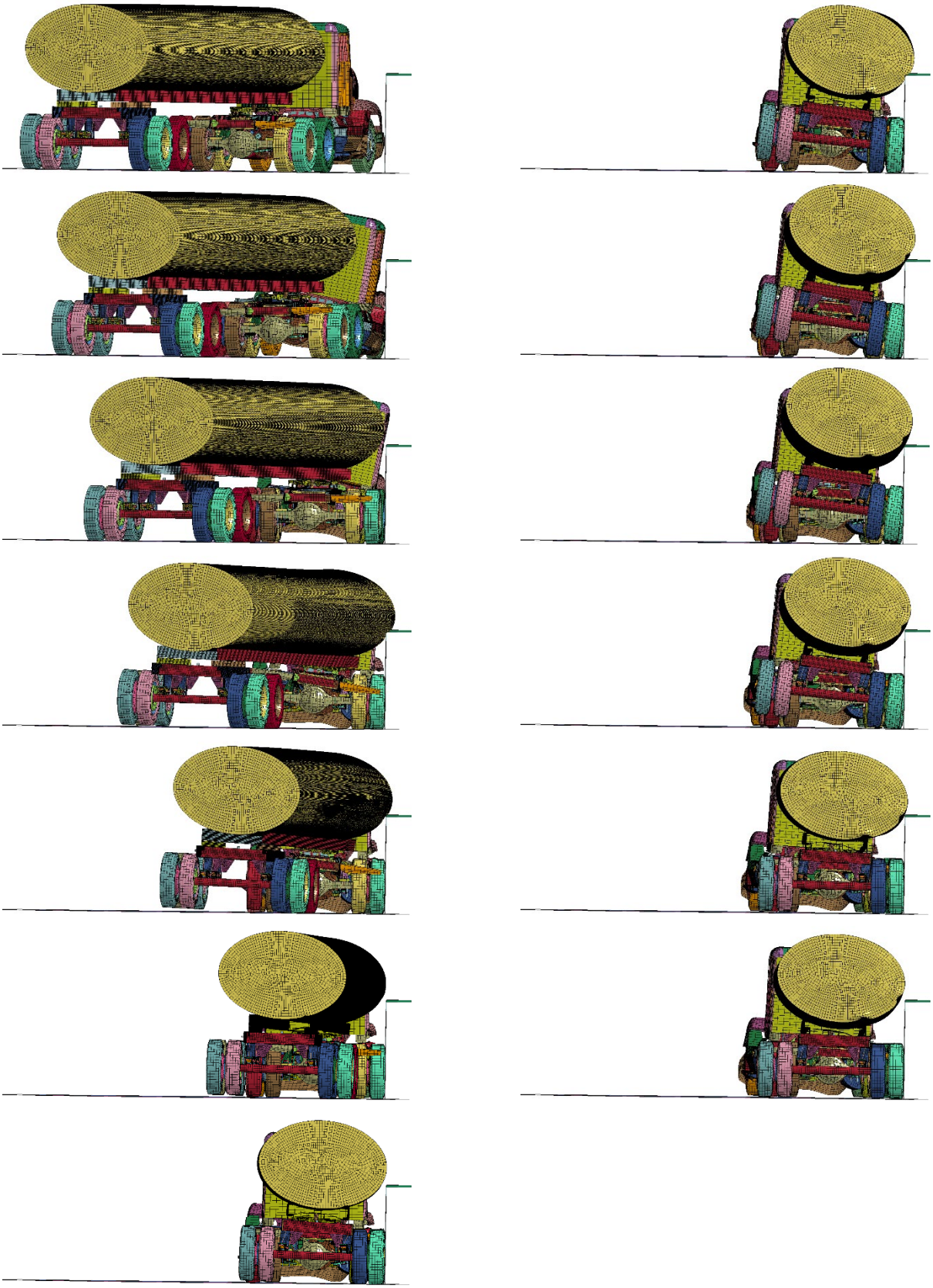

Figure 6.19 70-in. Barrier Sequentials (every 100 ms)

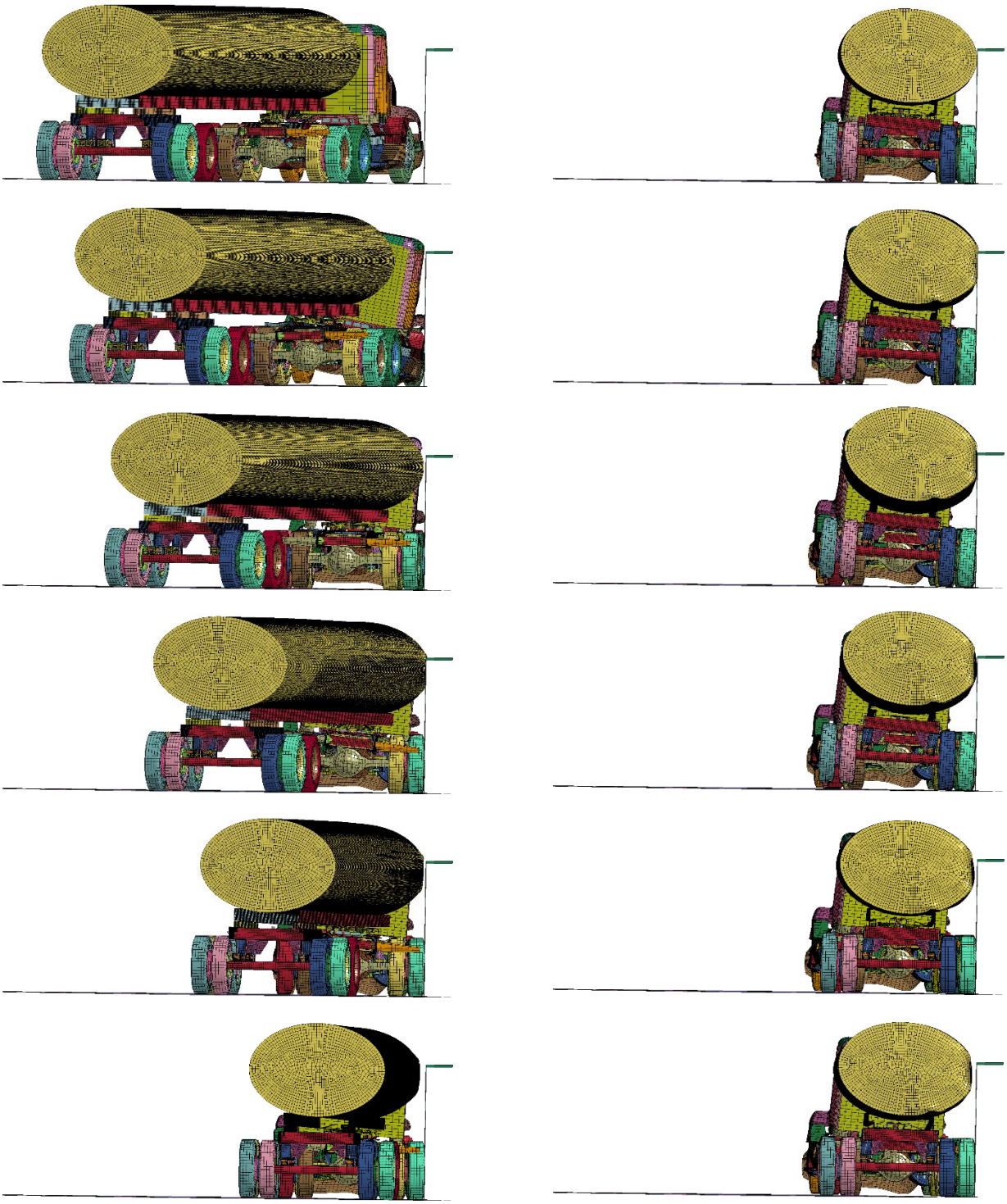

Figure 6.20 90-in. Barrier Sequentials (every 100 ms)

The roll, pitch, and yaw, lateral and vertical intrusion, impact forces, and other parameters were compared for different barrier heights, and recommendations for a minimum barrier height were derived.

The x, y, and z-rotational velocities, measured at the rear tandem axle of the trailer, were exported from the results for each simulation, and the Euler roll was calculated, as shown in figure 6.21. In the 50-in. tall barrier simulation, the truck rolled toward the barrier, but the simulation stopped at 1,171 ms. Although the simulation had an unresolvable error prior to being able to determine whether the vehicle would roll completely over the barrier or back toward the roadway, the roll angle was increasing at the simulation termination. The roll experienced with the 50-in. barrier model was much larger than the roll that would be desired in a full scale test, thus a 50-in. tall barrier was deemed too short.

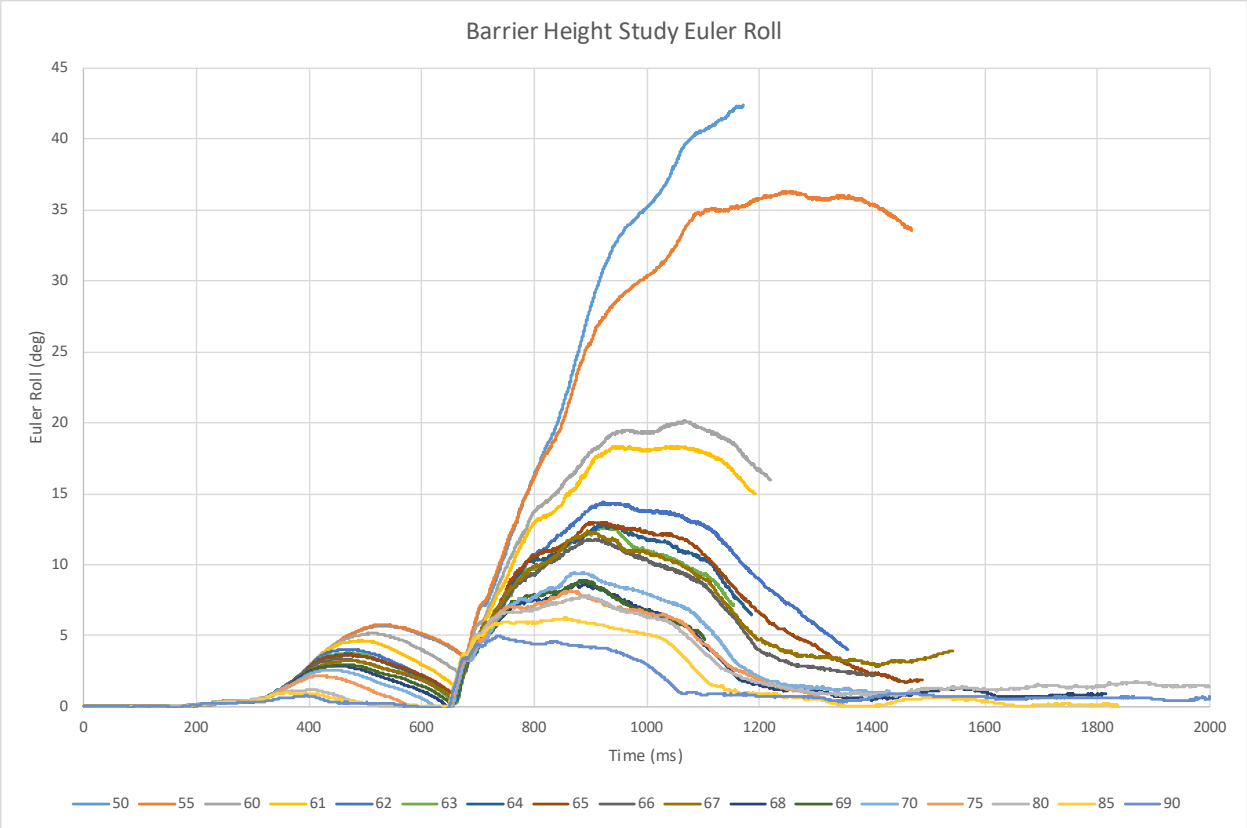

Figure 6.21 Barrier Height Study Euler Roll

The 55-in. barrier displayed similar initial results to the 50-in. barrier, but the vehicle began to roll back toward the roadway and did not roll over the barrier completely. Although the truck did not roll over, the researchers believed that this amount of roll was excessive, when considering the limitations noted previously. With larger barrier heights, a general trend of taller barriers resulting in less roll was clearly established. While many of the simulations did not run to completion due to unresolved errors, they ran long enough to determine that all barrier heights above 60 in. resulted in the truck rolling back toward the traffic side of the barrier.

The maximum roll vs. barrier height is shown in figure 6.22. There is not a known maximum roll value that is the threshold between a tractor-tank trailer vehicle rolling over or not rolling over a barrier. Whether or not the vehicle rolls over the barrier is dependent on the barrier

height, distribution of mass inside the tank, and shape of the barrier and tank, amongst many other factors. However, the researchers believe that moderate roll would be acceptable to prevent complete roll over of the top of the barrier and also prevent rollover on the front side of the barrier during a full scale crash test.

The maximum roll change between the 55- and 60-in. tall barriers was a substantial decrease of 16.2 degrees, and from 61 to 62 in. there was also another large decrease of 4.0 degrees. For barrier heights between 62 and 67 in., there was a general trend of decreasing maximum roll, but there were no substantial changes from one height to another. Between 67 and 68 in. tall barriers, there was another significant decrease in maximum roll of 3.7 degrees. For barrier heights above 68 in., the maximum roll is decreased minimally.

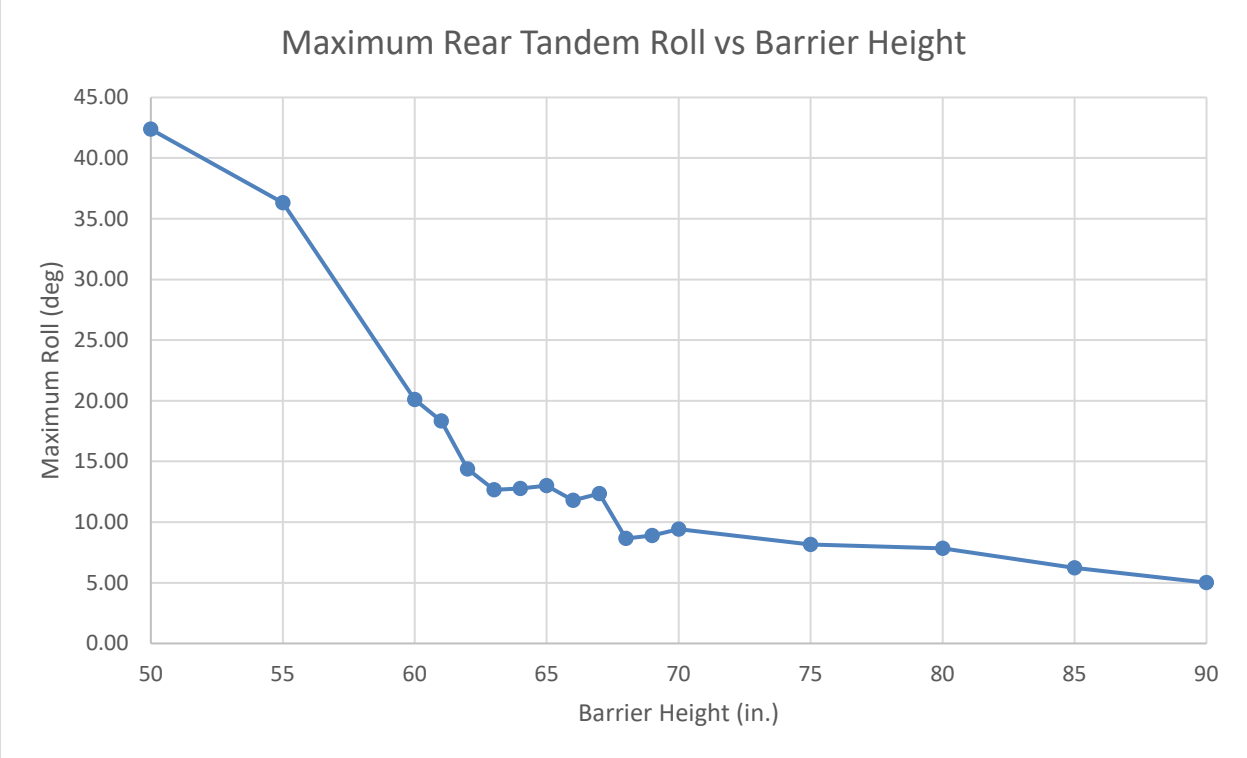

Figure 6.22 Barrier Height Study Maximum Roll

To illustrate the changes in maximum roll, figures 6.23 through 6.26 capture the instant of maximum roll for barrier heights of 50, 62, 70, and 90 in., with the time noted in ms. From the roll of the simulated vehicle, a barrier height of 62 in. was recommended due to the large decrease in roll from 61 to 62 in., the magnitude of the maximum roll (14.37 deg), and the general shape of the roll vs. time graph. This initial recommendation was somewhat conservative due to the limitations of the model. Thus, it may be possible to have a rigid, vertical-face barrier around 55 in. if height that prevents a tractor-trailer vehicle from rolling over the top of the barrier.

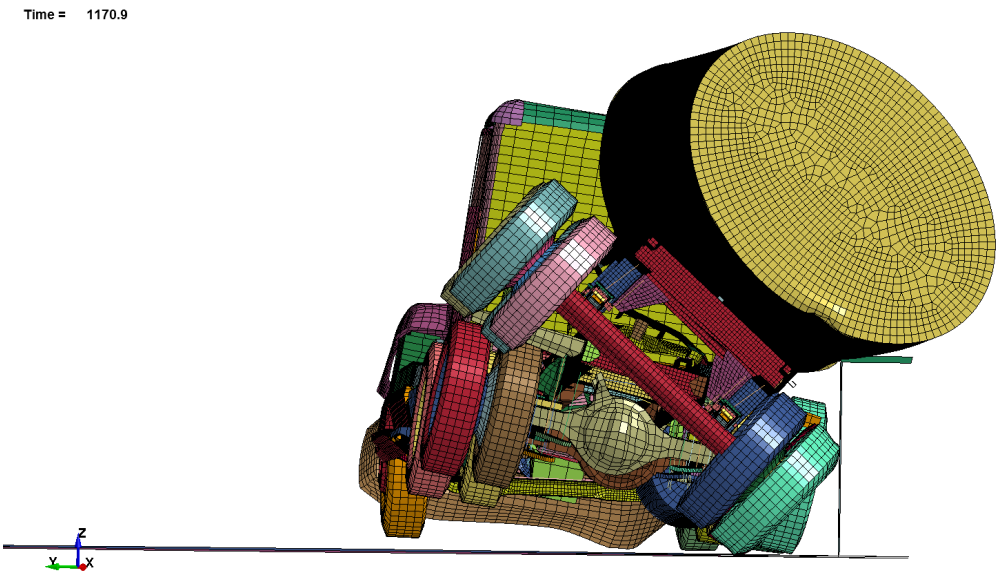

Figure 6.23 50-in. Barrier Maximum Roll

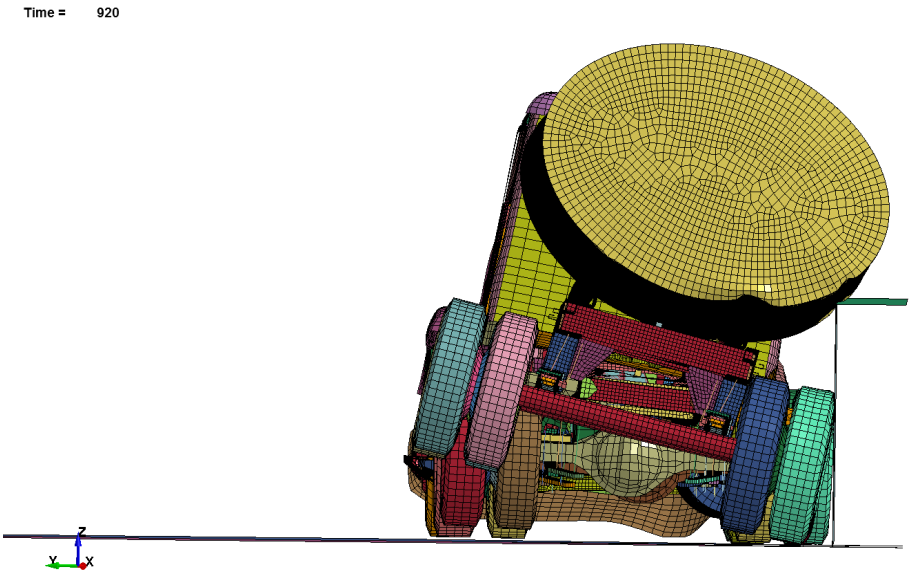

Figure 6.24 62-in. Barrier Maximum Roll

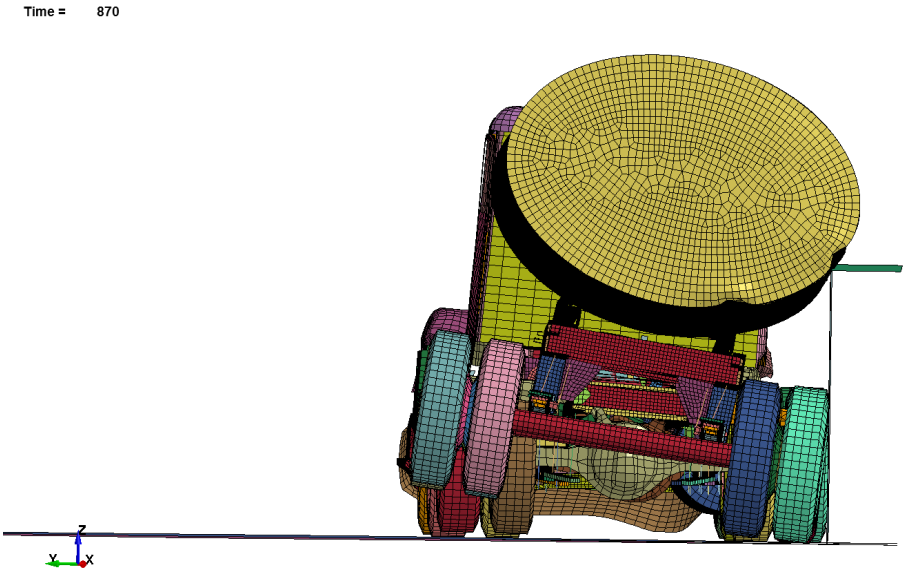

Figure 6.25 70-in. Barrier Maximum Roll

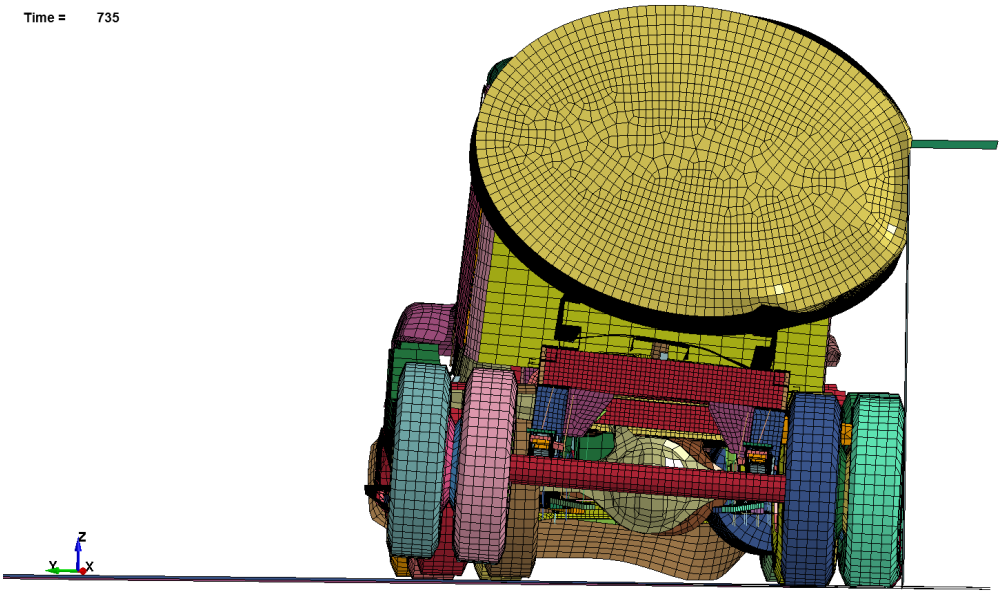

Figure 6.26 90-in. Barrier Maximum Roll

6.4 Barrier Height Study Intrusion

The second parameter that was used to estimate the minimum TL-6 barrier height was the level of intrusion, both laterally and vertically, of the extent of the tank behind the front face of the barrier. A schematic of these intrusions is shown in figure 6.27. This intrusion provided an indication of where an errant vehicle could impact a hazard on top of or behind the barrier.

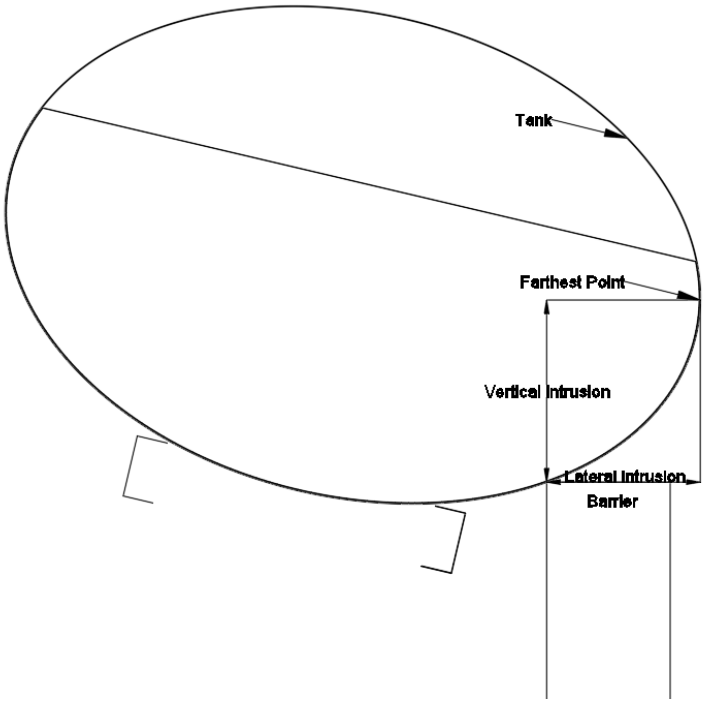

Figure 6.27 Trailer Intrusion Schematic

The lateral intrusion, or the distance from the front face of the barrier to the farthest edge of the tank, for the various barrier heights is shown in figure 6.28. The taller barriers experienced less lateral intrusion. The graph also appears to depict a diminishing return effect as the barrier height increases; that is to say that the change from a barrier height of 60 to 65 in. is larger than the change from a barrier height of 75 to 80 in. Two regions are of particular interest, 63 to 65 in. and 68 to 70 in. In these regions, there was minimal change in lateral intrusion between the different barrier heights.

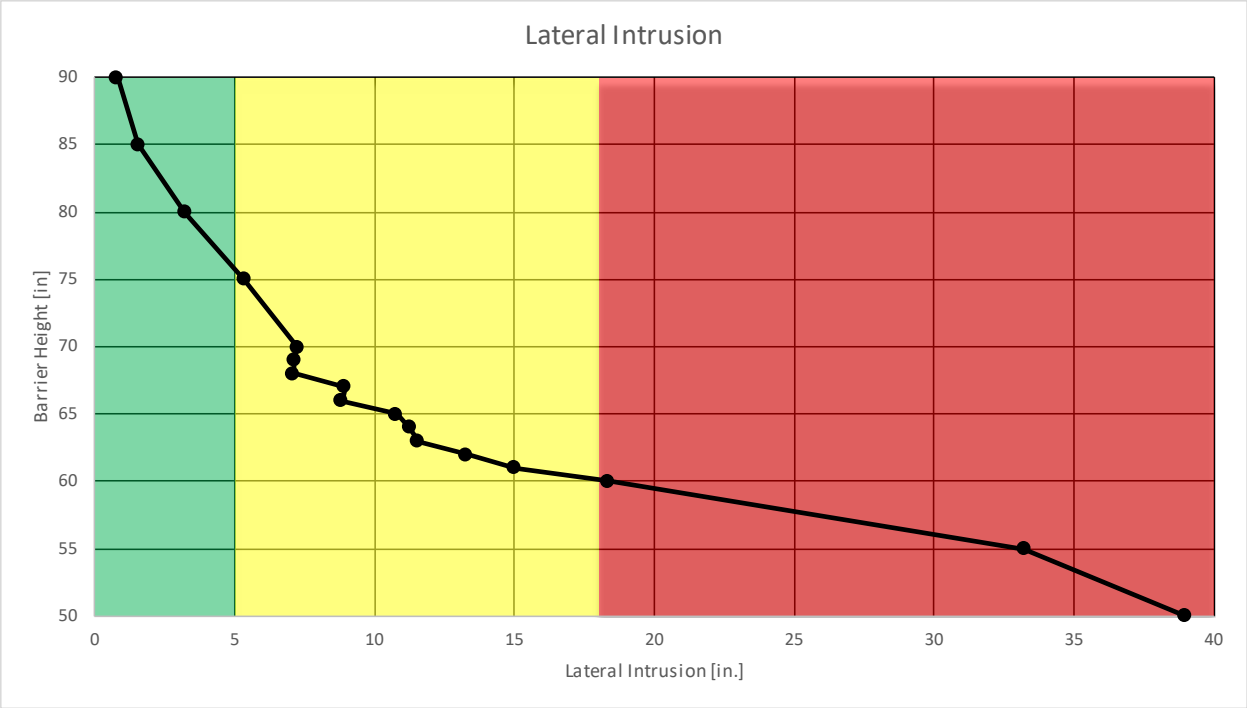

Figure 6.28 Lateral Intrusion

Three regions were created. The green region represented 0 to 5 in. of lateral intrusion, the yellow region represented 5 to 18 in. of lateral intrusion, and the red region was greater than 18 in. of lateral intrusion. The width of the barrier was targeted to be 18 in. in preliminary concepts. Thus, 18 in. was set as the division between the yellow and red regions so that the vehicle would not extend behind the barrier. However, these ranges could be adjusted. The yellow region was considered the most practical due to the allowance of some lateral intrusion and with the height being more optimized. Based on the trends observed and the magnitude of the intrusions, a barrier height of 61 in. was initially recommended to be ideal based on lateral intrusion of the tank behind the front face of the barrier. However, in installations were lateral intrusion is not a concern, the barrier height may be able to be lower than the initial recommendation.

The vertical intrusion, as shown in figure 6.29, illustrates the vertical distance from the ground to the top of the barrier and to the location of the farthest-extent of the tank behind the wall. The vertical intrusion varied minimally with the different barrier heights. Thus, vertical intrusion did not provide any definitive results in relation to determining a minimum barrier height.

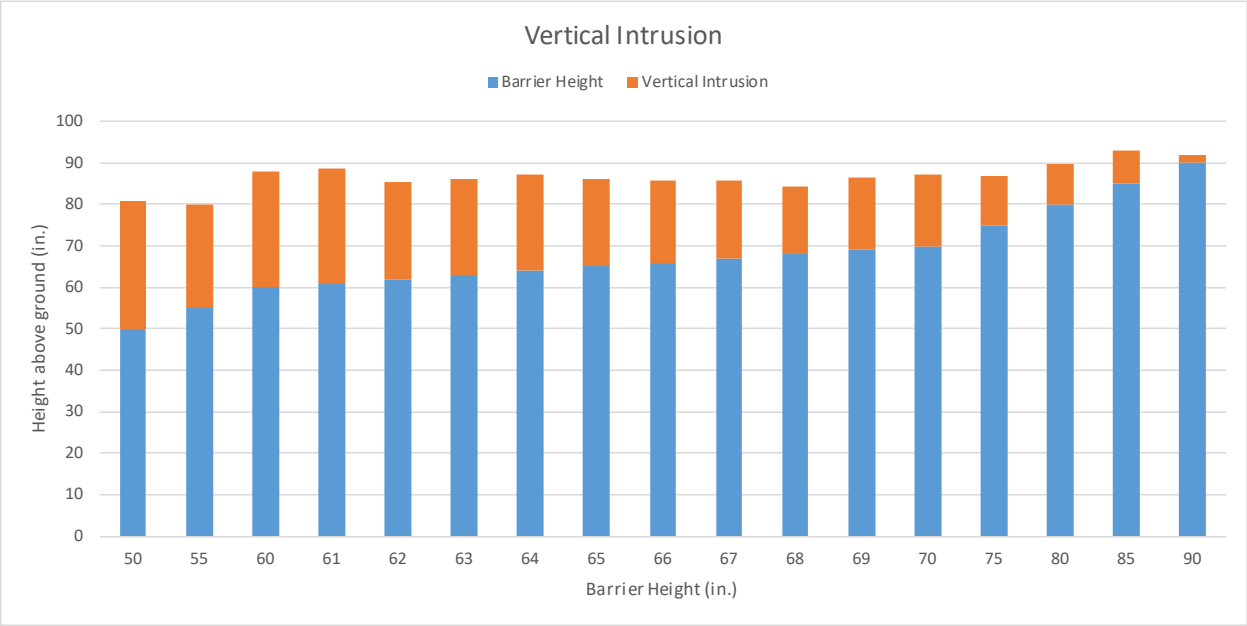

Figure 6.29 Vertical Intrusion

To better understand the position of the farthest extent of the tank behind the barrier in both the lateral and vertical direction, the vertical position above ground vs. the lateral position behind the front face was plotted, as shown in figure 6.30. It should be noted that the widest portion of the tank is located approximately 86¼ in. above the ground surface when on flat terrain with no angular motion. Similar to the lateral intrusion, green, yellow, and red ranges were established.

Both the 50- and 55-in. tall barriers result in the tank displacing far laterally in addition to vertically downward, which correlated to the large roll and instability shown previously. On the other end of the spectrum, the 80- to 90-in. tall barriers did not have much lateral intrusion which correlated to the vehicle being stable. While a stable vehicle was preferred, some roll and lateral intrusion was acceptable, thus barriers above 80 in. tall were likely not the optimal barrier heights.

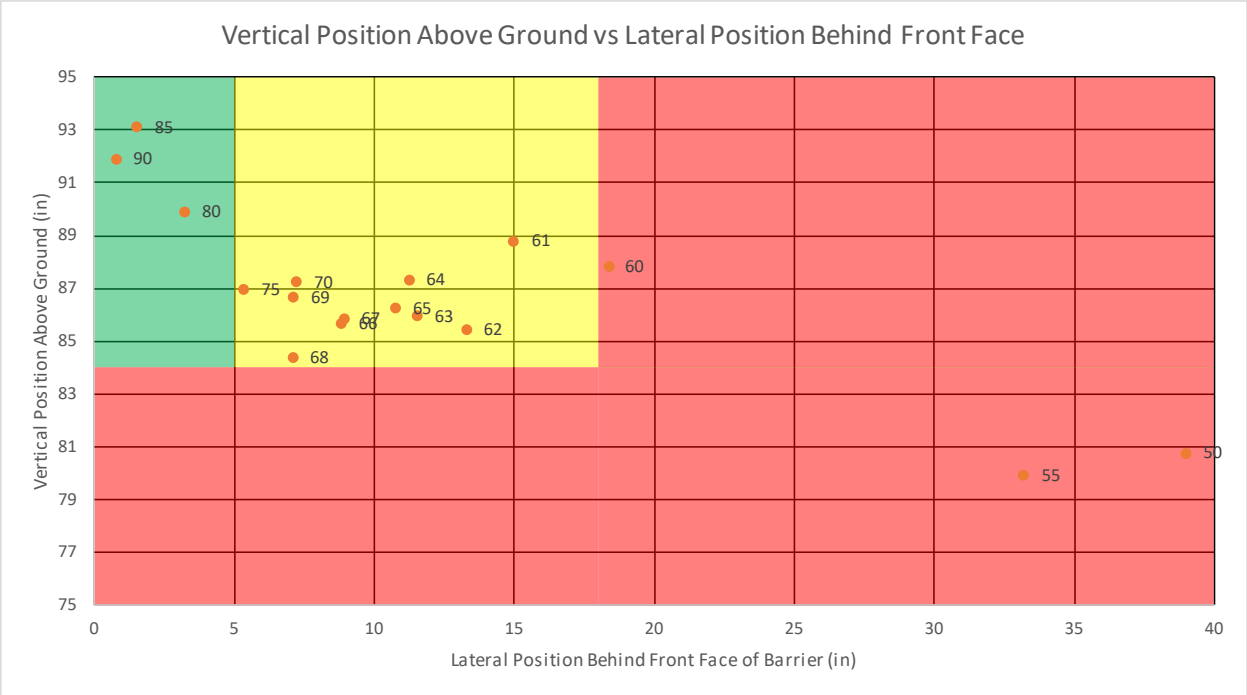

Figure 6.30 Vertical Intrusion vs. Lateral Intrusion

The preferred barrier height range was between 61 and 75 in. Thus, when lateral and vertical intrusion were considered, the recommended barrier height to contain a TL-6 truck was 61 in. A lower barrier height may be able to contain and redirect a TL-6 vehicle if lateral and vertical intrusion are not of concern.

6.5 Barrier Forces

Although not necessary to the determination of a minimum TL-6 barrier height, the forces exerted onto the barrier from the truck during impact are useful to the design of a new TL-6 barrier. The simulated barriers were created using rigidwalls, as shown in figure 6.31, thus the force in the walls can be extracted from the rwforc files. The benefit to using many different rigid walls is that each individual wall force can be investigated, or they can be summed together to determine the total force on the wall at any given time. The total force exerted on the barrier for barrier heights from 50 in. to 90 in. at 5-in. height intervals is shown in figure 6.32.

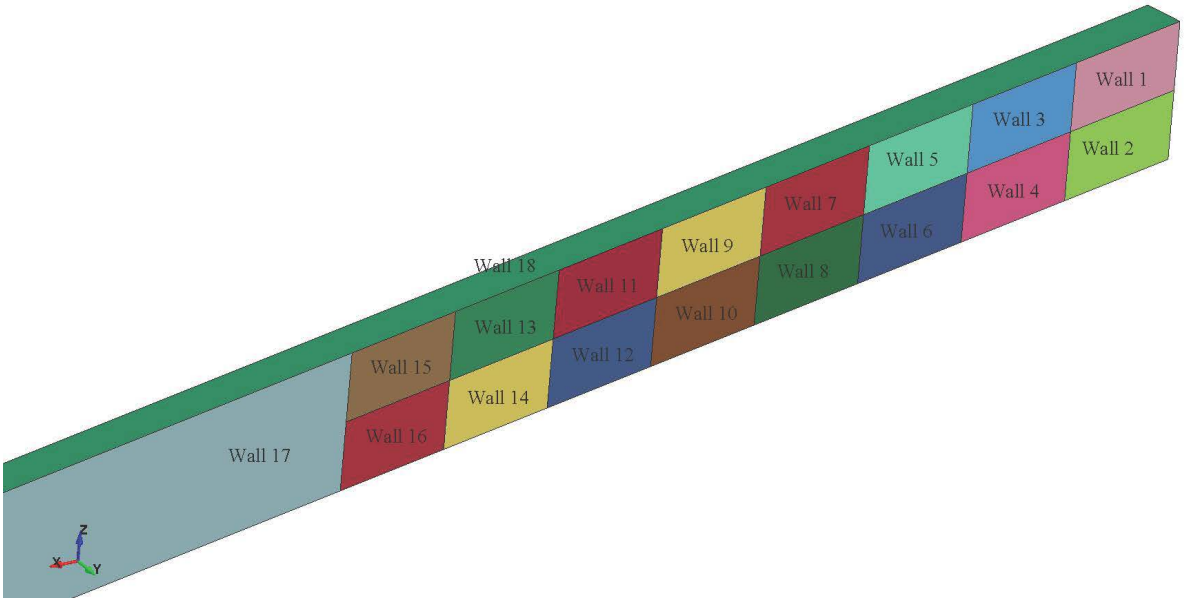

Figure 6.31 Rigidwall IDs

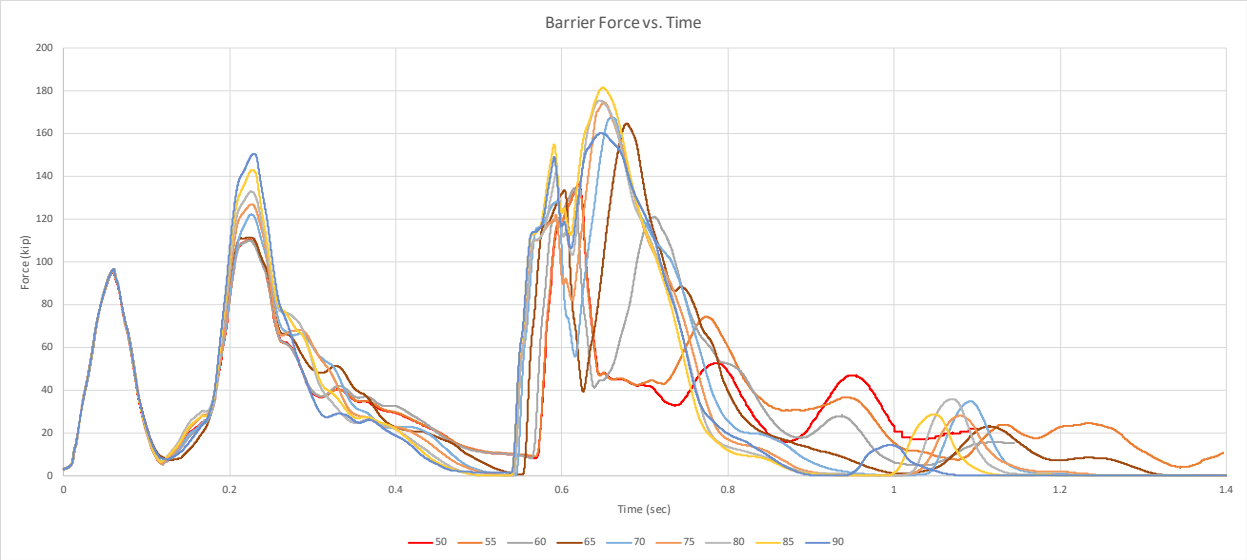

Figure 6.32 Total Barrier Force for Various Heights

The barrier heights of 50, 62, 70 and 90 in. were compared as exemplar heights. The forces on the individual rigid walls and the total force are shown in figures 6.33 through 6.36. The maximum impact forces were 136, 159, 168, and 160 kips for barrier heights of 50, 62, 70, and 90 in., respectively. As determined previously while trying to validate the model, these forces were much lower than what has occurred in prior crash tesst. When comparing the plot of the total force between the different barrier heights, the rear tandem impulse varied. For the 50-in. tall barrier model, there was one impulse with a peak of 136 kips. However, as the barrier height increased, a second impulse with a peak around 160 kips developed as a result of the tank rolling into and impacting the barrier. This impact did not occur in the 50-in. barrier impact, because the barrier was too short for the tank to contact the barrier. Overall, the impact force was similar with all barrier heights, with a slight increase as the barrier height increased.

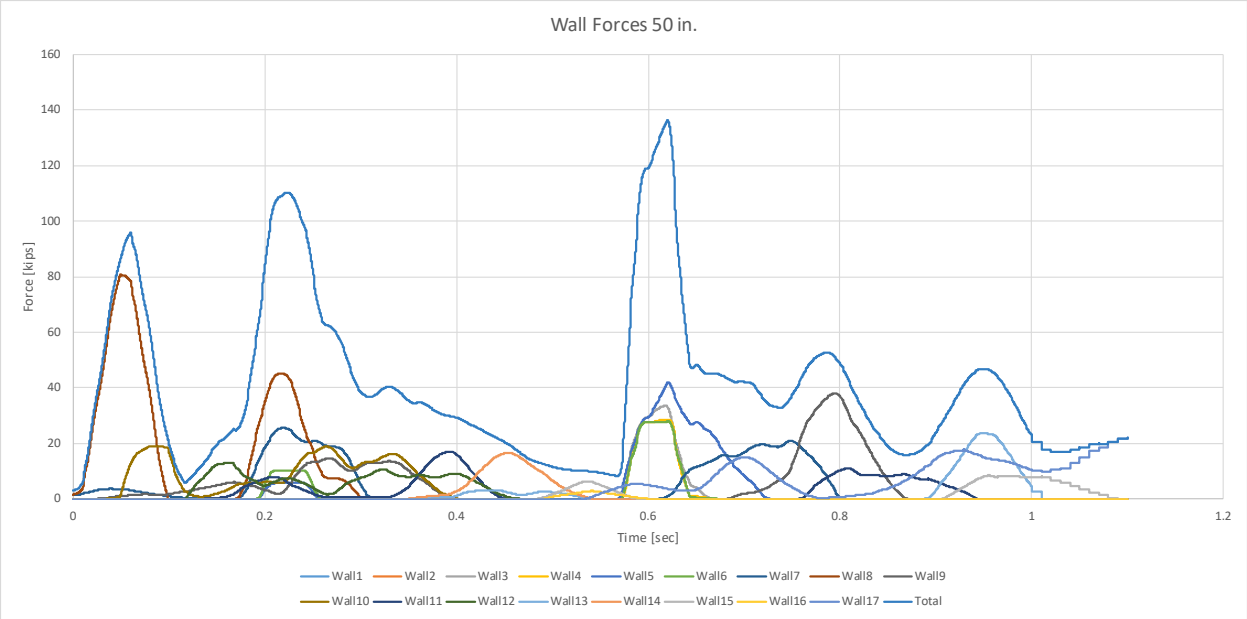

Figure 6.33 50-in. Barrier Impact Forces

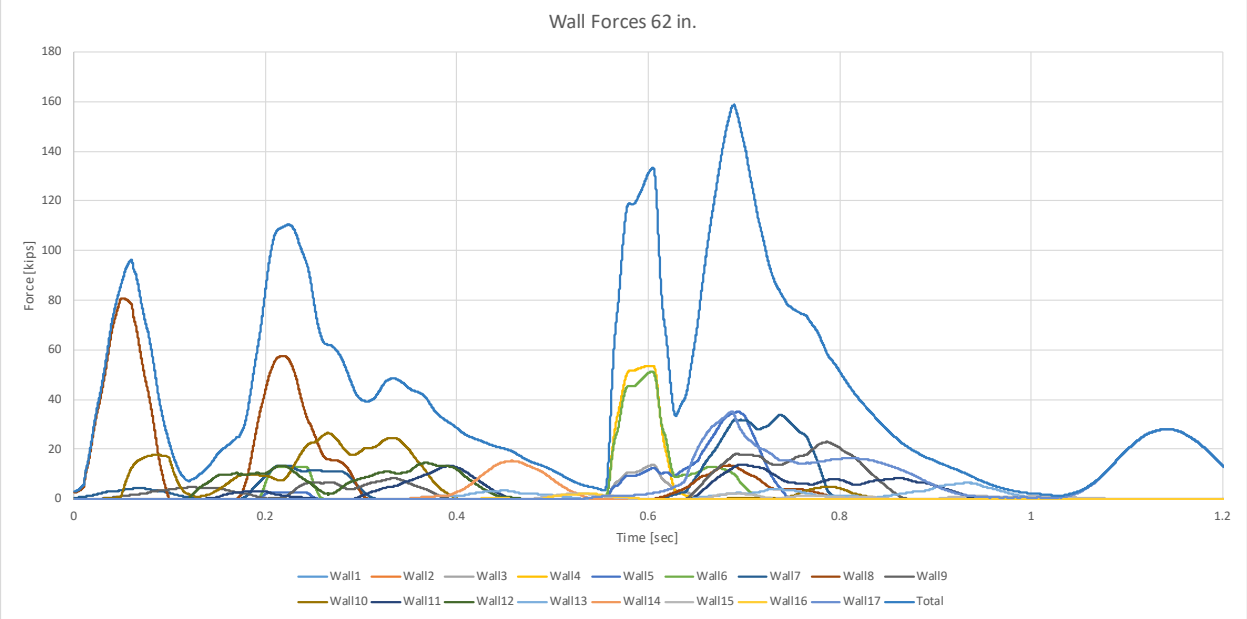

Figure 6.34 62-in. Barrier Impact Forces

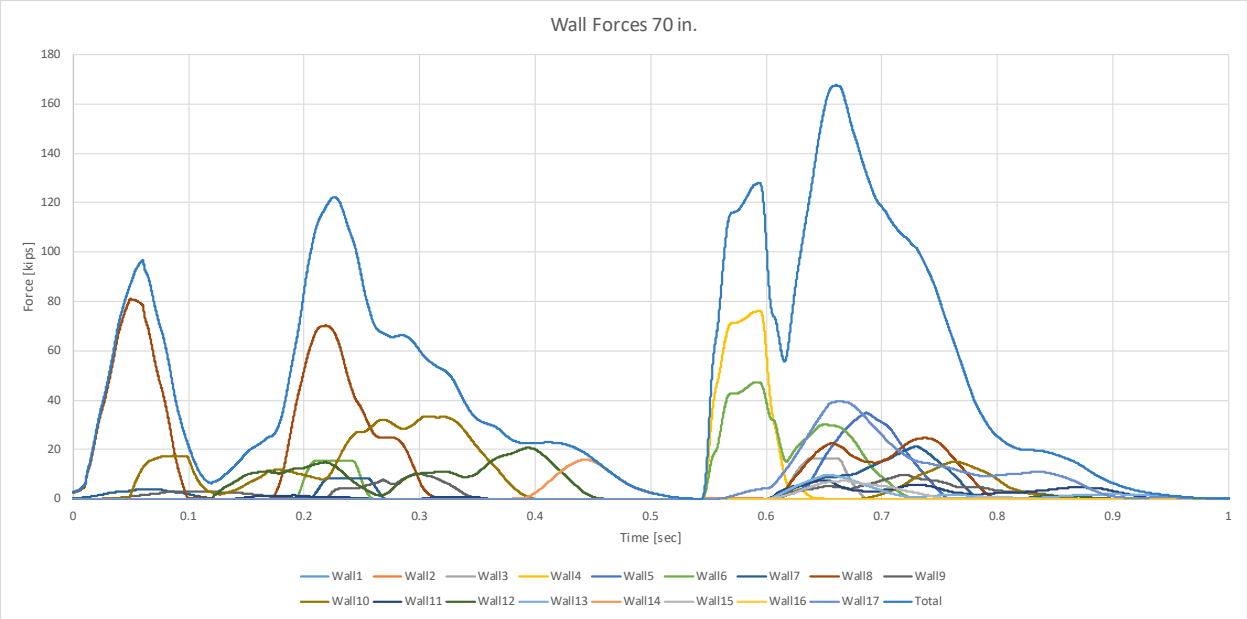

Figure 6.35 70-in. Barrier Impact Forces

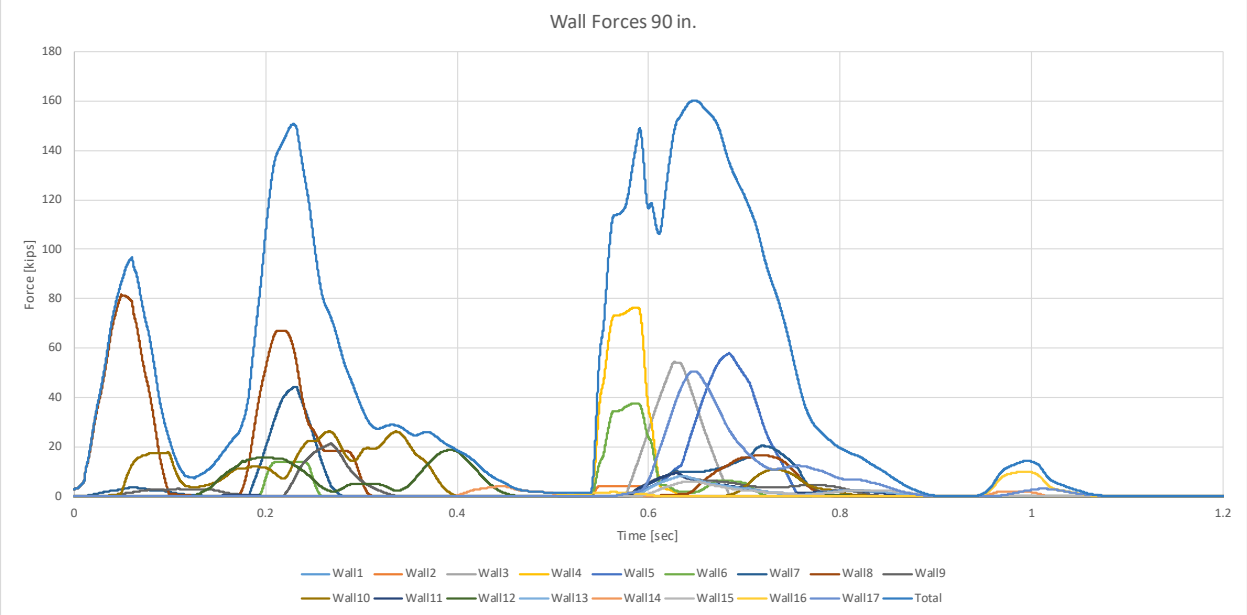

Figure 6.36 90-in. Barrier Impact Forces

6.6 Minimum Barrier Height Recommendation

Based on the data received from the various barrier height simulation results and the parameters investigated, the following minimum barrier heights were recommended based on each parameter: rear tandem axle roll – 62 in., lateral intrusion – 61 in., vertical intrusion – no

recommendation, and vertical and lateral intrusion – 61 in. Based on these results, the researchers believed that a barrier height of 62 in. could be adequate to prevent a TL-6 truck from rolling over a rigid wall. As discussed previously, there is not a known amount of roll to prevent a TL-6 vehicle from rolling over top of a barrier. Additionally, if lateral or vertical intrusion is not a concern, then these recommendations would not apply. Thus, these minimum barrier height recommendations may be conservative, and an even lower barrier height may be sufficient. However, this recommendation was only for a solid rigid parapet with a vertical face and horizontal top. The minimum barrier height is likely higher for varying shapes and for barriers that deform. Additionally, due to the limitations of the vehicle model, improvements to the vehicle were recommended, which may refine these recommendations in future phases. It is recommended to evaluate barrier heights between 50 and 70 in. with a refined vehicle model in the future.

Sequentials from the simulation of a MASH test designation no. 6-12 impact into a 62-in. rigid barrier are shown in figure 6.37. As the rear tandem impacted the barrier, the tank began to roll toward the barrier, making contact and leaning on the top of the barrier. The tank continued to ride on top of the barrier before beginning to roll back toward the traffic side of the barrier, at which point the simulation ends.

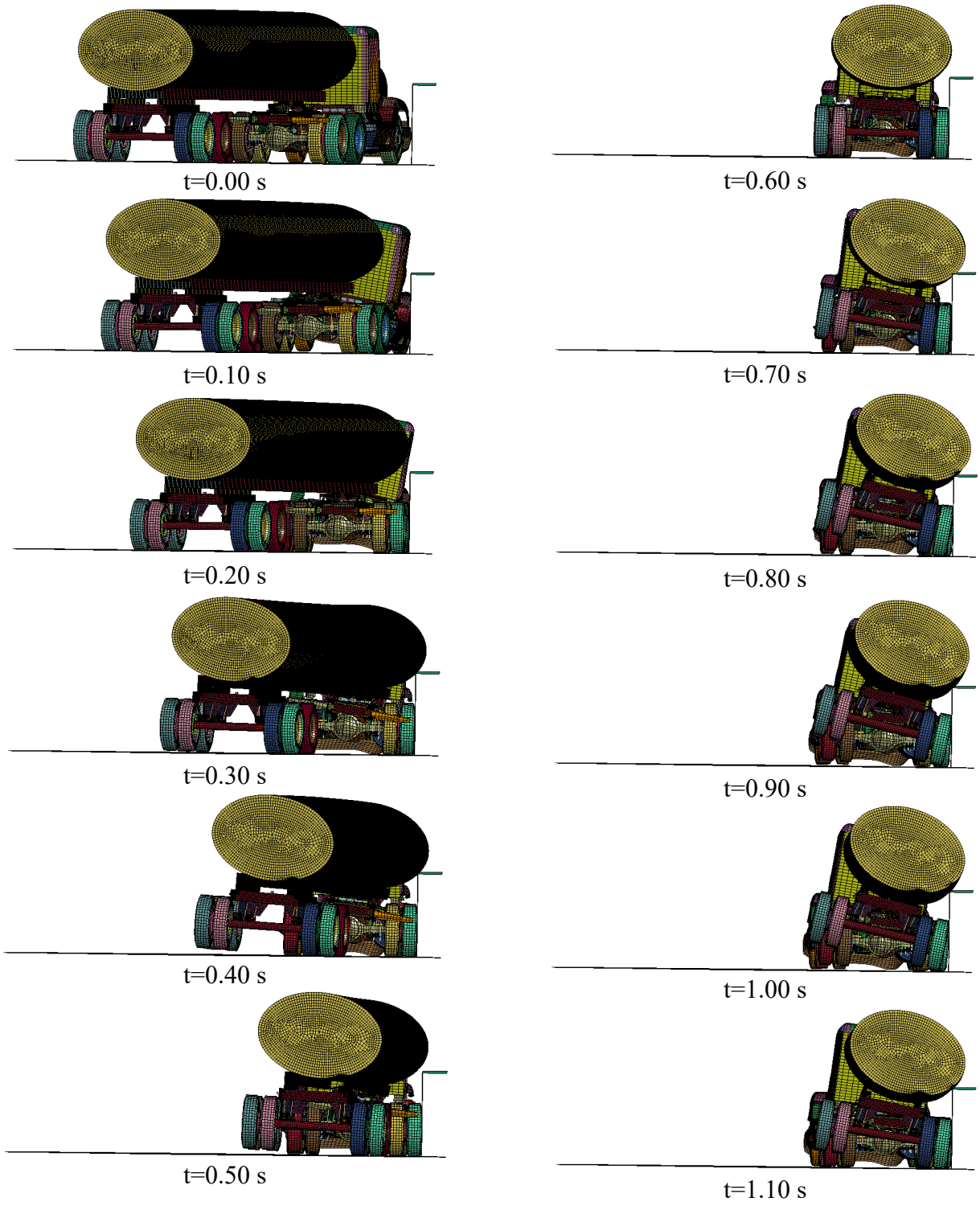

Figure 6.37 62-in. Barrier Simulation

Chapter 7 Summary, Conclusions, And Recommendations

The objective of this research project was to develop a new, cost-effective, MASH TL-6 barrier. A literature review on prior Test Level 5 and Test Level 6 barriers was conducted, and the cost of current TL-5 and TL-6 barriers was established. In total, twelve TL-5 and 2 TL-6 crash tests were reviewed. It was determined that the only existing TL-6 barrier was designed in 1984. This barrier was 90 in. tall and costs approximately $294/ft in current dollars, compared to current TL-5 barriers, which cost around $140/ft.

Existing barrier design procedures were investigated. Prior testing of instrumented wall in 1988 measured the maximum dynamic force imparted to the wall from a TL-6 vehicle to be 408 kips. From this test, two distinct loads were imparted to the barrier: one at a lower height that was applied the rear tandem axles of the trailer and one at a higher height that was applied by the tank. It was determined that there was no procedure to design a barrier for two large loads at varying heights. Thus, existing procedures were evaluated in an effort to develop a design procedure for a TL-6 barrier. However, the design procedure was dependent on the type of barrier (rigid, deformable, etc.)

Required, preferred, and optional design criteria for a new TL-6 barrier were established. Since some existing barrier design procedures tended to be conservative, two design loads were established. For a rigid barrier, a 350-kip load was used, and for a deformable or semi-rigid barrier, a 300-kip load was used. These loads were divided into two separate loads, with 2/3 of the impacting load occurring at the top of the barrier or up to a maximum height of 85 in, and the additional 1/3 of the impact load would be applied 21 in. above the roadway surface. The roadside configuration of the barrier must not have a base footprint width greater than 24 in. to be consistent with existing barriers. The barrier height will be minimized as much as possible, should not exceed 90 in., and was explored throughout this project The cost of the barrier must

be competitive with that of current TL-5 barriers from a benefit-cost perspective. The barrier must be able to withstand a secondary impact of any level after a TL-3 impact, at the same location as the TL-3 impact.

To determine the minimum barrier height necessary to contain and redirect a TL-6 truck impact, an existing TL-5 LS-DYNA truck model was modified by removing the box trailer and replacing it with a tank trailer to make a preliminary TL-6 vehicle model. The preliminary TL-6 vehicle model was to provide a simplified representation of tank trailers to obtain the general behavior of the tank trailer. The overall dimensions of the tank were determined by measuring ten tank trailers. The model was compared to the 1988 instrumented wall test to validate the vehicle model. While the model motion appeared to behave very similarly to the test, the forces imparted to the simulated wall was much lower than what had occurred in crash testing. Thus, there were some notable limitations of the vehicle model. The preliminary TL-6 model was then used to recommend a minimum TL-6 barrier height of 62 in. for rigid, vertical barriers only. It may be possible that an even lower minimum barrier height can be used to prevent rollover, which should be explored in future phases.

Several concepts were brainstormed, developed, and then evaluated based on their ability to meet the design criteria. From the seven concepts that were brainstormed and further refined, three were selected for further evaluation: the rigid solid wall, the rigid reinforced concrete parapet and rigid steel rail, and the rigid parapet with deformable steel rail.

Throughout the simulations to validate the TL-6 vehicle model and the simulations determining the minimum barrier height, the preliminary TL-6 vehicle model, while a good simplified model, did not accurately represent impact loads and accelerations from the Instrumented Wall test. Part of the discrepancy may be due to the differences in the 1968 test vehicle and the preliminary vehicle model, which was created from the geometry of a newer

tractor and trailer. However, there are several recommendations for improvements to the TL-6 vehicle model that may help enable it to behave more realistically. The TL-6 model should be updated to more accurately reflect the geometry and components of existing tank trailers including (1) the fifth wheel plate, (2) the connection between the fifth wheel plate and the tank, (3) the support rails and lateral bracing, (4) the baffles and bulk heads inside the tank, (5) the rails on the top of the tank, and (6) many of the additional tubes and additional components located underneath the tank. A detailed model of a new TL-6 trailer, as shown in figure 7.1, was obtained from LBT Inc. and is recommended to be used to create a more detailed tractor tank-trailer vehicle model.

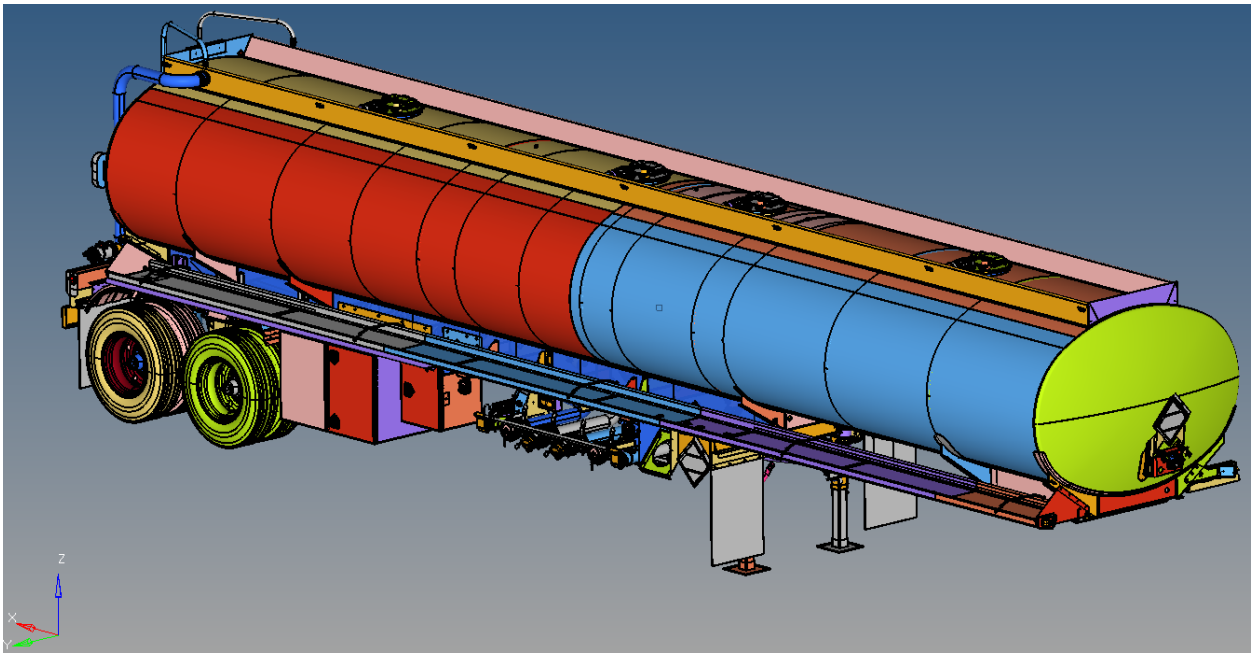

Figure 7.1 LBT Trailer Model

References

1. Ross, H.E., Sicking, D.L., Zimmer, R.A., and Michie, J.D., *Recommended Procedures for the Safety Performance Evaluation of Highway Features*, National Cooperative Highway Research Program (NCHRP) Report 350, Transportation Research Board, Washington, D.C., 1993.

2. *Manual for Assessing Safety Hardware (MASH)*, Second Edition, American Association of State Highway and Transportation Officials (AASHTO), Washington, D.C., 2016.

3. Michie, J.D., *Recommended Procedures for the Safety Performance Evaluation of Highway Appurtenances*, National Cooperative Highway Research Program (NCHRP) Report 230, Transportation Research Board, Washington, D.C., March 1981.

4. Hirsch, T.J., and Fairbanks, W.L., *Bridge Rail to Restrain and Redirect 80,000 lb Tank Trucks*, Report No. FHWA/TX-84/911-1F, Texas Transportation Institute, Texas A&M University, January 1984.

5. Toole, J.S., *Design Considerations for Prevention of Cargo Tank Rollovers*, Memorandum, Federal Highway Administration, U.S. Department of transportation, Washington, D.C., September 3, 2010.

6. *Highway Accident Report – Transport Company of Texas, Tractor-semitrailer (Tank) Collision with Bridge Column and Sudden Dispersal of Anhydrous Ammonia Cargo, I-610 at Southwest Freeway*, Report Number: NTSB-HAR-77-1, National Transportation Safety Board, Washington, D.C., April 14, 1977.

7. *Highway Accident Brief*, Accident Number: HWY-04-MH-012, National Transportation Safety Board, Washington, D.C.

8. *Rollover of a Truck-Tractor and Cargo Tank Semitrailer Carrying Liquefied Petroleum Gas and Subsequent Fire*, Accident Report Number: NTSB/HAR-11/01 PB2011-916201, National Transportation Safety Board, Washington, D.C.,

9. Hirsch, T.J., *Analytical Evaluation of Texas Bridge Rails to Contain Buses and Trucks*, Report No. FHWATX78-230-2, Texas Transportation Institute, Texas A&M University, August 1978.

10. Beason, W.L., and Hirsch, T.J., *Measurement of Heavy Vehicle Impact Forces and Inertia Properties*, Texas Transportation Institute, Texas A&M University, January 1989.

11. Rosenbaugh, S.K, Schmidt, J.D., Regier, E.M., and Faller, R.K., *Development of the Manitoba Constrained-Width, Tall Wall Barrier*, Report No. TRP-03-356-16, Midwest Roadside Safety Facility, University of Nebraska, September 26, 2016.

12. Rosenbaugh, S.K., Sicking, D.L., and Faller, R.K., *Development of a TL-5 Vertical Faced Concrete Median Barrier Incorporating Head Ejection Criteria*, Report No. TRP-03-194-07, Midwest Roadside Safety Facility, University of Nebraska, December 10, 2007.

13. Williams, W.F., Bligh, R.P., Menges, W.L., and Kuhn, D.L., *Crash Test Evaluation of the TXDOT T224 Bridge Rail*, FHWA/TX-15/9-1002-15-5, Texas Transportation Institute, Texas A&M University, December 2015.

14. Polivka, K.A., Faller, R.K., Holloway, J.C., Rohde, J.R, and Sicking, D.L., *Development, Testing, and Evaluation of NDOR's TL-5 Aesthetic Open Concrete Bridge Rail*, TRP-03-148-05, Midwest Roadside Safety Facility, University of Nebraska, December 1, 2005.

15. Hirsch, T.J., and Arnold A., *Bridge Rail to Restrain and Redirect 80,000 lb Trucks*, FHWA/TX-81/16+230-4F, Texas Transportation Institute, Texas A&M University, November 1981.

16. Alberson, D.C., Zimmer, R.A., and Menges W.L., *NCHRP Report 350 Compliance Test 5-12 of the 1.07-m Vertical Wall Bridge Railing*, FHWA-RD-96-199, Texas Transportation Institute, Texas A&M University, May 1996.

17. Hirsch, T.J., Fairbanks, Wm. L., and Buth, C.E., *Concrete Safety Shape with metal Rail on Top to Redirect 80,000 lb Trucks*, FHWA/TX-83/ +416-1F, Texas Transportation Institute, Texas A&M University, December 1984.

18. Mak, K.K., and Campise, W.L., *Test and Evaluation of Ontario "Tall Wall" Barrier with an 80,000-Pound Tractor-Trailer*, Texas Transportation Institute, Texas A&M University, September 1990.

19. Buth, C.E., and Menges, W.L., *MASH Test 5-12 on the Ryerson/Pultrall Parapet*, Texas Transportation Institute, Texas A&M University, February 2012.

20. Buth, C.E., and Menges, W.L., *MASH Test 5-12 of the Schöck ComBar Parapet*, Texas Transportation Institute, Texas A&M University, March 2011.

21. Sheikh, N.M., Carhuayano, R., Zdenek, M., and Riggs, D., *MASH Test Level 5 Steel Bridge Rail for Suspension Bridges*, Texas Transportation Institute, Texas A&M University, August 2016.

22. *AASHTO LRFD Bridge Design Specifications*, 6th Edition, American Association of State Highway and Transportation Officials, Washington, D.C., 2012.

23. Hirsch, T.J., *Analytical Evaluation of Texas Bridge Rails to Contain Buses and Trucks*, Research Report 230-2, Study 2-5-78-230, Texas Transportation Institute, Texas A&M University, 1978.

24. *1989 Guide Specifications for Bridge Railings*, American Association of State Highway and Transportation Officials, Washington, D.C., 1989.

25. *RISA-2D Educational,* RISA Tech Inc., https://risa.com/2deducational.html

26. *Ftool,* Marlin Ideias Criativas, Solucoes Digitas, https://www.ftool.com.br/Ftool/

27. Schmidt, J.D., *Development of a New Energy Absorbing Roadside/Median Barrier System with Restorable Elastomer Catridges*, Midwest Roadside Safety Facility, University of Nebraska – Lincoln, 2012

28. Hallquist, J.O., *LS-DYNA Keyword User's Manual*, LS-DYNA R7.1, Livermore Software Technology Corporation, Livermore, California, 2014.

29. Plaxico, C., and Kennedy–Battelle, J., *Enhanced Finite Element Analysis Crash Model of Tractor-Trailers (Phase A)*, Report No. #DTRT06G-0043, 2007.

30. Plaxico, C., and Kennedy–Battelle, J., *Enhanced Finite Element Analysis Crash Model of Tractor-Trailers (Phase C)*, Report No. #DTRT06G-0043, September, 2010.

31. Simunovic, S., Bennett, R., and Zisi., N., *Enhanced Finite Element Analysis Crash Model of Tractor-Trailers: Website and User's Manual*, Report No. DTRT06G-0043, June, 2009.

Appendices

Appendix A Vehicle Survey Dimensions

Date: 6/15/17 Test Number: _____

Tractor:
VIN No.: Unknown Make: Kenworth Model: W900
Year: Unknown Odometer: _____

Trailer:
VIN No.: 5WSAB442666N048076 Make: Walker Model: TTT-048076
Year: 2016

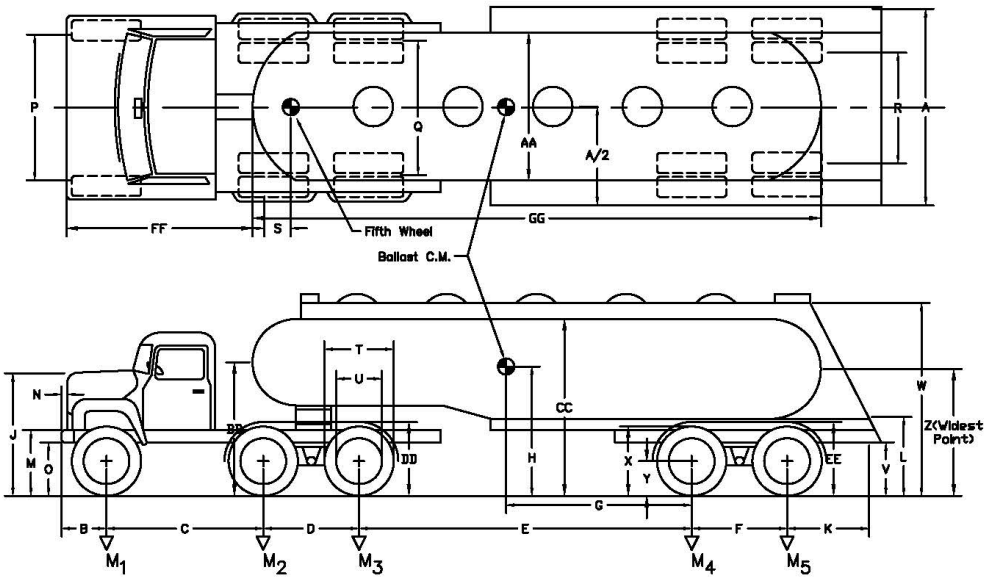

Vehicle Geometry – in. (mm)

A	94	J	77	R	59	Z	86
B	28 1/2	K	44	S	31	AA	74
C	230 1/2	L	54	T	40	BB	84
D	52	M	29 1/2	U	23	CC	120
E	337 1/2	N	0	V	31	DD	57
F	50	O	12	W	129	EE	44
G	Unknown	P	79	X	38 1/2	FF	228
H	Unknown	Q	73 1/2	Y	19 1/2	GG	500

Mass – lb (kg)	Curb	Test Inertial	Gross Static
M_1			
M_2			
M_3			
M_4			
M_5			
M_T			

Note any damage prior to test: _____

Figure A.1 Kenworth W900 Tractor with 2016 Walker Trailer Vehicle Dimensions

Date: 6/15/17 Test Number: _____

Tractor:
VIN No.: N/A Make: N/A Model: N/A
Year: N/A Odometer: _____

Trailer:
VIN No.: Unknown Make: Polar Model: Unkown
Year: Unknown

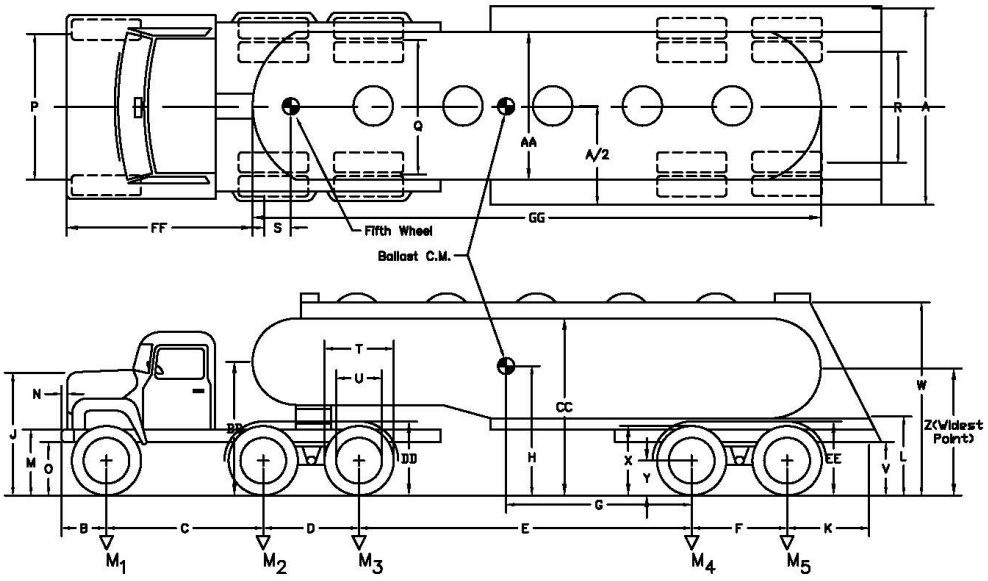

Vehicle Geometry – in. (mm)

A	100	J	N/A	R	78	Z	86
B	N/A	K	32	S	40	AA	72
C	N/A	L	52	T	N/A	BB	90 1/2
D	N/A	M	N/A	U	NA	CC	120
E	N/A	N	N/A	V	35	DD	N/A
F	106	O	N/A	W	120	EE	47 1/2
G	Unknown	P	N/A	X	41	FF	N/A
H	Unknown	Q	N/A	Y	20 1/2	GG	563

Mass – lb (kg)	Curb	Test Inertial	Gross Static
M_1			
M_2			
M_3			
M_4			
M_5			
M_T			

Note any damage prior to test: _____

Figure A.2 Polar Trailer Dimensions

Date: 6/15/17 Test Number: _____

Tractor:
VIN No.: N/A Make: N/A Model: N/A
Year: N/A Odometer: _____

Trailer:
VIN No.: 1203135 Make: Butler Model: Unkown
Year: 1971

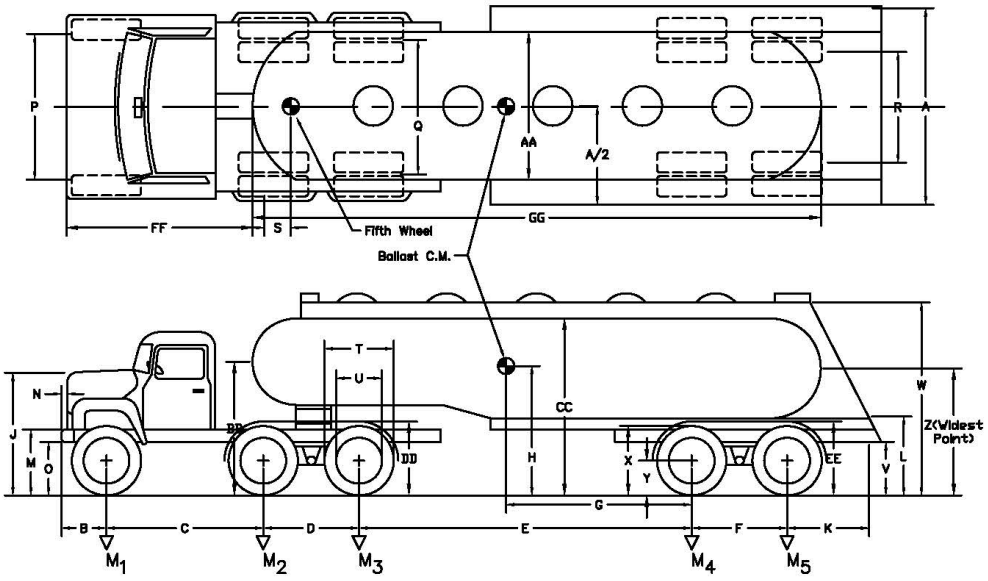

Vehicle Geometry – in. (mm)

A	95 3/4	J	N/A	R	59	Z	84
B	N/A	K	29 1/2	S	29 1/2	AA	70
C	N/A	L	48	T	N/A	BB	87
D	N/A	M	N/A	U	NA	CC	119
E	N/A	N	N/A	V	35	DD	53 1/2
F	49	O	N/A	W	123	EE	51
G	Unknown	P	N/A	X	40	FF	N/A
H	Unknown	Q	N/A	Y	19	GG	467

Mass – lb (kg)	Curb	Test Inertial	Gross Static
M_1			
M_2			
M_3			
M_4			
M_5			
M_T			

Note any damage prior to test: _____

Figure A.3 1971 Butler Trailer Dimensions

Date: 6/15/17 Test Number: _____

Tractor:
VIN No.: Unknown Make: Mack Model: Pinnacle
Year: Unknown Odometer: _____

Trailer:
VIN No.: 1W9S43210XN001508 Make: Walker Model: TTT/32508
Year: 1998

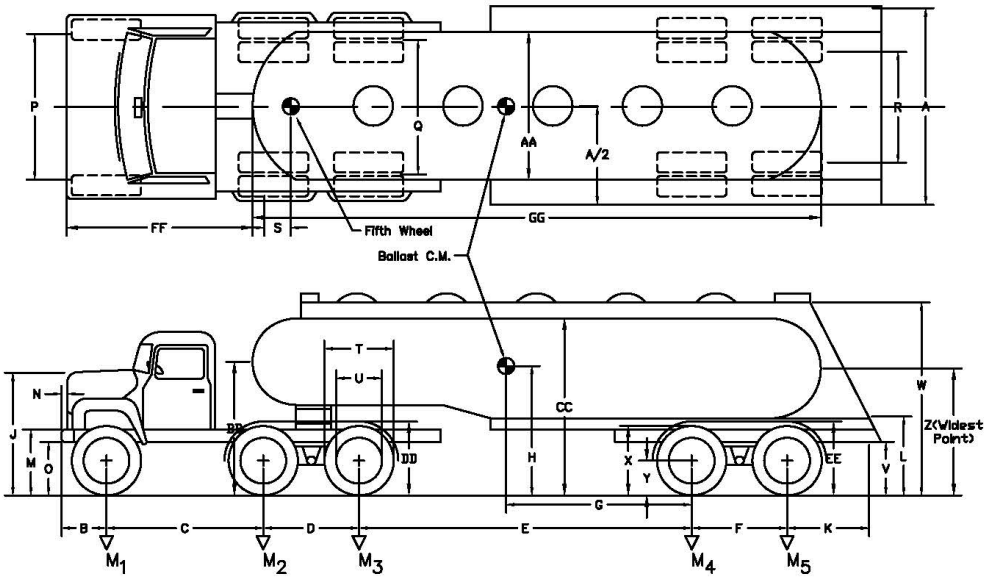

Vehicle Geometry – in. (mm)

A	94	J	65	R	58 1/2	Z	84
B	52	K	31	S	34	AA	73
C	188 1/2	L	50	T	40 1/2	BB	89
D	52	M	33	U	23	CC	120
E	383	N	0	V	33 1/2	DD	55 1/2
F	48	O	17 1/2	W	124	EE	48
G	Unknown	P	82	X	39	FF	245
H	Unknown	Q	74	Y	19 1/2	GG	500

Mass – lb (kg)	Curb	Test Inertial	Gross Static
M_1			
M_2			
M_3			
M_4			
M_5			
M_T			

Note any damage prior to test: _____

Figure A.4 Mack Pinnacle Tractor with 1998 Walker Trailer Vehicle Dimensions

Date: 6/15/17 Test Number: _____

Tractor:
VIN No.: N/A Make: N/A Model: N/A
Year: N/A Odometer: _____

Trailer:
VIN No.: 1202135 Make: Butler Model: Unkown
Year: 1971

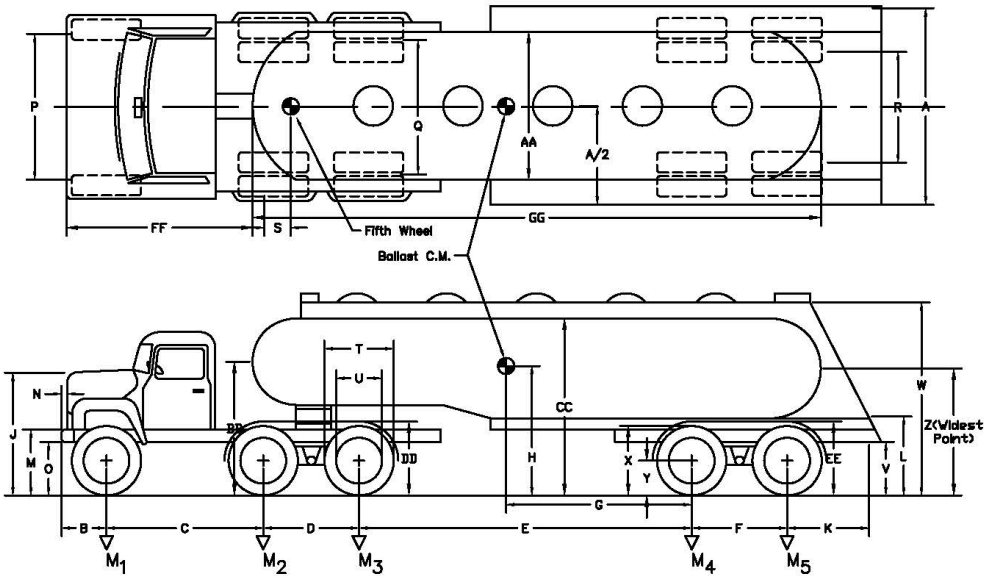

Vehicle Geometry – in. (mm)

A	96	J	N/A	R	58 1/2	Z	81
B	N/A	K	25 1/2	S	29 1/2	AA	78
C	N/A	L	46	T	N/A	BB	88
D	N/A	M	N/A	U	NA	CC	118
E	N/A	N	N/A	V	33	DD	54
F	48 1/2	O	N/A	W	122	EE	46
G	Unknown	P	N/A	X	30	FF	N/A
H	Unknown	Q	N/A	Y	19 1/2	GG	464

Mass – lb (kg)	Curb	Test Inertial	Gross Static
M_1			
M_2			
M_3			
M_4			
M_5			
M_T			

Note any damage prior to test: _____

Figure A.5 1971 Butler Trailer Dimensions

Date: 6/15/17 Test Number: _____

Tractor:
VIN No.: N/A Make: N/A Model: N/A
Year: N/A Odometer: _____

Trailer:
VIN No.: Unknown Make: Butler Model: Unkown
Year: 1969

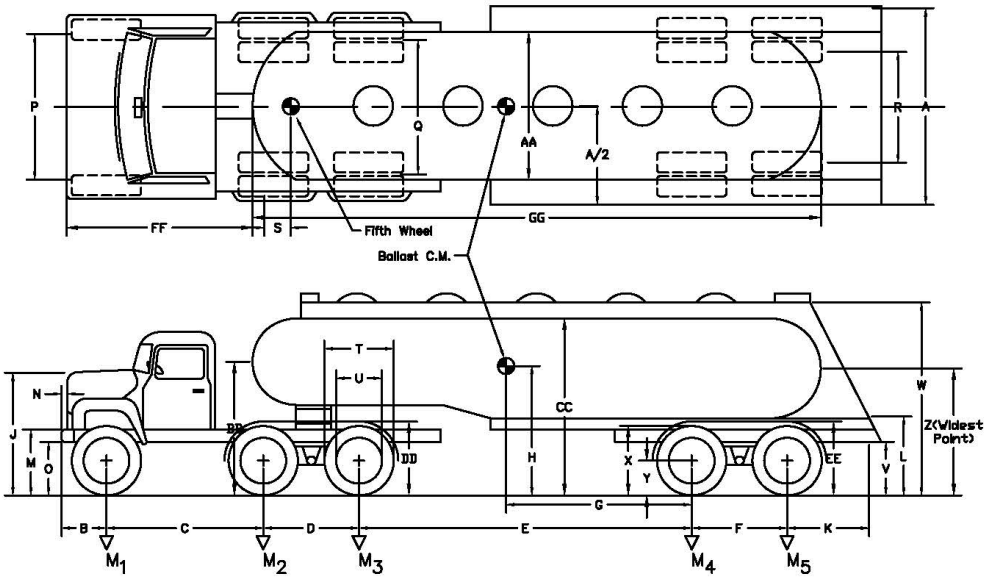

Vehicle Geometry – in. (mm)

A 96	J N/A	R 58 1/2	Z 81
B N/A	K 29	S 31	AA 71
C N/A	L 45	T N/A	BB 81
D N/A	M N/A	U NA	CC 118
E N/A	N N/A	V 31 1/2	DD 50 1/2
F 48	O N/A	W Unknown	EE 45
G Unknown	P N/A	X 39	FF N/A
H Unknown	Q N/A	Y 19	GG 438

Mass – lb (kg)	Curb	Test Inertial	Gross Static
M_1			
M_2			
M_3			
M_4			
M_5			
M_T			

Note any damage prior to test: _____

Figure A.6 1969 Butler Trailer Dimensions

Date: 6/15/17 Test Number: _____

Tractor:
VIN No.: Unknown Make: Mack Model: Pinnacle CXU
Year: 2014 Odometer: _____

Trailer:
VIN No.: Unknown Make: Fruehauf Model: TAG-F2-ESF-9200
Year: 1989

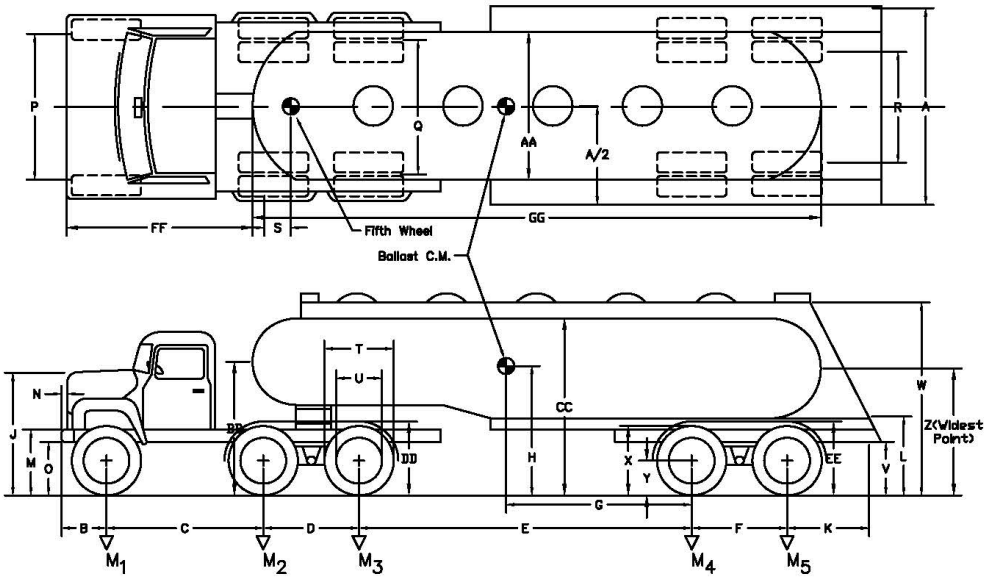

Vehicle Geometry – in. (mm)

A	95	J	65	R	59	Z	87 1/2
B	53	K	26	S	38	AA	92 1/2
C	160	L	55	T	41	BB	82
D	51	M	34	U	23	CC	118
E	355	N	0	V	35 1/2	DD	53
F	48	O	14	W	125	EE	49
G	Unknown	P	80	X	41	FF	188
H	Unknown	Q	75	Y	20 1/2	GG	488

Mass – lb (kg)	Curb	Test Inertial	Gross Static
M_1			
M_2			
M_3			
M_4			
M_5			
M_T			

Note any damage prior to test: _____

Figure A.7 2014 Mack Pinnacle CVU Tractor with 1989 Fruehauf Trailer Vehicle Dimensions

Date: 6/15/17 Test Number: _____

Tractor:
VIN No.: Unknown Make: Kenworth Model: T880
Year: 2017 Odometer: _____

Trailer:
VIN No.: Unknown Make: LBT Model: Unknown
Year: Unknown

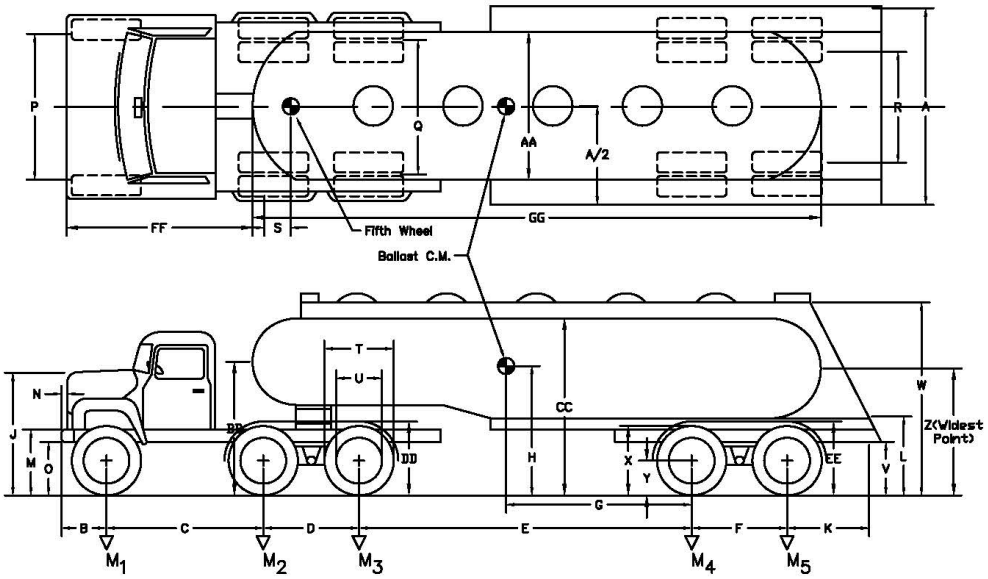

Vehicle Geometry – in. (mm)

A	96	J	67	R	60	Z	86
B	50	K	33	S	37	AA	92
C	185 1/2	L	55	T	41	BB	89 1/2
D	52	M	31	U	2	CC	117
E	347	N	0	V	36	DD	55
F	49	O	17	W	124	EE	51
G	Unknown	P	83	X	40	FF	209
H	Unknown	Q	75	Y	20	GG	488

Mass – lb (kg)	Curb	Test Inertial	Gross Static
M_1			
M_2			
M_3			
M_4			
M_5			
M_T			

Note any damage prior to test: _____

Figure A.8 2017 Kenworth T880 Tractor with LBT Trailer Vehicle Dimensions

Date: 6/15/17 Test Number: _____

Tractor:
VIN No.: Unknown Make: Kenworth Model: T880
Year: 2017 Odometer: _____

Trailer:
VIN No.: Unknown Make: LBT Model: TAG-F2-ESF-9200X5
Year: 1995

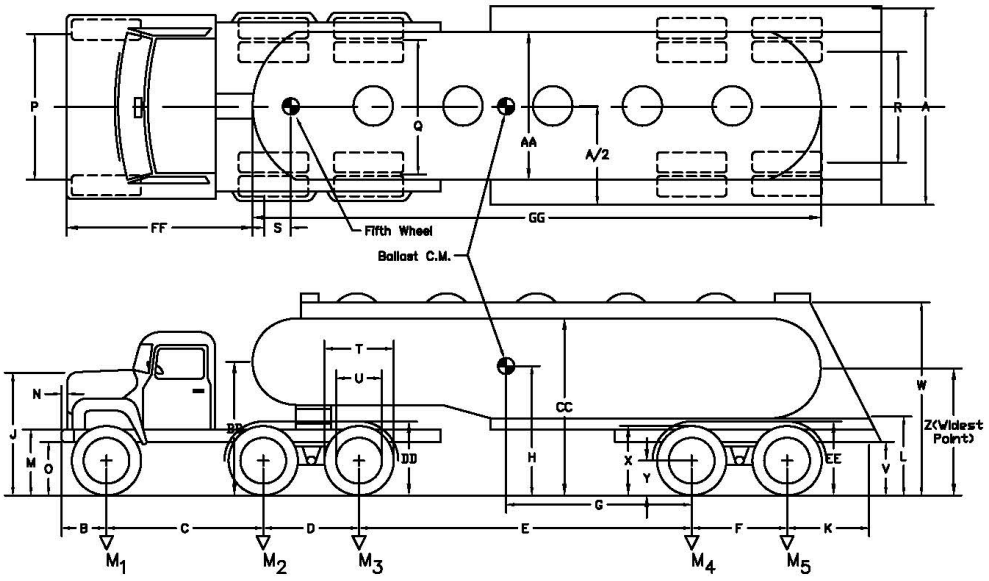

Vehicle Geometry – in. (mm)

A	96	J	68	R	60	Z	88
B	50	K	30	S	47	AA	93
C	184	L	55	T	41	BB	91
D	52	M	31	U	23	CC	119
E	370	N	0	V	37	DD	54
F	48 1/2	O	17	W	126	EE	52
G	Unknown	P	82	X	41	FF	N/A
H	Unknown	Q	74	Y	21	GG	489

Mass – lb (kg)	Curb	Test Inertial	Gross Static
M_1			
M_2			
M_3			
M_4			
M_5			
M_T			

Note any damage prior to test: _____

Figure A.9 2017 Kenworth T880 Tractor with 1995 LBT Trailer Vehicle Dimensions

Date: 6/15/17 Test Number: _____

Tractor:
VIN No.: Unknown Make: Peterbilt Model: Unknown
Year: Unknown Odometer: _____

Trailer:
VIN No.: Unknown Make: LBT Model: TAG-F2-ESF-9200X5SB
Year: 1994

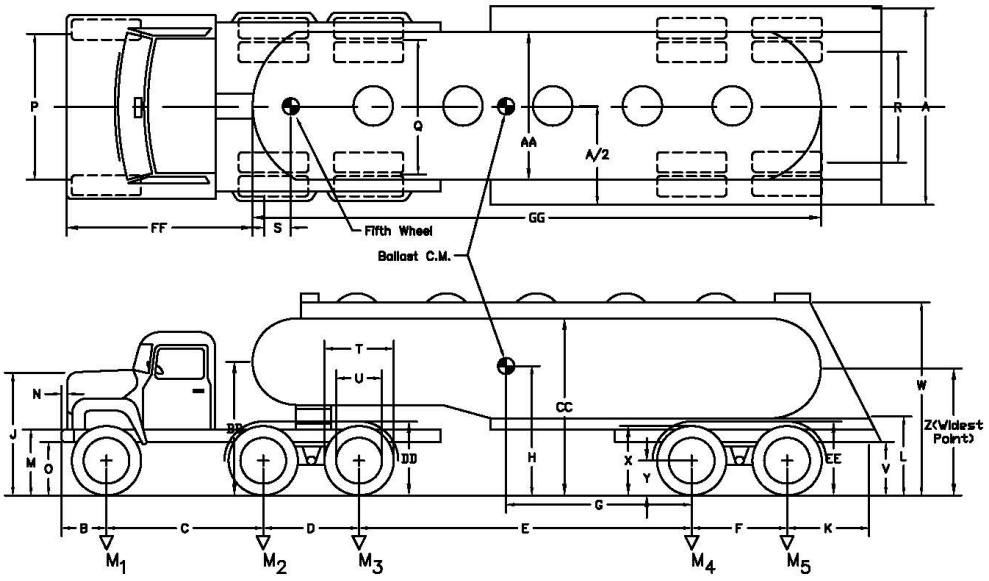

Vehicle Geometry – in. (mm)

A	96	J	74	R	60	Z	86
B	31	K	33	S	30	AA	89
C	239	L	53	T	40	BB	93
D	51	M	29	U	23	CC	117
E	350	N	0	V	36	DD	57
F	49	O	11	W	123 1/2	EE	50
G	Unknown	P	82	X	40	FF	252
H	Unknown	Q	74	Y	20	GG	486

Mass – lb (kg)	Curb	Test Inertial	Gross Static
M_1			
M_2			
M_3			
M_4			
M_5			
M_T			

Note any damage prior to test: _____

Figure A.10 Peterbilt Tractor with 1994 LBT Trailer Vehicle Dimensions

Appendix B TTI TL-6 Roman Wall Calculations

B.1 Yield Line Failure Section 1

Flexural Strength

Dean Whitfield — **Three Failure Mode**, **Failure Section 1 - Mb**, **1/3/2018**

Mu 9597 kip-in.

ε_{cu} 0.003

c= 3.475

a 2.953

Sum of forces 0.00

Design R/C & P/C ACI

ANSWER:

ϕ 0.90

ϕM, kip-in 2425 (2694.627044)

kip*ft 202.097

Av. β_1: 0.850

Units in kips and inches

Concrete Layers		f'c	Width, W	Thick., T	Depth, d_c	β_1	T_{upper}	T_{lower}	Revised T	Beta1 calcuation		Area	Force	M_n k-in.
	1	3.600	21.000	16.000	1.477	0.850	0.000	16.000	2.953	189.785467	223.27702	62.021	-189.79	-280.26
	2				16.000	0.850	16.000	16.000	0.000	0	0	0.000	0.00	0.00
	3				16.000	0.850	16.000	16.000	0.000	0	0	0.000	0.00	0.00
	4				16.000	0.850	16.000	16.000	0.000	0	0	0.000	0.00	0.00
	5				16.000	0.850	16.000	16.000	0.000	0	0	0.000	0.00	0.00
	6				16.000	0.850	16.000	16.000	0.000	0	0	0.000	0.00	0.00
	7				16.000	0.850	16.000	16.000	0.000	0	0	0.000	0.00	0.00
										189.785467	223.27702			

Steel Layers		Area A_{si}	Grade	Effective Prest.	Depth d_{si}	E_s	Q	fpy	R	K	ε_{s0}	$\Delta\varepsilon$	Total ε_s	Stress	Force	Moment	Modified stress	corresp. f'c
Grade 60 Bars	1	3.95	60	0	2.875	29000	0	60	100	1.096	0.0000	-0.0005	-0.0005	-15.01	-47.21	-135.74	-11.95	3.60
	2	3.95	60	0	13.125	29000	0	60	100	1.096	0.0000	0.0063	0.0063	60.00	237.00	3110.63	60.00	3.60
	3		60	0	12.688	29000	0	60	100	1.096	0.0000	0.0000	0.0060	60.00	0.00	0.00	60.00	3.60
	4		60	0	9.125	29000	0	60	100	1.096	0.0000	0.0000	0.0049	60.00	0.00	0.00	60.00	3.60
	5		60	0	11.750	29000	0	60	100	1.096	0.0000	0.0000	0.0071	60.00	0.00	0.00	60.00	3.60
	6		60	0	14.375	29000	0	60	100	1.096	0.0000	0.0000	0.0094	60.00	0.00	0.00	60.00	3.60
	7		60	0	17.000	29000	0	60	100	1.096	0.0000	0.0000	0.0117	60.00	0.00	0.00	60.00	0.00
	8		60	0	19.625	29000	0	60	100	1.096	0.0000	0.0000	0.0139	60.00	0.00	0.00	60.00	0.00
	9		60	0	22.250	29000	0	60	100	1.096	0.0000	0.0000	0.0162	60.00	0.00	0.00	60.00	0.00
	10		60	0	24.875	29000	0	60	100	1.096	0.0000	0.0000	0.0185	60.00	0.00	0.00	60.00	0.00
	11		60	0	27.500	29000	0	60	100	1.096	0.0000	0.0000	0.0207	60.00	0.00	0.00	60.00	0.00
	12		60	0	30.125	29000	0	60	100	1.096	0.0000	0.0000	0.0230	60.00	0.00	0.00	60.00	0.00
	13		60	0	32.750	29000	0	60	100	1.096	0.0000	0.0000	0.0253	60.00	0.00	0.00	60.00	0.00
Grade 70 Plate	1		70	0	0.000	29000	0	70	100	1.06	0.0000	0.0000	-0.0030	-70.00	0.00	0.00	-66.94	3.60
Gr. 120 Rods	1		120	0	5.125	29000	0.0217	81.00	4.224	1.01	0.0000	0.0000	0.0014	40.81	0.00	0.00	40.81	3.60
Gr. 150 Rods	1		150	0	5.125	29000	0.0217	120.00	4.224	1.01	0.0000	0.0000	0.0014	41.22	0.00	0.00	41.22	3.60
Gr 270	1		270	28	1.500	28500	0.031	243	7.36	1.043	0.0010	0.0000	-0.0007	-20.59	0.00	0.00	-17.53	3.60
Gr 270	2		270	28	5.500	28500	0.031	243	7.36	1.043	0.0010	0.0000	0.0027	77.84	0.00	0.00	77.84	3.60
Gr 270	3		270	160	10.000	28500	0.031	243	7.36	1.043	0.0056	0.0000	0.0112	250.14	0.00	0.00	250.14	3.60
Gr 270	4		270	160	10.750	28500	0.031	243	7.36	1.043	0.0063	0.0000	0.0115	251.27	0.00	0.00	251.27	3.60
	5		270	160	12.333	28500	0.031	243	7.36	1.043	0.0056	0.0000	0.0133	255.60	0.00	0.00	255.60	3.60
	6		270	160	14.667	28500	0.031	243	7.36	1.043	0.0056	0.0000	0.0153	258.47	0.00	0.00	258.47	3.60
	7		270	160	17.000	28500	0.031	243	7.36	1.043	0.0056	0.0000	0.0173	260.62	0.00	0.00	260.62	0.00
	8		270	160	19.333	28500	0.031	243	7.36	1.043	0.0056	0.0000	0.0193	262.54	0.00	0.00	262.54	0.00
	9		270	160	21.667	28500	0.031	243	7.36	1.043	0.0056	0.0000	0.0213	264.38	0.00	0.00	264.38	0.00
	10		270	160	24.000	28500	0.031	243	7.36	1.043	0.0056	0.0000	0.0233	266.18	0.00	0.00	266.18	0.00
	11		270	160	26.333	28500	0.031	243	7.36	1.043	0.0056	0.0000	0.0254	267.97	0.00	0.00	267.97	0.00
	12		270	160	28.667	28500	0.031	243	7.36	1.043	0.0056	0.0000	0.0274	269.76	0.00	0.00	269.76	0.00
	13		270	160	31.000	28500	0.031	243	7.36	1.043	0.0056	0.0000	0.0294	270.00	0.00	0.00	270.00	0.00
Sum of M										MAXIMUM	$\Delta\varepsilon$:	0.0083		Moment (K"	0.00	2694.63 kip*in		
																224.55 kip*ft		

$$\beta_{1SPA} = \sum_i (f'_{ci} A_{ci} \beta_1)_i / \sum_i (f'_{ci} A_{ci})_i$$

$$\varepsilon_{si} = \varepsilon_{cu}\left(\frac{d_i}{c} - 1\right) + \left(\frac{f_{se}}{E_s}\right)$$

P/C & R/C ACI: $0.65 \le \phi = (1.45 + 250\,\varepsilon_{extreme})/3 \le 0.9$
P/C AASHTO: $0.75 \le \phi = (1.75 + 250\,\varepsilon_{extreme})/3 \le 1.0$
R/C AASHTO: $0.75 \le \phi = 0.65 + 50\,\varepsilon_{extreme} \le 0.9$

Figure B.1 Yield Line Analysis Failure Section 1 Mb

Flexural Strength

Dean Whitfield — **Three Failure Mode** — **Failure Section 1 - Mc** — **1/3/2018**

Mu 9597 kip-in.

ε_{cu} 0.003

c= 2.053

a 1.745

Sum of forces 0.00

Design R/C & P/C ACI

ANSWER:

ϕ 0.90

ϕM_n kip-in 232 | 257.7822391 | Av. β_1 : 0.850

kip*ft 19.334

Units in kips and inches

Concrete Layers		f'c	Width, W	Thick., T	Depth, d_c	β_1	T_{upper}	T_{lower}	Revised T	Beta1calcuation		Area	Force	M_n k-in.
	1	3.600	12.000	8.000	0.873	0.850	0.000	8.000	1.745	64.08215659	75.3907725	20.942	-64.08	-55.92
	2				8.000	0.850	8.000	8.000	0.000	0	0	0.000	0.00	0.00
	3				8.000	0.850	8.000	8.000	0.000	0	0	0.000	0.00	0.00
	4				8.000	0.850	8.000	8.000	0.000	0	0	0.000	0.00	0.00
	5				8.000	0.850	8.000	8.000	0.000	0	0	0.000	0.00	0.00
	6				8.000	0.850	8.000	8.000	0.000	0	0	0.000	0.00	0.00
	7				8.000	0.850	8.000	8.000	0.000	0	0	0.000	0.00	0.00
										64.08215659	75.3907725			

Steel Layers		Area A_{si}	Grade	Effective Prest.	Depth d_{si}	E_s	Q	fpy	R	K	ε_{s0}	$\Delta\varepsilon$	Total ε_s	Stress	Force	Moment	Modified stress	corresp. f'c
Grade 60 Bars	1	0.84	60	0	2.438	29000	0	60	100	1.096	0.0000	0.0006	0.0006	16.29	13.68	33.35	16.29	3.60
	2	0.84	60	0	5.563	29000	0	60	100	1.096	0.0000	0.0051	0.0051	60.00	50.40	280.35	60.00	3.60
	3		60	0	12.688	29000	0	60	100	1.096	0.0000	0.0000	0.0155	60.00	0.00	0.00	60.00	0.00
	4		60	0	9.125	29000	0	60	100	1.096	0.0000	0.0000	0.0103	60.00	0.00	0.00	60.00	0.00
	5		60	0	11.750	29000	0	60	100	1.096	0.0000	0.0000	0.0142	60.00	0.00	0.00	60.00	0.00
	6		60	0	14.375	29000	0	60	100	1.096	0.0000	0.0000	0.0180	60.00	0.00	0.00	60.00	0.00
	7		60	0	17.000	29000	0	60	100	1.096	0.0000	0.0000	0.0218	60.00	0.00	0.00	60.00	0.00
	8		60	0	19.625	29000	0	60	100	1.096	0.0000	0.0000	0.0257	60.00	0.00	0.00	60.00	0.00
	9		60	0	22.250	29000	0	60	100	1.096	0.0000	0.0000	0.0295	60.00	0.00	0.00	60.00	0.00
	10		60	0	24.875	29000	0	60	100	1.096	0.0000	0.0000	0.0333	60.00	0.00	0.00	60.00	0.00
	11		60	0	27.500	29000	0	60	100	1.096	0.0000	0.0000	0.0372	60.00	0.00	0.00	60.00	0.00
	12		60	0	30.125	29000	0	60	100	1.096	0.0000	0.0000	0.0410	60.00	0.00	0.00	60.00	0.00
	13		60	0	32.750	29000	0	60	100	1.096	0.0000	0.0000	0.0449	60.00	0.00	0.00	60.00	0.00
Grade 70 Plate	1		70	0	0.000	29000	0	70	100	1.06	0.0000	0.0000	-0.0030	-70.00	0.00	0.00	-66.94	3.60
Gr. 120 Rods	1		120	0	5.125	29000	0.0217	81.00	4.224	1.01	0.0000	0.0000	0.0045	80.41	0.00	0.00	80.41	3.60
Gr. 150 Rods	1		150	0	5.125	29000	0.0217	120.00	4.224	1.01	0.0000	0.0000	0.0045	106.83	0.00	0.00	106.83	3.60
Gr 270	1		270	28	1.500	28500	0.031	243	7.36	1.043	0.0010	0.0000	0.0002	4.97	0.00	0.00	8.03	3.60
Gr 270	2		270	28	5.500	28500	0.031	243	7.36	1.043	0.0010	0.0000	0.0060	170.30	0.00	0.00	170.30	3.60
Gr 270	3		270	160	10.000	28500	0.031	243	7.36	1.043	0.0056	0.0000	0.0172	260.56	0.00	0.00	260.56	0.00
Gr 270	4		270	160	10.750	28500	0.031	243	7.36	1.043	0.0053	0.0000	0.0180	261.28	0.00	0.00	261.28	0.00
	5		270	160	12.333	28500	0.031	243	7.36	1.043	0.0056	0.0000	0.0206	263.76	0.00	0.00	263.76	0.00
	6		270	160	14.667	28500	0.031	243	7.36	1.043	0.0056	0.0000	0.0240	266.81	0.00	0.00	266.81	0.00
	7		270	160	17.000	28500	0.031	243	7.36	1.043	0.0056	0.0000	0.0275	269.84	0.00	0.00	269.84	0.00
	8		270	160	19.333	28500	0.031	243	7.36	1.043	0.0056	0.0000	0.0309	270.00	0.00	0.00	270.00	0.00
	9		270	160	21.667	28500	0.031	243	7.36	1.043	0.0056	0.0000	0.0343	270.00	0.00	0.00	270.00	0.00
	10		270	160	24.000	28500	0.031	243	7.36	1.043	0.0056	0.0000	0.0377	270.00	0.00	0.00	270.00	0.00
	11		270	160	26.333	28500	0.031	243	7.36	1.043	0.0056	0.0000	0.0411	270.00	0.00	0.00	270.00	0.00
	12		270	160	28.667	28500	0.031	243	7.36	1.043	0.0056	0.0000	0.0445	270.00	0.00	0.00	270.00	0.00
	13		270	160	31.000	28500	0.031	243	7.36	1.043	0.0056	0.0000	0.0479	270.00	0.00	0.00	270.00	0.00
Sum of M										MAXIMUM	$\Delta\varepsilon$:	0.0051		Moment (K"	0.00	257.78 kip*in		
																21.48 kip*f		

$$\beta_{1av} = \sum_1 (f'_c A_c \beta_1)_i / \sum_1 (f'_c A_c)_i$$

$$\varepsilon_{si} = \varepsilon_{cu}\left(\frac{d_i}{c} - 1\right) + \left(\frac{f_{se}}{E_s}\right)$$

P/C & R/C ACI: $0.65 \le \phi = (1.45 + 250\,\varepsilon_{extreme})/3 \le 0.9$
P/C AASHTO: $0.75 \le \phi = (1.75 + 250\,\varepsilon_{extreme})/3 \le 1.0$
R/C AASHTO: $0.75 \le \phi = 0.65 + 50\,\varepsilon_{extreme} \le 0.9$

Figure B.2 Yield Line Analysis Failure Section 1 Mc

$$L = \frac{8}{2} + \sqrt{\left(\frac{8}{2}\right)^2 + \frac{8 * (3.5) * 202.1}{19.33} - \frac{5 * 8}{2}} = 20.99$$

$$wl\left(\frac{20.99 - (8/2)}{20.99}\right) = \frac{8 * 202.1}{20.99} + \frac{19.33 * (20.99 - 5)}{(3.5)} = 204.26\ k$$

B.2 Yield Line Failure Section 2

Flexural Strength														Mu	9597	kip-in.			
Dean Whitfield		**Three Failure Mode**									ε_{cu}	0.003							
		Failure Section 2 - Mw									c=	1.905							
											a	1.620	Calculate						
											Sum of forces	0.00							
											Design	R/C & P/C ACI							
											ANSWER:								
											ϕ	0.90							
											ϕM_n kip-in	992	1102.151869	Av. β_1 :	0.850				
					Units in kips and inches						kip*ft	82.661							
Concrete Layers		**f'c**	**Width, W**	**Thick., T**	**Depth, d_c**	**β_1**	**T_{upper}**	**T_{lower}**	**Revised T**	**Beta1calcuation**				**Area**	**Force**	**M_n k-in.**			
	1	3.600	35.000	12.750	0.810	0.850	0.000	12.750	1.620	173.4645886	204.075987			56.688	-173.46	-140.48			
	2				12.750	0.850	12.750	12.750	0.000	0	0			0.000	0.00	0.00			
	3				12.750	0.850	12.750	12.750	0.000	0	0			0.000	0.00	0.00			
	4				12.750	0.850	12.750	12.750	0.000	0	0			0.000	0.00	0.00			
	5				12.750	0.850	12.750	12.750	0.000	0	0			0.000	0.00	0.00			
	6				12.750	0.850	12.750	12.750	0.000	0	0			0.000	0.00	0.00			
	7				12.750	0.850	12.750	12.750	0.000	0	0			0.000	0.00	0.00			
										173.4645886	204.075987						Modified	corresp.	
Steel Layers		**Area A_{sl}**	**Grade**	**Effective Prest.**	**Depth d_{sl}**	**E_s**	**Q**	**fpy**	**R**	**K**	**ε_{so}**	**$\Delta\varepsilon$**	**Total ε_s**	**Stress**	**Force**	**Moment**	**stress**	**f'c**	
Grade 60 Bars	1	1.76	60	0	2.750	29000	0	60	100	1.096	0.0000	0.0013	0.0013	38.56	67.86	186.63	38.56	3.60	
	2	1.76	60	0	10.000	29000	0	60	100	1.096	0.0000	0.0127	0.0127	60.00	105.60	1056.00	60.00	3.60	
	3		60	0	12.688	29000	0	60	100	1.096	0.0000	0.0000	0.0170	60.00	0.00	0.00	60.00	3.60	
	4		60	0	9.125	29000	0	60	100	1.096	0.0000	0.0000	0.0114	60.00	0.00	0.00	60.00	3.60	
	5		60	0	11.750	29000	0	60	100	1.096	0.0000	0.0000	0.0155	60.00	0.00	0.00	60.00	3.60	
	6		60	0	14.375	29000	0	60	100	1.096	0.0000	0.0000	0.0196	60.00	0.00	0.00	60.00	0.00	
	7		60	0	17.000	29000	0	60	100	1.096	0.0000	0.0000	0.0238	60.00	0.00	0.00	60.00	0.00	
	8		60	0	19.625	29000	0	60	100	1.096	0.0000	0.0000	0.0279	60.00	0.00	0.00	60.00	0.00	
	9		60	0	22.250	29000	0	60	100	1.096	0.0000	0.0000	0.0320	60.00	0.00	0.00	60.00	0.00	
	10		60	0	24.875	29000	0	60	100	1.096	0.0000	0.0000	0.0362	60.00	0.00	0.00	60.00	0.00	
	11		60	0	27.500	29000	0	60	100	1.096	0.0000	0.0000	0.0403	60.00	0.00	0.00	60.00	0.00	
	12		60	0	30.125	29000	0	60	100	1.096	0.0000	0.0000	0.0444	60.00	0.00	0.00	60.00	0.00	
	13		60	0	32.750	29000	0	60	100	1.096	0.0000	0.0000	0.0486	60.00	0.00	0.00	60.00	0.00	
Grade 70 Plate	1		70	0	0.000	29000	0	70	100	1.06	0.0000	0.0000	-0.0030	-70.00	0.00	0.00	-66.94	3.60	
Gr. 120 Rods	1		120	0	5.125	29000	0.0217	81.00	4.224	1.01	0.0000	0.0000	0.0051	81.71	0.00	0.00	81.71	3.60	
Gr. 150 Rods	1		150	0	5.125	29000	0.0217	120.00	4.224	1.01	0.0000	0.0000	0.0051	111.91	0.00	0.00	111.91	3.60	
Gr 270	1		270	28	1.500	28500	0.031	243	7.36	1.043	0.0010	0.0000	0.0003	9.81	0.00	0.00	12.87	3.60	
Gr 270	2		270	28	5.500	28500	0.031	243	7.36	1.043	0.0010	0.0000	0.0066	186.56	0.00	0.00	186.56	3.60	
Gr 270	3		270	160	10.000	28500	0.031	243	7.36	1.043	0.0056	0.0000	0.0184	261.65	0.00	0.00	261.65	3.60	
Gr 270	4		270	150	10.750	28500	0.031	243	7.36	1.043	0.0053	0.0000	0.0192	262.43	0.00	0.00	262.43	3.60	
	5		270	160	12.333	28500	0.031	243	7.36	1.043	0.0056	0.0000	0.0220	265.02	0.00	0.00	265.02	3.60	
	6		270	160	14.667	28500	0.031	243	7.36	1.043	0.0056	0.0000	0.0257	268.29	0.00	0.00	268.29	0.00	
	7		270	160	17.000	28500	0.031	243	7.36	1.043	0.0056	0.0000	0.0294	270.00	0.00	0.00	270.00	0.00	
	8		270	160	19.333	28500	0.031	243	7.36	1.043	0.0056	0.0000	0.0331	270.00	0.00	0.00	270.00	0.00	
	9		270	160	21.667	28500	0.031	243	7.36	1.043	0.0056	0.0000	0.0367	270.00	0.00	0.00	270.00	0.00	
	10		270	160	24.000	28500	0.031	243	7.36	1.043	0.0056	0.0000	0.0404	270.00	0.00	0.00	270.00	0.00	
	11		270	160	26.333	28500	0.031	243	7.36	1.043	0.0056	0.0000	0.0441	270.00	0.00	0.00	270.00	0.00	
	12		270	160	28.667	28500	0.031	243	7.36	1.043	0.0056	0.0000	0.0477	270.00	0.00	0.00	270.00	0.00	
	13		270	160	31.000	28500	0.031	243	7.36	1.043	0.0056	0.0000	0.0514	270.00	0.00	0.00	270.00	0.00	
	Sum of M									**MAXIMUM**	**$\Delta\varepsilon$:**	0.0127		**Moment (K'**	0.00	1102.15	kip*in		
																91.85	kip*f		

Figure B.3 Yield Line Analysis Section 2 Mw

Flexural Strength															Mu	9597	kip-in.		
Dean Whitfield		**Three Failure Mode**									ε_{cu}	0.003							
		Failure Section 2 - Mc									c=	1.824							
											a	1.551							
											Sum of forces	0.00	Calculate						
											Design	R/C & P/C ACI							
											ANSWER:								
											ϕ	0.90							
											ϕM_n kip-in	367	407.8830232	Av. β_1 :	0.850				
											kip*ft	30.591							
					Units in kips and inches														
Concrete Layers		**f'c**	**Width, W**	**Thick., T**	**Depth, d_c**	**β_1**	**T_{upper}**	**T_{lower}**	**Revised T**	**Beta1calcuation**					**Area**	**Force**	**M_n k-in.**		
	1	3.600	12.000	12.750	0.775	0.850	0.000	12.750	1.551	56.93714886	66.984881				18.607	-56.94	-44.14		
	2				12.750	0.850	12.750	12.750	0.000	0	0				0.000	0.00	0.00		
	3				12.750	0.850	12.750	12.750	0.000	0	0				0.000	0.00	0.00		
	4				12.750	0.850	12.750	12.750	0.000	0	0				0.000	0.00	0.00		
	5				12.750	0.850	12.750	12.750	0.000	0	0				0.000	0.00	0.00		
	6				12.750	0.850	12.750	12.750	0.000	0	0				0.000	0.00	0.00		
	7				12.750	0.850	12.750	12.750	0.000	0	0				0.000	0.00	0.00		
										56.93714886	66.984881							Modified	corresp.
Steel Layers		**Area A_{sl}**	**Grade**	**Effective Prest.**	**Depth d_{sl}**	**E_s**	**Q**	**fpy**	**R**	**K**	**ε_{so}**	**$\Delta\varepsilon$**	**Total ε_s**		**Stress**	**Force**	**Moment**	**stress**	**f'c**
Grade 60 Bars	1	0.66	60	0	2.375	29000	0	60	100	1.096	0.0000	0.0009	0.0009		26.27	17.34	41.18	26.27	3.60
	2	0.66	60	0	10.375	29000	0	60	100	1.096	0.0000	0.0141	0.0141		60.00	39.60	410.85	60.00	3.60
	3		60	0	12.688	29000	0	60	100	1.096	0.0000	0.0000	0.0179		60.00	0.00	0.00	60.00	3.60
	4		60	0	9.125	29000	0	60	100	1.096	0.0000	0.0000	0.0120		60.00	0.00	0.00	60.00	3.60
	5		60	0	11.750	29000	0	60	100	1.096	0.0000	0.0000	0.0163		60.00	0.00	0.00	60.00	3.60
	6		60	0	14.375	29000	0	60	100	1.096	0.0000	0.0000	0.0206		60.00	0.00	0.00	60.00	0.00
	7		60	0	17.000	29000	0	60	100	1.096	0.0000	0.0000	0.0250		60.00	0.00	0.00	60.00	0.00
	8		60	0	19.625	29000	0	60	100	1.096	0.0000	0.0000	0.0293		60.00	0.00	0.00	60.00	0.00
	9		60	0	22.250	29000	0	60	100	1.096	0.0000	0.0000	0.0336		60.00	0.00	0.00	60.00	0.00
	10		60	0	24.875	29000	0	60	100	1.096	0.0000	0.0000	0.0379		60.00	0.00	0.00	60.00	0.00
	11		60	0	27.500	29000	0	60	100	1.096	0.0000	0.0000	0.0422		60.00	0.00	0.00	60.00	0.00
	12		60	0	30.125	29000	0	60	100	1.096	0.0000	0.0000	0.0465		60.00	0.00	0.00	60.00	0.00
	13		60	0	32.750	29000	0	60	100	1.096	0.0000	0.0000	0.0509		60.00	0.00	0.00	60.00	0.00
Grade 70 Plate	1		70	0	0.000	29000	0	70	100	1.06	0.0000	0.0000	-0.0030		-70.00	0.00	0.00	-66.94	3.60
Gr. 120 Rods	1		120	0	5.125	29000	0.0217	81.00	4.224	1.01	0.0000	0.0000	0.0054		82.30	0.00	0.00	82.30	3.60
Gr. 150 Rods	1		150	0	5.125	29000	0.0217	120.00	4.224	1.01	0.0000	0.0000	0.0054		114.22	0.00	0.00	114.22	3.60
Gr 270	1		270	28	1.500	28500	0.031	243	7.36	1.043	0.0010	0.0000	0.0004		12.80	0.00	0.00	15.86	3.60
Gr 270	2		270	28	5.500	28500	0.031	243	7.36	1.043	0.0010	0.0000	0.0070		196.04	0.00	0.00	196.04	3.60
Gr 270	3		270	160	10.000	28500	0.031	243	7.36	1.043	0.0056	0.0000	0.0191		262.31	0.00	0.00	262.31	3.60
Gr 270	4		270	150	10.750	28500	0.031	243	7.36	1.043	0.0053	0.0000	0.0199		263.12	0.00	0.00	263.12	3.60
	5		270	160	12.333	28500	0.031	243	7.36	1.043	0.0056	0.0000	0.0229		265.79	0.00	0.00	265.79	3.60
	6		270	160	14.667	28500	0.031	243	7.36	1.043	0.0056	0.0000	0.0267		269.20	0.00	0.00	269.20	0.00
	7		270	160	17.000	28500	0.031	243	7.36	1.043	0.0056	0.0000	0.0306		270.00	0.00	0.00	270.00	0.00
	8		270	160	19.333	28500	0.031	243	7.36	1.043	0.0056	0.0000	0.0344		270.00	0.00	0.00	270.00	0.00
	9		270	160	21.667	28500	0.031	243	7.36	1.043	0.0056	0.0000	0.0382		270.00	0.00	0.00	270.00	0.00
	10		270	160	24.000	28500	0.031	243	7.36	1.043	0.0056	0.0000	0.0421		270.00	0.00	0.00	270.00	0.00
	11		270	160	26.333	28500	0.031	243	7.36	1.043	0.0056	0.0000	0.0459		270.00	0.00	0.00	270.00	0.00
	12		270	160	28.667	28500	0.031	243	7.36	1.043	0.0056	0.0000	0.0498		270.00	0.00	0.00	270.00	0.00
	13		270	160	31.000	28500	0.031	243	7.36	1.043	0.0056	0.0000	0.0536		270.00	0.00	0.00	270.00	0.00
	Sum of M									**MAXIMUM**	**$\Delta\varepsilon$:**	**0.0141**			**Moment (K'**	**0.00**	**407.88**	kip*in	
																	33.99	kip*f	

Figure B.4 Yield Line Analysis Failure Section 2 Mc

Flexural Strength															Mu	9597	kip-in.			
Dean Whitfield		**Three Failure Mode**									ε_{cu}	0.003								
		Failure Section 2 - Mb									c=	3.475								
											a	2.953								
											Sum of forces	0.00	Calculate							
											Design	R/C & P/C ACI								
											ANSWER:									
											ϕ	0.90								
											ϕM_n kip-in	2425	2694.627044	Av. β_1 :	0.850					
											kip*ft	202.097								
					Units in kips and inches															
Concrete Layers		f'c	Width, W	Thick., T	Depth, d_c	β_1	T_{upper}	T_{lower}	Revised T	Beta1calcuation					Area	Force	M_n k-in.			
	1	3.600	21.000	16.000	1.477	0.850	0.000	16.000	2.953	189.785467	223.27702				62.021	-189.79	-280.26			
	2				16.000	0.850	16.000	16.000	0.000	0	0				0.000	0.00	0.00			
	3				16.000	0.850	16.000	16.000	0.000	0	0				0.000	0.00	0.00			
	4				16.000	0.850	16.000	16.000	0.000	0	0				0.000	0.00	0.00			
	5				16.000	0.850	16.000	16.000	0.000	0	0				0.000	0.00	0.00			
	6				16.000	0.850	16.000	16.000	0.000	0	0				0.000	0.00	0.00			
	7				16.000	0.850	16.000	16.000	0.000	0	0				0.000	0.00	0.00			
										189.785467	223.27702								Modified	corresp.
Steel Layers		Area A_{sl}	Grade	Effective Prest.	Depth d_{sl}	E_s	Q	fpy	R	K	ε_{so}	$\Delta\varepsilon$	Total ε_s		Stress	Force	Moment		stress	f'c
Grade 60 Bars	1	3.95	60	0	2.875	29000	0	60	100	1.096	0.0000	-0.0005	-0.0005		-15.01	-47.21	-135.74		-11.95	3.60
	2	3.95	60	0	13.125	29000	0	60	100	1.096	0.0000	0.0083	0.0083		60.00	237.00	3110.63		60.00	3.60
	3		60	0	12.688	29000	0	60	100	1.096	0.0000	0.0000	0.0080		60.00	0.00	0.00		60.00	3.60
	4		60	0	9.125	29000	0	60	100	1.096	0.0000	0.0000	0.0049		60.00	0.00	0.00		60.00	3.60
	5		60	0	11.750	29000	0	60	100	1.096	0.0000	0.0000	0.0071		60.00	0.00	0.00		60.00	3.60
	6		60	0	14.375	29000	0	60	100	1.096	0.0000	0.0000	0.0094		60.00	0.00	0.00		60.00	3.60
	7		60	0	17.000	29000	0	60	100	1.096	0.0000	0.0000	0.0117		60.00	0.00	0.00		60.00	0.00
	8		60	0	19.625	29000	0	60	100	1.096	0.0000	0.0000	0.0139		60.00	0.00	0.00		60.00	0.00
	9		60	0	22.250	29000	0	60	100	1.096	0.0000	0.0000	0.0162		60.00	0.00	0.00		60.00	0.00
	10		60	0	24.875	29000	0	60	100	1.096	0.0000	0.0000	0.0185		60.00	0.00	0.00		60.00	0.00
	11		60	0	27.500	29000	0	60	100	1.096	0.0000	0.0000	0.0207		60.00	0.00	0.00		60.00	0.00
	12		60	0	30.125	29000	0	60	100	1.096	0.0000	0.0000	0.0230		60.00	0.00	0.00		60.00	0.00
	13		60	0	32.750	29000	0	60	100	1.096	0.0000	0.0000	0.0253		60.00	0.00	0.00		60.00	0.00
Grade 70 Plate	1		70	0	0.000	29000	0	70	100	1.06	0.0000	0.0000	-0.0030		-70.00	0.00	0.00		-66.94	3.60
Gr. 120 Rods	1		120	0	5.125	29000	0.0217	81.00	4.224	1.01	0.0000	0.0000	0.0014		40.81	0.00	0.00		40.81	3.60
Gr. 150 Rods	1		150	0	5.125	29000	0.0217	120.00	4.224	1.01	0.0000	0.0000	0.0014		41.22	0.00	0.00		41.22	3.60
Gr 270	1		270	28	1.500	28500	0.031	243	7.36	1.043	0.0010	0.0000	-0.0007		-20.59	0.00	0.00		-17.53	3.60
Gr 270	2		270	28	5.500	28500	0.031	243	7.36	1.043	0.0010	0.0000	0.0027		77.84	0.00	0.00		77.84	3.60
Gr 270	3		270	160	10.000	28500	0.031	243	7.36	1.043	0.0056	0.0000	0.0112		250.14	0.00	0.00		250.14	3.60
Gr 270	4		270	150	10.750	28500	0.031	243	7.36	1.043	0.0053	0.0000	0.0115		251.27	0.00	0.00		251.27	3.60
	5		270	160	12.333	28500	0.031	243	7.36	1.043	0.0056	0.0000	0.0133		255.60	0.00	0.00		255.60	3.60
	6		270	160	14.667	28500	0.031	243	7.36	1.043	0.0056	0.0000	0.0153		258.47	0.00	0.00		258.47	3.60
	7		270	160	17.000	28500	0.031	243	7.36	1.043	0.0056	0.0000	0.0173		260.62	0.00	0.00		260.62	3.60
	8		270	160	19.333	28500	0.031	243	7.36	1.043	0.0056	0.0000	0.0193		262.54	0.00	0.00		262.54	0.00
	9		270	160	21.667	28500	0.031	243	7.36	1.043	0.0056	0.0000	0.0213		264.38	0.00	0.00		264.38	0.00
	10		270	160	24.000	28500	0.031	243	7.36	1.043	0.0056	0.0000	0.0233		266.18	0.00	0.00		266.18	0.00
	11		270	160	26.333	28500	0.031	243	7.36	1.043	0.0056	0.0000	0.0254		267.97	0.00	0.00		267.97	0.00
	12		270	160	28.667	28500	0.031	243	7.36	1.043	0.0056	0.0000	0.0274		269.76	0.00	0.00		269.76	0.00
	13		270	160	31.000	28500	0.031	243	7.36	1.043	0.0056	0.0000	0.0294		270.00	0.00	0.00		270.00	0.00
	Sum of M									MAXIMUM	$\Delta\varepsilon$:	0.0083			Moment (K'	0.00	2694.63	kip*in		
																	224.55	kip*f		

Figure B.5 Yield Line Analysis Failure Section 2 Mb

$$L = \frac{8}{2} + \sqrt{\left(\frac{8}{2}\right)^2 + 8(6.41667)\left(\frac{202.1 + 82.66}{30.59}\right)} = 26.23\ ft$$

$$wl\left(\frac{26.23 - {}^{8}/_{2}}{26.23}\right) = \frac{8 * 202.1}{26.23} + \frac{8 * 82.66}{26.23} + \frac{30.59 * 26.23}{6.41667}$$

$$wl = 250.05\ k$$

B.3 Yield Line Failure Section 3

Flexural Strength														Mu	9597	kip-in.		
Dean Whitfield		**Three Failure Mode**									ε_{cu}	0.003						
		Failure Section 3 - Mw Upper																
											c=	2.046						
											a	1.739						
											Sum of forces	0.00	Calculate					
											Design	R/C & P/C ACI						
											ANSWER:							
											ϕ	0.90						
											ϕM_n kip-in	996	1106.552065	Av. β_1 :	0.850			
											kip*ft	82.991						
					Units in kips and inches													
Concrete Layers		f'c	Width, W	Thick., T	Depth, d_c	β_1	T_{upper}	T_{lower}	Revised T	Beta1calcuation				Area	Force	M_n k-in.		
	1	3.600	35.000	12.750	0.870	0.850	0.000	12.750	1.739	186.2990075	219.175303			60.882	-186.30	-162.03		
	2				12.750	0.850	12.750	12.750	0.000	0	0			0.000	0.00	0.00		
	3				12.750	0.850	12.750	12.750	0.000	0	0			0.000	0.00	0.00		
	4				12.750	0.850	12.750	12.750	0.000	0	0			0.000	0.00	0.00		
	5				12.750	0.850	12.750	12.750	0.000	0	0			0.000	0.00	0.00		
	6				12.750	0.850	12.750	12.750	0.000	0	0			0.000	0.00	0.00		
	7				12.750	0.850	12.750	12.750	0.000	0	0			0.000	0.00	0.00		
										186.2990075	219.175303							
Steel Layers		Area A_{si}	Grade	Effective Prest.	Depth d_{si}	E_s	Q	fpy	R	K	ε_{so}	$\Delta\varepsilon$	Total ε_s	Stress	Force	Moment	Modified stress	corresp. f'c
Grade 60 Bars	1	1.76	60	0	3.125	29000	0	60	100	1.096	0.0000	0.0016	0.0016	45.85	80.70	252.18	45.85	3.60
	2	1.76	60	0	9.625	29000	0	60	100	1.096	0.0000	0.0111	0.0111	60.00	105.60	1016.40	60.00	3.60
	3		60	0	12.688	29000	0	60	100	1.096	0.0000	0.0000	0.0156	60.00	0.00	0.00	60.00	3.60
	4		60	0	9.125	29000	0	60	100	1.096	0.0000	0.0000	0.0104	60.00	0.00	0.00	60.00	3.60
	5		60	0	11.750	29000	0	60	100	1.096	0.0000	0.0000	0.0142	60.00	0.00	0.00	60.00	3.60
	6		60	0	14.375	29000	0	60	100	1.096	0.0000	0.0000	0.0181	60.00	0.00	0.00	60.00	0.00
	7		60	0	17.000	29000	0	60	100	1.096	0.0000	0.0000	0.0219	60.00	0.00	0.00	60.00	0.00
	8		60	0	19.625	29000	0	60	100	1.096	0.0000	0.0000	0.0258	60.00	0.00	0.00	60.00	0.00
	9		60	0	22.250	29000	0	60	100	1.096	0.0000	0.0000	0.0296	60.00	0.00	0.00	60.00	0.00
	10		60	0	24.875	29000	0	60	100	1.096	0.0000	0.0000	0.0335	60.00	0.00	0.00	60.00	0.00
	11		60	0	27.500	29000	0	60	100	1.096	0.0000	0.0000	0.0373	60.00	0.00	0.00	60.00	0.00
	12		60	0	30.125	29000	0	60	100	1.096	0.0000	0.0000	0.0412	60.00	0.00	0.00	60.00	0.00
	13		60	0	32.750	29000	0	60	100	1.096	0.0000	0.0000	0.0450	60.00	0.00	0.00	60.00	0.00
Grade 70 Plate	1		70	0	0.000	29000	0	70	100	1.06	0.0000	0.0000	-0.0030	-70.00	0.00	0.00	-66.94	3.60
Gr. 120 Rods	1		120	0	5.125	29000	0.0217	81.00	4.224	1.01	0.0000	0.0000	0.0045	80.47	0.00	0.00	80.47	3.60
Gr. 150 Rods	1		150	0	5.125	29000	0.0217	120.00	4.224	1.01	0.0000	0.0000	0.0045	107.08	0.00	0.00	107.08	3.60
Gr 270	1		270	28	1.500	28500	0.031	243	7.36	1.043	0.0010	0.0000	0.0002	5.17	0.00	0.00	8.23	3.60
Gr 270	2		270	28	5.500	28500	0.031	243	7.36	1.043	0.0010	0.0000	0.0060	171.01	0.00	0.00	171.01	3.60
Gr 270	3		270	160	10.000	28500	0.031	243	7.36	1.043	0.0056	0.0000	0.0173	260.60	0.00	0.00	260.60	3.60
Gr 270	4		270	150	10.750	28500	0.031	243	7.36	1.043	0.0053	0.0000	0.0180	261.33	0.00	0.00	261.33	3.60
	5		270	160	12.333	28500	0.031	243	7.36	1.043	0.0056	0.0000	0.0207	263.81	0.00	0.00	263.81	3.60
	6		270	160	14.667	28500	0.031	243	7.36	1.043	0.0056	0.0000	0.0241	266.88	0.00	0.00	266.88	0.00
	7		270	160	17.000	28500	0.031	243	7.36	1.043	0.0056	0.0000	0.0275	269.91	0.00	0.00	269.91	0.00
	8		270	160	19.333	28500	0.031	243	7.36	1.043	0.0056	0.0000	0.0310	270.00	0.00	0.00	270.00	0.00
	9		270	160	21.667	28500	0.031	243	7.36	1.043	0.0056	0.0000	0.0344	270.00	0.00	0.00	270.00	0.00
	10		270	160	24.000	28500	0.031	243	7.36	1.043	0.0056	0.0000	0.0378	270.00	0.00	0.00	270.00	0.00
	11		270	160	26.333	28500	0.031	243	7.36	1.043	0.0056	0.0000	0.0412	270.00	0.00	0.00	270.00	0.00
	12		270	160	28.667	28500	0.031	243	7.36	1.043	0.0056	0.0000	0.0446	270.00	0.00	0.00	270.00	0.00
	13		270	160	31.000	28500	0.031	243	7.36	1.043	0.0056	0.0000	0.0481	270.00	0.00	0.00	270.00	0.00
	Sum of M									MAXIMUM	$\Delta\varepsilon$:	0.0111		Moment (K'	0.00	1106.55	kip*in	
																92.21	kip*f	

Figure B.6 Yield Line Analysis Failure Section 3 Mw Upper

Flexural Strength

Mu 9597 kip-in.

Dean Whitfield — **Three Failure Mode**
Failure Section 3 - Mw Lower

ε_{cu}	0.003
c=	1.562
a	1.327
Sum of forces	0.00
Design	R/C & P/C ACI
ANSWER:	
ϕ	0.90
ϕM_n kip-in	384
kip*ft	32.022

Calculate

426.959276 **Av. β_1 : 0.850**

Units in kips and inches

Concrete Layers		f'c	Width, W	Thick., T	Depth, d_c	β_1	T_{upper}	T_{lower}	Revised T	Beta1calcuation				Area	Force	M_n k-in.		
	1	3.600	13.000	17.500	0.664	0.850	0.000	17.500	1.327	52.8	62.1176471			17.255	-52.80	-35.04		
	2				17.500	0.850	17.500	17.500	0.000	0	0			0.000	0.00	0.00		
	3				17.500	0.850	17.500	17.500	0.000	0	0			0.000	0.00	0.00		
	4				17.500	0.850	17.500	17.500	0.000	0	0			0.000	0.00	0.00		
	5				17.500	0.850	17.500	17.500	0.000	0	0			0.000	0.00	0.00		
	6				17.500	0.850	17.500	17.500	0.000	0	0			0.000	0.00	0.00		
	7				17.500	0.850	17.500	17.500	0.000	0	0			0.000	0.00	0.00		
										52.8	62.1176471							
																	Modified	corresp.
Steel Layers		**Area A_{sl}**	**Grade**	**Effective Prest.**	**Depth d_{sl}**	**E_s**	**Q**	**fpy**	**R**	**K**	**ε_{so}**	**$\Delta\varepsilon$**	**Total ε_s**	**Stress**	**Force**	**Moment**	**stress**	**f'c**
Grade 60 Bars	1	0.44	60	0	3.125	29000	0	60	100	1.096	0.0000	0.0030	0.0030	60.00	26.40	82.50	60.00	3.60
	2	0.44	60	0	14.375	29000	0	60	100	1.096	0.0000	0.0246	0.0246	60.00	26.40	379.50	60.00	3.60
	3		60	0	12.688	29000	0	60	100	1.096	0.0000	0.0000	0.0214	60.00	0.00	0.00	60.00	3.60
	4		60	0	9.125	29000	0	60	100	1.096	0.0000	0.0000	0.0145	60.00	0.00	0.00	60.00	3.60
	5		60	0	11.750	29000	0	60	100	1.096	0.0000	0.0000	0.0196	60.00	0.00	0.00	60.00	3.60
	6		60	0	14.375	29000	0	60	100	1.096	0.0000	0.0000	0.0246	60.00	0.00	0.00	60.00	3.60
	7		60	0	17.000	29000	0	60	100	1.096	0.0000	0.0000	0.0297	60.00	0.00	0.00	60.00	3.60
	8		60	0	19.625	29000	0	60	100	1.096	0.0000	0.0000	0.0347	60.00	0.00	0.00	60.00	0.00
	9		60	0	22.250	29000	0	60	100	1.096	0.0000	0.0000	0.0397	60.00	0.00	0.00	60.00	0.00
	10		60	0	24.875	29000	0	60	100	1.096	0.0000	0.0000	0.0448	60.00	0.00	0.00	60.00	0.00
	11		60	0	27.500	29000	0	60	100	1.096	0.0000	0.0000	0.0498	60.00	0.00	0.00	60.00	0.00
	12		60	0	30.125	29000	0	60	100	1.096	0.0000	0.0000	0.0549	60.00	0.00	0.00	60.00	0.00
	13		60	0	32.750	29000	0	60	100	1.096	0.0000	0.0000	0.0599	60.00	0.00	0.00	60.00	0.00
Grade 70 Plate	1		70	0	0.000	29000	0	70	100	1.06	0.0000	0.0000	-0.0030	-70.00	0.00	0.00	-66.94	3.60
Gr. 120 Rods	1		120	0	5.125	29000	0.0217	81.00	4.224	1.01	0.0000	0.0000	0.0068	83.90	0.00	0.00	83.90	3.60
Gr. 150 Rods	1		150	0	5.125	29000	0.0217	120.00	4.224	1.01	0.0000	0.0000	0.0068	119.63	0.00	0.00	119.63	3.60
Gr 270	1		270	28	1.500	28500	0.031	243	7.36	1.043	0.0010	0.0000	0.0009	24.63	0.00	0.00	24.63	3.60
Gr 270	2		270	28	5.500	28500	0.031	243	7.36	1.043	0.0010	0.0000	0.0085	226.39	0.00	0.00	226.39	3.60
Gr 270	3		270	160	10.000	28500	0.031	243	7.36	1.043	0.0056	0.0000	0.0218	264.83	0.00	0.00	264.83	3.60
Gr 270	4		270	150	10.750	28500	0.031	243	7.36	1.043	0.0053	0.0000	0.0229	265.81	0.00	0.00	265.81	3.60
	5		270	160	12.333	28500	0.031	243	7.36	1.043	0.0056	0.0000	0.0263	268.82	0.00	0.00	268.82	3.60
	6		270	160	14.667	28500	0.031	243	7.36	1.043	0.0056	0.0000	0.0308	270.00	0.00	0.00	270.00	3.60
	7		270	160	17.000	28500	0.031	243	7.36	1.043	0.0056	0.0000	0.0353	270.00	0.00	0.00	270.00	3.60
	8		270	160	19.333	28500	0.031	243	7.36	1.043	0.0056	0.0000	0.0398	270.00	0.00	0.00	270.00	0.00
	9		270	160	21.667	28500	0.031	243	7.36	1.043	0.0056	0.0000	0.0442	270.00	0.00	0.00	270.00	0.00
	10		270	160	24.000	28500	0.031	243	7.36	1.043	0.0056	0.0000	0.0487	270.00	0.00	0.00	270.00	0.00
	11		270	160	26.333	28500	0.031	243	7.36	1.043	0.0056	0.0000	0.0532	270.00	0.00	0.00	270.00	0.00
	12		270	160	28.667	28500	0.031	243	7.36	1.043	0.0056	0.0000	0.0577	270.00	0.00	0.00	270.00	0.00
	13		270	160	31.000	28500	0.031	243	7.36	1.043	0.0056	0.0000	0.0622	270.00	0.00	0.00	270.00	0.00
	Sum of M									**MAXIMUM**	**$\Delta\varepsilon$:**	**0.0246**		**Moment (K'**	**0.00**	**426.96**	kip*in	
																35.58	kip*f	

Figure B.7 Yield Line Analysis Failure Section 3 Mw Lower

Flexural Strength															Mu	9597	kip-in.		
Dean Whitfield		**Three Failure Mode**									ε_{cu}	0.003							
		Failure Section 3 - Mc									c=	1.824							
											a	1.551							
											Sum of forces	0.00	Calculate						
											Design	R/C & P/C ACI							
											ANSWER:								
											ϕ	0.90							
											ϕM_n kip-in	679	754.3832143	Av. β_1 :	0.850				
											kip*ft	56.579							
				Units in kips and inches															
Concrete Layers		**f'c**	**Width, W**	**Thick., T**	**Depth, d_c**	**β_1**	**T_{upper}**	**T_{lower}**	**Revised T**	**Beta1calcuation**					**Area**	**Force**	**M_n k-in.**		
	1	3.600	12.000	21.500	0.775	0.850	0.000	21.500	1.551	56.93710794	66.9848329				18.607	-56.94	-44.14		
	2				21.500	0.850	21.500	21.500	0.000	0	0				0.000	0.00	0.00		
	3				21.500	0.850	21.500	21.500	0.000	0	0				0.000	0.00	0.00		
	4				21.500	0.850	21.500	21.500	0.000	0	0				0.000	0.00	0.00		
	5				21.500	0.850	21.500	21.500	0.000	0	0				0.000	0.00	0.00		
	6				21.500	0.850	21.500	21.500	0.000	0	0				0.000	0.00	0.00		
	7				21.500	0.850	21.500	21.500	0.000	0	0				0.000	0.00	0.00		
										56.93710794	66.9848329								
					4.134													Modified	corresp.
Steel Layers		**Area A_{si}**	**Grade**	**Effective Prest.**	**Depth d_{si}**	**E_s**	**Q**	**fpy**	**R**	**K**	**ε_{so}**	**$\Delta\varepsilon$**	**Total ε_s**		**Stress**	**Force**	**Moment**	**stress**	**f'c**
Grade 60 Bars	1	0.66	60	0	2.375	29000	0	60	100	1.096	0.0000	0.0009	0.0009		26.27	17.34	41.18	26.27	3.60
	2	0.66	60	0	19.125	29000	0	60	100	1.096	0.0000	0.0285	0.0285		60.00	39.60	757.35	60.00	3.60
	3		60	0	6.500	29000	0	60	100	1.096	0.0000	0.0000	0.0077		60.00	0.00	0.00	60.00	3.60
	4		60	0	9.125	29000	0	60	100	1.096	0.0000	0.0000	0.0120		60.00	0.00	0.00	60.00	3.60
	5		60	0	11.750	29000	0	60	100	1.096	0.0000	0.0000	0.0163		60.00	0.00	0.00	60.00	3.60
	6		60	0	14.375	29000	0	60	100	1.096	0.0000	0.0000	0.0206		60.00	0.00	0.00	60.00	3.60
	7		60	0	17.000	29000	0	60	100	1.096	0.0000	0.0000	0.0250		60.00	0.00	0.00	60.00	3.60
	8		60	0	19.625	29000	0	60	100	1.096	0.0000	0.0000	0.0293		60.00	0.00	0.00	60.00	3.60
	9		60	0	22.250	29000	0	60	100	1.096	0.0000	0.0000	0.0336		60.00	0.00	0.00	60.00	0.00
	10		60	0	24.875	29000	0	60	100	1.096	0.0000	0.0000	0.0379		60.00	0.00	0.00	60.00	0.00
	11		60	0	27.500	29000	0	60	100	1.096	0.0000	0.0000	0.0422		60.00	0.00	0.00	60.00	0.00
	12		60	0	30.125	29000	0	60	100	1.096	0.0000	0.0000	0.0465		60.00	0.00	0.00	60.00	0.00
	13		60	0	32.750	29000	0	60	100	1.096	0.0000	0.0000	0.0509		60.00	0.00	0.00	60.00	0.00
Grade 70 Plate	1		70	0	0.000	29000	0	70	100	1.06	0.0000	0.0000	-0.0030		-70.00	0.00	0.00	-66.94	3.60
Gr. 120 Rods	1		120	0	5.125	29000	0.0217	81.00	4.224	1.01	0.0000	0.0000	0.0054		82.30	0.00	0.00	82.30	3.60
Gr. 150 Rods	1		150	0	5.125	29000	0.0217	120.00	4.224	1.01	0.0000	0.0000	0.0054		114.22	0.00	0.00	114.22	3.60
Gr 270	1		270	28	1.500	28500	0.031	243	7.36	1.043	0.0010	0.0000	0.0004		12.80	0.00	0.00	15.86	3.60
Gr 270	2		270	28	5.500	28500	0.031	243	7.36	1.043	0.0010	0.0000	0.0070		196.04	0.00	0.00	196.04	3.60
Gr 270	3		270	160	10.000	28500	0.031	243	7.36	1.043	0.0056	0.0000	0.0191		262.31	0.00	0.00	262.31	3.60
Gr 270	4		270	150	10.750	28500	0.031	243	7.36	1.043	0.0053	0.0000	0.0199		263.12	0.00	0.00	263.12	3.60
	5		270	160	12.333	28500	0.031	243	7.36	1.043	0.0056	0.0000	0.0229		265.79	0.00	0.00	265.79	3.60
	6		270	160	14.667	28500	0.031	243	7.36	1.043	0.0056	0.0000	0.0267		269.20	0.00	0.00	269.20	3.60
	7		270	160	17.000	28500	0.031	243	7.36	1.043	0.0056	0.0000	0.0306		270.00	0.00	0.00	270.00	3.60
	8		270	160	19.333	28500	0.031	243	7.36	1.043	0.0056	0.0000	0.0344		270.00	0.00	0.00	270.00	3.60
	9		270	160	21.667	28500	0.031	243	7.36	1.043	0.0056	0.0000	0.0382		270.00	0.00	0.00	270.00	0.00
	10		270	160	24.000	28500	0.031	243	7.36	1.043	0.0056	0.0000	0.0421		270.00	0.00	0.00	270.00	0.00
	11		270	160	26.333	28500	0.031	243	7.36	1.043	0.0056	0.0000	0.0459		270.00	0.00	0.00	270.00	0.00
	12		270	160	28.667	28500	0.031	243	7.36	1.043	0.0056	0.0000	0.0498		270.00	0.00	0.00	270.00	0.00
	13		270	160	31.000	28500	0.031	243	7.36	1.043	0.0056	0.0000	0.0536		270.00	0.00	0.00	270.00	0.00
	Sum of M									**MAXIMUM**	**$\Delta\varepsilon$:**	**0.0285**			**Moment (k**	**0.00**	**754.38**	kip*in	
																	62.87	kip*f	

Figure B.8 Yield Line Analysis Failure Section 3 Mc

Flexural Strength															Mu	9597	kip-in.			
Dean Whitfield		**Three Failure Mode**									ε_{cu}	0.003								
		Failure Section 3 - Mb									c=	3.475								
											a	2.953								
											Sum of forces	0.00	Calculate							
											Design	R/C & P/C ACI								
											ANSWER:									
											ϕ	0.90								
											ϕM_n kip-in	2425	2694.627044	Av. β_1 :	0.850					
					Units in kips and inches						kip*ft	202.097								
Concrete Layers		f'c	Width, W	Thick., T	Depth, d_c	β_1	T_{upper}	T_{lower}	Revised T	Beta1calcuation					Area	Force	M_n k-in.			
	1	3.600	21.000	16.000	1.477	0.850	0.000	16.000	2.953	189.785467	223.27702				62.021	-189.79	-280.26			
	2				16.000	0.850	16.000	16.000	0.000	0	0				0.000	0.00	0.00			
	3				16.000	0.850	16.000	16.000	0.000	0	0				0.000	0.00	0.00			
	4				16.000	0.850	16.000	16.000	0.000	0	0				0.000	0.00	0.00			
	5				16.000	0.850	16.000	16.000	0.000	0	0				0.000	0.00	0.00			
	6				16.000	0.850	16.000	16.000	0.000	0	0				0.000	0.00	0.00			
	7				16.000	0.850	16.000	16.000	0.000	0	0				0.000	0.00	0.00			
										189.785467	223.27702								Modified	corresp.
Steel Layers		Area A_{sl}	Grade	Effective Prest.	Depth d_{sl}	E_s	Q	fpy	R	K	ε_{so}	$\Delta\varepsilon$	Total ε_s		Stress	Force	Moment		stress	f'c
Grade 60 Bars	1	3.95	60	0	2.875	29000	0	60	100	1.096	0.0000	-0.0005	-0.0005		-15.01	-47.21	-135.74		-11.95	3.60
	2	3.95	60	0	13.125	29000	0	60	100	1.096	0.0000	0.0083	0.0083		60.00	237.00	3110.63		60.00	3.60
	3		60	0	12.688	29000	0	60	100	1.096	0.0000	0.0000	0.0080		60.00	0.00	0.00		60.00	3.60
	4		60	0	9.125	29000	0	60	100	1.096	0.0000	0.0000	0.0049		60.00	0.00	0.00		60.00	3.60
	5		60	0	11.750	29000	0	60	100	1.096	0.0000	0.0000	0.0071		60.00	0.00	0.00		60.00	3.60
	6		60	0	14.375	29000	0	60	100	1.096	0.0000	0.0000	0.0094		60.00	0.00	0.00		60.00	3.60
	7		60	0	17.000	29000	0	60	100	1.096	0.0000	0.0000	0.0117		60.00	0.00	0.00		60.00	0.00
	8		60	0	19.625	29000	0	60	100	1.096	0.0000	0.0000	0.0139		60.00	0.00	0.00		60.00	0.00
	9		60	0	22.250	29000	0	60	100	1.096	0.0000	0.0000	0.0162		60.00	0.00	0.00		60.00	0.00
	10		60	0	24.875	29000	0	60	100	1.096	0.0000	0.0000	0.0185		60.00	0.00	0.00		60.00	0.00
	11		60	0	27.500	29000	0	60	100	1.096	0.0000	0.0000	0.0207		60.00	0.00	0.00		60.00	0.00
	12		60	0	30.125	29000	0	60	100	1.096	0.0000	0.0000	0.0230		60.00	0.00	0.00		60.00	0.00
	13		60	0	32.750	29000	0	60	100	1.096	0.0000	0.0000	0.0253		60.00	0.00	0.00		60.00	0.00
Grade 70 Plate	1		70	0	0.000	29000	0	70	100	1.06	0.0000	0.0000	-0.0030		-70.00	0.00	0.00		-66.94	3.60
Gr. 120 Rods	1		120	0	5.125	29000	0.0217	81.00	4.224	1.01	0.0000	0.0000	0.0014		40.81	0.00	0.00		40.81	3.60
Gr. 150 Rods	1		150	0	5.125	29000	0.0217	120.00	4.224	1.01	0.0000	0.0000	0.0014		41.22	0.00	0.00		41.22	3.60
Gr 270	1		270	28	1.500	28500	0.031	243	7.36	1.043	0.0010	0.0000	-0.0007		-20.59	0.00	0.00		-17.53	3.60
Gr 270	2		270	28	5.500	28500	0.031	243	7.36	1.043	0.0010	0.0000	0.0027		77.84	0.00	0.00		77.84	3.60
Gr 270	3		270	160	10.000	28500	0.031	243	7.36	1.043	0.0056	0.0000	0.0112		250.14	0.00	0.00		250.14	3.60
Gr 270	4		270	150	10.750	28500	0.031	243	7.36	1.043	0.0053	0.0000	0.0115		251.27	0.00	0.00		251.27	3.60
	5		270	160	12.333	28500	0.031	243	7.36	1.043	0.0056	0.0000	0.0133		255.60	0.00	0.00		255.60	3.60
	6		270	160	14.667	28500	0.031	243	7.36	1.043	0.0056	0.0000	0.0153		258.47	0.00	0.00		258.47	3.60
	7		270	160	17.000	28500	0.031	243	7.36	1.043	0.0056	0.0000	0.0173		260.62	0.00	0.00		260.62	0.00
	8		270	160	19.333	28500	0.031	243	7.36	1.043	0.0056	0.0000	0.0193		262.54	0.00	0.00		262.54	0.00
	9		270	160	21.667	28500	0.031	243	7.36	1.043	0.0056	0.0000	0.0213		264.38	0.00	0.00		264.38	0.00
	10		270	160	24.000	28500	0.031	243	7.36	1.043	0.0056	0.0000	0.0233		266.18	0.00	0.00		266.18	0.00
	11		270	160	26.333	28500	0.031	243	7.36	1.043	0.0056	0.0000	0.0254		267.97	0.00	0.00		267.97	0.00
	12		270	160	28.667	28500	0.031	243	7.36	1.043	0.0056	0.0000	0.0274		269.76	0.00	0.00		269.76	0.00
	13		270	160	31.000	28500	0.031	243	7.36	1.043	0.0056	0.0000	0.0294		270.00	0.00	0.00		270.00	0.00
	Sum of M									MAXIMUM	$\Delta\varepsilon$:	0.0083			Moment (K'	0.00	2694.63	kip*in		
																	224.55	kip*f		

Figure B.9 Yield Line Analysis Failure Section 3 Mb

$$L = \frac{8}{2} + \sqrt{\left(\frac{8}{2}\right)^2 + 8(7.5)\left(\frac{115.01 + 202.1}{56.58}\right)} = 22.77\ ft$$

$$wl\left(\frac{22.77 - {}^{8}/_{2}}{22.77}\right) = \frac{8 * 202.1}{22.77} + \frac{8 * 115.67}{22.77} + \frac{56.58 * 22.77}{7.5}$$

$$wl = 343.82\ kip$$

B.4 Incremental Analysis Method

$$\frac{P}{\Delta_{max}} = \frac{3*3457141psi*591.33in^4}{31.5^3} + \frac{2*3457141psi*591.33in^4}{9.5*31.5^2} \qquad (Eqn.\ 41)$$

$$k = \frac{P}{\Delta_{max}} = 644064.33\ {}^{lb}/_{in} = 7728.72\ {}^{k}/_{ft} \qquad (Eqn.\ 42)$$

Appendix C Concept Example Calculations

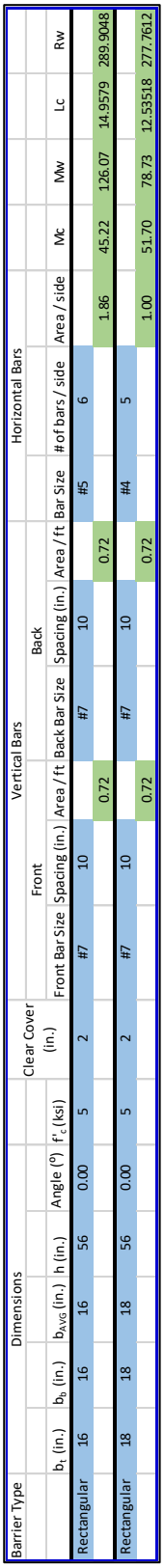

Barrier Type	Dimensions						Clear Cover (in.)	Vertical Bars						Horizontal Bars					
								Front			Back								
	b_t (in.)	b_b (in.)	b_{AVG} (in.)	h (in.)	Angle (°)	f'c (ksi)		Front Bar Size	Spacing (in.)	Area / ft	Back Bar Size	Spacing (in.)	Area / ft	Bar Size	# of bars / side	Area / side	Mc	Mw	Lc	Rw
Rectangular	16	16	16	56	0.00	5	2	#7	10	0.72	#7	10	0.72	#5	6	1.86	45.22	126.07	14.9579	289.9048
Rectangular	18	18	18	56	0.00	5	2	#7	10	0.72	#7	10	0.72	#4	5	1.00	51.70	78.73	12.53518	277.7612

Figure C.1 Concept 1 Example Calculations

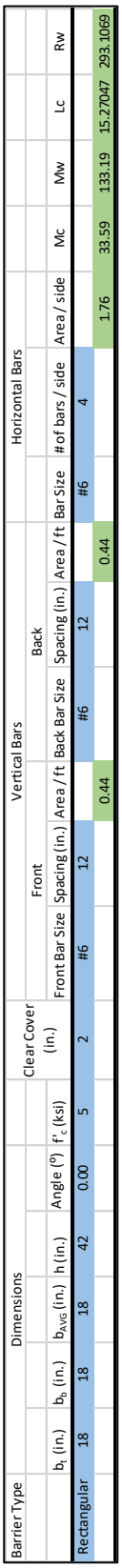

Barrier Type	Dimensions					Clear Cover (in.)	Vertical Bars						Horizontal Bars							
							Front			Back										
	b_t (in.)	b_b (in.)	b_{AVG} (in.)	h (in.)	Angle (°)	f'$_c$ (ksi)														
							Front Bar Size	Spacing (in.)	Area / ft	Back Bar Size	Spacing (in.)	Area / ft	Bar Size	# of bars / side	Area / side	Mc	Mw	Lc	Rw
Rectangular	18	18	18	42	0.00	5	#6	12	0.44	#6	12	0.44	#6	4	1.76	33.59	133.19	15.27047	293.1069

Figure C.2 Concept 2 Example Wall Calculations

Inputs:				
Rail:	HSS10X.625			
Posts:	h =	4	in.	height of the post (top of wall section to bottom of rail section)
	b =	2	in.	width of the post
	d =	8	in.	depth of the post
	L =	8	ft	span length
L_t =	8	ft	per AASHTO Chapter 13 requirements	
H_r =	11	in	height to the middle of the rail section	
Calculations:				
Loading:				
L=	8.0	ft		
a=	0.0	ft		
b=	8.0	ft		
c=	8	ft		
w=	29.125	k/ft		
x =	5	ft		
d=	4.00	ft		
Ra =	116.5	kip		
Rb =	116.5	kip		
Ma =	155.53	k-ft		
Mb =	155.53	k-ft		
M_{max} =	155.527	k-ft		
Rail:				
M_r =	2167.2	k-in		
	180.6	k-ft		
ΦM_r =	162.54	k-ft	Member is OK	
Posts:				
Z =	32	in^3		
M_p =	1036.8	k-in		
P_p=	74.0571	k	at top of rail	Post is OK

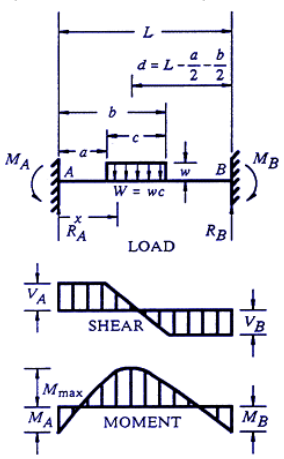

Figure C.3 Concept 2 Example Rail and Post Calculations

Barrier Type	Dimensions					Clear Cover (in.)	Vertical Bars						Horizontal Bars					
							Front			Back								
	b_t (in.)	b_b (in.)	b_{AVG} (in.)	h (in.)	Angle (°)	f'_c (ksi)		Front Bar Size	Spacing (in.)	Area / ft	Back Bar Size	Spacing (in.)	Area / ft	Bar Size	# of bars / side	Area / side	Mc	Mw	Lc	Rw
Rectangular	16	16	16	42	0.00	5	2	#6	12	0.44	#6	12	0.44	#5	5	1.55	29.63	104.33	14.70477	248.9737

Figure C.4 Concept 3 Example Wall Calculations

Inputs:				
Rail:	HSS7.5X.500			
Posts:	h =	6.5	in.	height of the post (top of wall section to bottom of rail section)
	b =	1.5	in.	width of the post
	d =	7	in.	depth of the post
	L =	8.0	ft	span length
L_t =	8	ft	per AASHTO Chapter 13 requirements	
Calculations:				
Rail:				
M_r =	1058	k-in	A500 Gr. C Fy=46	
	88.1667	k-ft		
ΦM_r =	79.35	k-ft		
Posts:				
Z =	18.375	in^3		
ΦM_p =	826.875	k-in	A572 Gr. 50	
P_p=	59.0625	k	at top bottom of rail	
Capacity:				
Spans	R (kip)			
1 span =	158.66			
2 span =	131.638			
3 span =	126.233			
4 span =	157.666			
5 span =	175.129			
6 span =	207.719			

Figure C.5 Concept 3 Example Rail and Post Calculations

Barrier Type	Dimensions					Clear Cover (in.)	Vertical Bars						Horizontal Bars					
							Front			Back								
	b_t (in.)	b_b (in.)	b_{AVG} (in.)	h (in.)	Angle (°)	f'_c (ksi)	Front Bar Size	Spacing (in.)	Area / ft	Back Bar Size	Spacing (in.)	Area / ft	Bar Size	# of bars / side	Area / side	Mc	Mw	Lc	Rw
Rectangular	16	16	16	42	0.00	5	#6	12	0.44	#6	12	0.44	#5	5	1.55	29.63	104.33	14.70477	248.9737

Figure C.6 Concept 4 Example Wall Calculations

Inputs:			Weight =	80000	lb							
Hardness =	80		Rear Weig	34000	lb							
Poissons =	0.5		Impact V =	50	mph							
Pad Area =	121	in^2	Impact θ =	15	deg							
Pad Height =	8	in	IS_{whole} =	447.8703	k-ft							
Δ_{max} =	8	in										
			Kinetic for Rear									
			Speed	15.5	mph							
Calculations:			Angle	90	deg							
E =	9.382421	Mpa	IS_{rear} =	273.0688	k-ft							
	1.360805	ksi		3276.826	k-in							
				468.118	k-in	1/7 of the rear IS						
G =	0.18	ksi										

The force due to the deformation of an elastomeric element shall be taken as:

$$H_{bu} = GA\frac{\Delta_u}{h_{rt}} \qquad (14.6.3.1\text{-}2)$$

where:

G = shear modulus of the elastomer (ksi)

A = plan area of elastomeric element or bearing ($in.^2$)

Δ_u = shear deformation from applicable strength and extreme event load combinations in Table 3.4.1-1 (in.)

h_{rt} = total elastomer thickness (in.)

Strength and extreme event limit states rolling forces shall be determined by testing.

Load	Pad Number																	
Spans	1	2	3	4	5	6	7	8	9	10	11	12	13	14	15	16	Sum	Average
2	21.78																21.78	21.78
3	14.52	14.52															29.04	14.52
4	10.89	21.78	10.89														43.56	14.52
5	8.712	17.424	17.424	8.712													52.272	13.068
6	7.26	14.52	21.78	14.52	7.26												65.34	13.068
7	6.222857	12.44571	18.66857	18.66857	12.44571	6.222857											74.67429	12.44571
8	5.445	10.89	16.335	21.78	16.335	10.89	5.445										87.12	12.44571
9	4.84	9.68	14.52	19.36	19.36	14.52	9.68	4.84									96.8	12.1
10	4.356	8.712	13.068	17.424	21.78	17.424	13.068	8.712	4.356								108.9	12.1
11	3.96	7.92	11.88	15.84	19.8	19.8	15.84	11.88	7.92	3.96							118.8	11.88
12	3.63	7.26	10.89	14.52	18.15	21.78	18.15	14.52	10.89	7.26	3.63						130.68	11.88
13	3.350769	6.701538	10.05231	13.40308	16.75385	20.10462	20.10462	16.75385	13.40308	10.05231	6.701538	3.350769					140.7323	11.72769
14	3.111429	6.222857	9.334286	12.44571	15.55714	18.66857	21.78	18.66857	15.55714	12.44571	9.334286	6.222857	3.111429				152.46	11.72769
15	2.904	5.808	8.712	11.616	14.52	17.424	20.328	20.328	17.424	14.52	11.616	8.712	5.808	2.904			162.624	11.616
16	2.7225	5.445	8.1675	10.89	13.6125	16.335	19.0575	21.78	19.0575	16.335	13.6125	10.89	8.1675	5.445	2.7225		174.24	11.616
17	2.562353	5.124706	7.687059	10.24941	12.81176	15.37412	17.93647	20.49882	20.49882	17.93647	15.37412	12.81176	10.24941	7.687059	5.124706	2.562353	184.4894	11.53059

Energy [k-in] with 0.5 x Force x Displacement									Pad Number									
Spans	1	2	3	4	5	6	7	8	9	10	11	12	13	14	15	16	Sum	Average
2	87.12																87.12	87.12
3	38.72	38.72															77.44	38.72
4	21.78	87.12	21.78														130.68	43.56
5	13.9392	55.7568	55.7568	13.9392													139.392	34.848
6	9.68	38.72	87.12	38.72	9.68												183.92	36.784
7	7.111837	28.44735	64.00653	64.00653	28.44735	7.111837											199.1314	33.18857
8	5.445	21.78	49.005	87.12	49.005	21.78	5.445										239.58	34.22571
9	4.302222	17.20889	38.72	68.83556	68.83556	38.72	17.20889	4.302222									258.1333	32.26667
10	3.4848	13.9392	31.3632	55.7568	87.12	55.7568	31.3632	13.9392	3.4848								296.208	32.912
11	2.88	11.52	25.92	46.08	72	72	46.08	25.92	11.52	2.88							316.8	31.68
12	2.42	9.68	21.78	38.72	60.5	87.12	60.5	38.72	21.78	9.68	2.42						353.32	32.12
13	2.062012	8.248047	18.55811	32.99219	51.5503	74.23243	74.23243	51.5503	32.99219	18.55811	8.248047	2.062012					375.2862	31.27385
14	1.777959	7.111837	16.00163	28.44735	44.44898	64.00653	74.67429	64.00653	44.44898	28.44735	16.00163	7.111837	1.777959				398.2629	30.6356
15	1.5488	6.1952	13.9392	24.7808	38.72	55.7568	75.8912	75.8912	55.7568	38.72	24.7808	13.9392	6.1952	1.5488			433.664	30.976
16	1.36125	5.445	12.25125	21.78	34.03125	49.005	66.70125	87.12	66.70125	49.005	34.03125	21.78	12.25125	5.445	1.36125		468.27	31.218
17	1.205813	4.823253	10.85232	19.29301	30.14533	43.40927	59.08484	77.17204	77.17204	59.08484	43.40927	30.14533	19.29301	10.85232	4.823253	1.205813	491.9718	30.74824

Figure C.7 Concept 4 Example Elastomer Post Calculations

Inputs:				
Rail:	HSS7X.375			
Posts:	h =	3	in.	height of the post (top of wall section to bottom of rail section)
	h tot =	12.625	in.	height from the top of the parapet to the top of the rail
	b =	1.5	in.	width of the post
	d =	5	in.	depth of the post
	L =	5	ft	span length
L_t =	8	ft	per AASHTO Chapter 13 requirements	
H_r =	11	in	height to the middle of the rail section	
Calculations:				
Rail:				
M_r =	651	k-in		
	54.25	k-ft		
Posts:				
Z =	9.375	in^3		
M_p =	337.5	k-in		
P_p=	24.1071	k	at top bottom of rail	
	20.50	k	load from elastomer posts	
Capacity:				
Spans	R (kip)			
1 span =	434			
2 span =	112.512			
3 span =	83.2857			
4 span =	87.3929			
5 span =	89.5442			
6 span =	100.14			
7 span =	107.318			
8 span =	119.198			
9 span =	128.181			
10 span =	140.452			
11 span =	150.317			
12 span =	162.724			
13 span =	173.098			
14 span =	185.553			
15 span =	196.254			
16 span =	208.718			
17 span =	219.644			

Figure C.8 Concept 4 Example Steel Rail Calculations

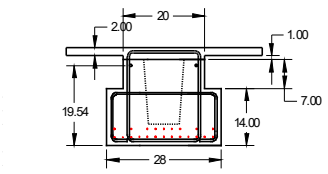

Section at Midspan at Beam and Topping

Flexural Strength

Bryan Beam **MKT** **2/7/2006**

ε_{cu}	0.003		
c=	2.671		
a	2.137		
Sum of forces	0.00	Calculate	
Design	R/C & P/C ACI		
ANSWER:			
ϕ	0.90		
ϕM_n kip-in	665	738.6281562	Av. β_1 : 0.800
kip*ft	55.397		

Mu 9597 kip-in.

Units in kips and inches

Concrete Layers		f'c	Width, W	Thick., T	Depth, d_c	β_1	T_{upper}	T_{lower}	Revised T	Beta1calcuation				Area	Force	M_n k-in.		
	1	5.000	8.000	14.000	1.068	0.800	0.000	14.000	2.137	68.37518452	85.4689806			17.094	-72.65	-77.62		
	2				14.000	0.850	14.000	14.000	0.000	0	0			0.000	0.00	0.00		
	3				14.000	0.850	14.000	14.000	0.000	0	0			0.000	0.00	0.00		
	4				14.000	0.850	14.000	14.000	0.000	0	0			0.000	0.00	0.00		
	5				14.000	0.850	14.000	14.000	0.000	0	0			0.000	0.00	0.00		
	6				14.000	0.850	14.000	14.000	0.000	0	0			0.000	0.00	0.00		
	7				14.000	0.850	14.000	14.000	0.000	0	0			0.000	0.00	0.00		
										68.37518452	85.4689806							
																	Modified	corresp.
Steel Layers		**Area A_{sl}**	**Grade**	**Effective Prest.**	**Depth d_{sl}**	**E_s**	**Q**	**fpy**	**R**	**K**	**ε_{so}**	**$\Delta\varepsilon$**	**Total ε_s**	**Stress**	**Force**	**Moment**	**stress**	**f'c**
Grade 60 Bars	1	1.2	60	0	2.688	29000	0	60	100	1.096	0.0000	0.0000	0.0000	0.54	0.65	1.74	0.54	5.00
	2	1.2	60	0	11.313	29000	0	60	100	1.096	0.0000	0.0097	0.0097	60.00	72.00	814.50	60.00	5.00
	3		60	0	12.688	29000	0	60	100	1.096	0.0000	0.0000	0.0113	60.00	0.00	0.00	60.00	5.00
	4		60	0	9.125	29000	0	60	100	1.096	0.0000	0.0000	0.0072	60.00	0.00	0.00	60.00	5.00
	5		60	0	11.750	29000	0	60	100	1.096	0.0000	0.0000	0.0102	60.00	0.00	0.00	60.00	5.00
	6		60	0	14.375	29000	0	60	100	1.096	0.0000	0.0000	0.0131	60.00	0.00	0.00	60.00	0.00
	7		60	0	17.000	29000	0	60	100	1.096	0.0000	0.0000	0.0161	60.00	0.00	0.00	60.00	0.00
	8		60	0	19.625	29000	0	60	100	1.096	0.0000	0.0000	0.0190	60.00	0.00	0.00	60.00	0.00
	9		60	0	22.250	29000	0	60	100	1.096	0.0000	0.0000	0.0220	60.00	0.00	0.00	60.00	0.00
	10		60	0	24.875	29000	0	60	100	1.096	0.0000	0.0000	0.0249	60.00	0.00	0.00	60.00	0.00
	11		60	0	27.500	29000	0	60	100	1.096	0.0000	0.0000	0.0279	60.00	0.00	0.00	60.00	0.00
	12		60	0	30.125	29000	0	60	100	1.096	0.0000	0.0000	0.0308	60.00	0.00	0.00	60.00	0.00
	13		60	0	32.750	29000	0	60	100	1.096	0.0000	0.0000	0.0338	60.00	0.00	0.00	60.00	0.00
Grade 70 Plate	1		70	0	0.000	29000	0	70	100	1.06	0.0000	0.0000	-0.0030	-70.00	0.00	0.00	-65.75	5.00
Gr. 120 Rods	1		120	0	5.125	29000	0.0217	81.00	4.224	1.01	0.0000	0.0000	0.0028	68.86	0.00	0.00	68.86	5.00
Gr. 150 Rods	1		150	0	5.125	29000	0.0217	120.00	4.224	1.01	0.0000	0.0000	0.0028	77.05	0.00	0.00	77.05	5.00
Gr 270	1		270	28	1.500	28500	0.031	243	7.36	1.043	0.0010	0.0000	-0.0003	-9.48	0.00	0.00	-5.23	5.00
Gr 270	2		270	28	5.500	28500	0.031	243	7.36	1.043	0.0010	0.0000	0.0042	118.51	0.00	0.00	118.51	5.00
Gr 270	3		270	160	10.000	28500	0.031	243	7.36	1.043	0.0056	0.0000	0.0138	256.57	0.00	0.00	256.57	5.00
Gr 270	4		270	150	10.750	28500	0.031	243	7.36	1.043	0.0053	0.0000	0.0143	257.28	0.00	0.00	257.28	5.00
	5		270	160	12.333	28500	0.031	243	7.36	1.043	0.0056	0.0000	0.0165	259.78	0.00	0.00	259.78	5.00
	6		270	160	14.667	28500	0.031	243	7.36	1.043	0.0056	0.0000	0.0191	262.34	0.00	0.00	262.34	0.00
	7		270	160	17.000	28500	0.031	243	7.36	1.043	0.0056	0.0000	0.0217	264.72	0.00	0.00	264.72	0.00
	8		270	160	19.333	28500	0.031	243	7.36	1.043	0.0056	0.0000	0.0243	267.07	0.00	0.00	267.07	0.00
	9		270	160	21.667	28500	0.031	243	7.36	1.043	0.0056	0.0000	0.0270	269.39	0.00	0.00	269.39	0.00
	10		270	160	24.000	28500	0.031	243	7.36	1.043	0.0056	0.0000	0.0296	270.00	0.00	0.00	270.00	0.00
	11		270	160	26.333	28500	0.031	243	7.36	1.043	0.0056	0.0000	0.0322	270.00	0.00	0.00	270.00	0.00
	12		270	160	28.667	28500	0.031	243	7.36	1.043	0.0056	0.0000	0.0348	270.00	0.00	0.00	270.00	0.00
	13		270	160	31.000	28500	0.031	243	7.36	1.043	0.0056	0.0000	0.0374	270.00	0.00	0.00	270.00	0.00
	Sum of M									MAXIMUM	$\Delta\varepsilon$:	0.0097		Moment (K'	0.00	738.63	kip*in	
																61.55	kip*f	

Figure C.9 Concept 4 Example Concrete Rail Calculations

Inputs:				
Rail:	HSS8.625X.375			
Posts:	h =	56	in.	height of the post (top of wall section to bottom of rail section)
	h tot =	56	in.	height from the top of the parapet to the top of the rail
	b =	3	in.	width of the post
	d =	12	in.	depth of the post
	L =	8	ft	span length
L_t =	8	ft	per AASHTO Chapter 13 requirements	
H_r =	56	in	height to the middle of the rail section	
Calculations:				
Rail:				
M_r =	1003.8	k-in		
	83.65	k-ft		
Posts:				
Z =	108	in^3		
M_p =	3888	k-in		
P_p=	69.4286	k	at top bottom of rail	
Capacity:				
Spans	R (kip)			
1 span =	501.9			
2 span =	259.871			
3 span =	211.466			
4 span =	230.394			
5 span =	240.91			
6 span =	272.848			
7 span =	294.959			
8 span =	329.689			
9 span =	356.246			

Figure C.10 Concept 5 Example System Calculations

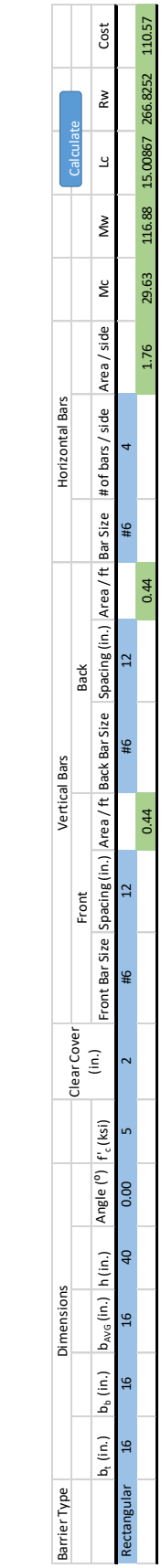

Barrier Type	Dimensions					Clear Cover (in.)	Vertical Bars				Horizontal Bars				Calculate		
							Front		Back								
	b_t (in.)	b_b (in.)	b_{AVG} (in.)	h (in.)	Angle (°)	f'c (ksi)		Front Bar Size	Spacing (in.)	Area / ft	Back Bar Size	Spacing (in.)	Area / ft	Bar Size	# of bars / side	Area / side	Mc	Mw	Lc	Rw	Cost
Rectangular	16	16	16	40	0.00	5	2	#6	12	0.44	#6	12	0.44	#6	4	1.76	29.63	116.88	15.00867	266.8252	110.57

Figure C.11 Concept 7 Wall Calculations

Inputs:							Weight =	80000	lb									
Hardness =	80						Rear Weig	34000	lb									
Poissons =	0.5						Impact V =	50	mph									
Pad Area =	400	in^2					Impact θ =	15	deg									
Pad Height =	16	in					IS_{whole} =	447.8703	k-ft									
Δ_{max} =	16.1	in																
							Kinetic for Rear											
							Speed	15.5	mph									
Calculations:							Angle	90	deg									
E =	9.382421	Mpa					IS_{rear} =	273.0688	k-ft									
	1.360805	ksi						3276.826	k-in									
								468.118	k-in	1/7 of the rear IS								
G =	0.18	ksi																

The force due to the deformation of an elastomeric element shall be taken as:

$$H_{bu} = GA\frac{\Delta_u}{h_{rt}} \qquad (14.6.3.1\text{-}2)$$

where:

G = shear modulus of the elastomer (ksi)

A = plan area of elastomeric element or bearing ($in.^2$)

Δ_u = shear deformation from applicable strength and extreme event load combinations in Table 3.4.1-1 (in.)

h_{rt} = total elastomer thickness (in.)

Strength and extreme event limit states rolling forces shall be determined by testing.

Load	Pad Number																	
Spans	1	2	3	4	5	6	7	8	9	10	11	12	13	14	15	16	Sum	Average
2	72.45																72.45	72.45
3	48.3	48.3															96.6	48.3
4	36.225	72.45	36.225														144.9	48.3
5	28.98	57.96	57.96	28.98													173.88	43.47
6	24.15	48.3	72.45	48.3	24.15												217.35	43.47
7	20.7	41.4	62.1	62.1	41.4	20.7											248.4	41.4
8	18.1125	36.225	54.3375	72.45	54.3375	36.225	18.1125										289.8	41.4
9	16.1	32.2	48.3	64.4	64.4	48.3	32.2	16.1									322	40.25
10	14.49	28.98	43.47	57.96	72.45	57.96	43.47	28.98	14.49								362.25	40.25
11	13.17273	26.34545	39.51818	52.69091	65.86364	65.86364	52.69091	39.51818	26.34545	13.17273							395.1818	39.51818
12	12.075	24.15	36.225	48.3	60.375	72.45	60.375	48.3	36.225	24.15	12.075						434.7	39.51818
13	11.14615	22.29231	33.43846	44.58462	55.73077	66.87692	66.87692	55.73077	44.58462	33.43846	22.29231	11.14615					468.1385	39.01154
14	10.35	20.7	31.05	41.4	51.75	62.1	72.45	62.1	51.75	41.4	31.05	20.7	10.35				507.15	39.01154
15	9.66	19.32	28.98	38.64	48.3	57.96	67.62	67.62	57.96	48.3	38.64	28.98	19.32	9.66			540.96	38.64
16	9.05625	18.1125	27.16875	36.225	45.28125	54.3375	63.39375	72.45	63.39375	54.3375	45.28125	36.225	27.16875	18.1125	9.05625		579.6	38.64
17	8.523529	17.04706	25.57059	34.09412	42.61765	51.14118	59.66471	68.18824	68.18824	59.66471	51.14118	42.61765	34.09412	25.57059	17.04706	8.523529	613.6941	38.35588

Energy [k-in] with 0.5 x Force x Displacement									Pad Number									
Spans	1	2	3	4	5	6	7	8	9	10	11	12	13	14	15	16	Sum	Average
2	583.2225																583.2225	583.2225
3	259.21	259.21															518.42	259.21
4	145.8056	583.2225	145.8056														874.8338	291.6113
5	93.3156	373.2624	373.2624	93.3156													933.156	233.289
6	64.8025	259.21	583.2225	259.21	64.8025												1231.248	246.2495
7	47.61	190.44	428.49	428.49	190.44	47.61											1333.08	222.18
8	36.45141	145.8056	328.0627	583.2225	328.0627	145.8056	36.45141										1603.862	229.1231
9	28.80111	115.2044	259.21	460.8178	460.8178	259.21	115.2044	28.80111									1728.067	216.0083
10	23.3289	93.3156	209.9601	373.2624	583.2225	373.2624	209.9601	93.3156	23.3289								1982.957	220.3285
11	19.28008	77.12033	173.5207	308.4813	482.0021	482.0021	308.4813	173.5207	77.12033	19.28008							2120.809	212.0809
12	16.20063	64.8025	145.8056	259.21	405.0156	583.2225	405.0156	259.21	145.8056	64.8025	16.20063						2365.291	215.0265
13	13.80408	55.21633	124.2367	220.8653	345.1021	496.947	496.947	345.1021	220.8653	124.2367	55.21633	13.80408					2512.343	209.3619
14	11.9025	47.61	107.1225	190.44	297.5625	428.49	499.905	428.49	297.5625	190.44	107.1225	47.61	11.9025				2666.16	205.0892
15	10.3684	41.4736	93.3156	165.8944	259.21	373.2624	508.0516	508.0516	373.2624	259.21	165.8944	93.3156	41.4736	10.3684			2903.152	207.368
16	9.112852	36.45141	82.01566	145.8056	227.8213	328.0627	446.5297	583.2225	446.5297	328.0627	227.8213	145.8056	82.01566	36.45141	9.112852		3134.821	208.9881
17	8.072284	32.28913	72.65055	129.1565	201.8071	290.6022	395.5419	516.6262	516.6262	395.5419	290.6022	201.8071	129.1565	72.65055	32.28913	8.072284	3293.492	205.8432

Figure C.12 Concept 7 Elastomer Post Calculations

END OF DOCUMENT